University of Kentucky
UKnowledge

Theses and Dissertations--Microbiology, Immunology, and Molecular Genetics

Microbiology, Immunology, and Molecular Genetics

2023

Investigating the relationship between metabolic reprogramming and peripheral CD4+ T-cell inflammation in human type 2 diabetes pathogenesis

Gabriella Kalantar
University of Kentucky, ghpu222@uky.edu
Author ORCID Identifier:
https://orcid.org/0000-0003-1573-3787
Digital Object Identifier: https://doi.org/10.13023/etd.2023.386

Right click to open a feedback form in a new tab to let us know how this document benefits you.

Recommended Citation

Kalantar, Gabriella, "Investigating the relationship between metabolic reprogramming and peripheral CD4+ T-cell inflammation in human type 2 diabetes pathogenesis" (2023). *Theses and Dissertations--Microbiology, Immunology, and Molecular Genetics*. 28.
https://uknowledge.uky.edu/microbio_etds/28

This Doctoral Dissertation is brought to you for free and open access by the Microbiology, Immunology, and Molecular Genetics at UKnowledge. It has been accepted for inclusion in Theses and Dissertations--Microbiology, Immunology, and Molecular Genetics by an authorized administrator of UKnowledge. For more information, please contact UKnowledge@lsv.uky.edu.

STUDENT AGREEMENT:

I represent that my thesis or dissertation and abstract are my original work. Proper attribution has been given to all outside sources. I understand that I am solely responsible for obtaining any needed copyright permissions. I have obtained needed written permission statement(s) from the owner(s) of each third-party copyrighted matter to be included in my work, allowing electronic distribution (if such use is not permitted by the fair use doctrine) which will be submitted to UKnowledge as Additional File.

I hereby grant to The University of Kentucky and its agents the irrevocable, non-exclusive, and royalty-free license to archive and make accessible my work in whole or in part in all forms of media, now or hereafter known. I agree that the document mentioned above may be made available immediately for worldwide access unless an embargo applies.

I retain all other ownership rights to the copyright of my work. I also retain the right to use in future works (such as articles or books) all or part of my work. I understand that I am free to register the copyright to my work.

REVIEW, APPROVAL AND ACCEPTANCE

The document mentioned above has been reviewed and accepted by the student's advisor, on behalf of the advisory committee, and by the Director of Graduate Studies (DGS), on behalf of the program; we verify that this is the final, approved version of the student's thesis including all changes required by the advisory committee. The undersigned agree to abide by the statements above.

Gabriella Kalantar, Student

Barbara S. Nikolajczyk, Major Professor

Brett Spear, Director of Graduate Studies

INVESTIGATING THE RELATIONSHIP BETWEEN METABOLIC REPROGRAMMING AND PERIPHERAL $CD4^+$ T-CELL INFLAMMATION IN HUMAN TYPE 2 DIABETES PATHOGENESIS

DISSERTATION

A dissertation submitted in partial fulfillment of the
requirements for the degree of Doctor of Philosophy in the
College of Medicine
at the University of Kentucky

By

Gabriella Hope Kalantar

Lexington, Kentucky

Co- Directors: Dr. Barbara S. Nikolajczyk, Professor of Pharmacology and Nutritional Sciences

and Dr. Subbarao Bondada, Professor of Microbiology, Immunology, and Molecular Genetics

Lexington, Kentucky

2023

Copyright © Gabriella Hope Kalantar 2023
https://orcid.org/0000-0003-1573-3787

ABSTRACT OF DISSERTATION

INVESTIGATING THE RELATIONSHIP BETWEEN METABOLIC REPROGRAMMING AND PERIPHERAL $CD4^+$ T-CELL INFLAMMATION IN HUMAN TYPE 2 DIABETES PATHOGENESIS

Chronic, low-grade systemic inflammation rises in obesity and promotes type 2 diabetes (T2D). Circulating immune cells are key indicators of obesity and T2D pathogenesis. T cells outnumber monocytes, in blood, suggesting that T cells might fuel peripheral inflammation in obesity/T2D. Our lab's work supports this idea by identification of a Th17 cytokine profile in T2D from T-cell stimulated peripheral blood mononuclear cells. Work described herein further supported this work by demonstrating that T cells dominate peripheral inflammation over monocytes across the spectrum of obesity and glycemic control. Our lab has also recently shown that inflammation changes during prediabetes (preT2D), identified bioinformatically by a Th1/Th2 cytokine profile that shared similarities with T cells from people with normal glucose tolerance (NGT), suggesting a potential compensatory mechanism to shift inflammation away from T2D pathogenesis. T cells from preT2D donors also had higher oxidative phosphorylation (OXPHOS) activity, thus supporting the relationship between T-cell metabolism and function, leading to our hypothesis that enhanced mitochondrial function in $CD4^+$ T cells promotes peripheral inflammation in preT2D.

We first tested mitochondrial function parameters, which were indistinguishable amongst NGT, preT2D, and T2D donors. Thus, high T-cell OXPHOS in preT2D was not due to changes in mitochondrial function. We next tested the possibility that differential mitochondrial fuel metabolism promotes high T-cell OXPHOS in preT2D and the differences between preT2D and T2D-associated cytokine profiles. Of the fuel sources tested, we saw a profound reduction in OXPHOS activity in both preT2D and T2D cells by glutaminolysis restriction via glutaminase-1 (GLS-1) inhibition, of which also reduced Th1/Th17 cytokines from T-effector cells. While GLS-1 inhibition reduced mTORC1 activity, reductions in Th1/Th17 cytokines were not dependent on mTORC1. Therefore, GLS-1 activity supports high OXPHOS and T2D-associated inflammation independent of the positive feedback loop between glutamine and mTORC1. Alternatively, GLS-1 function could be downstream of mTORC1. These results provide a novel mechanism that links metabolic reprogramming in preT2D T cells to T2D pathogenesis. We hypothesize that changes in metabolism occur in T cells prior to onset of T2D-associated inflammation, of which we think happens later in T2D development through glutaminolysis reliance. Data from this work could have promising clinical implications in potential efforts to repurpose the glycemic control drug peroxisome proliferator-activated receptor-gamma agonists for T2D-associated inflammation as they have been shown to inhibit GLS-1 activity and Th17 function.

KEYWORDS: Type 2 diabetes, obesity, prediabetes, $CD4^+$ T cells, metabolism, mitochondria

Gabriella Hope Kalantar

08/03/2023

INVESTIGATING THE RELATIONSHIP BETWEEN METABOLIC REPROGRAMMING AND PERIPHERAL $CD4^+$ T CELL INFLAMMATION IN HUMAN TYPE 2 DIABETES PATHOGENESIS

By
Gabriella Hope Kalantar

Dr. Barbara S. Nikolajczyk
Co-Director of Dissertation

Dr. Subbarao Bondada
Co-Director of Dissertation

Dr. Brett Spear
Director of Graduate Studies

08/03/2023
Date

DEDICATION

To my husband, Alborz, for your unwavering love and support. Your efforts to both celebrate my victories and embrace me through failures served as the lifejacket that kept me afloat. You were truly the light that diminished the darkness in times that I couldn’t find the switch. I love you, my oso.

ACKNOWLEDGEMENTS

I would first like to thank my mentor and dissertation advisor, Dr. Barbara Nikolajczyk for teaching me how to be an independent scientist and critical thinker. The growth I have experienced in the lab, both personally and professionally, over the last four years has allowed me to realize my full potential and I have become an overall more confident person and scientist. Thank you for your guidance, patience, kindness, and words of wisdom. I would also like to thank my advisory committee Dr. Subbarao Bondada, Sarah D'Orazio, Nancy Webb, Jamie Sturgill, and Charles Snow for their invaluable insights. Each of you have individually shaped my scientific career by always encouraging me to step back and look at the bigger picture and have profoundly influenced my professional development.

I would also like to acknowledge Dr. Madhur Agrawal who not only helped fuel my decision to join the Nikolakczyk lab, but also welcomed me with open arms through the growing pains of being a new graduate student and answering my many questions that had obvious answers without judgement. Madhur also assisted with and provided training on flow cytometry panels and cytokine measurements. I would also like to thank Dr. Jin Chen, Dr. Sajjad Fouladvand, Dr. Xiaohua Douglas Zhang, and Shubh Saraswat for bioinformatic analyses, patient and clear explanations of complex statistical models, and overall invaluable contributions to this body of work. Additional thanks to the microbiology, immunology, and molecular genetics department for not only providing me with outstanding Ph.D. training, but for also giving me a sense of community and belonging, and for providing a safe space to express my ideas and grow

professionally. I also received technical assistance from Dr. Leena P. Bharath from Merrimack College (confocal microscopy), Anne C. Hawk during her rotation in our lab (quantitative real-time polymerase chain reaction experiments), and Dr. Sara SantaCruz-Calvo in the Nikolajczyk lab (reactive oxygen species measurements and dose titration pilot studies for BPTES and NV-5138 treatments). This brings me to my next acknowledgment, to a person I could not thank enough, Sara. You were a second mentor to me and challenged me to think deeper and never hesitated to offer a helping hand, or a shoulder to cry on. I not only gained a mentor, but I also gained a lifelong friend. Thank you for everything.

I'd like to take a moment to thank my outstanding support system. To my husband, Alborz, the dedication page says it all. I couldn't have made it through this challenging process without your comforting presence and roaring laughter. You never failed to remind me of the truly important things in life and that hardship is only temporary. You have been my rock since day one. To my parents, I am so grateful to be your daughter and I know that I've made you and our small Appalachian hometown proud. Your endless encouragement has meant more than I could ever put into words. Last, but certainly not least, I'd like to thank the irreplaceable friends that I've made in the MIMG department, particularly, Mackenzie, Zaria, and Jamila. Our movie nights will forever be part of some of my most cherished memories. I only regret that we didn't start them sooner. Thank you for accepting me, laughing at my jokes (even when I tell too many), and for supporting me. I am so lucky to have gone through this journey with you all.

TABLE OF CONTENTS

ACKNOWLEDGEMENTS iii

LIST OF TABLES viii

LIST OF FIGURES ix

CHAPTER 1. INTRODUCTION AND BACKGROUND 1

1.1 Introduction 1

1.2 Regulation of insulin sensitivity and glucose tolerance 3

1.2.1 Nutrient and endocrine mediated regulation 3

1.2.2 Immune cell-mediated regulation 8

1.3 Pathophysiology of obesity-associated T2D 10

1.3.1 Pancreatic β-cell impairment 10

1.3.2 Meta-inflammation feeds systemic insulin resistance 12

1.3.3 Diagnosis, management of T2D and risk assessment 15

1.4 The role of metabolic reprogramming in T cell fate and function 18

1.4.1 Regulation of metabolism during quiescence 19

1.4.2 Metabolic reprogramming during activation and differentiation 23

1.4.3 Th1 lineage 25

1.4.4 Th2 lineage 26

1.4.5 Th17 lineage 27

1.5 Hypothesis 28

CHAPTER 2. MATERIALS AND METHODS 30

2.1 Description of human donors 30

2.2 PBMC isolation and archiving 30

2.3 Total $CD4^+$ T cell and T_{eff} cell isolation 32

2.4 Cell thawing, culture conditions, and cytokine measurements 33

2.5 Flow cytometry 34

2.6 Extracellular flux analysis 35

CHAPTER 3. T CELLS DOMINATE PERIPHERAL INFLAMMATION IN OBESITY-ASSOCIATED T2D 37

3.1 Disclaimer 37

3.2 Introduction 37

3.3 Objective and Summary 38

3.4 Materials and methods 39

3.4.1 Donor description and demographics 39

3.4.2 Cell manipulations 41

3.4.3 Flow cytometry 41

3.4.4 Statistical Analysis 42

3.5 Results 44

3.5.1 PBMCs increase cytokine production over time following T-cell stimulation but not myeloid stimulation 44

3.5.2 T cell and myeloid cell cytokine changes accompany metabolic decline 47

3.5.3 T cell- compared to myeloid-stimulated PBMCs produce more TNF-α 49

3.5.4 T cell cytokine competency disproportionately contributes to diabetes-associated meta-inflammation 54

3.6 Discussion 56

CHAPTER 4. MITOCHONDRIAL TRAITS ARE NOT ALTERED IN PERIPHERAL $CD4^+$ T CELLS IN T2D PATHOGENESIS 58

4.1 Introduction 58

4.2 Materials and methods 62

4.2.1 Donor description and demographics 62

4.2.2 Mitotracker probes 64

4.2.3 Quantitative real-time PCR 65

4.2.4 ROS Measurements 66

4.2.5 Western Blot 67

4.2.6 Confocal microscopy 68

4.2.7 Statistical analysis 69

4.3 Results 69

4.3.1 Functional mitochondria and lower autophagy are indicative of higher bioenergetics in preT2D T cells 69

4.3.2 Mitochondrial mass and membrane dynamics are not altered in T cells from preT2D donors 73

4.4 Discussion 77

CHAPTER 5. GLUTAMINOLYSIS SUPPORTS HIGH METABOLISM AND $CD4^+$ T CELL INFLAMMATION IN T2D PATHOGENESIS 79

5.1 Introduction 79

5.2 Objective 80

5.3 Materials and methods 80

5.3.1 Donor description and demographics 80

5.3.2 Cell manipulations: Total $CD4^+$ T cells 82

5.3.3 Cell manipulations: T_{eff} cells 82

5.3.4 Lactate Measurements 83

5.3.5 mTORC1 ELISA 83

5.3.6 Statistical analysis 84

5.4 Results 85

5.4.1 Mitochondrial pyruvate import is dispensable for T-cell metabolism and effector cytokine production 85

5.4.2 Blocking Cpt1a to limit FAO changes $CD4^+$ T-cell metabolism and T_{eff} cytokine production through disease-independent mechanisms 89

5.4.3 Glutaminolysis supports high OXPHOS and proinflammatory effector responses in T2D pathogenesis 91

5.4.4 GLS-1 inhibition reduces mTORC1 activity in preT2D and T2D independent of inflammation 98

5.5 Discussion 102

CHAPTER 6. SUMMARY AND FUTURE DIRECTIONS 104

APPENDICES 112

REFERENCES 124

VITA 157

LIST OF TABLES

Table 1.1 Clinical cut-off values for diabetes risk/severity assessment[163] 16
Table 3.1 Description of human donors 40
Table 3.2 List of glycemic and lipid control medications and smoker status 41
Table 3.3 Surface marker antibody panel 42
Table 3.4 Intracellular marker antibody panel 42
Table 4.1 Description of human donors 63
Table 4.2 List of glycemic and lipid control medications and smoker status 64
Table 4.3 PCR Primer Sequences 66
Table 5.1 Description of human donors 81
Table 5.2 List of glycemic and lipid control medications and smoker status 82

LIST OF FIGURES

Figure 1.1 Schematic diagram of T-cell quiescence 22
Figure 3.1 Cytokine responses to T cell-targeting, but not myeloid-targeting, stimuli change over time and are impacted by T2D 45
Figure 3.2 Loss of glycemic control associates with changes in T cell cytokine production 48
Figure 3.3 Loss of glycemic control associates with changes in LPS-stimulated cytokine production 50
Figure 3.4 T cell stimulation elicits more TNF-α than myeloid stimulation of PBMCs from all participants with obesity 52
Figure 3.5 Intracellular staining confirms that the CD4+ T cells produce more TNF-α than myeloid cells at 40- or 20-hours post-stimulation, respectively 53
Figure 3.6 Combinatorial models indicate that T cell cytokines are more important than myeloid cytokines for T2D-associated inflammation 55
Figure 4.1 Schematic diagram of mitochondrial structure, membrane dynamics, OXPHOS activity and ROS production 61
Figure 4.2 Mitochondrial transmembrane potential remains functional in T cells from preT2D and T2D donors 70
Figure 4.3 High T-cell OXPHOS in preT2D does not associate with oxidative stress or enhanced autophagy 72
Figure 4.4 T cell mitochondrial mass and abundance are comparable amongst donor cohorts 75
Figure 4.5 Mitochondrial membrane dynamics do not explain high OXPHOS in T cells in preT2D 76
Figure 5.1 Mitochondrial pyruvate import minimally contributes to high T cell OXPHOS in preT2D 86
Figure 5.2 Mitochondrial pyruvate import uncouples T-cell metabolism from function.... 88
Figure 5.3 T cells from preT2D and T2D donors are insensitive to mild stress-induced changes to OXPHOS activity from Cpt1a inhibition 90
Figure 5.4 Cpt-1a inhibition uncouples T-cell metabolism from function 92
Figure 5.5 Glutaminolysis supports high T-cell OXPHOS in preT2D and T2D 94
Figure 5.6 GLS-1 inhibition reduces Th1 and Th17 cytokines 96
Figure 5.7 Alpha-ketoglutarate supplementation does not reverse the effects of GLS-1 inhibition on metabolism and inflammation 97
Figure 5.8 GLS-1 inhibition reduces mTORC1 activity in T2D T cells and mTOR inhibition mimics effects of GLS-1 on Th1 and Th17 cytokines 100
Figure 5.9 mTORC1 agonism does not reverse effects of GLS-1 inhibition on inflammation 101
Figure 6.1 Schematic diagram of proposed mechanisms supporting $CD4^+$ T-cell metabolism and T_{eff} cytokine production in preT2D 110
Figure 6.2 Schematic diagram of proposed mechanisms supporting $CD4^+$ T-cell metabolism and T_{eff} cytokine production in T2D 111

CHAPTER 1. INTRODUCTION AND BACKGROUND

1.1 Introduction

Obesity rates have steadily increased over the last two decades, resulting in its classification as a global health issue. Approximately 50% of the U.S. adult population has obesity, coupled with the distressing emergence of pediatric cases (>13 million).[1-3] Escalating obesity rates are a major public health concern as obesity is a critical risk factor for several chronic diseases that account for half of the leading causes of death in the U.S. including heart disease, chronic liver disease, and type 2 diabetes (T2D).[4,5]

Many of the factors that contribute to T2D risk support obesity onset. The highest obesity prevalence is reported in rural regions.[6] Rural counties are profoundly affected by poverty, often accompanied by food insecurity, lack of recreational centers/parks and proper health education, and poor healthcare quality/access.[7] Social and environmental factors heavily influence the contributions of obesity and lifestyle to T2D risk, supported by Kentucky and Western Virginia leading the nation in obesity prevalence and ranking within the top ten states in T2D cases.[6] According to the 2019 KY Diabetes Report from the cabinet of health and family services, Kentucky ranked fifth in the nation in 2017[8,9] for highest mortality rate due to diabetes-associated deaths, a profound rationale to improve T2D management, care, and prevention in under-served communities.

The progression from normal glucose tolerance (NGT) to T2D is a multifactorial process that is seldom a linear path. Although obesity and lifestyle are hallmark indicators of T2D risk, it is important to note the combinatorial nature of disease development such as family history of T2D and the social determinants described above.[7,10,11] Together, these make for a complex disease mechanism that can take several years to display obvious clinical manifestations, making early detection and prevention efforts challenging. Although obesity is but one of the many contributors to T2D development, it plays a critical role in its pathophysiology, primarily through alterations in key metabolic signaling pathways induced by long-term nutrient excess. Pinpointing how and when to intervene is

crucial to improving diabetes risk (i.e., prediabetes) and prevalence as made alarmingly evident by the current 37 million U.S. adults with T2D and an estimated 96 million with prediabetes (preT2D).[9]

Chronic nutrient excess induces systemic changes to metabolic pathways such as glucose and fatty acid (FA) metabolism. Postprandial increases in peripheral glucose and free FA (FFA) levels signal insulin secretion from pancreatic islet cells that are mostly comprised of insulin-secreting β-cells (~60%).[12] One primary function of the pancreas is to respond to high blood glucose concentrations by releasing insulin from insulin-storing granules, thereby allowing glucose to be taken out of the bloodstream and into insulin-responsive tissues to be used for energy (e.g., skeletal muscle, adipose tissue, and liver).[13-18] High blood glucose levels (i.e., hyperglycemia) stimulates pancreatic β-cells to increase insulin secretion demand. Pancreatic β-cells have the ability to compensate for a high insulin demand and this is why some people may never develop T2D as this period is long-lasting, often generating increased β-cell mass and abundance.[19-21] Over time, compensatory increases in insulin secretion can lead to β-cell dysfunction due to exhaustion and endoplasmic reticulum (ER) stress, ultimately resulting in cell death, insulin insufficiency and persistent hyperglycemia, and systemic insulin resistance (IR).[22-24] As this process advances, most people with T2D require exogenous insulin treatment to handle peripheral glucose uptake. Hyperglycemia can also be improved in people with T2D through the availability of a wide range of hypoglycemic drugs that help improve lifespan as poor glycemic control augments the development of macrovascular and microvascular complications such as renal disease and neuropathy, respectively, and thus elevate risk of mortality.[25-27]

To add further complexity to disease progression, low-grade systemic inflammation (i.e., meta-inflammation) has been demonstrated to arise during obesity, even without IR, and persists into T2D development- emphasizing early and progressive immune cell involvement in obesity-associated comorbidities. Circulating and tissue-resident immune cells provide both positive and negative regulation to insulin responses. Immune cells influence metabolic function by

cytokine-mediated signal transduction elicited on target cells like adipocytes, hepatocytes, skeletal muscle fibers, and pancreatic β cells to generally enhance or limit glucose and FA uptake/metabolism in response to nutrient fluctuations, thus directly impacting bioenergetics and functional outcomes of insulin-responsive tissues.[28-36] In obesity and T2D, systemic immune cell subset distribution and the cytokine milieu shift from classically anti-inflammatory type-2 immune responses to pro-inflammatory type-1 and type-17 immune responses, as defined in the context of metabolic disease.[37-40] The culmination of an altered immune landscape, both in circulation and in tissue microenvironments, leads to overactivation of negative regulatory pathways in insulin signaling, thereby supporting IR. Until recently, cells of the innate immune system such as macrophages, have been credited as the predominant source of chronic, low-grade systemic inflammation (i.e., meta-inflammation) in obesity and T2D. However, evidence from our lab and others has revealed an instrumental role of the adaptive immune system (B and T lymphocytes) in IR and T2D pathogenesis with promising potential for clinical applications, particularly in $CD4^+$ T cell-mediated inflammation.[40-46]

The purpose of this dissertation is to explore the role of obesity-associated nutrient milieu shifts on T-cell function in T2D pathogenesis through alterations in metabolism and/or mitochondrial function. We hypothesized that $CD4^+$ T cells are a significant source of T2D-associated meta-inflammation that is driven by altered T-cell metabolism as early as preT2D, particularly through enhanced mitochondrial function. This work proposes a novel mechanism that links T-cell mitochondrial metabolism in preT2D to T2D immunopathogenesis and identifies potential drug targets to alleviate T2D-associated meta-inflammation.

1.2 Regulation of insulin sensitivity and glucose tolerance

1.2.1 Nutrient and endocrine mediated regulation

Obesity typically arises from a persistent positive energy balance, meaning calorie consumption exceeds calorie expenditure. Caloric excess generally leads

to increased energy storage in adipocytes, primarily in the form of triglycerides (TG), while β-cells upregulate insulin secretion to resolve hyperglycemia. T2D onset is triggered by a combination of impaired insulin secretion by β-cells and IR in peripheral tissues. Peripheral glucose increments are sensed by the glucose transporter GLUT2 expressed on β-cells to facilitate glucose uptake and subsequent catabolism by glycolysis.[47,48] Glucose import triggers activation of the phosphoinositide-3 kinase (PI3K)-protein kinase B (Akt) cascade.[49] The PI3K-Akt pathway helps maintain glycolysis by stimulating production of fructose-2,6-bisphosphate, a product of glycolysis that allosterically activates the rate-limiting enzyme phosphofructokinase 1 (PFK1) to catalyze the irreversible conversion of fructose-6-phosphate (F-6P). F-6P is also an essential substrate for the hexosamine biosynthesis pathway, thus PI3K-Akt activation maximizes F-6P availability for glycolysis as rapid ATP production is necessary to meet the high bioenergetic demands of pancreatic beta-cells upon post-prandial (i.e., post-meal) insulin secretion.

Higher rates of glycolysis increase intracellular adenosine triphosphate (ATP) levels that initiate closing of ATP-dependent K^+ channels, thereby depolarizing the β-cell membrane to allow Ca^{2+} influx. Intracellular Ca^{2+} accumulation is further aided by phospholipase C (PLC) activation potentiated by FFAs bound to G-protein coupled receptors (GPCRs) expressed on β cells, collectively triggering insulin-containing granules to fuse to the plasma membrane and release insulin into the periphery by exocytosis.[50,51] Preproinsulin, the single-chain polypeptide precursor for insulin, undergoes ER modifications to generate proinsulin. Proinsulin is folded in the ER lumen before translocation to the Golgi apparatus to be packaged into secretory vesicles where it's cleaved to yield the mature and final form of insulin.[52] Insulin production places a high protein biosynthesis burden on β-cells as each cell contains 100-500 units of insulin, approximately 10-days' worth of insulin supply.[53] Although β-cells are designed to handle a high rate of protein synthesis, as evidenced by their highly developed ER structures that are relatively larger,[54] the long-lasting compensatory ability of β-cells remains an impressive phenomenon and reveals an actionable window of

time for intervention; however, this window is somewhat elusive due to lack of obvious symptomology during the compensatory period.[55]

Optimal insulin secretion from the pancreas relies on essential hormone signals provided by adipose tissue (AT) and specialized enteroendocrine cells of the gastrointestinal (GI) tract, referred to as the G-P-A axis.[56] Many glycemic control drugs prescribed for T2D management target essential mechanisms of the G-P-A axis, emphasizing dysfunctional network integration as a critical component of disease progression. AT produces two indispensable hormones for insulin regulation (i.e., incretins): adiponectin and leptin. Adiponectin is one of the most abundant hormones in circulation, with optimal levels observed in metabolically healthy individuals, and possesses insulin-sensitizing properties including gluconeogenesis suppression, promoting FA oxidation (FAO) within β-cells and insulin-responsive tissues, and downstream activation of peroxisome proliferator activated receptor-alpha (PPAR-α) to support glucose-stimulated insulin secretion.[57-59] Leptin, popularly known as the satiety hormone, undergoes increased expression after insulin secretion to serve as a negative feedback regulator and protect against excess insulin secretion.[60] In turn, insulin acts on adipocytes to stimulate glucose uptake and activate PPAR-γ to restrict lipolysis- a process that mobilizes AT energy stores, typically during exercise or fasting.[61,62] Lipolysis restriction enables adipocytes to synthesize and store TGs to maintain an adequate energy reservoir for periods of fasting.[63] PPAR-γ is an important master regulator of lipid metabolism, adipocyte function, and systemic insulin sensitivity. In adipocytes, PPAR-γ enhances adipogenesis in response to insulin secretion by inducing differentiation of preadipocytes to mature adipocytes in subcutaneous white AT (SAT) in ex vivo human AT and supports the switch from white AT (WAT) to brown (AT) by activating uncoupling proteins (UCP), which carry out thermogenesis.[64-66] PPAR-γ helps maintain systemic insulin sensitivity by enhancing glucose uptake in both skeletal muscle and AT through activation of the

PI3K-Akt pathway and promoting adiponectin production from AT to sustain insulin secretion and limit gluconeogenesis.

Glucagon-like peptide 1 (GLP-1) produced by enteroendocrine cells is an incretin that enhances the expression of adiponectin and binds to GLP-1 receptors (GLP-1R) on pancreatic β cells- activating adenylate cyclase and cAMP accumulation, thereby supporting protein synthesis and cell growth.[67,68] Glucose transport across the apical side to the basolateral side of enteroendocrine cells is facilitated by sodium-glucose cotransporter (SGLT) 1, stimulating release of glucose-dependent insulinotropic peptide (GIP)[69] to exert dual effects on insulin secretion, both directly on the β cell and indirectly through promoting glucagon secretion from pancreatic α cells.[70] GIP further displays duel regulatory actions on insulin secretion by decreasing and increasing adiponectin and leptin expression, respectively.[71] GLP-1 and GIP are inactivated through cleavage and subsequent degradation by dipeptidyl peptidase 4 (DPP4), an enzyme that is widely-expressed/secreted by numerous tissues such as endothelial cells in vasculature and immune cells, primarily T cells in humans.[72,73] The compensatory period of insulin secretion in obesity and preT2D is supported by increases in GLP-1 (β-cell hypertrophy) that is eventually downregulated in T2D,[74] and increases in GIP production, which persists in T2D development and supports upregulated gluconeogenesis and leptin resistance.[75] Compensatory increases in GLP-1 and GIP are also accompanied by enhanced DPP4 secretion that persists in T2D development, supporting insulin resistance.[76]

The importance of the incretins in coordinating pathways involved in glucose-stimulated insulin secretion is made clear by their use as therapeutic targets in glycemic control medications for T2D. The most commonly prescribed glycemic control drug for T2D management is metformin. Metformin is a biguanide that is distributed across the small intestine, kidney, and liver with peak concentrations observed in the hepatic portal vein, thus its actions are mainly in the liver to decrease hepatic glucose output.[77-79] The primary mechanism of action of metformin is activation of adenosine monophosphate kinase (AMPK, a master regulator of cellular quiescence).[80,81] AMPK activation reduces gluconeogenesis

through inhibition of transcription factors that promote expression of gluconeogenic enzymes.[82] Moreover, metformin usage is associated with increases in GLP-1 secretion, posing an additional mechanism by which metformin suppresses gluconeogenesis.[83,84] Metformin has also been controversially identified as an electron transport chain (ETC) complex I inhibitor, reducing metabolic activity of hepatocytes and AT, and reactive oxygen species (ROS) production, ultimately combatting oxidative stress-induced inflammatory responses that can exacerbate T2D progression in people with obesity and impaired glucose tolerance (IGT).[85-88]

Contradictory evidence on metformin as a complex I inhibitor outweighs the supporting evidence. Complex I inhibition by metformin has been shown to occur only at supraphysiological concentrations.[88] In fact, physiological concentrations of metformin increase mitochondrial respiration and turnover in hepatocytes of DIO mice through AMPK activation, thereby improving mitochondrial function in obesity and IR.[89] Additionally, metformin's effect on gluconeogenesis inhibition is dependent on acute increases in cytosolic ROS, indicating that the mechanism of action for metformin in the liver is redox-dependent.[88] Although metformin is an attractive candidate for people with preT2D to delay/prevent T2D onset, especially considering its effects on weight loss in combination with lifestyle interventions, its use in preT2D remains controversial amongst clinicians.[90,91]

Agonists for PPAR-γ, a drug class referred to as thiazolidinediones (TZDs), improve insulin sensitivity in AT and skeletal muscle.[92,93] Prescription of TZDs has waned over the years due to undesirable side effects such as weight gain, edema, and congestive heart failure. Hence, TZDs pose considerable risk for exacerbating obesity and obesity-associated comorbidities, which people with T2D are already at elevated risk of developing.[94] GLP-1R agonists and SGLT inhibitors produce favorable outcomes in glycemic control, particularly when implemented in combination therapy either together or with other glycemic control drugs.[74,95-98] In addition to glycemic control benefits, drugs like metformin, TZDs, and DPP4 inhibitors have reported anti-inflammatory properties in either T2D or preT2D human donors; however, consistency/reproducibility of anti-inflammatory effects from these drugs remains an issue and limit use in clinical practice for T2D

prevention/delay.[99-102] Additionally, some glycemic control drugs induce a degree of immunosuppression such as impaired Th1 immunity against intracellular pathogens, emphasizing effects on immune cell function and the potential utility of glycemic control drugs to target inflammation associated with T2D.[103-105]

1.2.2 Immune cell-mediated regulation

The current understanding of T2D largely focuses on the endocrine arm of disease pathogenesis, hence the variety of existing hypoglycemic drugs. While an irrefutably important component of T2D development, it only addresses part of the problem. Circulating and tissue-resident immune cells play a vital role in the regulation of insulin signaling, largely through cytokine-mediated signal transduction in target cells. Pancreatic β-cells express a variety of cytokine receptors (e.g., IL-1R, TNF-R1, IL-6R)[106-108] to aid in the response to hyperglycemia predominantly by modulating activity of insulin receptor substrate (IRS) proteins and activation of c-Jun N-terminal kinases (JNK). Insulin receptors (InsR) expressed on peripheral tissues belong to the receptor tyrosine kinase (RTK) family, which are sensitive to immunomodulatory effects. Binding of insulin to the InsR induces tyrosine phosphorylation of IRS proteins. Active IRS proteins bind to and activate the PI3K-Akt pathway to enable nutrient uptake and metabolism.[109] Furthermore, both FA and cytokine signals activate JNKs-serine/threonine kinases of the mitogen activated protein kinase (MAPK) family that are expressed ubiquitously across insulin-responsive tissues. JNKs act primarily to downregulate the insulin response by activation signals from TNF-α and PI3K to phosphorylate IRS proteins on serine residues, rendering them inactive.[110-112]

Signal transduction mediated by cytokines associated with type-2 immunity, such as interleukin (IL) 4, IL-5, and IL-13, induces tyrosine phosphorylation of IRS proteins, suppress gluconeogenesis and lipogenesis, and upregulate glucose transporter expression in AT and skeletal muscle, thus supporting systemic insulin sensitivity and glucose tolerance.[28-30,34-36,113] Type 2 immune responses further act to keep type-1 and type-17 immune responses, like TNF-α, IFN-γ, and IL-17 at low

levels as these cytokines act to repress insulin signaling through serine phosphorylation of IRS proteins, enhancement of gluconeogenesis, and glucose transporter overexpression.[33,114-116] Immune cells that produce type 2 inflammatory responses such as T-helper 2 (Th2), regulatory T cells (T_{reg}), invariant natural killer T cells (iNKT), “alternative-switched” M2-polarized macrophages, eosinophils, and type 2 innate lymphoid cells (ILC2) are recruited to white AT (WAT) after T_{regs} are seeded postnatally and become tissue-resident memory (T_{RM}) cells as demonstrated in mice.[117] T_{RM} cells in WAT are replenished throughout the lifespan by chemokine recruitment and their phenotype/overall viability is supported by adiponectin production, underscoring the fundamental relationship between immune cells and insulin signaling in peripheral tissues.[118,119] Furthermore, type 1 and type 17 immune cells are not found in post-natal WAT and are thought to infiltrate exclusively by recruitment to restrict pro-inflammatory immune cell dominance.[120]

Nutrient fluctuations influence immune cell trafficking and function. Oral glucose load in fasted donors with either NGT or T2D results in $CD4^+$ and $CD8^+$ T cell accumulation in peripheral blood, likely in response to chemotactic signals induced by insulin secretion and InsR activation.[121] Moreover, high fat consumption appears to have negative effects on type 2 cytokines as demonstrated by reduced IL-5 and IL-13 in active young (< 60 years old) and old (> 60) individuals after a high fat meal, posing a potential mechanism by which type 1/17 responses eventually dominate meta-inflammation in obesity and T2D.[122] Systemic post-prandial increases in cytokine production are commonly reported, particularly higher IL-1β, IL-6, and TNF-α.[31,123] IL-1β increases insulin abundance and granule docking in pancreatic β-cells. Moreover, IL-1β stimulates NLRP3 inflammasome activation and subsequent IL-1β production/release from β-cells to promote a feedback loop between macrophages and the pancreas.[124] Production of IL-1β in the post-prandial insulin response must be balanced as

higher than normal levels promote ER stress and the UPR pathway, and caspase activation- triggering dysfunction and apoptosis of pancreatic β-cells.[125]

Contrary to IL-1β, TNF-α and IL-6 elicit suppressive functions on the peripheral insulin response by activating JNKs and the Janus kinase (JAK)/signal transducers of activation and transcription (STAT) cascade, respectively. JAK/STAT signaling integrate cellular responses to cytokine signals. During insulin signaling, IL-6/IL-6R or TNF-α/TNFR binding induces phosphorylation of JAK/STAT3.[115,126] Activated STAT3 dissociates with JAK and forms heterodimers with STAT1 before translocating to the nucleus to promote transcription of the suppressor of cytokine signaling (SOCS) 1 and 3 proteins. SOCS1 and SOC3 act to disrupt InsR activity by inducing proteosomal degradation of IRS-1 and IRS-2 proteins. In turn, SOCS1 and SOCS3 downregulate JAK/STAT signaling as a negative feedback mechanism to prevent excessive downregulation of InsR activity.[127,128]

In summary, post-prandial nutrient increases stimulate immune cell trafficking through insulin-responsive tissues and induce cytokine production for insulin response regulation. Parabiosis studies suggest that infiltrating immune cells can traffic back out of insulin-responsive tissues and into circulation,[129] thus immune cells in peripheral blood may have interacted within individual microenvironments of metabolic tissues, potentially priming them to elicit certain inflammatory properties during effector memory responses upon re-activation. Given the sensitivity of immune cell subset distribution and function to nutrient milieu shifts, chronic nutrient excess in obesity and T2D is a potential critical mediator of inflammatory changes associated with disease pathogenesis, thereby bridging endocrine and immunological mechanisms in T2D onset/progression.

1.3 Pathophysiology of obesity-associated T2D

1.3.1 Pancreatic β-cell impairment

Gradually, as hyperglycemia and hyperlipidemia persist, the compensatory increase of insulin synthesis in response to hyperglycemia generates more

misfolded insulin proteins as the influx of nascent unfolded polypeptides exceeds the folding capacity of the ER, activating the unfolded protein response (UPR) and chronic ER stress. Excess saturated FAs (SFAs), such as palmitate, are elevated in circulation in obesity and further exacerbate ER stress through UPR activation.[130] A hallmark sign of ER stress is excess Ca^{2+} flux and the mitochondria are often a primary victim of this pathogenic process as mitochondrial Ca^{2+} influx is required to maintain optimal respiratory chain (electron transport chain [ETC]) activity. An overload of Ca^{2+} in mitochondria results in overproduction of mitochondrial ROS (mtROS), notably superoxide. Insufficient neutralization of mtROS due to glutathione (GSH) depletion[131] from ER stress supports mitochondrial dysfunction/death, leaving β-cell function compromised. Moreover, ROS accumulation diminishes Ca^{2+} flux, ultimately promoting β-cell dysfunction by impairing insulin secretion.[132] Accrual of dysfunctional β-cells mediates progressive β-cell loss by eventual death and apoptosis. Marked β-cell apoptosis correlates with T2D severity as this progressive loss leads to exogenous insulin dependence.[133] Impaired β-cell function is often accompanied and exacerbated by pathogenic alterations throughout a multitude of organ systems that are impacted by obesity and hyperglycemia. These changes are described as the “ominous octet” of chronic hyperglycemia,[134] describing changes that occur in AT, skeletal muscle, liver, pancreas, vasculature, brain, renal system, and systemic inflammation that collectively support T2D.

WAT, both subcutaneous (SAT) and visceral (VAT), undergo major physiological changes during obesity that are critical to T2D pathology. Notably, adipocytes undergo hypertrophy and hyperplasia in addition to higher rates of lipolysis. Enhanced lipolysis in obesity is a common consequence of ectopic accumulation of circulating FAs, which impairs AT insulin sensitivity and thus the antilipolytic effect of insulin. Lipolysis enables adipocytes to release glycerol and FFAs that are taken up into circulation, thereby supporting the effects of glucotoxicity and lipotoxicity on IR.[135,136] Furthermore, an elevated rate of adipocyte death releases other cellular components like ATP and advanced glycated end products (AGE).[137] These components, along with FFAs, fall under

the category of damage-associated molecular patterns (DAMPs) and, with the help of chemokines released from surrounding adipocytes, will aid in recruitment of circulating immune cells such as neutrophils, macrophages, and cytotoxic T cells ($CD8^+$ T cells) to clear cellular debris and initiate an inflammatory response to the damaged tissue.[138-140] Since enhanced lipolysis and adipocyte death is ongoing in long-term obesity, this sustains a chronic inflammatory loop between adipocytes and resident/circulating immune cells that involves ROS accumulation, ER stress, and mitochondrial dysfunction.[141]

1.3.2 Meta-inflammation feeds systemic insulin resistance

$CD8^+$ T cells have been shown to traffic through WAT early after diet-induced obesity initiation[139] and are thought to help facilitate initial recruitment of circulating monocytes that subsequently mature into macrophages through signals received by both AT and T-helper cells (also known as T-effector cells). Cytokines produced by Th2 and Tregs support the “alternative-switched” M2 phenotype in macrophages, characterized by production of type-2 immunity cytokines. Conversely, Th1 cells stimulate TNF-α, IL-1β, and IL-6 release from macrophages- a phenotype referred to as “classically switched” M1 macrophages. This response elicits further recruitment of proinflammatory immune cell subsets like T-helper 1 (Th1) and T-helper 17 (Th17) cells. The role of the innate immune system, namely monocytes and macrophages, has been the focus of inflammation studies in obesity and IR. These studies utilize mouse models to emphasize AT inflammation and macrophage accumulation as the dominant driver of IR and are disproportionately represented in the literature relative to AT or peripheral inflammation studies in human obesity/T2D.

Macrophages have been credited as the primary mediators of IR and glucose intolerance, primarily by potentiating pathogenic effects through IL-1β, TNF-α, and IL-6 production, particularly in WAT.[140,142-145] However, assessment of macrophage populations (i.e., M1 and M2) pre- and post-bariatric surgery showed no change in WAT macrophage (ATM) populations after significant weight loss and that ATM population frequencies did not correlate with WAT IR.[146] These data are

further supported by work from Dr. Alyssa Hasty's lab showing that weight loss in HFD-fed mice does not change ATM phenotype or pro-inflammatory cytokine production, which becomes further exacerbated upon weight cycling (i.e., weight re-gain).[147] Together, these data expose a critical gap in translating our current understanding and points to underappreciated cellular sources of inflammation in T2D.

Serum cytokine levels of IL-1β, TNF-α, IL-6, and C reactive protein are elevated in people with obesity/T2D and are thought to reflect macrophage-mediated severity of meta-inflammation.[32,148-150] Serum cytokines can be utilized as clinical predictors of T2D risk; however, these are not reflective of meta-inflammation in T2D as they are not taken up from circulation into tissue, have short half-lives, and have been shown to be comparable to NGT donors. [32,148-150] Serum cytokine levels are also highly sensitive to a host of factors such as fasting, medications, physical activity, and proper blood processing, making it an overall unreliable measure and an uninformative indicator of T2D-associated inflammation.[149] Nonetheless, serum cytokine levels are still used as a major readout of inflammation in human T2D studies, even though these assessments do not reveal cellular sources of inflammation. This could explain, in part, why targeting individual cytokines, like IL-1β and TNF-α, do not improve glycemia long-term in people with T2D.[151-153]

As described earlier in this chapter, T cells are instrumental in maintaining inflammation, particularly through essential signals provided by T-effector cells (the more inflammatory T cell subset, herein 'T_{eff}') that are required to support the phenotype/function and survival of surrounding immune cells. RAG-1 knockout mice (i.e., lymphocyte-deficient) fail to develop IR in diet-induced obesity (DIO) mouse models,[41] underscoring the central role of the adaptive immune system to T2D pathophysiology. Since $CD4^+$ T cells can control responses of other immune cells, a closer examination of how $CD4^+$ T cells help drive meta-inflammation in obesity and T2D could reveal suitable mechanisms to target for anti-inflammatory therapies against T2D-associated meta-inflammation. As previously stated, type 1 and type 17 immune cells are not part of the T_{RM} landscape in WAT, thus these

immune cell subsets show up in WAT upon chemokine recruitment from circulation to primarily downregulate insulin signaling and potentiate a pro-inflammatory cascade in the context of obesity/T2D. While this highlights the importance of immune cell recruitment from circulation to peripheral insulin-sensitive tissues in promoting IR, there are few existing data on the role of circulating immune cells on meta-inflammation since the predominant research focus has been on AT in murine DIO. Therefore, shifting our focus from AT to the periphery is critical to deepen our understanding of how meta-inflammation promotes T2D.

T cells make up 60-80% of the peripheral blood mononuclear cell (PBMC) fraction and is mostly comprised of $CD4^+$ T cells relative to $CD8^+$ T cells (an approximate 2:1 ratio).[154] In the context of morbid obesity, the total $CD4^+$ T cell frequency is higher in PBMCs relative to SAT or VAT, suggesting that peripheral $CD4^+$ T cell accumulation may begin during obesity.[40] In healthy individuals, the $CD4^+$ T-cell fraction in PBMCs is mostly made up of naïve $CD4^+$ T cells, whereas T_{eff} memory (T_{EM}) cells comprise approximately 35% of the total circulating T-cell pool, which declines with age.[155] Conversely, the PBMC fraction in people with T2D was shown to exhibit lower naïve $CD4^+$ T cell frequencies and higher T_{EM} abundance.[156] Likewise, migratory capacity was impaired in *ex vivo* peripheral $CD4^+$ T_{EM} cells co-cultured with high endothelial venule cells and primed with dendritic cells. Impaired migratory capacity was more pronounced in senescent T_{EM} subsets that were present in higher frequencies in T2D donors compared to individuals with NGT, indicating that peripheral T-cell exhaustion associates with T2D. Impaired T-cell migration is hypothesized to be induced by oxidative stress from hyperglycemia, which likely promotes T-cell exhaustion.[157-159] Peripheral $CD4^+$ T cell accumulation and impaired migration in concordance with aberrant activation, as demonstrated by CD69 expression on fresh *ex vivo* T cells,[160] potentially enhance microvascular and macrovascular diabetic complications mediated by cytokine signaling in vasculature and nerve fibers.

Published data from our lab has characterized a pro-inflammatory T-cell signature in T cell-stimulated PBMCs in obesity-associated T2D that is bioinformatically distinct from obesity and normoglycemia, the latter predicted by a

Th1/Th2-dominated cytokine signature.[43] Additionally, Th17 cytokines were shown to promote TNF-α production from PBMCs,[43] thus emphasizing the contribution of T cells in production of a “myeloid-centric” cytokine. PBMC cultures lacking B cells significantly reduced Th17 cytokine production by T2D donor cells, supporting previous demonstrations that B cells are crucial for the $CD4^+$ T cell contribution to obesity-associated inflammation.[42,161,162] Additional analysis of T cell-stimulated PBMCs in T2D donors revealed that changes in FAO by alterations in lipid flux and FAO machinery, characterized by a low carnitine acylcarnitine transferase (CACT) to carnitine palmitoyltransferase 1a (Cpt1a) ratio. Changes in FAO fueled the T2D-associated peripheral Th17 dominance as confirmed by long-chain FA (LCFA) supplementation and CACT overexpression in cells from normoglycemic donors.[46] Together, these data not only reveal a robust pro-inflammatory T cell profile that delineates T2D, but also points to alterations in T cell metabolism as a critical driver of T2D meta-inflammation. Unifying glycemic control therapies through both endocrine and immunological mechanisms by targeting the way immune cells utilize fuel sources, which is likely shifted in obesity and T2D from peripheral glucotoxicity and lipotoxicity, may be an effective treatment option to promote cytokine action on insulin-sensitization.

1.3.3 Diagnosis, management of T2D and risk assessment

Along T2D progression, there is typically a transition from NGT to preT2D. Both preT2D and T2D are clinically defined by three laboratory measures: fasting blood glucose (FBG), hemoglobin A1C (HbA1C), and an oral glucose tolerance test (OGTT). FBG is defined as the concentration of glucose in the bloodstream during periods of fasting and is a measure of basal glycemic control. Cut-off FBG values for NGT, preT2D, & T2D are outlined in Table 1.1. FBG is only one measure of T2D risk and comes with its own disadvantages.[163] For example, increased levels of cortisol, a hormone secreted during stress, can have a profound impact on FBG levels. Cortisol signals to hepatocytes to initiate gluconeogenesis- a process by which hepatocytes convert glucagon to glucose and secrete it to the periphery. This process can temporarily result in hyperglycemia, thereby

potentially skewing results to mimic preT2D or T2D. Additionally, fasting has been shown to increase parameters of stress, though the evidence to support this hypothesis is equally met with contradictory evidence suggesting that fasting can be beneficial for stress and anxiety.[164] Due to these constraints, additional measures are often assessed to confirm glycemic control status, apart from individuals displaying clear signs of hyperglycemia, such as hyperglycemic crisis, by which FBG is sufficient for a T2D diagnosis.[163]

Table 1.1 Clinical cut-off values for diabetes risk/severity assessment[163]

Classification	FBG mg/dl	HbA1c, %	OGTT
NGT	80 - 98	< 5.7 %	120 - 139
preT2D	99 - 124	5.7 – 6.3%	140 - 159
T2D	≥ 125	≥ 6.4%	160 - 200

Another key parameter of T2D risk/management is HbA1c percentage. HbA1c is a form of hemoglobin that is chemically linked to sugar via glycosylation.[163] In the bloodstream, monosaccharides like glucose spontaneously bind to hemoglobin. In the event of chronically high blood glucose levels, the relative abundance of glycosylated hemoglobin becomes higher; therefore, HbA1c is a long-term correlate of hyperglycemia (see cut-off values in Table 1.1). HbA1c results are often considered in combination with FBG levels to determine a person's risk of T2D development in addition to monitoring the severity of T2D in a diagnosed individual. HbA1c collection presents many advantages over FBG measurements, such as no fasting requirement, being more closely linked to chronic complications like cardiovascular disease, is more efficient at capturing chronic hyperglycemia, and has improved bench-top stability compared to plasma glucose.[165] Conversely, HbA1c results can also be skewed by certain factors and have raised concerns on how well this measure indicates T2D risk/progression. Conditions that enhance red blood cell turnover, as observed in sickle cell, hemodialysis, and second-third trimester pregnancy can result in a false negative for T2D or high T2D risk.[153] Furthermore, HbA1c does not capture transient and intermittent hyperglycemia, which refers to blood glucose variations that occurs in

human preT2D and T2D.[166] An individual who is early in preT2D development may have an HbA1c reading that is in the upper limit of the NGT range, so elevated T2D risk might not be captured.[153] In this event, FBG levels and an OGTT are more representative of T2D risk.

In the circumstance where an OGTT is necessary, as in T2D risk/severity assessment, a 60g oral glucose load is administered after a time zero reading (FBG), then blood glucose is measured every 30-minutes for 2 hours.[151] While each interval reading can be indicative of T2D risk/severity, the 2-hour timepoint reading is often used as the clinical determinant. Similar to FBG, OGTT readings can be skewed by the stress response, thus providing potentially false positive results. An important consideration for administering an OGTT include the risk to those who have already developed T2D, particularly if there is poor glycemic control as an OGTT can lead to hyperglycemic crisis.[151,152] This critical point is typically why HbA1c and FBG are sufficient criteria for a T2D diagnosis. If HbA1c and FBG provide disparate results, the test that produced the higher reading is typically repeated.[152]

In summary, T2D risk and development arises from a combination of lifestyle, genetic, and/or social determinants. Distinguishing features of NGT, preT2D, and T2D are FBG concentrations and HbA1c percentage, with OGTT levels used as complementary data primarily for assessing T2D risk. Early detection of diabetes risk is currently the most effective strategy for T2D prevention as preT2D is a reversible condition if a proper intervention plan is implemented; however, this should not be mistaken as a simple task. The multifactorial nature of T2D development and the complex mechanisms involved in the pathophysiology of obesity/T2D generate numerous challenges in designing effective prevention strategies. Most prevention strategies include lifestyle modifications such as exercise and reducing carbohydrate and fat intake, particularly SFAs.[167] If a person with preT2D presents with a serious obesity-associated comorbidity such as cardiovascular disease, glycemic control drugs are typically prescribed to help limit both T2D development and worsening of the comorbidity.[151] Together, these prevention strategies are often successful, particularly if lifestyle modifications are

sustained;[154] however, social determinants of T2D risk/development complicate sustainability of lifestyle modifications. Further, lifestyle changes have a greater success rate of T2D prevention the earlier they are implemented in preT2D development, which is a rather enigmatic time point to identify. Thus, critical gaps remain in our understanding of mechanisms that fuel T2D progression that could reveal more suitable targets for clinical prevention/delay strategies.

1.4 The role of metabolic reprogramming in T cell fate and function

The fate of immune cell differentiation is, in part, reliant on metabolic programs initiated upon activation, a phenomenon termed metabolic reprogramming.[168] In essence, metabolic reprogramming elicits the appropriate balance between catabolic and anabolic processes to properly meet the high bioenergetic and biosynthetic demands of the activated immune cell. Products of catabolism can be used for anabolic processes by which certain metabolites can serve as precursors for biosynthesis of nucleotides and proteins. In the absence of activating stimuli (i.e., rest or quiescence), immune cells predominantly favor catabolism over anabolism to generate enough adenosine triphosphate (ATP) to meet basal energy requirements. Upon activation, immune cells will upregulate both catabolism and anabolism to meet the demands of rapid proliferation. Metabolic reprogramming in the activated state enhances uptake of nutrients that will provide precursors and metabolites for a variety of essential cell signaling functions such as replenishing carbon loss from amplified biosynthesis (i.e., TCA cycle anaplerosis), supporting production of reducing equivalents for the ETC, stimulating nucleotide/amino acid biosynthesis and glutathione (GSH) reduction to combat oxidative stress via the pentose phosphate pathway (PPP). Metabolic reprogramming presents similarities amongst immune cell subsets; however, key differences help guide the differentiation of distinct subsets. In addition, the nutrient surplus in circulation and within insulin-responsive tissues during obesity and T2D likely alter metabolic reprogramming to favor certain transcriptional programs in T-cell differentiation and function. As the experimental design outlined in this dissertation largely focuses on total $CD4^+$ T cells and $CD4^+$ T_{eff} cells, the following

background on metabolic reprogramming will focus exclusively on these specific cell types.

1.4.1 Regulation of metabolism during quiescence

At rest, adenosine monophosphate kinase (AMPK) acts as the master regulator of quiescence. AMPK is a heterotrimeric complex made up of α, β, and γ subunits that can translocate between the cytoplasm and nucleus. AMPK functions to conserve ATP stores through catabolic pathways for cell survival maintenance. AMPK is activated under resting conditions by elevated levels of adenosine monophosphate (AMP) relative to ATP by an allosteric mechanism in which AMP binds to the γ-subunit, enabling AMPK to respond to AMP-ATP fluctuations.[169] Binding of AMP to AMPK induces stimulatory phosphorylation in the α-subunit by several upstream kinases (e.g., tumor suppressor kinase LBK1 and Ca^{2+}-sensitive kinase CAMKK2)[170], allowing AMPK to primarily limit anabolic pathways as these are major consumers of ATP. AMPK reduces lipid and sterol synthesis via inactivation of Acetyl-CoA carboxylases (e.g., ACC1 and ACC2) and HMG-CoA reductase,[171,172] in addition to blocking hexosamine biosynthesis by phosphorylating glucose-fructose amidotransferase 1 (GFAT1), the enzyme that converts glucose-derived fructose-6-phosphate (F-6P) to glucosamine-6P.[173] Inhibition of the hexosamine biosynthesis pathway is a key mechanism by which AMPK restricts anabolic processes because hexosamine biosynthesis provides UDP-GlcNAc, a substrate required for protein glycosylation through O-GlcNAcylation (a reversible post-translational modification) and N-linked glycosylation,[174,175] thereby supporting immunity pathways that are upregulated during cellular activation and consume considerable amounts of ATP.[176] Examples of key transcription factors targeted by O-GlcNAcylation in immune cells are nuclear factor kappa B (NF-κB), nuclear factor of activated T-cells (NFAT), and c-Myc to activate cytokine production, support proliferation, and enhance catabolism.[174]

Another critical mechanism by which AMPK inhibits anabolic processes is through inhibition of the multi-protein complex mammalian target of rapamycin

complex I (mTORC1), a master regulator of cellular growth and proliferation, consisting of the serine/threonine kinase mTOR, the adapter protein regulatory-associated protein (RAPTOR) that positively regulates mTORC1 activation, and the proline-rich substrate of Akt of 40 kDa (PRAS40).[177-179] Several components of mTORC1 are shared with mTORC2, such as mammalian lethal with Sec13 protein 8 (mLST8), which enables mTOR's serine/threonine kinase activity, and deptor (the negative regulator of mLST8). The absence of RAPTOR and presence of rictor is a key distinction of mTORC2 from mTORC1, which renders mTORC2 insensitive to rapamycin inhibition. AMPK inhibits mTORC1 activity by activating a component of the tuberin complex,[180] TSC2, a negative regulator of mTORC1 by inhibition of RAPTOR. By these distinct mechanisms, AMPK ensures that growth signaling pathways and protein synthesis are restricted to conserve energy stores.

During quiescence, immune cells still need to take up and metabolize nutrients to survive but will do so at a low, optimal rate as bioenergetic demands are much lower in a non-proliferative state. AMPK replenishes ATP primarily through stimulating low-grade glucose uptake/metabolism and oxidation of FAs.[171] AMPK stimulates expression of glucose transporters on the plasma membrane to promote glucose uptake for subsequent breakdown to pyruvate. T cells express several glucose transporters (GLUT1, 3, 6, and 8), but these do not exhibit redundant functions as GLUT1 was found to be indispensable for $CD4^+$ T cell proliferation and viability.[181,182] AMPK primarily stimulates glucose uptake by inhibitory phosphorylation of thioredoxin interacting protein (TXNIP), a protein that directly suppresses glucose uptake by recycling GLUT1 from the plasma membrane.[183] During quiescence, the glycolytic end-product pyruvate will predominantly be oxidized into acetyl-CoA[184] and shunted into the TCA cycle to maintain generation of the reducing equivalents NADH and $FADH_2$ for the ETC and oxidative phosphorylation (OXPHOS). Further, AMPK supports FAO by decreasing the pool of malonyl-CoA through inhibition of ACC1, an enzyme that catalyzes the rate-limiting step of FA synthesis (FAS) by converting acetyl-CoA to malonyl-CoA.[185] Malonyl-CoA acts as a negative regulator of the trimeric outer mitochondrial membrane (OMM) enzyme Cpt1a, which carries out the first and

rate-limiting step of FAO by converting FA-derived acyl-CoA into acylcarnitine, a form of FAs that can be transported across the inner mitochondrial membrane (IMM). By decreasing malonyl-CoA production, Cpt1a activity is enhanced, thereby increasing the rate of FA import into the mitochondria for subsequent breakdown by β-oxidation.

While AMPK limits several anabolic pathways to conserve ATP and achieves basal energy requirements through OXPHOS, T-cell viability is also critically maintained by tonic T-cell receptor (TCR) and/or survival signals from the local microenvironment. An important survival signal for quiescent T cells is IL-7. A primary source of IL-7 comes from stromal cells in the thymus[186] and bone marrow[187] during lymphocyte development but is also produced by a variety of epithelial and endothelial cells in secondary lymphoid organs, skin, liver, and lung.[188-193] Additionally, these cell types produce a circulating form of IL-7 that supports peripheral T-cell survival.[194-196] IL-7 promotes T-cell survival by binding to IL-7Rα, inducing STAT3 dimerization and subsequent translocation to the nucleus. STAT3-mediated translation of the class O of forkhead box (FOXO) family of transcription factors serves to limit proliferation and maintain cell survival by further sustaining IL-7 and IL-7Rα expression. Quiescent naïve T cells in lymphoid tissue receive tonic TCR signals through transient interactions with self-peripheral major histocompatibility complex (MHC) II complexes, providing weak TCR interactions to moderately induce phosphorylation of immunoreceptor tyrosine-based activation motifs (ITAMs).[197] On the other hand, circulating naïve and memory T cells do not receive tonic TCR signals.[198] Instead, sphingosine-1-phosphate (S1P) derived from RBCs[199] or endothelial cells[200] binds to the S1P receptor, S1PR1, which is expressed on T cells and will support STAT3 activity.[201] Further, S1P-S1PR1 engagement supports OXPHOS in quiescent T cells by inhibition of the mitophagy protein PINK1 to restrict mitophagy and promote mitochondrial biogenesis[202] (summary outlined in Figure 1.1).

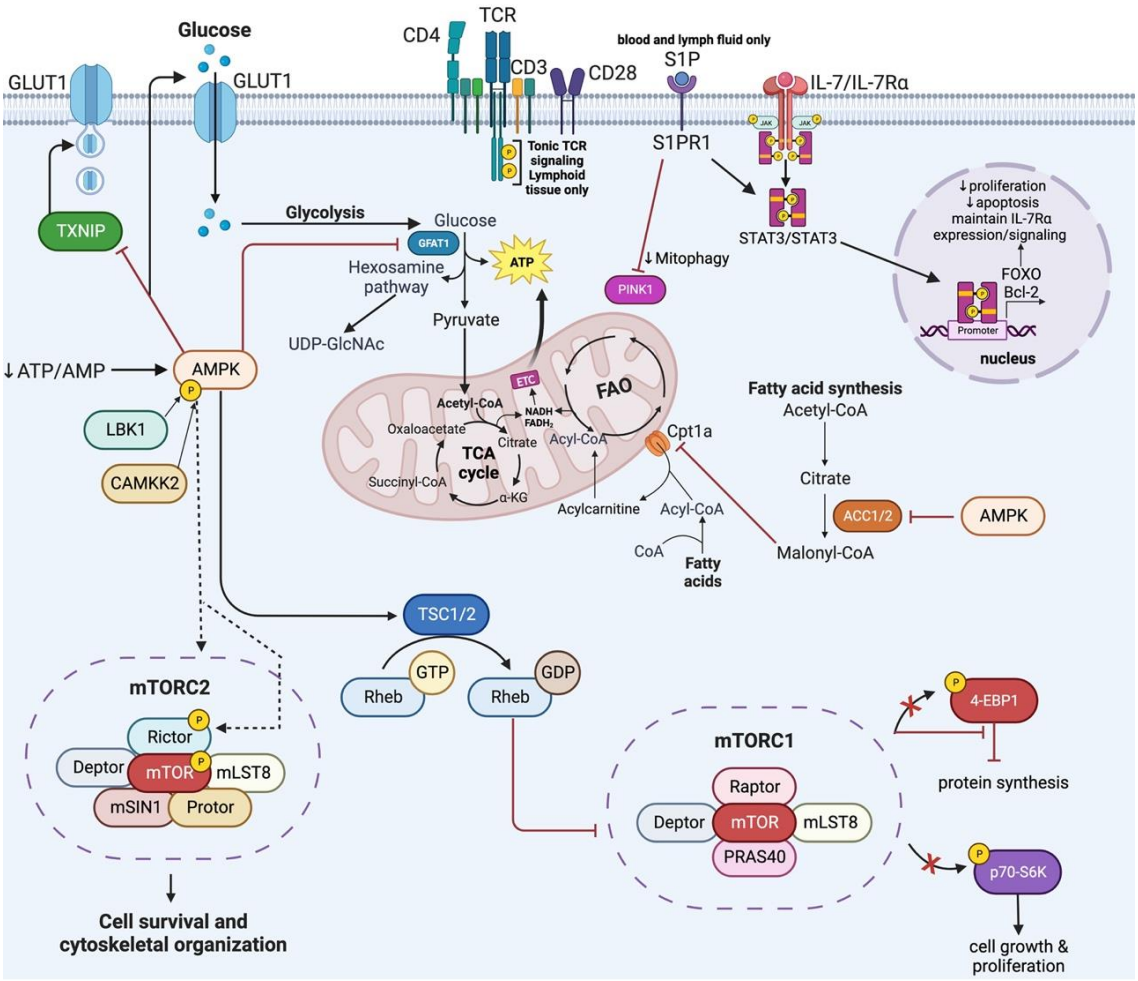

Figure 1.1 Schematic diagram of T-cell quiescence
Summary of AMPK activation-mediated regulation of T cell quiescence by inhibition of anabolic pathways (hexosamine biosynthesis, fatty acid synthesis, protein synthesis, and cellular growth/proliferation) and maintenance of low-level catabolism by sustaining GLUT1 expression to promote glucose uptake and glycolysis (supported by low level mTORC2 activation) and fatty acid oxidation by downregulating acetyl-CoA carboxylase 1 and 2 (ACC1/2). Tonic T cell receptor (TCR) signals (lymphoid tissue only), sphingosine 1 phosphate (S1P) engagement with the S1P receptor (S1PR1) (blood and lymph fluid only), and IL-7/IL-7R signal transduction of JAK/STAT pathways aids in maintaining cell survival, limiting proliferation, and preserving mitochondrial function by downregulating mitophagy.

1.4.2 Metabolic reprogramming during activation and differentiation

Contrary to quiescence, immune cell activation necessitates rapid cellular growth and proliferation. Naïve $CD4^+$ T-cell activation requires interaction with APCs to recognize cognate antigen loaded on MHC-II, also known as human leukocyte antigen II (HLA-II) when referring to humans. Antigen recognition results in TCR engagement/cross-linking and activation of the TCR signaling molecule CD3. TCR engagement is the first step of naïve T-cell activation but remains incomplete without co-stimulatory molecule interactions. The T cell and APC interaction forms the immunological synapse, which allows binding of co-stimulatory partners and recruitment of critical signaling molecules to the TCR that are necessary for T-cell activation. T cells and APCs express a variety of co-stimulatory molecules and their respective ligands, a common example including T cell-expressed CD28 binding to the B7 family ligands B7-1 and B7-2 on APCs.[181,203] Propagation of TCR and CD28 proximal signals initiate nutrient uptake and biosynthetic pathways, and enhancement of catabolic processes.[181,204,205]

Costimulatory interactions sequester the catalytic subunit of phosphoinositide-3 kinase (PI3K), p110δ, to the immune synapse and will subsequently activate protein kinase B (Akt). Akt ultimately functions to promote cell survival and glycolysis by upregulating anti-apoptotic transcription factors like the Bcl-2 family and enhancing glucose transporter expression, respectively.[206,207] Additionally, PI3K and AKT activate mTORC1 by inhibition of the tuberin complex (TSC1, TSC2, and TBC1D7),[208] which acts primarily through TSC2's functions as a GTPase-activating protein that inhibits the Ras family GTPase Rheb (a positive regulator of mTORC1).[209] Furthermore, early studies on metabolic reprogramming in $CD4^+$ T cells have shown that the PI3K-Akt-mTORC1 pathway is indispensable for differentiation and survival of $CD4^+$ T_{eff} and T_{reg} cells.[210-212] Together, these data highlight the integral role of TCR-costimulatory signals in rewiring metabolism upon activation and supporting subset differentiation.

While PI3K-Akt orchestrate mTORC1 and mTORC2 activation, amino acids, particularly leucine, glutamine, and arginine also tightly regulate mTORC1

activity; whereas, amino acid uptake is dispensable for mTORC2 activation.[213] In fact, absence of leucine or glutamine results in diminished mTORC1 activation,[214] revealing a critical role of amino acid uptake in metabolic reprogramming. Like glucose, leucine and glutamine uptake/metabolism support mTOR functions. [215,216] Specifically, leucine and glutamine support upregulation of protein synthesis by mTORC1-mediated phosphorylation of 4-EBP1 and association of mTORC1 to the autophagosome to restrict autophagy, respectively, to promote overall T cell function and survival.[216] Additionally, there's a positive feedback loop between mTORC1 activation and glutamine metabolism as mTORC1 enhances glutaminolysis through activation of glutamate dehydrogenase (GDH), the enzyme that converts glutamate to alpha-ketoglutarate (α-KG).[217] Glutamine can also further stimulate uptake/metabolism of other key fuel sources as demonstrated most notably by impaired glucose uptake/metabolism in $CD4^+$ T cells when the glutamine transporter (Slc1a5) is genetically knocked-down,[205] thus glutamine uptake/metabolism bridges glycolytic and oxidative metabolism.

Metabolites generated from glycolysis and glutaminolysis serve as precursors for amino acid, nucleotide, and lipid biosynthesis,[184,218] and display coordinated functions to support post-translational modifications of key proteins in T-cell activation. For example, glucose conversion to F-6P and the donation of an amine group from glutamine during glutamate conversion supports the hexosamine biosynthesis pathway to generate UDP-GlcNAc. O-GlcNAcylation of intracellular proteins/transcription factors and N-glycosylation of cell surface receptors and cluster of differentiation (CD) molecules (e.g., TCR, CD25, CD69, etc.) requires UDP-GlcNAc, and modulates T-cell activation, lineage, and effector functions.[174,218,219] Aside from supporting mTORC1 activity, glutaminolysis provides a bioenergetic advantage to rapidly proliferating cells. The dominant carbon flux into the TCA cycle switches from glucose to glutaminolysis upon activation as glutaminolysis is a rapid process, and is thus more efficient at replenishing carbon loss than glycolysis and subsequent pyruvate oxidation.[220] Moreover, glutamine-derived metabolites support early naïve T-cell activation. Nonvesicular release of glutamate in the immunological synapse, particularly from

macrophages and dendritic cells, enhances T-cell activation and protects activated T cells from apoptosis by supporting redox balance.[221-223]

1.4.3 Th1 lineage

Upon activation, naïve $CD4^+$ T cells can differentiate into a variety of subsets depending on the differentiation signals and growth factors provided by the local microenvironment. Differentiation programs are primarily initiated by signals transmitted to the cell by fate-specifying cytokines that are produced by surrounding immune cells and non-hematopoietic cells (e.g., stromal cells, endothelial/epithelial cells, etc). Naïve $CD4^+$ T cells differentiate into Th1 cells predominantly by IL-12 produced by APCs and can also be influenced by IFN-γ production from $CD8^+$ T cells and natural killer (NK) cells. IL-12 induces JAK2-STAT4 signal transduction, promoting STAT4 dimerization with STAT1 and translocation to the nucleus where it binds to the promoter region of *Tbx21*- the gene that transcribes the Th1-specific transcription factor T-bet. Together, IL-12 and T-bet signals stimulate production of characteristic Th1 cytokines: IFN-γ, TNF-α, IL-12, lymphotoxin-α (Ltα or TNF-β), and granulocyte-macrophage colony-stimulating factor (GM-CSF)[224]. Production of these cytokines allows Th1 cells to function in cell-mediated immunity against intracellular bacteria and viruses by promoting cytotoxic functions of $CD8^+$ T cells and NK cells, enhancing phagocytic activity of macrophages and dendritic cells, and inducing B cell class-switching to IgG2a for pathogen opsonization.

In the context of sterile inflammation, as in chronic inflammatory disease, Th1 cells play an instrumental role in maintaining a pro-inflammatory cascade, predominantly through TNF-α production. TNF-α is capable of shutting down important anti-inflammatory mechanisms by activating the UPR pathway, inducing serine phosphorylation of RTKs, and suppressing Foxp3 expression in T_{regs}.[114,115] Th1 cells further boost pro-inflammatory functions by maintaining $CD8^+$ T cell and NK cell-mediated cytotoxicity and M1-macrophage polarization, a significant source of TNF-α production. M1 macrophages are also the dominant source of IL-

1β, which induces local tissue damage, activates caspase-mediated cell death, and exacerbates inflammation through TNF-α.[225]

Th1 differentiation is positively regulated by IL-12 and IFN-γ,[44,226] and negatively regulated by suppressor of cytokine signaling (SOCS) protein 3. SOCS3 inhibits Th1 differentiation by preventing IL-12-induced STAT4 activation. Th1 differentiation is thought to partially rely on mTORC1 activity,[227] independent of PI3K,[228] as SOCS3 function is blocked by mTORC1 via an undefined mechanism. Activation of mTORC1 supports glycolysis and glutaminolysis and is one reason these pathways are reportedly required for Th1 differentiation and effector function.[182,229,230] Th1 cells cultured in the absence of glutamine take on T_{reg}-like properties such as Foxp3 expression,[229] demonstrating the impact of different fuel sources/metabolic pathways in not only T cell lineage commitment but also in T-cell plasticity.

1.4.4 Th2 lineage

Type 2 immune responses are primarily associated with promoting humoral immunity against extracellular parasitic infections but are also instrumental in the pathogenesis of certain chronic inflammatory conditions like allergic asthma and atopic dermatitis.[177] Th2 cells are critical mediators of type 2 immunity by inducing B cell class-switching to IgE, eosinophil and mast cell activation by IL-5 production, and M2-macrophage polarization by IL-4 and IL-13 actions.[231] Th2 differentiation is mainly driven by IL-4;[28,232] however, APC-produced IL-6 has been demonstrated to provide initial support of Th2 differentiation by promoting IL-4 production in naïve $CD4^+$ T cells[233] but, in turn, elicits dual effects by also limiting Th2 responses to prevent allergic pathogenesis, hence the role of IL-6 in Th2 commitment is context-dependent.

Signal transduction by IL-4 in naïve $CD4^+$ T cells stimulates JAK1/STAT6 signaling and subsequent STAT6/STAT5 translocation to the nucleus. STAT6/STAT5 induces GATA-3 activation, the Th2-defining transcription factor that stimulates IL-4, IL-5, and IL-13 production[234]. APC-produced IL-33 binding to membrane-bound ST2 (IL-1RL1)[231] also stimulates GATA-3 expression through

p38 activation and can additionally upregulate Foxp3 expression in T_{regs} or in Th2 cells to elicit T_{reg}-like properties such as IL-10 production. IL-4 also activates PPAR-γ in Th2 cells, which promotes lipid metabolism, cytokine production, and ST2 expression.[232] In addition to JAK/STAT signaling, IL-4 also induces PI3K-Akt activation and downstream mTORC2.[231] Inhibition of Th2 differentiation is coordinated by SOCS5, which is inhibited by mTORC2. Additionally, mTORC2 coordinates RhoA functions in cytoskeletal rearrangement[235] during cell growth, of which Th2 cells are sensitive to relative to other effector subsets, thus Th2 cells are considered to rely more on mTORC2 activity during differentiation.

The importance of mTORC2 in Th2 fate doesn't necessarily mean that mTORC1 is dispensable for Th2 differentiation and/or function. Like in Th1 cells, knockdown of mTORC1 fails to induce Th2 differentiation.[234] Moreover, both mTORC1 and mTORC2 support Th2 cytokine production by stimulating aerobic glycolysis and promoting FAO by PPAR-γ activation; therefore, glycolysis and FAO support Th2 fate and effector functions. Given the key role of both mTOR complexes in Th2 differentiation and cytokine production, it is more likely that fine-tuning of different magnitudes of mTORC1 and mTORC2 activation dictate T cell fate/function rather than one complex solely dominating fate decisions. This idea was proposed by Hongbo Chi and colleagues as the "Goldilocks hypothesis" on mTOR involvement in metabolic reprogramming of T cells.[236]

1.4.5 Th17 lineage

Th17 cells are a more recently identified $CD4^+$ subset relative to Th1 and Th2 cells, of which were formally discovered in 1986.[231] Despite its later reveal, the role of Th17 cells in health and disease has been extensively characterized since its debut nearly 20 years ago.[237,238] Known for their protective role in mucosal immunity, Th17 cells can also elicit robust pathogenic responses in chronic inflammatory disease as demonstrated by a strong Th17 component in many autoimmune diseases.[239,240] Th17 commitment is facilitated by APC-produced IL-6 and TGF-β activation of JAK2/STAT3 signal transduction, subsequently releasing activated STAT3 to undergo homodimerization and translocation to the

nucleus. STAT3 dimers promote expression of ROR-γt, the Th17-defining transcription factor. Activation of ROR-γt induces production of characteristic Th17 cytokines like IL-17A, IL-17F, IL-21, and IL-22 [237,238]. APC-produced IL-23 further promotes Th17 commitment through its actions on STAT3 activation.[238]

Th17 cells are generally subcategorized as protective or pathogenic. Pathogenic Th17 responses are supported by APC-produced IL-23 and IL-1β[162,237]. Like Th1 cells, differentiation of Th17 cells is negatively regulated by SOCS3, supporting the theory that Th17 cells also rely more on mTORC1 activity for differentiation. In addition, the catalytic subunit of PI3K was required for Th17 differentiation along with concordance of glutaminolysis and mTORC1 activation as demonstrated by ameliorated proinflammatory T cell cytokine responses (Th1 and Th17) by knockdown of the glutamine transporter Scl1a5; however, it is important to consider that Slc1a5 deficiency was not modeled specifically in T cells.[205] Moreover, glutamine is required for T cell survival/expansion[203] regardless of phenotype, excluding T_{regs}, which appear to survive and even thrive in glutamine deprivation conditions.[229] Therefore, reduced cytokine responses previously reported could be due to functional impairments induced by glutamine deprivation.

Another mechanism by which glutamine metabolism has been proposed to support Th17 differentiation is by the transcription factor inducible cAMP early repressor (ICER) as demonstrated by reduced OXPHOS, GLS-1 expression, and Th17 differentiation in ICER-deficient murine T cells cultured in the presence of glutamine.[125] The ICER transcription factor was found to directly bind to the GLS-1 promoter and enhance its activity, thereby establishing another mechanism by which GLS-1 activity promotes Th17 differentiation. Collectively, these data reveal glutamine metabolism as a potential target for mitigating Th17-induced inflammation.

1.5 Hypothesis

The monocyte and macrophage contribution to meta-inflammation has been extensively characterized in a disproportionate number of murine models of DIO and AT inflammation relative to the work done in human T2D AT and

peripheral inflammation. Work from our lab and others has characterized peripheral $CD4^+$ T cells as critical mediators of T2D-associated meta-inflammation. Our goal is to unify disparate claims in the literature and determine the relative contribution of myeloid cells and T cells to meta-inflammation across the spectrum of obesity. As part of our efforts to identify a point of intervention for T2D delay/prevention, we further aim to characterize the peripheral inflammatory signature in preT2D and elucidate how changes in inflammation, if any, link preT2D to T2D immunopathogenesis. We hypothesize that $CD4^+$ T cells are a significant source of T2D-associated inflammation and are at least as important as myeloid cells in the overall contribution to meta-inflammation across the spectrum of obesity. Moreover, we hypothesize that nutrient milieu fluctuations during obesity impact progression of inflammation during T2D pathogenesis by shifting fuel utilization in T cells to support characteristic cytokine profiles.

CHAPTER 2. MATERIALS AND METHODS

2.1 Description of human donors

The University of Kentucky Institutional Review Board approved this cross-sectional study in accordance with the Declaration of Helsinki. Donors were recruited from the community by the University of Kentucky Center for Clinical and Translational Sciences from Fall 2018 to Spring 2023. Descriptions of donor cohorts are described in subsequent chapters. Percentage HbA1c, FBG levels, and/or 2-hr OGTT were used, as per the American Association of Diabetes guidelines[163], to classify preT2D and T2D donors and is listed for NGT donors who had this information available. Exclusion criteria are as previously published[241] and included inflammatory/autoimmune diseases (polycystic ovarian syndrome, type 1 diabetes, rheumatoid arthritis, etc.), medical history of cancer < 5 years past, chronic kidney disease as determined by an estimated glomerular filtration rate < 45, liver disease, and use of antihistamines or non-steroidal anti-inflammatory drugs (NSAIDs) < 72hr prior to blood collection. Individuals with T2D did not use > 100 U/d of insulin. People with obesity/T2D often present with other comorbidities such as declines in cardiovascular health; therefore, excluding these donors would likely limit recruitment. Thus, people with stable coronary disease and/or taking statins, ≤ 81 mg/d of aspirin, angiotensin-converting enzyme (ACE) inhibitors, and/or taking glycemic control drugs such as metformin were included as these are commonly prescribed for T2D management.

2.2 PBMC isolation and archiving

Aeseptic technique was used for all blood processing and cell culture experiments under BSL-2 safety conditions. Recruited donors fasted overnight and provided 100-200mL of blood collected by venous puncture into acid/citrate/dextrose-containing tubes (10mL each). Two tubes of blood (from the same donor only) were combined into one 50mL conical tube containing 15mL 1X Dulbecco's phosphate-buffered saline (DPBS) (Corning, Corning, NY). Each

conical tube of diluted blood was slowly applied by a gravity setting along the side of a 50mL SepMate conical tube (STEM Cell Technologies, Vancouver, Canada) containing 15mL Ficol-Paque Premium Centrifugation Media (Cytiva, Marlborough, MA). The 15mL volume of Ficol is a critical volume to adhere to as it goes slightly above the separation chamber and will allow for proper separation of blood layers. All centrifugation steps were performed using a Thermo Sorvall Legend XTR refrigerated centrifuge (Thermo Fisher Scientific, Waltham, MA) with a TX-750 rotor and set to room temp. SepMate tubes were centrifuged for 20-min at 2,500rpm with the deceleration/brake set to 3 to prevent perturbation of blood layers. After centrifugation, RBCs and granulocytes were separated under the tube's separation layer with the Ficol media, while PBMCS and plasma were above the separation layer. The top layer was quickly poured into a new 50mL conical tube, then split into two tubes and the volume was brought up to 50mL with 1X buffer 1 warmed to room-temperature. A 1X buffer 1 stock is made by diluting from a 10X buffer 1 stock: 1.0L 10X DPBS (Corning), 20mM EDTA (Gibco), and 10g/L bovine serum albumin (Millipore Sigma) in 1X DBPS.

Conical tubes were centrifuged at 1,200rpm for 10-min (herein, 'standard setting'). Supernatants were discarded and cell pellets (PBMCs) were combined into one 50mL conical tube by resuspending one pellet in 1X buffer 1 and transferring to each pellet until all were combined into one tube before pelleting. The PBMC pellet was resuspended in 1-4mL of 1X RBC lysis buffer, which was diluted from the 10X manufacturer's stock (BioLegend) in sterile cell culture-grade water (Cytiva). The resuspended pellet was incubated with 1X RBC lysis buffer at room temperature for 1-5 minutes. The volume of RBC lysis buffer and time of incubation was dependent on the number of RBCs present in the pellet, which was estimated visually by the intensity of red color in the pellet. Although RBCs were separated underneath the SepMate tube's separation layer with the Ficol gradient, some RBCs remain or leak back through the separation layer when the top layer was poured into fresh conical tubes. After RBC lysis incubation, the lysis reaction was stopped by adding 1X buffer 1 up to 50mL and cells were pelleted. Cells were resuspended in 1X buffer 1 up to 50mL then counted by adding 10μL of cell

suspension to 90μL of trypan blue, then dispensed into a hemocytometer chamber. Cells were visualized in the hemocytometer with a light microscope. Cells were counted manually using a hand counter, counting all cells in each of the four quadrants (Q), using the following equation to determine total cell volume:

$$Q1 + Q2 + Q3 + Q4 \div 4 = Avg \times 10x^4 \; x \; dilution \; factor \times total \; vol$$

After cell volume was determined, cells were pelleted then resuspended in freezing medium (fetal bovine serum [FBS]) containing 1% dimethylsulfoxide (DMSO) (Millipore Sigma) in a volume that achieves a density of 10^7 cells/mL. One-mL of cell suspension was aliquoted into cryovials, which were then placed in a Mr. Frostie (Nalgene, Rochester, NY) containing 250mL of 99% isopropyl alcohol and placed overnight in the -80°C freezer to achieve a cooling rate of 1°C/min. The next day, frozen PBMCs were transferred to a cryotank supplied with liquid nitrogen (LN2) as needed and stored there until ready for use.

2.3 Total $CD4^+$ T cell and T_{eff} cell isolation

Total $CD4^+$ T cells and T_{eff} cells were either purified from fresh or archived PBMCs. Archived total $CD4^+$ T cells used for extracellular flux analysis were always isolated from fresh PBMCs. Cells isolated from fresh PBMCs were purified by magnetic bead separation using a negative selection kit for total $CD4^+$ T cells including antibodies against non-$CD4^+$ T cells using the following markers: CD8, CD14, CD15, CD16, CD19, CD36, CD56, CD123, TCR γ/δ, and CD235a). T_{eff} cells ($CD25^-$) were further purified from the $CD4^+$ T cell population (Miltenyi Biotec, Gaithersburg, MD) then archived as described in section 2.2 at a density of 5 x 10^6 cells/mL. Cells that were isolated from archived PBMCs were resuspended in Zombie Aqua viability dye (BioLegend) at a 1:100 dilution in 1X DPBS (Corning) for 30 minutes at 4°C. For total $CD4^+$ T cells, cells were labeled with anti-human CD4-FITC (BioLegend, Clone OKT4, 1:100 in 1X buffer 1). For T_{eff} cells, a combination of anti-human CD4-FITC and anti-human CD25-APC (BioLegend, Clone M-A251) were added at a 1:100 dilution in 1X buffer 1. For both cell types,

cells were incubated with surface marker antibodies for 30 minutes at 4°C. Cells were purified by fluorescence-activated cell sorting (FACS) with a Sony sy3200 Cell Sorter on $CD4^{hi}$ or $CD4^{hi}CD25^{-}$ fluorescence intensity (FI) for total $CD4^{+}$ and T_{eff} cells, respectively. Sorted cells were used immediately as they cannot withstand re-freezing.

2.4 Cell thawing, culture conditions, and cytokine measurements

For all experiments involving cell culture, archived cells were taken out of LN_2 storage and transported on dry ice. Cells were thawed quickly in a 37°C water bath with agitation, then transferred to 10-15mL conical tubes containing Roswell Park Memorial Institute 1640 (RPMI-1640) (Gibco) cell culture medium. RPMI-1640 contained 11mM D-glucose, 25mM N-2-hydroxyethylpiperaine-N'-2-ethanesulfonic acid (HEPES) and 4mM L-glutamine. RPMI-1640 was also supplemented with 10% heat-inactivated fetal bovine serum (FBS) (Gibco), 1% Na-pyruvate (Gibco), and 1% penicillin-streptomycin (Gibco). To calculate total cell volume, all cell culture experiments followed the counting procedure described in section 2.2 with dilution factor and total volume adjusted. After counting, cells were pelleted (1,200rpm for 10-min using a Thermo Sorvall Legend XTR refrigerated centrifuge with a TX-750 rotor and set to room temp) and resuspended in RPMI-1640 at a volume that achieved a cell density of 10^6 cells/mL. All cell culture incubations took place at 37°C with 5% CO_2. Additions/alterations to this procedure are outlined as they apply in subsequent chapters. Cytokines were quantified using a 25-plex human Th17 magnetic bead kit (EMD Millipore), and a Bio-Rad FLEXMAP 3D with Luminex xPONENT v4.2 and data was analyzed Bio-plex Manager software (Bio-Rad) v6.1. Cytokines that commonly exceed the upper limit of quantification (ULOQ) when cells are stimulated were measured separately with

a 6-plex Th17 magnetic bead kit (EMD Millipore) with supernatants diluted 1:10 (PBMCs) or 1:50 (purified T cells).

2.5 Flow cytometry

In experiments that measured intracellular cytokines, stimulated cells were cultured with 1000X Brefeldin A at a 1X concentration (eBioscience, San Diego, CA) added in the last 5 hours of stimulation. Cells were collected (detachment of adherent cells described in chapter 3, section 3.2.3) and transferred to a 96-well V-bottom plate (ThermoFisher Scientific). Cells stimulated with CD3/CD28 dynabeads (Gibco) had beads removed by magnetic separation prior to transfer. Cells in all flow cytometry experiments were resuspended in Zombie NIR viability stain (BioLegend, San Diego, CA) at a 1:250 dilution in 1X DPBS at 4°C, in the dark, for 30 minutes (or at room temp, in the dark, for 15 minutes for mitotracker red staining, described in chapter 4). Cells were washed, pelleted at 1,200rpm for 10-min using a Thermo Sorvall Legend XTR refrigerated centrifuge with a TX-750 rotor and set to 4°C, and resuspended with a master mix of antibodies against target surface markers (described in subsequent chapters) in 1X buffer 1. Surface marker antibody incubation was at 4°C, in the dark, for 30 minutes followed by a repeated wash and pellet step with the centrifuge temperature set to 4°C to sustain cell viability hereafter. If intracellular staining was performed, cells were resuspended in fixation buffer (Invitrogen, Waltham, MA) and incubated at room temperature, in the dark, for 30 minutes. If intracellular staining was not performed, cells were washed and pelleted again, then fixed by resuspending in 1% paraformaldehyde (PFA) (Santa Cruz Biotechnology, Santa Cruz, CA) in 1X DPBS and stored at 4°C for no longer than 24hr if cells were not immediately analyzed by the flow cytometer.

If a fixation buffer step was performed, cells were washed in 1X permeabilization buffer (Invitrogen) after incubation and pelleted. A wash with permeabilization buffer and centrifugation were repeated to maximize cell permeability. Cells were resuspended in a master mix of antibodies against

intracellular targets (described in subsequent chapters) in 1X permeabilization buffer for 30 minutes, in the dark, at 4°C before pelleting and resuspending in 1% PFA. Cells were either analyzed immediately by flow cytometry or analyzed within 24hr of staining (stored in the dark at 4°C). UltraComp eBeads (Invitrogen) were singly stained with all antibodies within individual experimental design panels, except viability stain which requires cells, to perform compensation. For all flow cytometry experiments that used PBMCs, fluorescence minus one (FMO) controls were used to validate gating of different immune cell subsets since PBMCs are a dense heterogeneous population. Flow cytometric analyses were performed on a Beckman Coulter CytoFLEX using the CytExpert software. Data were analyzed using FlowJo v11.

2.6 Extracellular flux analysis

The protocol used in this work for performing an extracellular flux analysis in whole live cells using a mitochondrial stress test was as previously described.[46,242] Total $CD4^+$ T cells that were isolated from fresh PBMCs and were archived $\leq$ 6 months were stimulated with CD3/CD28 dynabeads for 40h (additional manipulations described in subsequent chapters as they apply). After incubation, cells were counted as described in section 2.2, adjusting for total volume (volume remaining in cell culture well post-incubation). Cells were pelleted at 1,200 rpm for 10-min using a Thermo Sorvall Legend XTR refrigerated centrifuge with a TX-750 rotor and set to room temp. Supernatants were harvested for 25-plex and 6-plex cytokine assays. Cells were resuspended in the appropriate volume to achieve a cell density of 2.5 x 10^5 cells/175uL in pre-warmed phenol red-free seahorse XF DMEM (Agilent, Santa Clara, CA) containing HEPES and supplemented with 10mM D-glucose, 4mM L-glutamine, and 2mM Na-pyruvate (Agilent). Cells were plated in triplicate or quadruplicate per treatment condition in poly-D-lysine-coated (Sigma Aldrich) 96-well cell culture microplates (Agilent). Plated cells were centrifuged at 450 x g with deceleration set to 0, then the plate was rotated 180° and centrifuged again with the speed changed to 650 x g. The stop button was pressed as soon as the centrifuge reached the speed setting. The

purpose of these subsequent centrifugation steps was to allow cells to adhere to the bottom of the plate since T cells are suspension cells. After centrifugation steps, plated cells were incubated for 1hr at 37°C without CO_2 to de-gas the plate. Sensor cartridges were hydrated as per the manufacturer's instructions (Agilent). After incubation, a standard mitochondrial stress test was performed involving use of subsequent injections of the ATP synthase inhibitor oligomycin (Calbiochem, San Diego, CA), mitochondrial protonophore carbonyl cyanide-p-trifluoromethoxyphenylhydrazone (FCCP) (Enzo Life Sciences, Farmingdale, NY), and a combination of rotenone and antimycin A (Enzo Life Sciences) to block iron sulfite clusters in ETC complexes I and III, respectively. Final concentrations of each inhibitor was 3.5μM for oligomycin, 1μM for FCCP, and 14μM each for rotenone and antimycin A, all of which were determined in a previously published study from our lab.[242] Oxygen consumption rate (OCR) and extracellular acidification rate (ECAR) were measured as a direct measure of OXPHOS and a surrogate measure of glycolysis, respectively, with a Seahorse XF 96fe Analyzer (Agilent) by O_2 and pH sensors within the sensor cartridge. Data were analyzed using the Wave software v2.6 (Agilent).

CHAPTER 3. T CELLS DOMINATE PERIPHERAL INFLAMMATION IN OBESITY-ASSOCIATED T2D

3.1 Disclaimer

The work described in this chapter was previously published[241] and copyright permission was granted by John Wiley and Sons, Inc. (WILEY) to Gabriella Kalantar and the University of Kentucky to be reused for this dissertation only. Copyright license number 5601101054908 granted on August 2, 2023.

3.2 Introduction

Inflammatory sequelae of obesity are induced by peripheral changes in immunomodulatory lipids, immune cell expansion in classical metabolic tissues like AT, and proinflammatory hormones.[41,140,243,244] Our current understanding of meta-inflammation in obesity and T2D is largely based on studies using mouse models that have highlighted the importance of proinflammatory macrophages in AT and other metabolic tissues.[37,145] Although macrophages are irrefutably important to metabolic immunopathogenesis, the frequency of T cells in VAT is higher in nonobese primates/humans compared with mice,[245] suggesting that the contribution of T cells to human metabolic disease is underappreciated.

Peripheral inflammation in human obesity and T2D, which is likely influenced by recirculation of immune cells through the expanded AT,[129] remains less understood than mouse AT inflammation.[246] Both the serum and AT of lean people and mice have higher concentrations of cytokines characteristic of noninflammatory immune cells (IL-10, IL-13, and IL-33),[39] which maintain metabolic and immunological homeostasis within insulin-sensitive tissues. Conversely, IL-1β, IL-6, and TNF-α are higher in people with obesity and are used to clinically predict T2D risk.[32,148] Additionally, PBMCs from people with obesity/T2D have higher competency (ability of immune cells to contribute to an inflammatory response) to produce the proinflammatory cytokines generally attributed to $CD4^+$ T cells (TNF-β, IL-17, and IL-21) that overlap with the T cell

profile in human AT.[40,43,44] Given that both $CD4^+$ and $CD8^+$ T cells are relatively abundant in human blood and increase IFN-γ production in response to obesity/T2D,[139,161] these data suggest that an insufficient understanding of the contribution of T cells to peripheral inflammation in obesity may explain why clinical trials of immunomodulatory drugs for diabetes have generally not been successful and, therefore, not broadly adopted.[247]

Crosstalk among immune cells adds further complexity to the search for modifiable cell types that disproportionately contribute to T2D-associated inflammation. Many investigations indicate that myeloid cells are the source of TNF-α in obesity and T2D; our work showed that $CD4^+$ and $CD8^+$ T cell TNF-α is activated by IL-17F, a product of Th17 cells.[43] Closer scrutiny of our own work and others' demonstrated that both a Th17 profile and an underlying Th1 profile (including TNF-α) characterize T2D-associated inflammation, in concordance with murine and human analyses.[40,42,43,46,161] Methods used in these studies often did not allow attribution of cytokines to myeloid or T cells; therefore, the relative contribution of these two major sources of peripheral meta-inflammation remains unclear.

To quantify the relative contributions of circulating T and mononuclear myeloid ("myeloid" herein) cells to peripheral inflammation in obesity and metabolic decline, we measured cytokine production by stimulated PBMCs to assess cytokine competency, the ability of cells to contribute to overall inflammation. In diseases such as obesity, which lack a definitive single PBMC stimulant despite convincing evidence of immune cell activation, pan-stimulation of the large number of circulating immune cells available from blood, which recirculate through the expanded AT,[129] has been critical for our understanding of mechanisms driving meta-inflammation and comparison among studies.

3.3 Objective and Summary

The purpose of this study was to determine the relative contributions of T cells and myeloid cells in obesity and T2D-associated peripheral inflammation to unify disparate claims in the literature between mouse models and human data.

The work discussed in this chapter establishes that stimulation duration impacts PBMC responses to T cell- (CD3/CD28), but not myeloid- (lipopolysaccharide [LPS]), targeted stimuli, regardless of the donor's metabolic health. Therefore, the acute response of myeloid cells is diluted by the sustained contribution of T cells to overall "inflammation." $CD4^+$ T cells also have the competency to contribute more TNF-α to peripheral meta-inflammation than myeloid cells, regardless of time point. Finally, models that combine cytokine production from both cell types have shown that cytokines generated by T cell stimulation rank higher for defining peripheral meta-inflammation. These results indicate a major role of T cells in peripheral inflammation in human obesity and T2D to significantly extend our understanding of immune cells as dominant sources of meta-inflammation.

3.4 Materials and methods

3.4.1 Donor description and demographics

Recruitment method, inclusion criteria, and exclusion criteria were as described in chapter 2. Cohorts for this study were age-matched and BMI-matched as described in Table 3.1. A list of medications as they relate to inflammation and/or glycemic control are outlined in Table 3.2.

Table 3.1 Description of human donors

	Overweight/obesity + (non-diabetes [ND])	Overweight/obesity + preT2D	Overweight/ obesity + T2D
Age, years [median(range)]	56 (45-66)	56 (50-72)	60 (47-64)
BMI, kg m^2 [median(range)]	34.03 (27-40)	36.7 (31 – 38)	34.5 (26-38)
FBG, mg dl$^-$ [median(range)]	95 (88-107)	104.5 (98-110) ‡	*Not measured for T2D donors
A1c, % [median(range)]	5.4 (5.1-5.6) 7/9	5.4 (5.1-5.7) 9/10	7 (5.6-10.3) † 11/11
Total *N*	9	10	11
Females	6	8	6
Males	3	2	5
White	8	9	8
Black/AA	1	1	3

*Clinical diagnosis of type 2 diabetes sufficient for subjects on glycemic control drugs; ND or preT2D was confirmed in some subjects based on 2hr oral glucose tolerance test blood glucose measures (not shown).
†Indicates a significant difference between ND and T2D donors based on ANOVA and ‡significant difference between ND and preT2D donors based on Student's t-test ($P < 0.05$)

Table 3.2 List of glycemic and lipid control medications and smoker status

Medications	ND	preT2D	T2D
Metformin (*N*)	0/9	0/10	9/11
Thiazolidinediones (*N*)	0/9	0/10	1/11
DPP-4 Inhibitors (*N*)	0/9	0/10	3/11
Sulfonylureas (*N*)	0/9	0/10	2/11
Statins (*N*)	3/9	4/10	7/11
ACE Inhibitors (*N*)	2/9	2/10	3/11
Smoker (*N*)	0/9	1/10	0/11

3.4.2 Cell manipulations

PBMCs were used in all experiments within this chapter. PBMCs were isolated, archived, thawed, and cultured in complete RPMI-1630 cell culture medium as outlined in chapter 2. Cells were treated +/- lipopolysaccharide (LPS) from *Escherichia coli* O111:B4 (25 ng/mL, Millipore Sigma) to primarily stimulate myeloid cells or CD3/CD28 dynabeads (Gibco) to primarily stimulate T cells for 20-72 hours. Supernatants were harvested and used for a 25-plex cytokine array as described in chapter 2. Cells were used for flow cytometric analysis of intracellular cytokine production from individual PBMC subsets.

3.4.3 Flow cytometry

To gate for $CD4^+$ T cells and $CD11b^+/CD14^+$ myeloid cells, we stained for common surface markers of the predominant populations within the PBMC fraction. BFA treatment and flow staining protocol was as described in chapter 2. LPS-treated cells were incubated on ice with 2.5mM EDTA (Gibco) for 30-min to detach adherent cells. Cells remaining adherent were removed with a rubber

scraper (CytOne) and cold PBS washes. Alternatively, CD3/CD28-stimulated cells were pelleted and beads were removed with a magnet. Tables 3.3 and 3.4 list the antibodies and their respective clones that were used for surface marker and intracellular cytokine staining.

Table 3.3 Surface marker antibody panel

Antibody (anti-human)	Clone, Fluorophore (Manufacturer)	Dilution
anti-CD4	OKT4, FITC (BioLegend)	1:200
anti-CD8	SK1, BV785 (BioLegend)	1:200
anti-CD14	63D3, PE/Cyanine 7 (Biolegend)	1:200
anti-CD19	SJ25C1, BV510 (BD Biosciences)	1:100
anti-CD161	DX12, BB700 (BD Biosciences)	1:100
anti-CD11b	D12, BV605 (BD Biosciences)	1:50

Table 3.4 Intracellular marker antibody panel

Antibody (anti-human)	Clone, Fluorophore (Manufacturer)	Dilution
anti-TNF-α	MAb11, PE (BD Biosciences)	1:50
anti-IFN-γ	B27, PE-CSF (BD Biosciences)	1:50

3.4.4 Statistical Analysis

We used GraphPad Prism v8 for an ANOVA mixed-effects analysis (restricted maximum likelihood) with Tukey's multiple comparisons to assess temporal differences in cytokines. One-way ANOVA with Bonferroni multiple comparisons (Gaussian data) or a Kruskal-Wallis test with Dunn multiple comparisons (non-Gaussian data), both with a 95% confidence interval, determined cohort-specific differences in stimuli responses.

Bioinformatic analyses were performed by our collaborators Dr. Sajjad Fouladvand, Dr. Jin Chen, and Dr. Xiaohua Douglas Zhang at the University of Kentucky in the department of biostatistics. Maximum Relevance and Minimum Redundancy (mRMR)[248] and extreme gradient boosting (XGBoost)[249] were used to perform feature engineering and classification tasks, respectively. The mRMR model ranked features based on their relevance to outcome variable and feature

redundancy. The top five features selected by mRMR were used to train XGBoost models. The XGBoost algorithm used an additive manner to optimize the objective function in Equation (1).

$$\hat{y}_i = \sum_{k=1}^{K} f_k(x_i), \qquad f_k \in \mathcal{F} \tag{1}$$

Where $\hat{y}_i$ was the prediction, x_i was the input, K was the number of additive functions and $\mathcal{F} = (q: \mathbb{R}^m \rightarrow T, w \in \mathbb{R}^T)$ was the regression tree space. Scikit-learn [250] and XGBoost [249] libraries were used to implement predictive models. Leave one out cross validation trained and tested the models; averaged values across all samples were reported. Precision (equation 2), recall (equation 3), F1-score (equation 4) and Area Under the Curve (AUC) assessed model performances as follows.

$$Precision = \frac{True\ Positives}{True\ Positives + False\ Positives} \tag{2}$$

$$Recall = \frac{True\ Positives}{True\ Positives + False\ Negatives} \tag{3}$$

$$F1 - score = \frac{2 \times (Precision \times Recall)}{(Precision + Recall)} \tag{4}$$

For the partial least-squares discriminant analysis (PLSDA),[250] cytokine data were log-transformed to mitigate skewing. Cytokines with a small range of values had the option to be as/more important than cytokines with a large range of values. Therefore, we scaled each cytokine to zero mean and unit variance before applying PLSDA. After all data preprocessing (based on exploratory analysis), PLSDA was applied using the R function splsda() in the “mixOmics” package.[251] Data were analyzed using each of 2 options: 1) two components, each with all 25

cytokines; or 2) using R function tune.splsda() to automatically find an optimal number of cytokines to separate groups. The top ranked cytokines are shown.

3.5 Results

3.5.1 PBMCs increase cytokine production over time following T-cell stimulation but not myeloid stimulation

To determine the relative contributions of myeloid and T cells to obesity-associated inflammation in the periphery, we first established the importance of stimulation time for cytokine production. We used CD3/CD28 dynabeads to primarily stimulate T cells or *E. coli* LPS to primarily stimulate myeloid cells in PBMCs from donors with obesity and normal glucose tolerance, who were classified as non-diabetes (ND), preT2D, or T2D, for 20 to 72 hours and then used PLSDA constrained by donor type to ask how time impacts cytokine profiles in PBMCs responding to T cell- or monocyte-targeted stimulation. The shift in inflammation defined by a mathematical combination of all cytokines projected in two dimensions showed that CD3/CD28-activated inflammation shifted over time (Figure 3.1A-C, top panel). A focus on the five cytokines that were most important for distinguishing profile shifts indicated cohort-dependent differences in cytokines that distinguished the CD3/CD28 response (bracket on bar graphs, Figure 3.1A-C). A mixed Th17/Th1 profile (IL-17F/A/IFN-γ/TNF-β), generated at 72 hours, dominated “inflammation” in PBMCs from donors with T2D (Figure 1A, lower panel, red bars; note lack of importance of cytokines produced at 20 hours and 40 hours, gray and black bars). A similar 72-hour Th17/Th1 profile (TNF-β, IL-17F/A/granulocyte-macrophage colony-stimulating factor [GM-CSF]) dominated inflammation in preT2D (Figure 3.1B, lower panel), although 72-hour IFN-γ was somewhat less important for defining inflammation in preT2D compared to T2D cultures (compare Figure 3.1A,B in which IFN-γ is ranked second or eighth most important for T2D or preT2D, respectively). Cytokines related to type 2 immune responses (IL-9, -13, and -21)[252,253] were more important in CD3/CD28-elicited inflammation in cultures from donors with obesity and NGT or non-diabetes (ND,

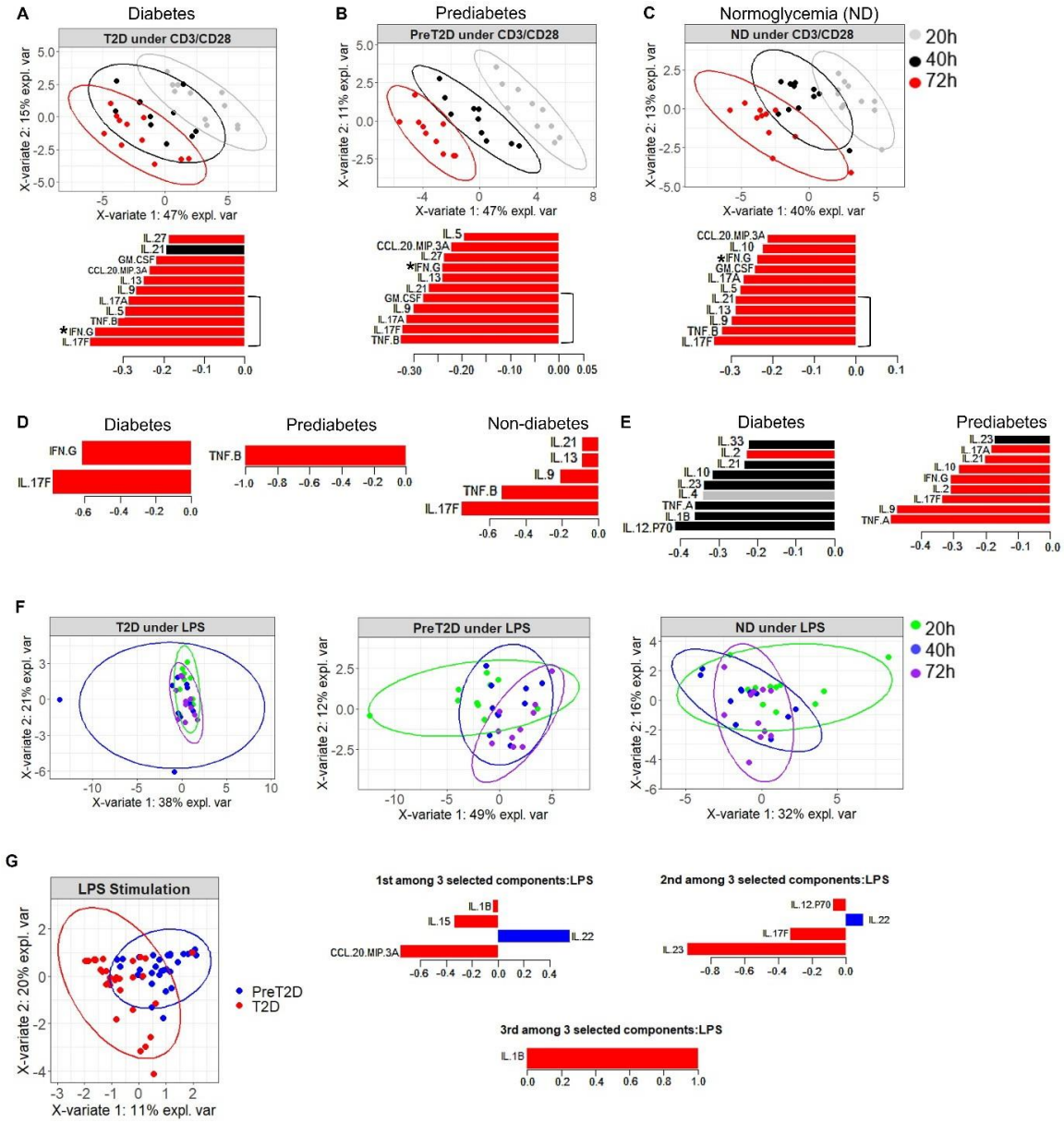

Figure 3.1 Cytokine responses to T cell-targeting, but not myeloid-targeting, stimuli change over time and are impacted by T2D

PLSDA of inflammatory profiles by combining all cytokines measured after PBMC stimulation with CD3/CD28 for 20 (gray), 40 (black), or 72 (red) hours. PBMCs were from donors with a high overweight or obesity BMI and (A) T2D, (B) preT2D, or (C) normal glycemic control (ND). Top panels show 2D projections of cytokine profiles in the first (most distinguishing) component, colored and grouped by time point; bottom panels rank cytokines produced at all time points from most (bottom) to least (top) important for defining responses most characteristic of cells from the donor cohort indicated. (D) Autoselection of cytokines/time points that distinguished CD3/CD28-elicited inflammation from donor cohorts as indicated to distinguish cytokines and eliminate background "noise." (E) Cytokines that were the second most distinguishing components of inflammation for cells from the donor cohort as indicated. (G) Autoselection of cytokines/time points that distinguished LPS-elicited inflammation for cells from donors *(continued on next page)*

Figure 3.1 (continued) preT2D (blue) or T2D (red) rank as described above to differentiate responses. Analysis and figures were generated by X.D. Zhang.

Figure 3.1C), suggesting that loss of a type 2 profile associates with metabolic decline in obesity. Cytokine production at 40 hours post CD3/CD28 was overrepresented as a secondary component for defining inflammation for all participants' cells (Figure A2.1). Mixed-effects analysis of individual cytokines over time for each cohort supported the PLSDA demonstration that cytokines produced by PBMCs stimulated with CD3/CD28 (but neither LPS nor lack of stimulating ligands) increased over time (Figure A2.2).

Follow-up analysis used R to automatically find the optimal number of cytokine values/time points that distinguished inflammation for cells from each of the three participant cohorts to focus on important distinguishing cytokines while eliminating background "noise." Automated cytokine selection showed that 72-hour production of IL-17F and IFN-γ dominated the first component of CD3/CD28-elicited cytokines in T2D, consistent with our previous identification of a mixed Th17/Th1 profile in T2D,[43,46] whereas TNF-β (lymphotoxin A; a Th1 cytokine)[254] at 72 hours was most distinguishing for preT2D. The autoselected first component for CD3/CD28-stimulated ND cells included cytokines from all major $CD4^+$ T effector subsets (Th1,2,17; Figure 3.1D). The second component profiles for CD3/CD28-stimulated PBMCs included cytokine production at 40 hours in both donors with T2D and ND donors (Figure 3.1E, left; black/gray bars and data not shown) but remained dominated by 72-hour cytokine amounts in preT2D (Figure 3.1E, right; red bars). Taken together, these data indicate that shifts in CD3/CD28-elicited responses over time are impacted by metabolic status of the cell donor and/or T2D drugs. In sharp contrast, treatment time had little effect on cytokine production by both LPS-stimulated and unstimulated PBMCs (Figure 3.1F and Figure A1.1 and Figure A1.2). Although LPS responses insignificantly changed over time, automated selection of cytokines elicited from PBMCs by LPS showed significant separation of profiles between donors with T2D and preT2D (but not ND) and highlighted three components that differentially supported T2D.

Chemokine (CC motif) ligand 20 (CCL-20) was most important for response of cells from T2D subjects, with IL-22 dominating preT2D cell responses in the first component. IL-23 and IL-1β were lesser contributors to T2D-specific inflammation (components 2 and 3, respectively; Figure 3.1G). We conclude, from both CD3/CD28- and LPS-elicited profiles, that metabolic status impacts cytokine competency in cells from donors with obesity, consistent with our work on purified $CD4^+$ T cells.[45]

3.5.2 T cell and myeloid cell cytokine changes accompany metabolic decline

Our work indicated that combinatorial cytokine profiles differentiated ND from T2D inflammation.[43,46] To better understand the unique cytokine competency of PBMCs from participants with obesity and preT2D and to put our combinatorial findings (Figure 3.1) into the more traditional context of the literature, we compared amounts of individual cytokines produced by stimulated PBMCs among all participant groups. Consistent with previous findings,[43,44] CD3/CD28 stimulation for 40 to 72 hours elicited more IL-17A, IFN-γ, and/or IL-17F, although not additional cytokines, by cells from donors with preT2D or T2D compared with donors with normoglycemia (Figure 3.2A,B and data not shown). Although a direct comparison of cytokine production by CD3/CD28-stimulated PBMCs from our past data to outcomes herein is problematic owing to equipment changes, sample storage time, and other technical differences, comparisons between outcomes from newly recruited participants with T2D from our historical and present sites (Boston, Massachusetts metro area and Kentucky, respectively) have shown trends toward less production of signature Th17 cytokines by cultures from clinically and demographically similar Kentucky participants (Figure 3.2C).

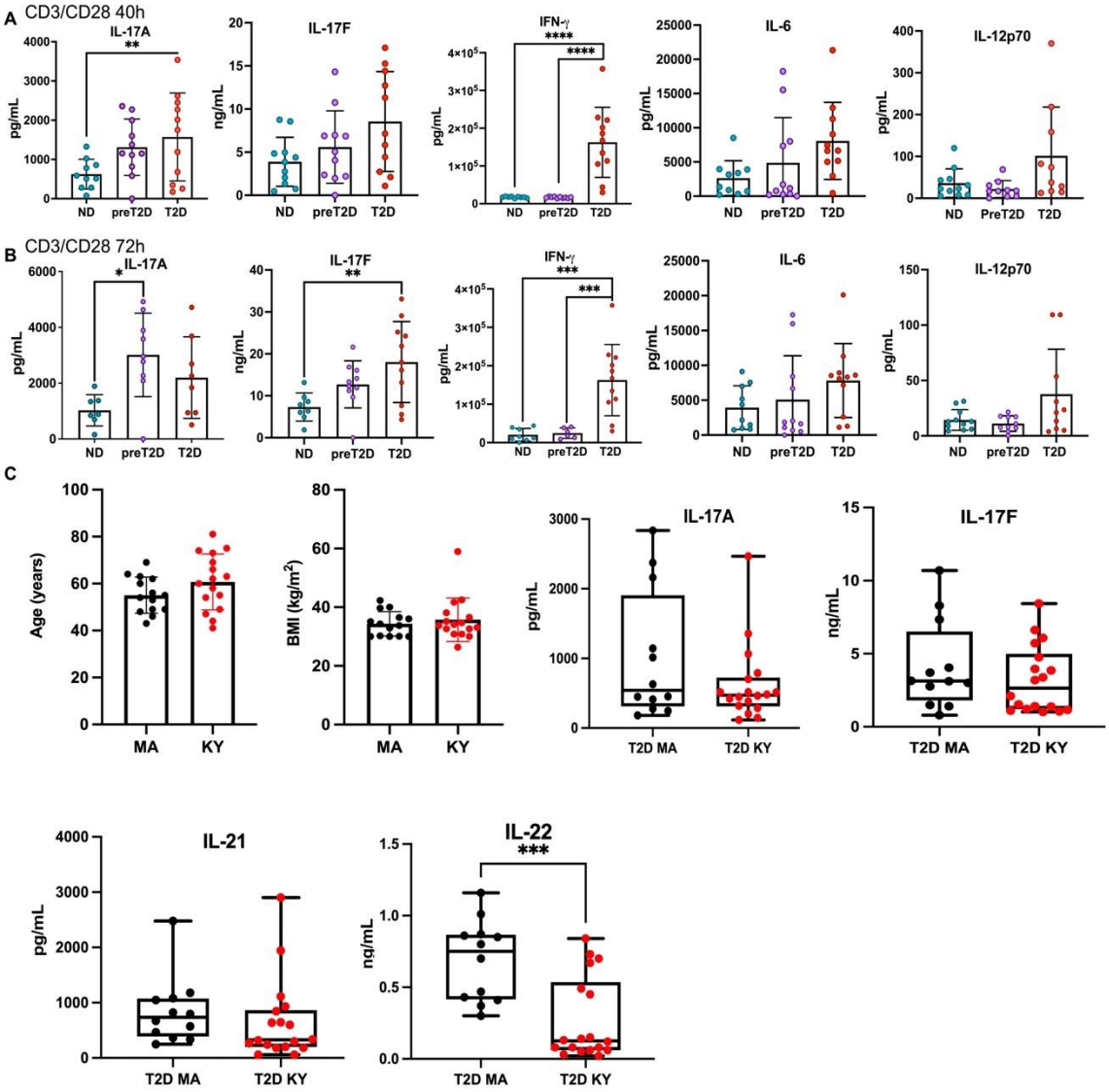

Figure 3.2 Loss of glycemic control associates with changes in T cell cytokine production

PBMCs from ND (blue dots), preT2D (purple dots), and T2D (red dots) cohort donors were activated with T cell-targeted stimuli and cytokine production was quantified after (**A**) 40 or (**B**) 72 hours. Differences in cytokine production based on glycemic controls of the PBMC donors were identified by one-way ANOVA. (**C**) Cytokine production by PBMCs from participants with T2D recruited from the Boston, MA metro area (left, black dots n = 17; 12 males) or at the University of Kentucky (right, red dots, n = 12; 10 males). Panels at left show subjects were matched for BMI and age. Trends toward differential production of multiple Th17 signature cytokines are shown (unpaired two-tailed t test). Experiments, data collection, and data analysis in panel C was performed by S. SantaCruz-Calvo.

Cultures from Kentuckians with T2D had higher amounts of the Th1 cytokine IFN-γ and trends of others such as IL-6 and IL-12p70, similar to our findings in the Boston cohort (Figure 3.2A,B).[43,46] The dominance of IFN-γ is unlikely to be caused by the high prevalence of smokers in Kentucky, which supports Th1 polarization,[255] as we recruited one versus zero active smokers in the Kentucky and Boston T2D cohorts, respectively. Regardless of location-associated difference, these analyses confirm the conclusion that time-dependent changes in cytokine competency are shaped by metabolic status in CD3/CD28-stimulated PBMCs.

To similarly challenge the bioinformatic indication that metabolic status impacts an early peak of LPS-activated cytokines (Figure 3.1G), we compared production of single cytokines following 20-hour LPS stimulation in PBMCs from all participant cohorts. About half the cytokines were produced in higher amounts as disease progressed, although some, such as IL-1β and TNF-α, failed to meet statistical criteria for increases (Figure 3.3, and data not shown). These data independently indicate the potential contribution of myeloid inflammation increases with obesity-associated metabolic decline independent of culture time.

3.5.3 T cell- compared to myeloid-stimulated PBMCs produce more TNF-α

Given the unexpected evidence that T cells may contribute more to meta-inflammation in the long run (Figure 3.1), we focused our analysis on production of TNF-α, the first cytokine linked to obesity-associated metabolic disease.[256,257] Both T cells and monocytes from donors with obesity make TNF-α,[43] but myeloid cells are often the sole focus of TNF-α production in obesity, as first recognized in mouse AT.[144] We compared production of TNF-α by 20-hour LPS-stimulated and 20-, 40-, or 72-hour CD3/CD28-stimulated PBMCs among cohorts. Irrespective of time point or metabolic status, CD3/28 stimulation produced more TNF-α than LPS; although, IL-6 (another T2D-associated cytokine) was produced at higher concentrations by myeloid stimulation of T2D cells, regardless of the comparator T cell time point (Figure 3.4A,B and Figure A2.3). Cytokines made predominantly by myeloid cells (IL-1β; Figure 3.4C) or by T cells (IFN-γ and IL-12p70; Figure 3.4D) were elicited by the expected stimulus, whereas some cytokines were

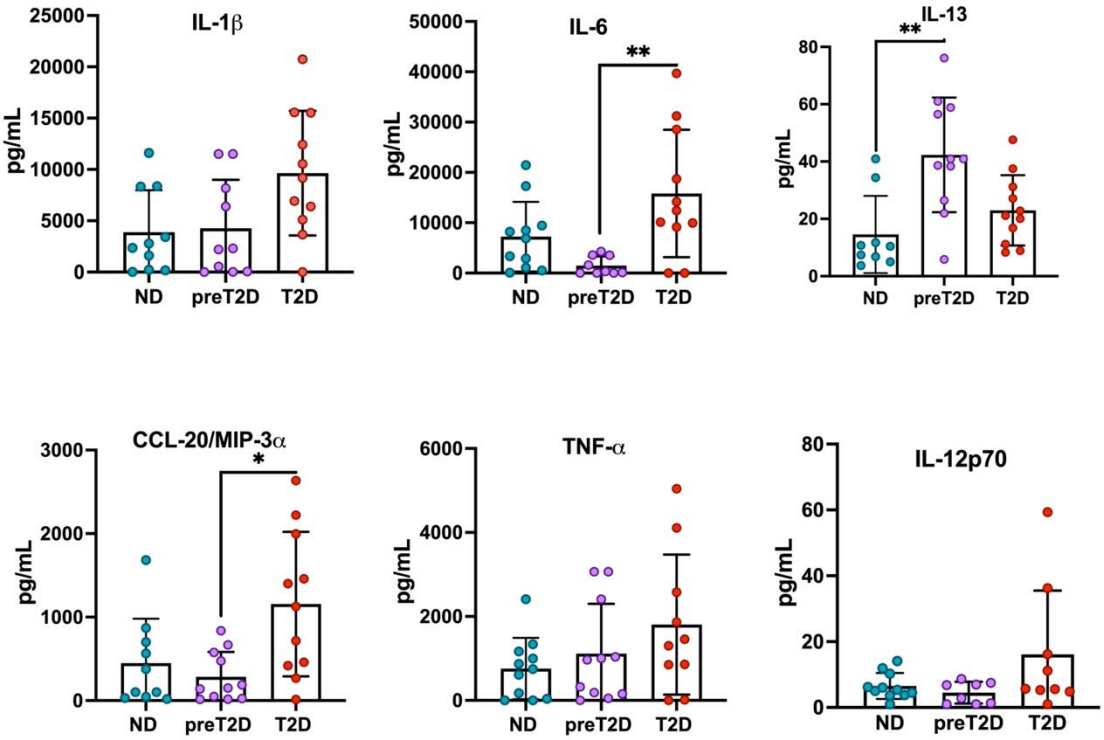

Figure 3.3 Loss of glycemic control associates with changes in LPS-stimulated cytokine production

PBMCs from participants with ND (blue dots), preT2D (purple dots), or T2D (red dots) were activated with a myeloid-targeting stimulus (LPS), and cytokine production was quantified after 20 hours. Cytokines that were detectable in a majority of the samples are shown. Differences in cytokine production was quantified after 20 hours. Differences in cytokine production based on glycemic control of the PBMC donor were identified by two-way ANOVA, with trends for IL-1β and TNF-α failing to reach statistical significance. Plungers represent SD and significance level is as defined in figure 3.1.

similarly produced (CCL-20; Figure 3.4F and Figure A2.3).

We used intracellular staining (Figure A1.4) to challenge the possibility that circulating $CD4^+$ T cells produce more TNF-α than myeloid cells in response to canonical stimuli and whether metabolic status or immune cell subset frequency affects this response. Control experiments showed that frequencies of $CD11b^+$ myeloid cells, $CD14^+$ myelo-monocytes, $CD4^+$ T cells, and TNF-α^+ cells within each subset were similar among the three cohorts and within expected frequencies for human PBMCs (Figure 3.5A and Figure A1.5), consistent with previous analyses.[46,258] Follow-up work compared TNF-α production by 20-hour LPS- and 40-hour CD3/CD28-stimulated PBMCs to capture the earliest times of maximal TNF-α elicitation for each stimulus and compared TNF-α production based on mean fluorescence intensity (MFI), a measure of average cytokine production/cell. The average $CD11b^+$ cell produced <10% of the TNF-α produced by $CD14^+$ cells in LPS-responding PBMCs (Figure 3.5B). Each $CD4^+$ T cell from CD3/CD28-stimulated PBMCs produced approximately 12x or 1.3x more TNF-α on average than $CD11b^+$ or $CD14^+$ cells, respectively, in LPS-stimulated PBMCs, and only a small fraction of $CD11b^+$ and even fewer $CD14^+$ cells produced a small amount of TNF-α^+ (i.e., MFI) following CD3/CD28 stimulation, adding little to the overall TNF-α production in culture supernatants (Figure 3.5B,C). $CD4^+$ cells also trended to produce more TNF-α on average than each $CD14^+$ cell in ND and T2D samples, but this difference failed to reach statistical significance (Figure 3.5D). Given the much higher frequency of TNF-α-producing $CD4^+$ cells and higher (or for $CD14^+$, similar) TNF-α production per cell (i.e., MFI), intracellular staining supports the Bio-Plex conclusion that activated peripheral blood $CD4^+$ T lymphocytes produce more TNF-α than myeloid cells in obesity and obesity-associated T2D; therefore, T cells may contribute more to peripheral meta-inflammation than myeloid cells.

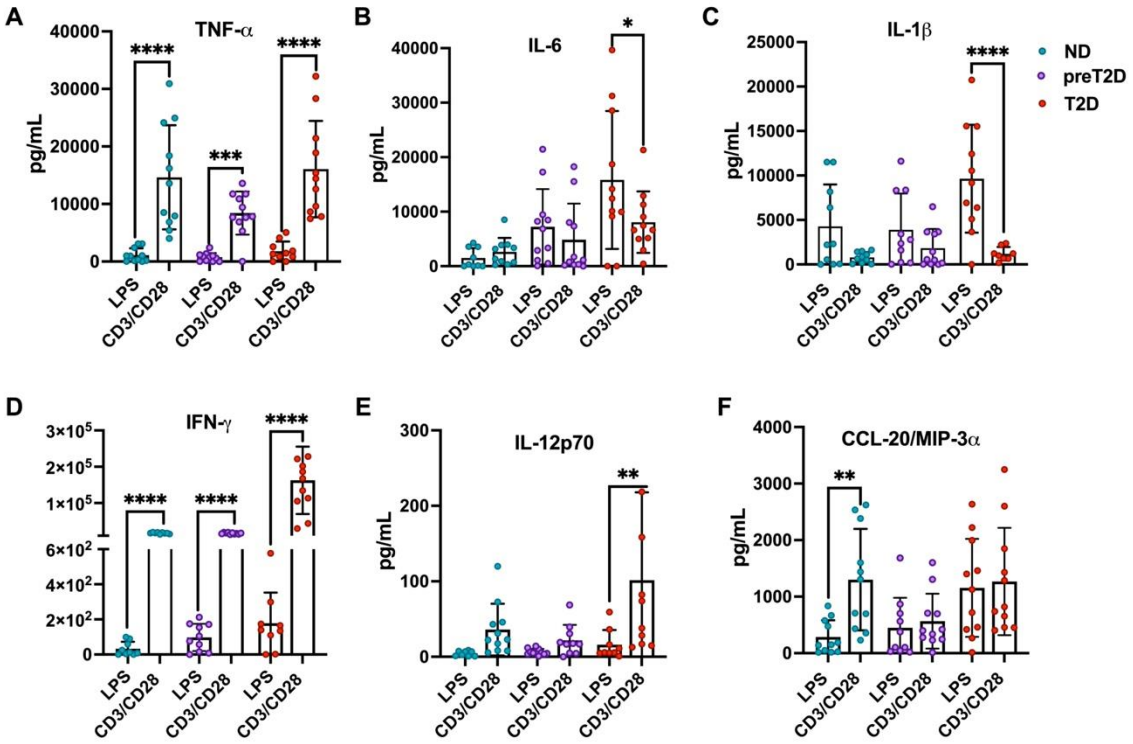

Figure 3.4 T cell stimulation elicits more TNF-α than myeloid stimulation of PBMCs from all participants with obesity

Direct comparison of cytokines elicited by 20-hour stimulation of PBMCs from participants with ND (blue dots), preT2D (purple dots), and T2D (red dots) as indicated. Differences identified by a two-way ANOVA mixed-effects analysis are indicated. Bars show average and SD. **$p < 0.01$; ***$p < 0.001$; ****$p < 0.0001$.

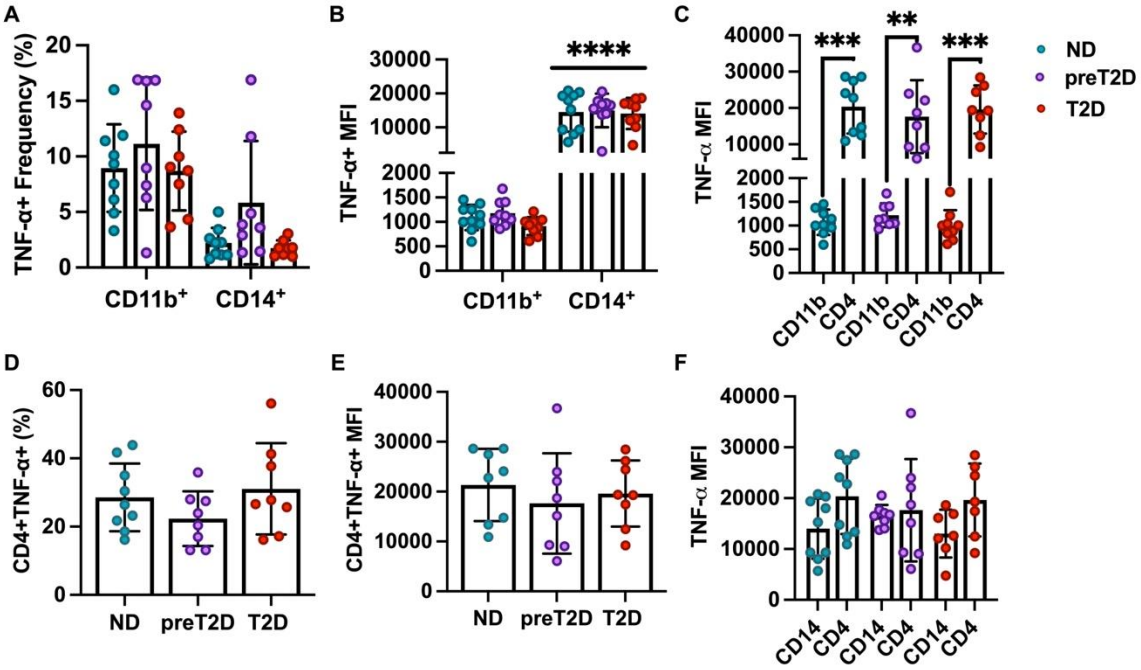

Figure 3.5 Intracellular staining confirms that the CD4+ T cells produce more TNF-α than myeloid cells at 40- or 20-hours post-stimulation, respectively

(**A**) Frequency of (top) CD11b$^+$ myeloid cells and CD14$^+$ monocytes or (bottom) CD4$^+$ T cells from ND (blue dots), preT2D (purple dots), T2D (red dots) PBMCs stained positive for TNF-α. Frequency was relative to total PBMCs. (**B**) MFI indicates the average number of TNF-α molecules produced on a per cell basis in the cell types indicated. A direct comparison of intracellular TNF-α as measure by MFI in CD4$^+$ T cells verses CD11b$^+$ (**C**) or CD14$^+$ monocytes (**D**). Differences were assessed by one-way ANOVA with Bonferroni multiple comparisons. **$p < 0.01$; ***$p < 0.001$; ****$p < 0.0001$.

3.5.4 T cell cytokine competency disproportionately contributes to diabetes-associated meta-inflammation

Despite the demonstrated role of TNF-α in meta-inflammation,[259] TNF-α is not a top cytokine for differentiating CD3/CD28 from LPS responses in obesity alone or in combination with metabolic decline (Figure 3.1). We combined cytokine measures from all stimulation conditions (CD3/CD28, LPS, and unstimulated for 20, 40, and 72 hours) in PLSDA as an unbiased approach to address the relative importance of CD3/CD28- versus LPS-generated cytokines in meta-inflammation. CD3/CD28 cytokines elicited at 72 hours (Figure 3.6A, left; red bars) were most important for defining diabetes-associated inflammation, with dominance of LPS (20 hours)-elicited IL-1β and, to a lesser extent, IL-23 and IL-6 as an underlying (second) component of T2D inflammation (Figure 3.6A, right; green bars). To independently challenge this indication that CD3/28 responses dominate peripheral inflammation in T2D, we reanalyzed cytokine data by mRMR, a principal components method that combined cytokines produced by all participants' samples following each of the two stimuli for all time points. Separation of cytokine data from all time points and stimuli by participant types (ND, preT2D, T2D) produced a model with poor performance for differentiating cytokine values from ND compared with participants with preT2D (0.500 precision) although accuracy of prediction of T2D from cytokines was 0.909 (Table A2.1)

Due to poor model performance with the three cohorts separated, we combined cytokine data from both types of participants without T2D (ND + preT2D, designated ND+) to ask which cytokines, elicited by which stimulus, and at which time post stimulation, best differentiated T2D from ND+ samples. Three of the top five cytokine measures that differentiated T2D were IFN-γ produced by CD3/CD28 stimulation of PBMC for 72, 40, or 20 hours (Figure 3.6B). LPS elicited two of the top ranked cytokines (IL-33 at 40 hours and CCL-20 at 20 hours). Principal component analysis of these top five cytokines shows clear visual distinction of T2D compared with ND+ inflammation, with confidence in the model boosted by very high precision (Figure 3.6C,D). The arguably lower prominence of IFN-γ in the PLSDA model (Figure 3.6A) compared with the mRMR model (Figure 3.6B)

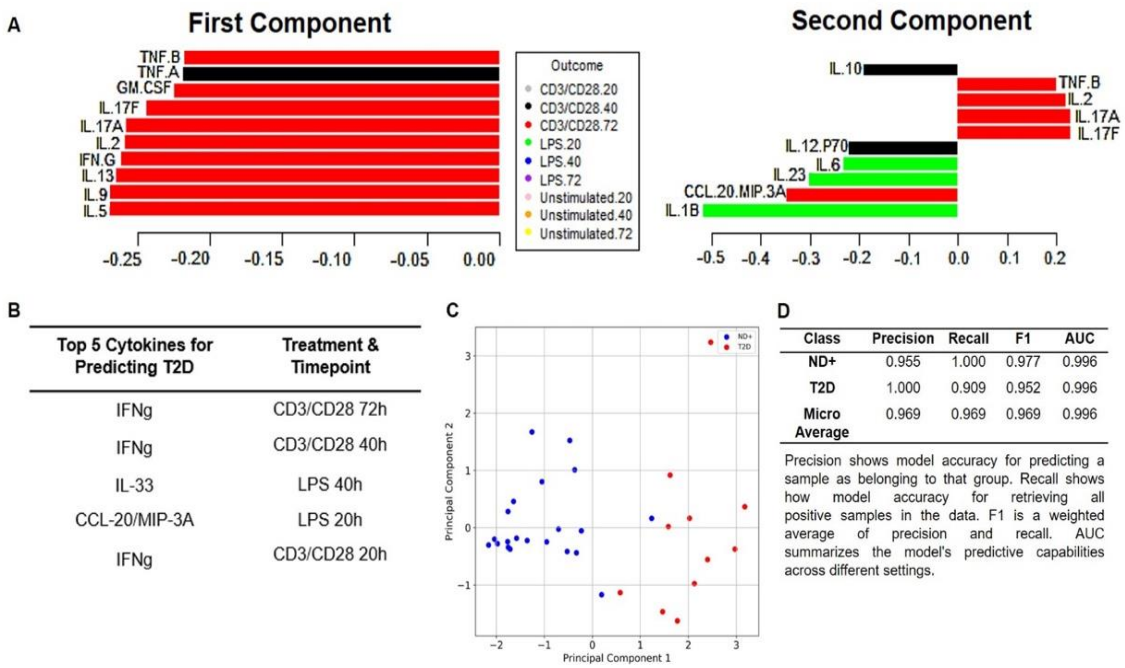

Top 5 Cytokines for Predicting T2D	Treatment & Timepoint
IFNg	CD3/CD28 72h
IFNg	CD3/CD28 40h
IL-33	LPS 40h
CCL-20/MIP-3A	LPS 20h
IFNg	CD3/CD28 20h

Class	Precision	Recall	F1	AUC
ND+	0.955	1.000	0.977	0.996
T2D	1.000	0.909	0.952	0.996
Micro Average	0.969	0.969	0.969	0.996

Precision shows model accuracy for predicting a sample as belonging to that group. Recall shows how model accuracy for retrieving all positive samples in the data. F1 is a weighted average of precision and recall. AUC summarizes the model's predictive capabilities across different settings.

Figure 3.6 Combinatorial models indicate that T cell cytokines are more important than myeloid cytokines for T2D-associated inflammation

(**A**) PLSDA model that combined cytokines produced by PBMCs stimulated as indicated in the Outcome key and then ranked cytokines produced by each condition/samples from most (bottom) to least (top) important for defining inflammation in T2D. Left panel shows cytokines in the first component (dimension) that distinguishes T2D. Right panel ranks cytokines in the second component. (**B**) Ranking of top five cytokines that differentiate T2D from ND^+ (a combination outcomes from ND and preT2D cells) samples identified by mRMR. (C) Two-dimensional representation of profiles derived from mathematical combination of the top five cytokines identified in panel **B**. Blue and red dots indicate "inflammation" from participants with ND+ or T2D, respectively. (**D**) Quantification of mRMR model quality. A perfect model would have values of 1.0 for all parameters, which are defined under the table. AUC: area under the curve. Data and figures for panel A were analyzed and generated by X.D. Zhang. Data and figures for panels B-D were analyzed and generated by S. Fouladvand and J. Chen.

may, in part, be explained by exclusion of cytokines produced by unstimulated cells from the latter model. Regardless, based on both PLSDA and mRMR, we conclude that T cell cytokines, perhaps fueled in part by the Th1 cytokine IFN-γ and a lesser contribution by TNF-α, ranked highly as an indicator of T2D in several analyses (Figures 3.1A-D and Figures 3.4-3.6) and contribute a greater amount of disease-defining peripheral inflammation to human T2D than do myeloid cells.

3.6 Discussion

Our kinetic analysis defined inflammatory profiles produced by PBMCs from ND, preT2D, and T2D participants with obesity and showed that primary stimulation of T cells, but not myeloid cells, produced a profile that changed over time. Temporal changes indicated that multiple analyses were needed to test the relative contributions of myeloid and T cells to peripheral inflammation in obesity-associated metabolic decline. T cells impact peripheral inflammation over longer time points, suggesting that focus on TNF-α would test the possibility that T cells significantly contribute to peripheral meta-inflammation. Our data show that T cells contribute at least as much TNF-α as myeloid cells to systemic meta-inflammation. More comprehensive analyses supported the same conclusion: T cells dominate systemic inflammation in obesity-associated T2D. Our work translates the relative importance of myeloid and T cells in metabolic disease first identified in animal models to a conceptually new demonstration of the relative role of T cells in peripheral meta-inflammation and thereby obesity sequelae.[260,261]

Responses to T cell-targeted CD3/CD28 underscored the distinctiveness of preT2D inflammation first indicated by our analysis of cytokine competency of purified $CD4^+$ T cells,[45] and significantly extends existing analyses of cytokines in preT2D plasma/serum.[262,263] The acute myeloid response, combined with the more sustained response to CD3/CD28 that dominates overall “inflammation” at 72 hours, is consistent with a canonical immune response in which innate immune cells respond quickly to prime a sustained adaptive immune response. Whether this temporal pattern is mimicked by shifts in the undefined ligands that regulate chronic low-level inflammation in obesity-associated metabolic decline or explains

the suboptimal immune responses to, for example, vaccines and viruses in obesity/T2D remains unclear.[264,265]

The prominence of IFN-γ as an indicator of T2D with likely codominance of Th17 cytokines (IL-17A/F, -21, and -22) is consistent with our demonstrations of mixed peripheral Th1/Th17 profiles in human T2D, although mechanistic support of these two $CD4^+$ subsets differ.[43,46] Our findings are consistent with more IFN-γ-secreting T cells/mRNA expression in AT from mice and humans with obesity[266] and demonstrations that IFN-$\gamma^{-/-}$ mice on a high-fat diet are metabolically more healthy than wild-types.[267] The similar profile generated by Kentucky compared with Boston samples is surprising given a lower trend of concentrations of Th17 cytokines by CD3/CD28 stimulation of PBMCs from Kentuckians. The underlying cause of this geographical difference remains unclear and is a limitation of the study, as variables such as stress, diet, and activity almost certainly contribute, although all Boston participants were generally in areas known for less social determinants of T2D risk/development. Numerous analyses indicate Northeastern United State residents are healthier, as indicated by greater life expectancy, than those in the Southeast (including our catchment areas in Kentucky[268]), but this conclusion is counterintuitive to our findings of higher amounts of selected inflammatory cytokines produced by samples from Northeasterners. The number of participants in each group, although appropriate for bioinformatic analysis, is not appropriate to analyze data by sex or race. Given that both $CD4^+$ Th1 and $CD8^+$ T cells produce IFN-γ in response to CD3/CD28 stimulation (amid low myeloid IFN-γ competency), it is possible that population differences in T cell subsets, including a lower frequency of $CD8^+$ cells in T2D samples in Boston,[46] but not Kentucky along with differences in the model assumptions contribute to the prominence of IFN-γ in the mRMR model. These outcomes stress the benefit of using multiple analytical tools and comparisons to best understand systemic disorders through the lens of inflammation and thereby target treatments that take advantage of existing Food and Drug Administration approved pharmaceuticals.

CHAPTER 4. MITOCHONDRIAL TRAITS ARE NOT ALTERED IN PERIPHERAL CD4$^+$ T CELLS IN T2D PATHOGENESIS

4.1 Introduction

As described in chapter 3, CD4$^+$ T cells are a significant and dominating driver of peripheral inflammation in obesity and T2D. We also observed that both monocyte and T cell responses in PBMCs from people with preT2D have similarities to cells from people with obesity and NGT (non-diabetes) as well as people with T2D- emphasizing the intermediate nature of preT2D in disease progression, through an inflammatory lens. Notably, LPS-induced IL-13 was higher in preT2D, whereas CD3/CD28-induced IFN-γ production was lower compared to cells from T2D donors, suggesting there might be a unique peripheral cytokine profile in preT2D that skews more toward NGT immune profiles. Recent work from our lab has revealed that purified and stimulated T_{eff} are bioinformatically distinguished from those of T2D donors on a mixed cytokine profile dominated by Th1 (GM-CSF and TNF-α)[224] and Th2 (IL-4, IL-5, and IL-13) cytokines. The presence of Th1 cytokines amongst the top 5 rankings is consistent with the data presented in chapter 3 where Th1 cytokines like TNF-α were produced in high amounts across the spectrum of obesity.[241] These data collectively support the well-established role of Th1 cytokines in obesity-associated meta-inflammation and T2D pathogenesis.[40,44,260,266,269,270]

Additional PLSDA analysis between preT2D T_{eff} and T_{eff} from lean NGT donors showed similarities in IL-4, IL-5, and IL-13 production as these did not rank in the top distinguishing features between the two groups. Rather, other Th1 (IFN-γ and IL-12) and Th2 (IL-6 and IL-10)[126,231] cytokines ranked as most highly characteristic of lean NGT donors compared to preT2D, consistent with the demonstrations in chapter 3 that IFN-γ is not predictive of preT2D. Additionally, the Th17-produced cytokine CCL-20/MIP-3α[240] was ranked as a predictor of preT2D, revealing a minor Th17 component in the preT2D inflammatory profile when compared to the absence of obesity or IR.[45] This is a novel characterization of

peripheral inflammation in preT2D as earlier studies in human preT2D, albeit few, had only measured a wide-ranging and non-specific array of serum cytokines.[262,263,271] Since type-2 immunity is considered the more favorable profile in the context of metabolic disease, the dominance of Th2 cytokines in the preT2D profile supports our hypothesis that T cells in preT2D may have a compensatory mechanism against T2D-associated inflammation- a potential consequence of the compensatory period of β-cell insulin secretion.

Since preT2D presents with a unique peripheral cytokine profile and given what we know of the influence of metabolic reprogramming on T-cell function, it is reasonable to posit that the metabolic threshold and/or the utilization of fuel sources in T cells changes during T2D progression to support different inflammatory phenotypes. Our previous work showed that T_{eff} cells from preT2D donors have 2-3x higher OXPHOS activity compared to cells from lean NGT and T2D donors. Oxygen consumption rate (OCR), a measure of OXPHOS activity, was lower in preT2D donors when T_{eff} cells were co-cultured with T_{regs}; nonetheless, overall OCR was still relatively high, indicating that peripheral T cells have enhanced bioenergetic requirements during preT2D that are met through higher mitochondrial metabolism. Bioenergetic augmentation might appear before pathogenic cytokine dominance or could be a part of our proposed compensatory mechanism to drive preT2D T cells away from T2D pathogenesis. Together, these results lead us to hypothesize that enhanced mitochondrial function supports high OXPHOS and the preT2D-associated inflammatory profile from peripheral $CD4^+$ T cells in preT2D.

Mitochondria are commonly known for their required role in energy production, lending itself the title of “powerhouse of the cell.” However, mitochondria are now appreciated mediators of cellular function. Mitochondria act as key cell signaling platforms, initially revealed by their critical role in apoptosis regulation.[272-274] Mitochondria are highly dynamic organelles, and their morphology can dictate the intensity of OXPHOS activity. The outer mitochondrial membrane (OMM) contains proteins that recruit catalysts of membrane fission (budding or fragmentation) such as phosphorylated dynamin-related protein 1

(DRP1), which is recruited from the cytoplasm to the accessory protein Fis-1.[275] Additionally, the OMM expresses transmembrane GTPases that mediate membrane fusion of 2 or more mitochondria response to cellular stress/damage[276] or nutrient fluctuations,[277,278] and can create mitochondrial contact sites with other subcellular compartments (e.g., the ER)[279] (Figure 4.1A,B). The proteins responsible for OMM fusion are heterodimeric complexes made up of mitofusin-1 (Mfn-1) and mitofusin-2 (Mfn-2) belonging to the dynamin-related family of GTPases (Figure 4.1B).[280] After OMM fusion is complete, a combination of short and long variants of the cristae-localized inner mitochondrial membrane (IMM) protein OPA-1 creates homodimers with adjacent OPA-1 molecules (Figure 4.1B);[281] additionally, OPA-1 helps sustain cristae structure- a crucial component of OXPHOS efficiency.[282,283] Substrates provided by the TCA cycle and FAO donate electrons to be transferred through ETC complexes I-IV as protons are pumped out of the mitochondrial matrix and into the intermembrane space, which will then be pumped back into the mitochondrial matrix by ATP synthase (complex V) to generate ATP (Figure 4.1C).

Together with pH (proton concentration), mitochondrial transmembrane potential ($\Delta\psi m$; the electrochemical proton gradient) generates the protonmotive (Δp) force that orchestrates H^+ flux across the IMM (Figure 4.1C).[284] During electron transfer through complexes I, II, and III, electrons prematurely leak into the intermembrane space with most electron leak coming from iron-sulfer clusters in complexes I and II.[285,286] Electron leak leads to the generation of mitochondrial ROS, primarily superoxide ($O_2\bullet^-$) (Figure 4.1 C). Mitochondrial $O_2\bullet^-$ can be further reduced by manganese-superoxide (Mn-SOD) to yield hydrogen peroxide (H_2O_2) radicals (Figure 4.1C). Low levels of ROS are vital to cell viability and proper immune function,[287-289] whereas excess production can be cytotoxic.[272,274] ROS levels can also influence T cell lineage as demonstrated by impaired Th17 differentiation/function under high ROS levels.[290,291] In summary, OXPHOS activity is influenced by important determinants of mitochondrial function such as the electrochemical gradient, mitochondrial biogenesis and mass, membrane dynamics, and ROS production. Higher T-cell OXPHOS activity in preT2D

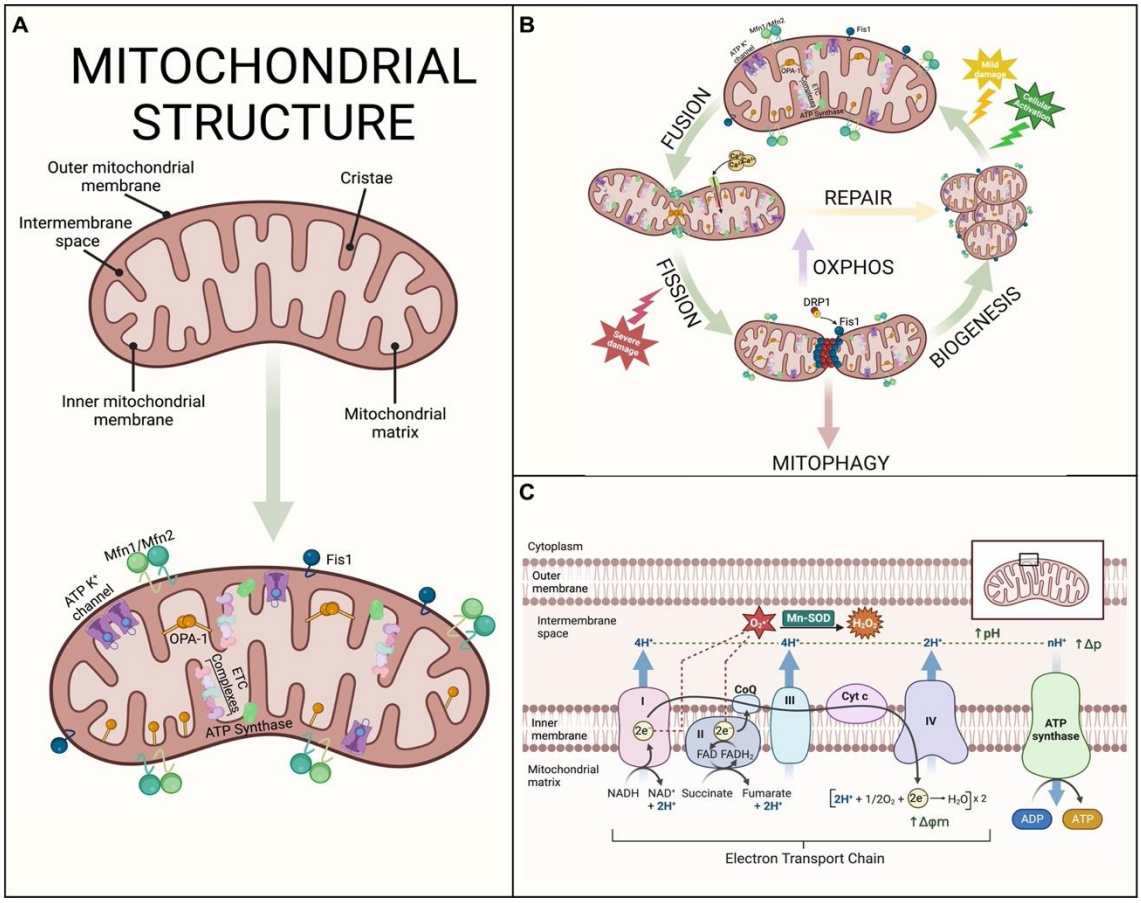

Figure 4.1 Schematic diagram of mitochondrial structure, membrane dynamics, OXPHOS activity and ROS production

(**A**) Mitochondrial components and matrix are separated by an outer membrane, intermembrane space and inner membrane. The outer membrane contains membrane dynamics proteins Fis-1 (fission) and dimeric complexes of Mfn-1 and Mfn-2 (fusion). The inner membrane contains ETC complexes I-IV and ATP synthase within cristae. Cristae structure and inner membrane fusion are maintained by the OPA-1 protein. (**B**) Cellular activation or mild cellular stress stimulate mitochondria to fuse by homotypic Mfn-1/Mfn-2 and OPA-1 interactions, supporting increases in OXPHOS by opening of ATP-sensitive K+ channels, Ca^{2+} influx, and cristae tightening. Under mild stress, fusion mitigates mitochondrial damage by mixing matrix content then separates by fission mediated by Fis1 recruitment of phosphorylated cytoplasmic DRP-1. Activation-induced fission events enhance mitochondrial abundance (biogenesis); however, severe stress/ will increase rate of fission to induce mitophagy. (**C**) Reducing equivalents NADH and $FADH_2$ donate electrons, passed through complexes I-IV as protons are pumped into the intermembrane space, with consequential superoxide and peroxide production from electron leak. Increases in proton concentration (pH) and the electrochemical gradient ($\Delta\varphi m$) drive protonmotive force (Δp) to pump protons back into the mitochondrial matrix through ATP synthase, generating ATP.

suggests potentially enhanced mitochondrial function. To begin to identify the mechanism(s) driving high T-cell OXPHOS in preT2D, we measured mitochondrial function parameters in total $CD4^+$ T cells in age-matched cohorts with either a lean BMI and NGT (lean NGT), or an obesity BMI with either preT2D or T2D since inflammatory profiles generated from T cells from preT2D and obese NGT donors were too similar to distinguish in previous bioinformatic models,[241] and to keep comparisons consistent with previously published data.[45]

4.2 Materials and methods

4.2.1 Donor description and demographics

Recruitment method, inclusion criteria, and exclusion criteria were as described in chapter 2. Cohorts for this study were age-matched and obesity cohorts were BMI-matched as described in Table 4.1. A list of medications as they relate to inflammation and/or glycemic control are outlined in Table 4.2.

Table 4.1 Description of human donors

	Lean + NGT	Overweight/obesity + preT2D	Overweight/obesity + T2D
Age, years (median [range])	47 (36 – 61)	56 (39 – 64)	56 (45 – 62)
BMI, kg m^2 (median [range])	23 (18 – 24)[&†]	37 (28 – 43)	35.5 (29 – 35)
FBG, mg dl$^-$ (median [range])	98 (93-98) 6/13	101 (90-116) 9/19	Not measured for T2D donors*
A1c, % (median [range])	5.2 (4.9 – 5.4) 6/13	5.5 (4.8 – 6.5) 13/14	6.8 (5.4 – 7.7) [†‡] 7/7
Total *N*	13	14	7
Females	11	12	2
Males	2	2	5
White	12	14	5
Black/AA	0	0	2
Native American	1	0	0

*Clinical diagnosis of type 2 diabetes sufficient for subjects on glycemic control drugs; NGT or preT2D was confirmed in some subjects based on 2hr oral glucose tolerance test blood glucose measures (not shown).

[&] Indicates a significant difference between leanNGT and T2D donors based on Student's t-test ($P < 0.05$)

†Indicates a significant difference between leanNGT and T2D donors and ‡significant difference between preT2D and T2D donors based on Student's t-test ($P < 0.05$)

Table 4.2 List of glycemic and lipid control medications and smoker status

Medications	LeanNGT	preT2D	T2D
Metformin (*N*)	0/13	0/14	5/7
Thiazolidinediones (*N*)	0/13	0/14	0/7
DPP-4 Inhibitors (*N*)	0/13	0/14	1/7
Sulfonylureas (*N*)	0/13	0/14	0/7
Statins (*N*)	0/13	4/14	6/7
ACE Inhibitors (*N*)	0/13	2/14	1/7
SGLT2 Inhibitors (*N*)	0/13	0/14	2/7
GLP-1R agonists (*N*)	0/13	0/14	027
Smoker (*N*)	0/13	0/14	0/7

4.2.2 Mitotracker probes

To quantify mitochondrial transmembrane potential and mass, we utilized mitochondrial fluorescent probes mitotracker red CMXRos (Invitrogen) and mitotracker green (Cell Signaling Technology, Danvers, MA) at 400nM and 40nM concentrations, respectively, in resting and CD3/CD28-stimulated total $CD4^+$ T cells. Mitotracker red is a fixable dye, whereas mitotracker green is not fixable; therefore, we quantified mitotracker red MFI by flow cytometry as demonstrated in the literature[292] and mitotracker green MFI by a microplate reader at 490nm. Both dyes were resuspended in DMSO then brought to their respective concentrations in pre-warmed complete RPMI lacking phenol red (Gibco). Cells were pelleted and resuspended in 100μL of each probe, separately. Cells stained with either dye were transferred to black flat-bottom 96-well plates (Grenier Bio-One, Monroe, NC). Both plates were covered with non-clear plate lids to protect from light. Cells stained with either dye were incubated for 30 minutes at 37°C with 5% CO_2.

During the last 10-minutes of incubation, FCCP (100nM) was added to control wells in the mitotracker red plate as a positive control for staining. After incubation, cells stained with mitotracker green were immediately measured for fluorescence at 490 nm in a ThermoFisher Scientific Varioskan Lux microplate reader. Cells stained with mitotracker red quickly underwent magnetic bead removal, then were pelleted, and resuspended in a master mix of Zombie NIR viability stain (BioLegend) and anti-CD4-FITC (BioLegend, Clone OKT4, anti-human) at 1:250 and 1:200, respectively, in 1X DPBS. Cells were incubated, in the dark, at room temp for 15-minutes, washed, then pelleted. Cells were fixed with 1% PFA/DPBS and stored at 4C for no more than 24hr after staining if cells were not immediately analyzed by flow cytometry. Single-stained cells were used as compensation controls, including unstained cells.

4.2.3 Quantitative real-time PCR

Resting and CD3/CD28-stimulated (40h) total $CD4^+$ T cells were harvested and used for genomic DNA (gDNA) isolation using the DNeasy blood and tissue kit (Qiagen, Germantown, MD) and the manufacturer's protocol for cultured cells. Purity and yield of gDNA was quantified using a nanodrop (Life Technologies, Carlsbad, CA), and only samples yielding a 260/280 ratio of ~1.8 were used for qPCR analysis. Samples and primers were prepared per the manufacturer's instructions for a standard curve assay using SYBR green (Life Technologies). For the standard curve, samples that were treated with CD3/CD28 beads were pooled (10μL each) and measured for gDNA purity and yield. DNA samples from cells that were not stimulated (i.e., resting) were pooled and quantitated by nanodrop, and were used as the calibrant for normalization. The standard curve was created by four 1:10-fold serial dilutions of pooled stimulated samples. Primer sequences (purchased from IDT and designed as published)[293] are listed in table 4.3. Lyophilized primers were reconstituted in 1X Tris-HCl/EDTA (TE) buffer to make a 100μM stock. Primer stocks were diluted to a final concentration of $8x10^3$ nM and each DNA sample was diluted in 1X TE buffer to 5ng/μL per the manufacturer protocol, and aliquoted (stored at -20°C). Primer and DNA sample aliquots were

discarded after 2 freeze-thaw cycles. SYBR green master mix volumes used were as listed in the manufacturer protocol. Each plate included one mitochondrial DNA (mtDNA) and one nuclear DNA (nDNA) target in addition to the 2 housekeeping genes actin and ubiquitin cyclase 9 (UBC9), both of which were previously identified as having stable expression in primary human T cells.[294] PCR plates were analyzed by a QuantStudio 6 (Life Technologies) using the SYBR standard curve assay protocol. Data were analyzed per the published protocol from Dr. Philip Kern's lab[293] by comparing the geometric Ct mean of mtDNA targets to that of nDNA targets. Fold-change for each sample was normalized to each housekeeping (ΔCt) gene and compared to the calibrant ($2^{-\Delta\Delta Ct}$). These experiments were performed with the help of Anne Caroline Hawk, a rotating student in the UKY Integrated Biomedical Sciences Program.

Table 4.3 PCR Primer Sequences

Target	Description	Forward	Reverse
Mt-ND1	NADH dehydrogenase 1 (Complex I subunit)	GGGCTACTACAACCCTTCGC	TGGTGAGAGCTAAGGTCGGG
Mt-ND4	NADH dehydrogenase 4 (Complex I subunit)	CATAATCGCCCACGGGCTTA	GGTAAGGCGAGGTTAGCGAG
Mt-ND6	NADH dehydrogenase 6 (Complex I subunit)	ATTCCCCCGAGCAATCTCAAT	CGGGAGGATCCTATTGGTGC
NEB-1	Nuclear envelope budding-1	GGCACCTCTTGATATGCTCC	TATGCCTTCTTGGCAAGGTCC
BECN-1	Beclin-1	GAAGTTTTCCGGCGGCTAC	CCGTCACCCAAGTCCGGT
CYPB	Cyclophilin-B	CCTCTCCGAACGCAACATGAA	CTTTGGGCCCCTTCTTCTTCT
ACTB	Actin	GAGCACAGAGCCTCGCCTTT	CGCGGCGATATCATCATCCAT
UBC9	Ubiquitin cyclase 9	CTGGAAGATGGTCGTACCCTG	GGTCTTGCCAGTGAGTGTCT

4.2.4 ROS Measurements

Total $CD4^+$ T cells were incubated in 96-well U-bottom tissue-treated cell culture plates (Falcon) with CD3/CD28 beads for 40h at a total density of $2.5x10^5$ cells/well (experiments performed by G.H. Kalantar). After incubation, cells were

pelleted and resuspended in complete phenol red-free RPMI 1640 containing fluorescent dyes that act as free radical sensors against total superoxide by dihydroethidium (DHE), total peroxides by 2',7'–dichlorofluorescin diacetate (DCFDA) fluorescence (ThermoFisher Scientific), and mitochondrial superoxide by MitoSOX Red (Invitrogen) per the manufacturer's instructions with unstained cells in media used as a blank (experiments performed by S. Santa-Cruz Calvo). Cells were plated in a black 96-well optical flat-bottom plate (Greiner Bio) to protect from light reactivity and fluorescence was measured by a ThermoFisher Scientific Varioskan Lux microplate reader at 518/606 nm (DHE), 472/517 nm (DCFDA), and 396/610 nm (MitoSOX Red).

4.2.5 Western Blot

Total $CD4^+$ T cells were incubated with CD3/CD28 beads for 40h. Cells were harvested and pelleted, then lysed in 35-40μL 1X cell lysis buffer (Cell Signaling Technology) containing a protease/phosphatase inhibitor cocktail (Invitrogen), on ice for 30 minutes with agitation by vortex every 10 minutes. Cell lysates were pelleted to remove debris at 13,000 rpm for 15 minutes at 4°C. Supernatants were transferred to fresh tubes and kept on ice. Protein quantity was measured using the Pierce BCA assay (ThermoScientific) per the manufacturer's protocol, adjusting for loaded sample volume (5μL) while keeping the volume of BCA standards the same. Lysates exceeding $2x10^6$ cells were diluted 5-fold with ddH2O. Sample volumes were calculated for desired protein concentration (20μg) and were diluted in 1X cell lysis buffer containing Laemelli buffer and β-mercaptoethanol, boiled at 95°C for 5 minutes. Proteins were separated by SDS-PAGE in 10-well 4-20% polyacrylamide gels (Bio-Rad) at 100V for 20 minutes, then 140V for 40-55 minutes. Separated proteins were transferred to polyvinylidene difluoride (PVDF) membranes that were activated by HPLC-grade methanol for 10 minutes, at 100V for 100 minutes. Successful protein transfer was determined by incubating membranes in Ponceau S stain for 5 minutes, washed 3x with 1X TBS containing 0.5% Tween-20 (TBST) (Bio-Rad) then blocked with 5% BSA/TBST for 1hr. After blocking, BSA solution was discarded and primary

antibody (clones and dilutions listed in Table 5.3) in 3% BSA/TBST was added for overnight incubation at 4°C with gentle rocking. The next day, membranes were washed 3x with 1X TBST, incubated at RT with HRP-conjugated secondary antibody for 1hr followed by the wash step. Membranes were incubated at RT for 5 minutes with a 1:1 ratio of Clarify ECL substrate (Bio-Rad) and visualized by chemiluminescence with a Bio-Rad ChemiDoc. Because most of the fusion and fission markers had similar molecular weights, membranes were stripped 5x using Pearce Stripping buffer at room temp for 22 minutes and washed 3x with 1X TBST before re-blocking and re-probing. Protein expression was quantified using the ImageJ software and normalized to β-actin expression (loading control).

4.2.6 Confocal microscopy

$CD4^+$ T cells were cultured for 40h with αCD3/αCD28 beads. The cells were collected and plated on poly-D-lysine coated coverslips in 12-well plates (Corning). The cells were centrifuged (1200 rpm, 10 min using the Thermo Sorvall refrigerated centrifuge with a TX-750 rotor set to room temp), washed 2x with 1X PBS and incubated in 4% paraformaldehyde for 30-min at room temp. The coverslips were washed 2x with PBS and 0.1% triton X-100 (PBST) and shipped on ice packs to Merrimack college for imaging by Dr. Leena Bharath. For imaging, the coverslips were washed 2X with PBST and were blocked for 30 min in 5% BSA/PBST. Antibodies to LC3, LAMP-1, and pSer616-DRP1 (Cell Signaling Technology) were added at a 1:50 dilution for overnight incubation at 4ºC. The coverslips were washed 2x with PBST and incubated with fluorophore-tagged secondary antibodies 1:500 (anti-mouse Alexa 488 or anti- rabbit Alexa 680) (Rockland Immunochemicals, Limerick, PA) for 2h at RT. The coverslips were washed 2x with PBST and mounted on glass slides using Fluromount G (Southern Biotech, Birmingham, AL). Cell imaging along with Z-stack captures were performed using 63X oil immersion lens in a Zeiss LSM 800 confocal microscope. Approximately 3-4 cells/field and 3-4 fields/slide were imaged for each donor and data were analyzed using FIJI/Image J.[295,296] Microscopy images were processed as described.[297] Expression of proteins were reported as MFI and colocalization

between two proteins were reported as Pearson's Colocalization Coefficient (PCC). PCC is a well-established method that quantifies the degree of overlap between fluorescence in the channels. PCC is unaffected by changes to the offset and is independent of gain. PCC has a range of +1 (perfect correlation) to −1 (perfect but negative correlation). PCC is not sensitive to differences in signal intensity between the components of an image caused by different labeling with fluorochromes, photobleaching or different settings of amplifiers.[298,299]

4.2.7 Statistical analysis

We used GraphPad Prism v8 to prepare figures and assessed differences by a one-way ANOVA or two-way ANOVA with Bonferroni's multiple comparisons as they apply (described in figure legends).

4.3 Results

4.3.1 Functional mitochondria and lower autophagy are indicative of higher bioenergetics in preT2D T cells

ETC complexes assembled throughout cristae can simultaneously display different $\Delta\psi m$ intensities, owing to the tightening of cristae upon increased respiration, which allows for enhanced OXPHOS efficiency.[300-304] Abnormally low $\Delta\psi m$ can be indicative of damaged or dying mitochondria whereas increasing $\Delta\psi m$ indicates magnitude of OXPHOS activity.[284,292] To identify whether high OXPHOS activity in $CD4^+$ T cells from preT2D donors is explained by alterations in $\Delta\psi m$, we stimulated total $CD4^+$ T cells from lean NGT, preT2D, and T2D donors (Table 4.1) and stained cells with the mitotracker red CMXRos probe (Figure 4.1A), which passively diffuses across the plasma membrane and accumulates in mitochondria based on $\Delta\psi m$. As expected, membrane potential increases upon T-cell activation (Figure 4.1B), which is comparable amongst cohorts. Treatment of cells with FCCP confirms the dye's accumulation is dependent on $\Delta\psi m$ (Figure 4.1B). These data suggest that high OXPHOS in preT2D T cells is not a consequence of

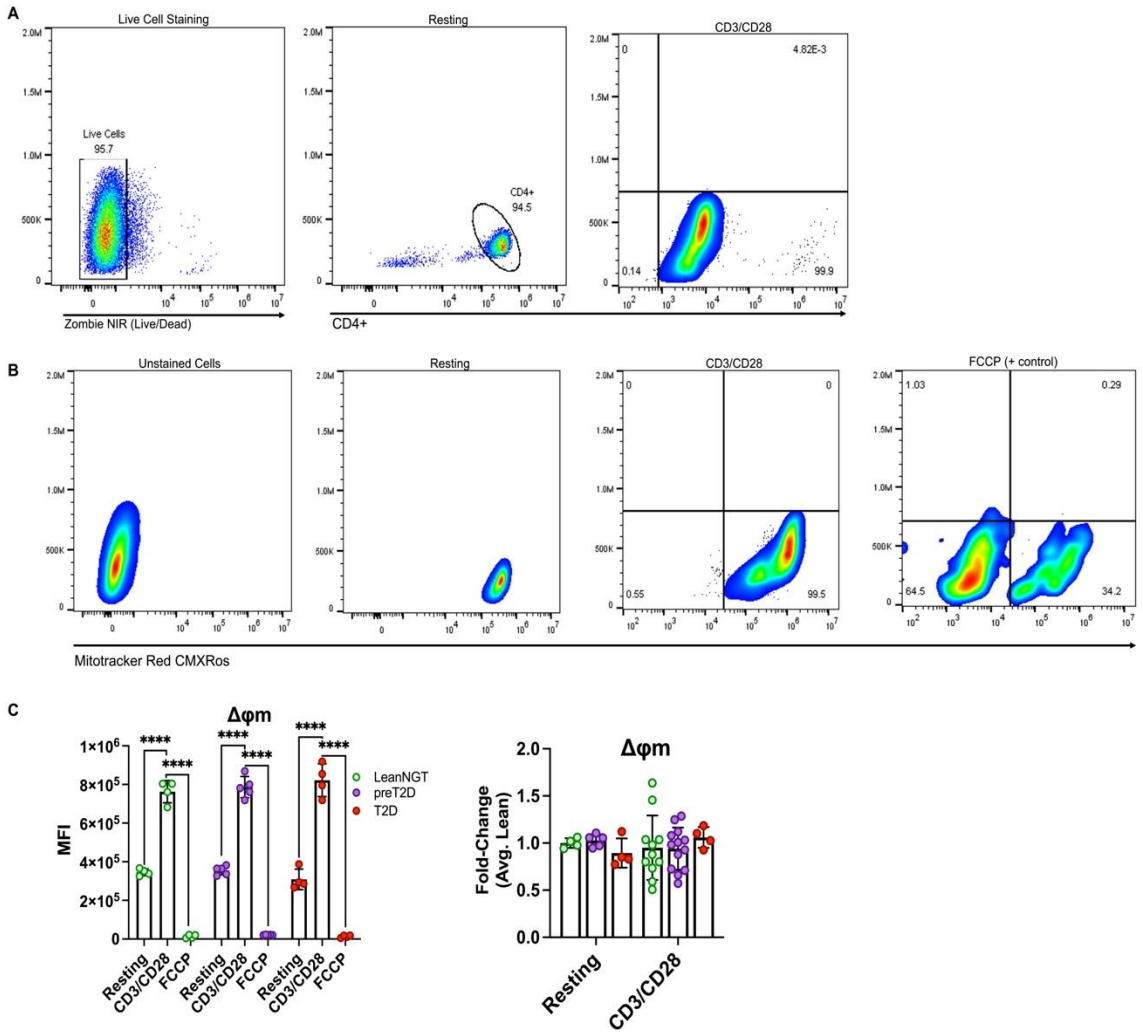

Figure 4.2 Mitochondrial transmembrane potential remains functional in T cells from preT2D and T2D donors

Mitochondrial transmembrane potential was measured by mitotracker red staining and flow cytometric analysis in total CD4⁺ T cells from lean NGT (green), preT2D (purple), and T2D (red) donors after 40h +/- CD3/CD28 stimulation. Gating strategy and purity check for (**A**) live CD4⁺ cells under resting (middle) or stimulated (right) conditions. (**B**) Mitotracker red staining of unstained cells (left- negative control), resting cells (middle left), stimulated cells (middle right) and FCCP-treated stimulated cells as a positive control of mitotracker staining (left- FCCP treated cells represented in lower left quadrant as mitotracker negative). (**C**) Mitotracker red MFI under the described conditions (left) and fold-change to the average of the leanNGT group per condition (right). Bars represent average and SD. Differences were assessed by two-way ANOVA and Bonferroni's multiple comparisons. ****$p < 0.0001$.

enhancements in $\Delta\psi m$ nor does it seem that T cell mitochondria become dysfunctional, even in T2D.

ROS are produced at low-moderate levels as a natural consequence of cellular respiration. Higher respiratory activity could generate excess ROS if antioxidants fail to concomitantly increase, potentially eliciting pathogenic changes. To further confirm whether T-cell mitochondrial dysfunction, as indicated by excess ROS, associates with T2D pathogenesis, we measured ROS production by fluorescent probes against total superoxide, mitochondrial superoxide, and total peroxides as three distinguishable ROS species. Stimulated $CD4^+$ T cells from preT2D and T2D donors exhibited normal levels of ROS production (Figure 4.2A) as compared to lean NGT donors, except mitochondrial superoxide being lower in T2D T cells (Figure 4.2A- middle). Lower mtROS in T2D T cells could be due to metformin usage.[81,87,305] Alternatively, lower mtROS could be a consequence of the T2D-associated Th17 cytokine profile as Th17 cells require low to moderate amounts of ROS, particularly mtROS, for differentiation and function.[291,306] These data suggest that preT2D T cells do not produce more ROS despite higher OXPHOS and thus T-cell mitochondria are likely not stimulating ROS accumulation. We conclude that high OXPHOS is preT2D is not associated with pathogenic effects that eventually initiate mitochondrial dysfunction.

Mitochondria play an essential role in regulating autophagy. Moderate to high levels of ROS produced during OXPHOS activity has been shown to support autophagy by activation of autophagy-regulating protease 4, which is required for microtubule-associated protein 1A/1B-light chain 3 (LC3) deconjugation from phosphatidylethanolamine. Unconjugated LC3 and lysosomal associated membrane protein 1 (LAMP-1) can co-localize for autophagosome formation.[307] Moreover, the selective form of autophagy, mitophagy, utilizes already formed autophagosomes and initiates autophagosome formation, thus autophagosome formation measurements can also be an indirect indicator of mitophagy. To assess whether autophagy changes in T cells during T2D pathogenesis, we prepared stimulated total $CD4^+$ T cells for confocal microscopy to quantify autophagosome formation by LC3 and LAMP-1 expression and co-localization (Figure 4.3B).

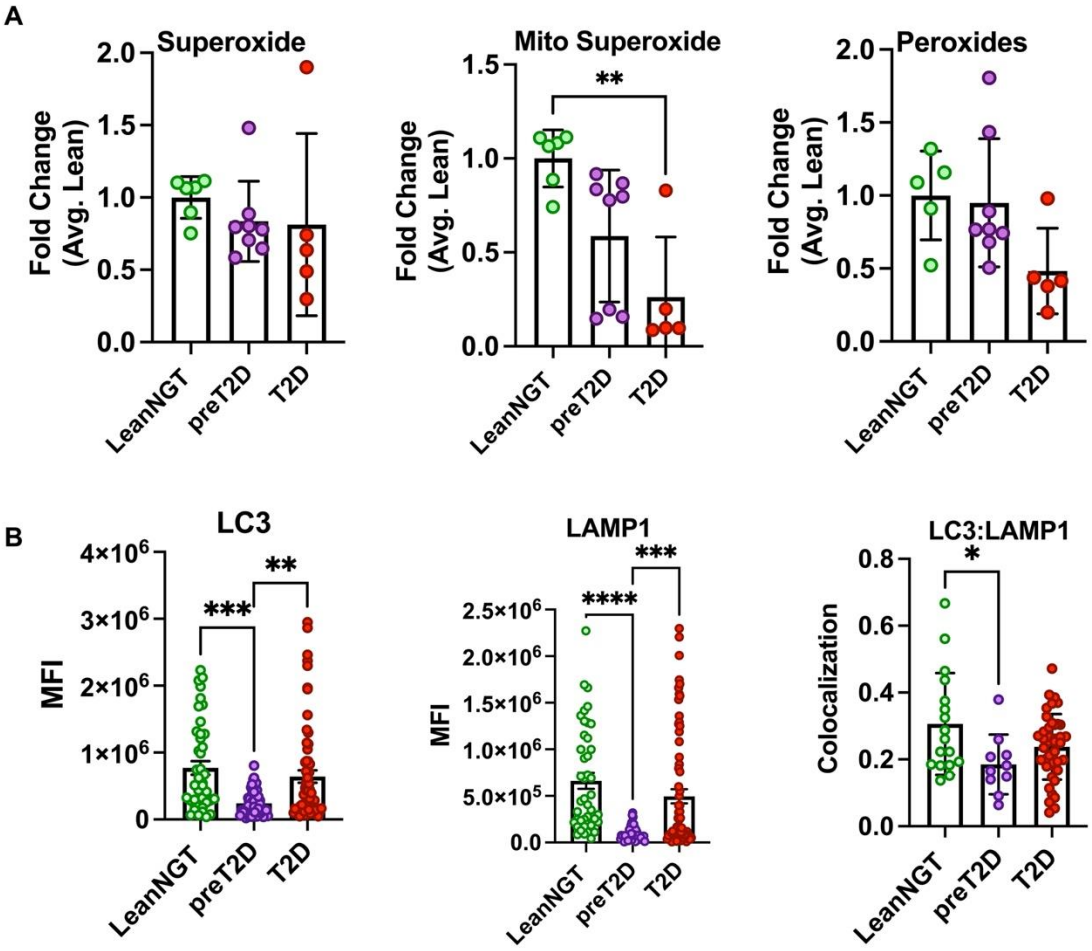

Figure 4.3 High T-cell OXPHOS in preT2D does not associate with oxidative stress or enhanced autophagy

ROS production and autophagosome formation was measured and quantified in total $CD4^+$ T cells from leanNGT, preT2D, and T2D donors after 40h stimulation. (**A**) Intracellular total superoxide (left), mitochondrial superoxide (middle), and total peroxide (right) production. (**B**) Confocal microscopy quantification of autophagy markers LC3 (left), LAMP-1 (middle), and colocalization to measure autophagosome formation (right). Bars represent average and SD. Differences were assessed by a one-way ANOVA and Bonferroni's multiple comparisons. *$p < 0.05$; **$p < 0.01$; ***$p < 0.001$; ****$p < 0.0001$. ROS measurements and data analysis in panel A was performed by S. SantaCruz-Calvo. Data in panel B were quantified and analyzed by L.P. Bharath.

Individual expression of LC3 and LAMP1 was comparable between lean NGT and T2D donors but was significantly lower in preT2D T cells (Figure 4.3B- left, middle). Likewise, autophagosome formation was lower in preT2D (Figure 4.3B- right). Lack of increased cellular turnover was expected as ROS did not exceed normal levels, as established by lean NGT donor cells. Lower rates of autophagy are reflective of higher metabolic activity since activation of nutrient sensors like mTORC1 prevents autophagosome formation;[216] therefore, high T-cell OXPHOS in preT2D donors might protect T cells from autophagy.

4.3.2 Mitochondrial mass and membrane dynamics are not altered in T cells from preT2D donors

The net balance between mitochondrial formation and degradation, defined as mitochondrial. mass, is a key indicator of mitochondrial function.[308] To determine if high OXPHOS in preT2D T cells is a consequence of changes in mitochondrial mass and/or abundance, we stained resting and stimulated $CD4^+$ T cells with the fluorescent mitotracker green (MtG) probe, which accumulates in the mitochondrial matrix independent of $\Delta\psi m$. Greater accumulation of MtG can denote greater mitochondrial matrix content (i.e., mitochondrial formation), whereas less accumulation of MtG can be indicative of lower matrix content (i.e., mitochondrial degradation). MtG MFI was indistinguishable between resting and stimulated T cells (Figure 4.4A- left) and was comparable amongst cohorts (Figure 4.4A- right). Comparable mass between resting and stimulated conditions is surprising considering that cellular quiescence is associated with smaller mitochondria with a spherical morphology, which is an early indicator of mitophagy; however, this has only been demonstrated in yeast.[309] Stimulation of $CD4^+$ T cells may ultimately support mitochondrial biogenesis through balanced fusion and fission rather than sustaining and/or enhancing mitochondrial formation as demonstrated in T_{eff} cells;[310] therefore, mitochondrial mass changes may not be detected by MtG staining as mitochondrial morphology could be similar in resting and stimulated T cells. It's worth noting that MtG probes are an imperfect measure

of mass with claims of sensitivity to fluctuations in $\Delta\psi m$, but this has been demonstrated only in HeLa cells and is contradicted by data in other studies.[311,312]

We next quantified relative abundance of mtDNA to nDNA by SYBR green master mix and qRT-PCR to determine if changes in mitochondrial abundance help explain high T-cell OXPHOS in preT2D T cells. Abundance of mtDNA and the mtDNA/nDNA ratio was comparable amongst cohorts (Figure 4.4B,C). Moreover, mtDNA abundance was 2- to 6-fold higher in stimulated cells compared to the calibrator (resting T cells) as represented by $2^{-\Delta\Delta Ct}$ (Figure 4.4C). These data indicate that comparable mitotracker green intensity between resting and stimulated cells may be due to morphological similarities between fragmented mitochondria and mitochondrial biogenesis; therefore, mitotracker green is likely more reflective of mitochondrial shape than abundance. Furthermore, mitochondrial mass and abundance did not differ amongst cohorts in activated T cells, suggesting that mitochondrial biogenesis and mtDNA abundance are not likely to be the cause of higher T-cell OXPHOS in preT2D.

Mitochondrial membrane dynamics tightly control OXPHOS activity, primarily through cristae remodeling.[301] Both mitochondrial biogenesis and mitophagy, mediated by fission proteins DRP1 and Fis-1, support increased OXPHOS activity. Mitochondrial fusion facilitated by Mfn-1/Mfn-2 heterodimers and OPA-1 homodimers promotes enhanced OXPHOS efficiency.[301,302,304] To identify if changes in mitochondrial fusion or fission explain high T-cell OXPHOS in preT2D, we quantified protein expression of fission and fusion markers in stimulated $CD4^+$ T cells by western blot analysis and confocal microscopy (Figure 4.5A,D). Total DRP1 and Fis-1 were not differentially expressed in T cells from preT2D or T2D donors compared to those of lean NGT donors (Figure 4.5B). Confocal microscopy quantification of pSer616-DRP1 expression (Figure

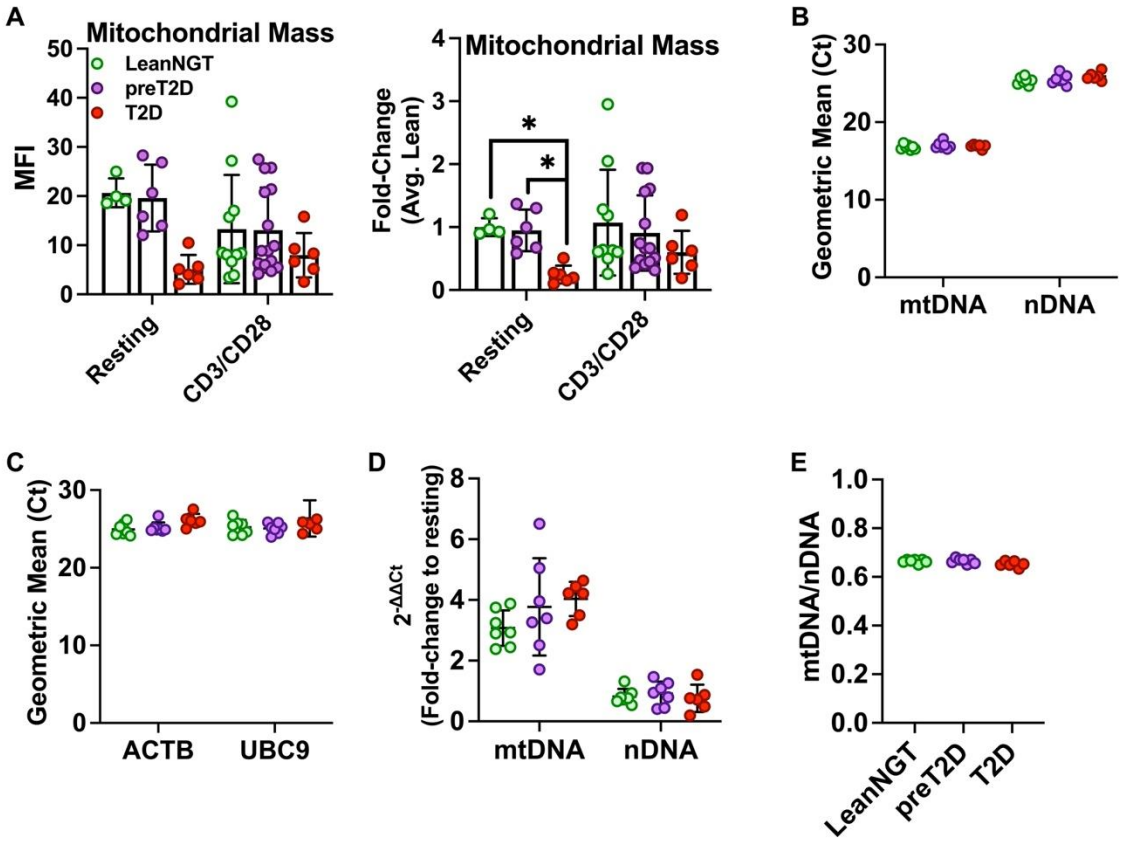

Figure 4.4 T cell mitochondrial mass and abundance are comparable amongst donor cohorts

(**A**) Mitochondrial mass was measured by fluorescent detection of mitotracker green in total $CD4^+$ T cells +/- CD3/CD28 stimulation (40h), represented as MFI (left) and fold-change to the average MFI of the leanNGT group resting cells or stimulated cells (right). Quantitative real-time PCR of mitochondrial DNA (mtDNA) targets and nuclear DNA (nDNA) targets to quantify mitochondrial abundance/biogenesis by the geometric mean of cycle threshold (Ct) values of mtDNA or nDNA targets (**B**) relative to actin and UBC9 housekeeping gene abundance (geometric mean of Ct values across plates) (**C**) and compared to pooled resting T cells (calibrant), represented as fold-change ($2^{-\Delta\Delta Ct}$) (**D**) and ratio of mtDNA to nDNA (**E**). Bars represent average and SD. Differences were assessed by a two-way ANOVA (**A-D**) or one-way ANOVA (**E**). *$p < 0.05$.

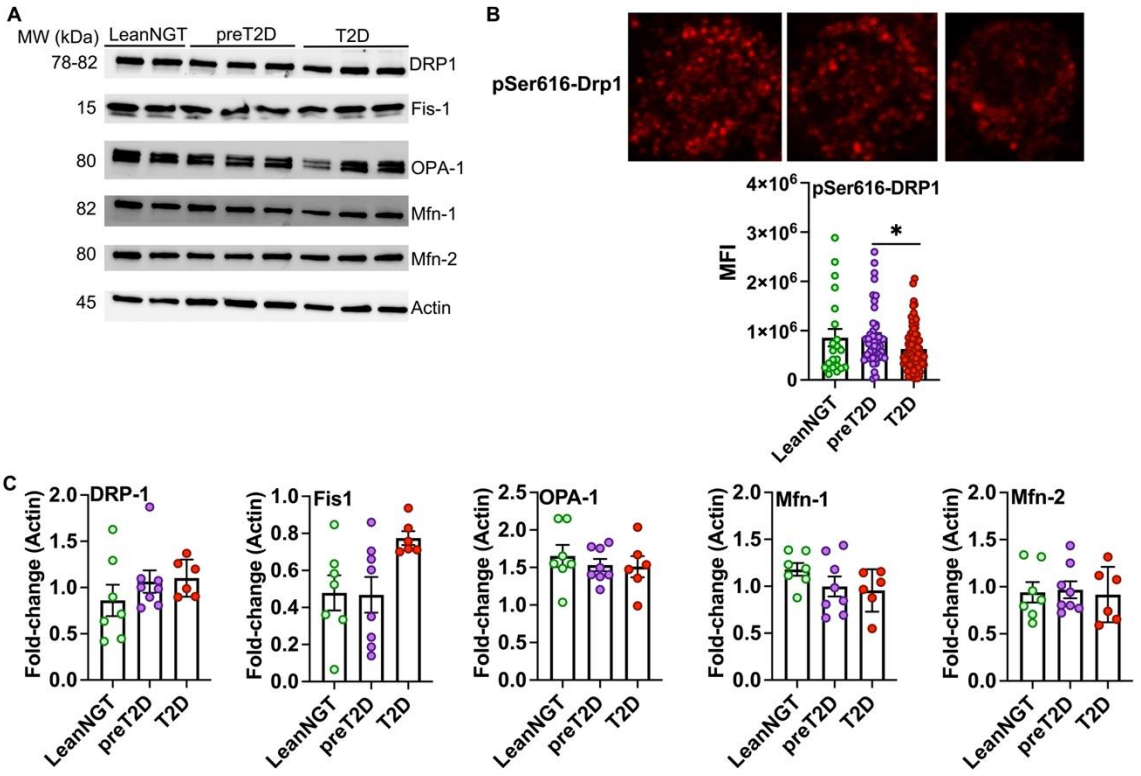

Figure 4.5 Mitochondrial membrane dynamics do not explain high OXPHOS in T cells in preT2D

Western blot (**A**) and confocal microscopy (**B**) quantification of mitochondrial fission markers pSer616-DRP1 (**B**), total DRP1, and Fis1**,** and fusion markers OPA-1, Mfn-1, and Mfn-2 (**C**) in total CD4⁺ T cells from leanNGT (green dots), preT2D (purple dots), and T2D (red dots) donors after 40h CD3/CD28 stimulation. Protein expression analysis by western blot is presented as fold-change to actin (leanNGT n = 7, preT2D n = 8, T2D n = 6). For confocal microscopy, approximately 3-4 cells/field and 3-4 fields/slide were imaged for each donor (leanNGT n = 5, preT2D n = 4, T2D n = 6). Differences were assessed by a one-way ANOVA with Bonferroni's multiple comparisons. *$p < 0.05$.

4.5D) revealed similar expression between lean NGT and preT2D or lean NGT and T2D groups (Figure 4.5D). However, pSer616-DRP1 MFI was modestly lower in T2D T cells compared to preT2D- another possible effect of metformin usage in T2D donors since it reportedly inhibits DRP1-mediated fission by reducing DRP1 GTPase activity.[313] Further assessment of mitochondrial fusion markers revealed no significant difference in protein expression by T cells from all 3 cohorts (Figure 4.5C). Together, these data imply that mitochondrial function is not compromised in T cells during preT2D or T2D, and high OXPHOS in preT2D T cells is unlikely a consequence of enhanced mitochondrial fission or fusion, hence higher OXPHOS in preT2D T cells remains unexplained and may rather be due to differences in mitochondrial fuel utilization, thus generating more ETC substrates and ultimately more ATP production.

4.4 Discussion

Enhanced T-cell bioenergetics in preT2D is not due to differences in $\Delta\psi m$ and ROS production, nor mitochondrial mass and quantity. Lower mitochondrial $O_2\bullet^-$ and pSer616-DRP1 in T cells from T2D donors could be attributed to metformin usage (Table 4.2), which has been shown to significantly reduce mitochondrial ROS production and DRP1 activation.[87,313] Alternatively, lower mitochondrial $O_2\bullet^-$ could be associated with the Th17 cytokine profile in T2D as low to moderate levels of ROS are required for Th17 differentiation and function.[290,291,306] Similarities in mitochondrial mass between resting and stimulated T cells could be due to harvesting cells at the 40hr time point. Mitochondrial biogenesis is usually associated with cellular proliferation and T cells do not undergo substantial proliferation *in vitro* within 40hr. Distinct T-cell proliferation is usually not detected until least 72hr post-stimulation and often requires IL-2 supplementation in the cell culture medium; however, similarities in mitochondrial morphology between resting and stimulated T cells is more likely since we demonstrated that mtDNA abundance increases upon stimulation, which is more reflective of mitochondrial biogenesis than total mitochondrial mass. Additionally, changes in membrane dynamics may be better detected earlier in T-

cell stimulation as in the first 12-24 hours, demonstrated by *ex vivo* retention of circadian regulation of membrane dynamics.[314] However, elevated OCR in preT2D T cells is observed at 40h post-stimulation, so higher rates of mitochondrial fusion or biogenesis are unlikely explanations for enhanced OXPHOS. Transmission electron microscopy would provide the best resolution for imaging mitochondria and could be most informative in confirming mitochondrial abundance and morphology in T cells.

Substrates from catabolic metabolism, predominantly from the TCA cycle, are supplied to the ETC to act as electron donors through complexes I-IV. Thus, high OXPHOS activity may associate with more available ETC complexes; however, this was not the case for T cells in preT2D donors, thus pointing to possible differential involvement of nutrient-sensing mechanisms in T-cell metabolic reprogramming. Metabolic reprogramming is associated with lower rates of autophagy from PI3K-Akt-mTORC1 activation in response to increased ATP levels.[181,182] Autophagy markers and autophagosome formation was lower in T cells from preT2D donors coincides with high metabolism in preT2D; therefore, supporting the idea that high T-cell OXPHOS in preT2D could be due to differences in mitochondrial fuel utilization rather than changes in mitochondrial function.

CHAPTER 5. GLUTAMINOLYSIS SUPPORTS HIGH METABOLISM AND CD4$^+$ T CELL INFLAMMATION IN T2D PATHOGENESIS

5.1 Introduction

High OXPHOS in preT2D T cells is not a consequence of higher mitochondrial mass/quantity, transmembrane potential, membrane dynamics, or ROS production. These parameters were also unchanged in cells from T2D donors, except lower pSer616-DRP1 and mitochondrial superoxide likely due to metformin usage, indicating that mitochondrial health and function are not altered in peripheral CD4$^+$ T cells during T2D pathogenesis. Autophagy is tightly regulated by nutrient-sensing mechanisms, particularly the PI3K-Akt-mTOR pathway.[315,316] Lower autophagosome formation indicated less autophagy in preT2D T cells, consistent with higher metabolic activity. Together these data point to the possibility that high T-cell OXPHOS in preT2D could be supported by enhanced fuel utilization and subsequent activation of nutrient-sensing pathways.

Both mTORC1 and mTORC2 promote cellular growth, survival, and differentiation. While mTORC2 supports glycolysis by sustaining Akt activation, mTORC1 is reported to have greater involvement in supporting cellular metabolism upon activation through promoting glucose uptake and glycolysis via HIF-1α activation,[317] TCA anaplerosis by glutamine uptake and glutaminolysis,[216] lipid metabolism through downstream activation of SREBP1 and PPAR-γ,[318,319] and OXPHOS by mitochondrial biogenesis. Moreover, different T cell subsets have been demonstrated to differentially rely on mTORC1 and mTORC2 activity. Th1 and Th17 cells are generally thought to depend more on mTORC1 activity for differentiation and effector functions, whereas mTORC2 activity is considered more critical for Th2 cells; however, these are generalizations that do not necessarily imply that one mTOR complex solely controls T-cell fate over the other complex. Given previous reports of metabolic reprogramming influencing T-cell function, we hypothesized that T cell inflammation and high OXPHOS in preT2D is due to changes in metabolic reprogramming, particularly through enhanced

mitochondrial fuel utilization- a probable consequence of the *in vivo* nutrient-rich environment of peripheral blood in obesity.

5.2 Objective

To uncover the mechanism that drives preT2D-associated T-cell inflammation and high OXPHOS, we designed manipulation experiments against TCA cycle anaplerosis to test the impact of three primary mitochondrial fuel sources in T cell metabolism and T_{eff} cytokine production: pyruvate, fatty acids, and glutamine. Cells typically upregulate one or more anaplerotic sources when another source dips to maintain replenishment of carbon loss during anabolism. Blocking the breakdown of each fuel source within the mitochondria effectively and feasibly allows for postulation of how each fuel contributes to baseline metabolism and inflammatory outcomes in NGT, preT2D, and T2D. Alterations in metabolic reprogramming offer potential clinical application in T2D prevention/delay strategies by revealing mechanisms that might become altered during preT2D that could serve as actionable goals against T2D pathogenesis.

5.3 Materials and methods

5.3.1 Donor description and demographics

Donors were recruited per the guidelines described in chapter 2 and are further described in Table 5.1 and Table 5.2. Most donors recruited to this study did not have FBG or A1c measured at time of blood collection, thus information for these parameters is limited.

Table 5.1 Description of human donors

	Lean BMI + NGT	Overweight/obesity BMI + preT2D	Overweight/obesity BMI + T2D
Age, years (median[range])	52 (36-67)	53 (36-66)	47 (37-62)
BMI, kg m^2 (median[range])	23 (18-24)[&,†]	34.6 (26 – 45)	35.5 (28-40)
FBG, mg dl^- (median[range])	Not measured for lean donors	101 (90-116) 9/19	Not measured for T2D donors*
A1c, % (median[range])	5.4 (5.2-5.4) 3/18	5.5 (4.8-6.8) 18/19	6.8 (5.4-10.8)[†‡] 15/16
Total *N*	18	19	16
Females	14	14	7
Males	4	5	9
White	16	18	11
Black/AA	0	0	5
Native American	2	1	0

*Clinical diagnosis of type 2 diabetes sufficient for subjects on glycemic control drugs; NGT or preT2D was confirmed in some subjects based on 2hr oral glucose tolerance test blood glucose measures (not shown).
[&]Indicates a significant difference between leanNGT and T2D donors based on Student's t-test ($P < 0.05$)
†Indicates a significant difference between leanNGT and T2D donors and ‡significant difference between preT2D and T2D donors based on Student's t-test ($P < 0.05$)

Table 5.2 List of glycemic and lipid control medications and smoker status

Medications	LeanNGT	preT2D	T2D
Metformin (*N*)	0/18	1/19	11/16
Thiazolidinediones (*N*)	0/18	0/19	0/16
DPP-4 Inhibitors (*N*)	0/18	0/19	1/16
Sulfonylureas (*N*)	0/18	5/19	3/16
Statins (*N*)	0/18	5/19	11/16
ACE Inhibitors (*N*)	0/18	3/19	4/16
SGLT2 Inhibitors (*N*)	0/18	0/19	2/16
GLP-1R agonists (*N*)	0/18	0/19	2/16
Smoker (*N*)	0/18	0/19	0/16

5.3.2 Cell manipulations: Total $CD4^+$ T cells

Total $CD4^+$ T cells were isolated, archived, and thawed as described in chapter 2. Both cell types were plated at a density of 10^6 cells/mL in either 6-well tissue culture-treated plates (total CD4s) or 24-well tissue culture-treated plates (Corning) and treated with vehicle (DMSO for all experiments involving treatments, Millipore Sigma), 10μM BPTES (Millipore Sigma), 3μM etomoxir (Millipore Sigma), UK5099 (2μM Tocris, Minneapolis, MN), or 100μM NV-5138 (MedChem Express, Monmouth Junction, NJ) and stimulated with CD3/CD28 beads. Total $CD4^+$ T cell cultures were subjected to a mitochondrial stress test as described in chapter 2.

5.3.3 Cell manipulations: T_{eff} cells

$CD4^+$ T_{eff} cells were isolated, archived, and thawed as described in chapter 2. T_{eff} cells were plated in 24-well tissue culture-treated plates (T_{eff}) and treated with vehicle, 10μM BPTES (Sigma Aldrich), 3μM etomoxir (Sigma Aldrich), 2μM

UK5099 (Tocris), 10μM dimethyl-2-ketoglutarate (DM2KG) (Cayman Chemical, Ann Arbor, MI), or 0.01μM everolimus (Sigma Aldrich) and stimulated with CD3/CD28 beads for 40h. DM2KG was added 20h and 32h post-stimulation since we demonstrated in chapter 3 that cytokine production does not begin to peak until after 20-hours of stimulation. Supernatants were harvested for cytokine measurements as described in chapter 2 and cell pellets were stored at -80°C, then lysed and quantified for protein by BCA assay as described in chapter 2 for protein expression quantification of mTORC1 activity by ELISA (section 5.3.5).

5.3.4 Lactate Measurements

Lactate concentration in cell culture supernatants from activated total CD4+ T cells harvested prior to extracellular flux analysis (experiments performed by G.H. Kalantar) was measured by a colorimetric assay kit (BioVision) (performed by Dr. Sara SantaCruz-Calvo). Cell culture supernatants were archived in -80 °C before analysis, then thawed and diluted by 100-fold for lactate concentration measurement. We experienced issues with oversaturation of samples compared to the standard curve, despite 100-fold dilution, which worked previously; therefore, data are displayed as MFI instead of concentration.

5.3.5 mTORC1 ELISA

T_{eff} cells described in section 5.3.3 were thawed from -80°C on ice, lysed, and used for protein quantification by BCA assay per the protocol described in chapter 4. To determine mTORC1 activity +/- BPTES treatment, Teff lysates were used for protein expression of total and pThr389-S6K detected by PathScan Sandwich ELISA kits (Cell Signaling Technology). Pilot experiments determined that 0.5ug of protein was sufficient for total S6K detection and 1.5ug of protein for pThr389-S6K. Sandwich ELISAs were performed per the manufacturer's protocol, bringing well volumes up to 25uL with sample diluent (individual dilution factors were calculated and used in data analysis), and samples were incubated overnight on the antibody-coated wells. Control cell extracts for total S6K (untreated MCF7 cells) and pThr389-S6K (IGF-1 treated MCF7 cells) (Cell Signaling Technology)

were used as positive and negative controls for each assay. Protein expression was determined using a ThermoFisher Scientific Varioskan Lux microplate reader to measure absorbance at 450nm.

5.3.6 Statistical analysis

We used GraphPad Prism v8 to prepare figures for individual cytokine measurements and extracellular flux analysis, and to assess differences by a two-way ANOVA or one-way ANOVA with Bonferroni's multiple comparisons where applicable. Significance was defined as $p < 0.05$.

Bioinformatic analysis was performed by Dr. Xiaohua Douglas Zhang and his mentee Shubh Saraswat in the department of statistics at the University of Kentucky. For the partial least square discriminant analysis (PLSDA),[241,251,320] cytokine data were log-transformed to mitigate skewing. Cytokines with a small range of values had the option to be as or more important than cytokines with a large range of values. We thus scaled each cytokine to zero mean and unit variance before applying PLSDA. We excluded 7 cytokines for further analysis because their concentration is lower than the LLOQ in every sample. The 7 excluded cytokines are "IL.15", "IL.1B", "IL.33", "IL.17E.IL.25", "IL.27", "IL.31", and "IL.28A". After all data preprocessing (based on exploratory analysis), PLSDA was applied mainly using the R function *splsda()* in the "mixOmics" package with the R version R4.2.2. The key comparisons of cytokine profiles included activated $CD4^+$ Teff cells from cohorts described in section 5.3.1 treated with vehicle versus UK5099, vehicle versus etomoxir, and vehicle versus BPTES treatment for each cohort. In each comparison, we used the first two PLSDA components to display the classification results based on the cytokines with variable importance in the projection (VIP) score greater than 1.

5.4 Results

5.4.1 Mitochondrial pyruvate import is dispensable for T-cell metabolism and effector cytokine production

Since mitochondrial traits and function are not altered in T2D pathogenesis, high OXPHOS in preT2D T cells may be due to enhanced mitochondrial fuel utilization; particularly, fuels that critically maintain TCA cycle anaplerosis and generation of reducing equivalents for the ETC. Therefore, we utilized pharmacological inhibitors against three primary mitochondrial substrates (pyruvate, fatty acids, and glutamine) to manipulate TCA cycle anaplerosis and ETC efficiency in activated $CD4^+$ T cells. We first tested the contribution of pyruvate oxidation to T-cell metabolism using UK5099, a cell-permeable α-cyanocinnamate compound that acts as a potent active site thiol modifier in the mitochondrial pyruvate carrier (MPC) to block the bidirectional transport of pyruvate across the IMM.[321] To avoid off-targets effects, such as blocking plasma membrane monocarboxylate transporters (e.g., lactate transporters), we used a concentration below 10μM as published.[322] A mitochondrial stress test revealed UK5099 did not change OCR nor ECAR in stimulated $CD4^+$ T cells across all cohorts (Figure 5.1A-B). As expected, OCR parameters such as basal, maximal, and ATP-linked respiration were also unchanged with MPC inhibition (Figure 5.1C), although spare respiratory capacity (SRC) was modestly reduced in the preT2D group (Figure 5.1C), indicating that mitochondrial pyruvate metabolism is modestly important for preT2D T cells to respond to increases in energy demand/stress. ECAR and secreted lactate were also unchanged by MPC inhibition. (Figure 5.1D). Together, these data suggest that pyruvate oxidation is dispensable for $CD4^+$ T-cell metabolism as T cells appear to sufficiently compensate for loss of pyruvate's contribution to the TCA cycle and is consistent with previous findings that MPC function does not impact pyruvate reduction.[220] Consistent with previously published in preT2D T_{eff} cells, total $CD4^+$ T cells from preT2D

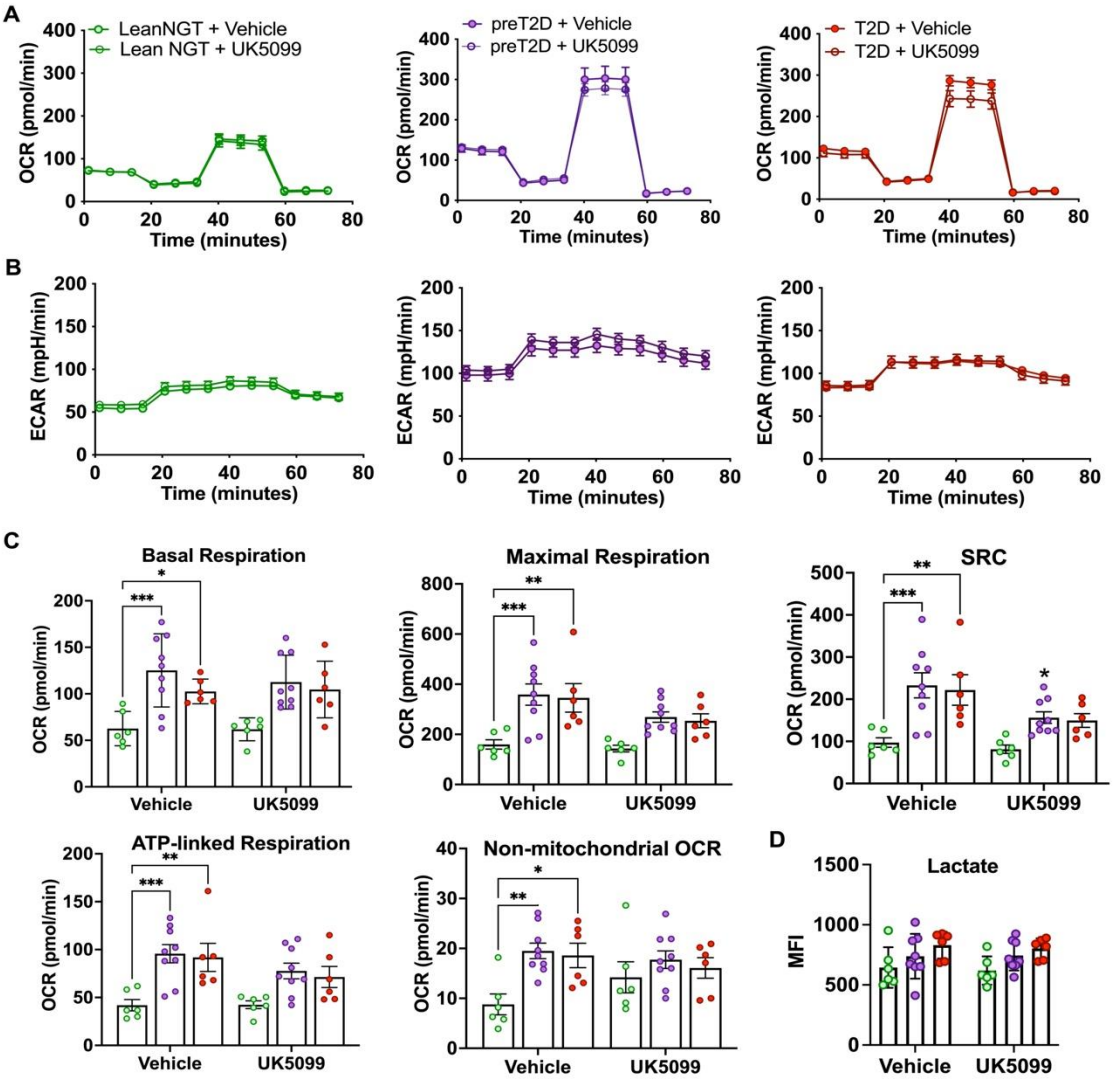

Figure 5.1 Mitochondrial pyruvate import minimally contributes to high T cell OXPHOS in preT2D

Mitochondrial stress test of CD3/CD28-stimulated total $CD4^+$ T cells treated with vehicle (DMSO- filled dots) or UK5099 (2μM- open dots) from LeanNGT (green dots- *n* = 6), preT2D (purple dots- *n* = 9), and T2D (red dots- *n* = 6) donors. OCR (**A**) and ECAR (**B**) plots as representations of OXPHOS and glycolysis, respectively. Dots at each time point represent the average OCR of samples as a group/treatment and plungers represent SEM. (**C**) OXPHOS parameters calculated as described in chapter 2. Bars represent average and SEM. Differences amongst cohorts by treatment and within cohorts by treatment were assessed by a two-way ANOVA with Bonferroni's multiple comparisons. *p < 0.05; **p < 0.01; ***p < 0.001.

donors display higher OXPHOS (Figure 5.1A), but also exhibit higher ECAR (Figure 5.1B), indicating overall higher metabolic threshold; however, no differences in secreted lactate were observed amongst cohorts (Figure 5.1D), consistent with our previously published data that high OXPHOS is the underlying mechanism driving differences in T cell function in preT2D. Total $CD4^+$ T cells from T2D donors also displayed higher metabolism similarly to preT2D, though closer examination of data distribution in OXPHOS parameters showed OCR in T2D T cells to be more similar to T cells from the lean NGT group as significance level was lower compared to preT2D comparison to lean NGT cells; therefore, these data are consistent with our previous work and potentially links similarities in metabolic reprogramming of T cells in preT2D to T2D pathogenesis.

To determine how mitochondrial fuel utilization impacts T-cell inflammation, we also inhibited the MPC in T_{eff} cells as stimulated T_{eff} cells, like total $CD4^+$ T cells, in preT2D displayed a unique cytokine profile from T2D and lean NGT donors.[45] PLSDA analysis revealed that overall cytokine production was increased with MPC inhibition (Figure 5.2A-B), independent of T2D risk/diagnosis, and displayed reliable model predictions (Figure 5.2A, accuracy $\geq$ 70% for all cohorts) despite the inability of MPC inhibition to change metabolism as measured by extracellular flux. Changes in cytokine production were similar amongst cohorts, particularly with increased Th2 cytokines ranked as the top predictors of MPC inhibition (Fig 5.2B, green labels). These data support previous reports that Th2 cells primarily utilize aerobic glycolysis for cytokine production.[235] Enhanced cytokine production (individually represented in Figure 5.2C-F) without changing bioenergetic requirements uncouples T-cell metabolism from function and highlights that certain metabolites likely have greater influence on effector function; therefore, we conclude that high T-cell OXPHOS in preT2D is independent of pyruvate oxidation.

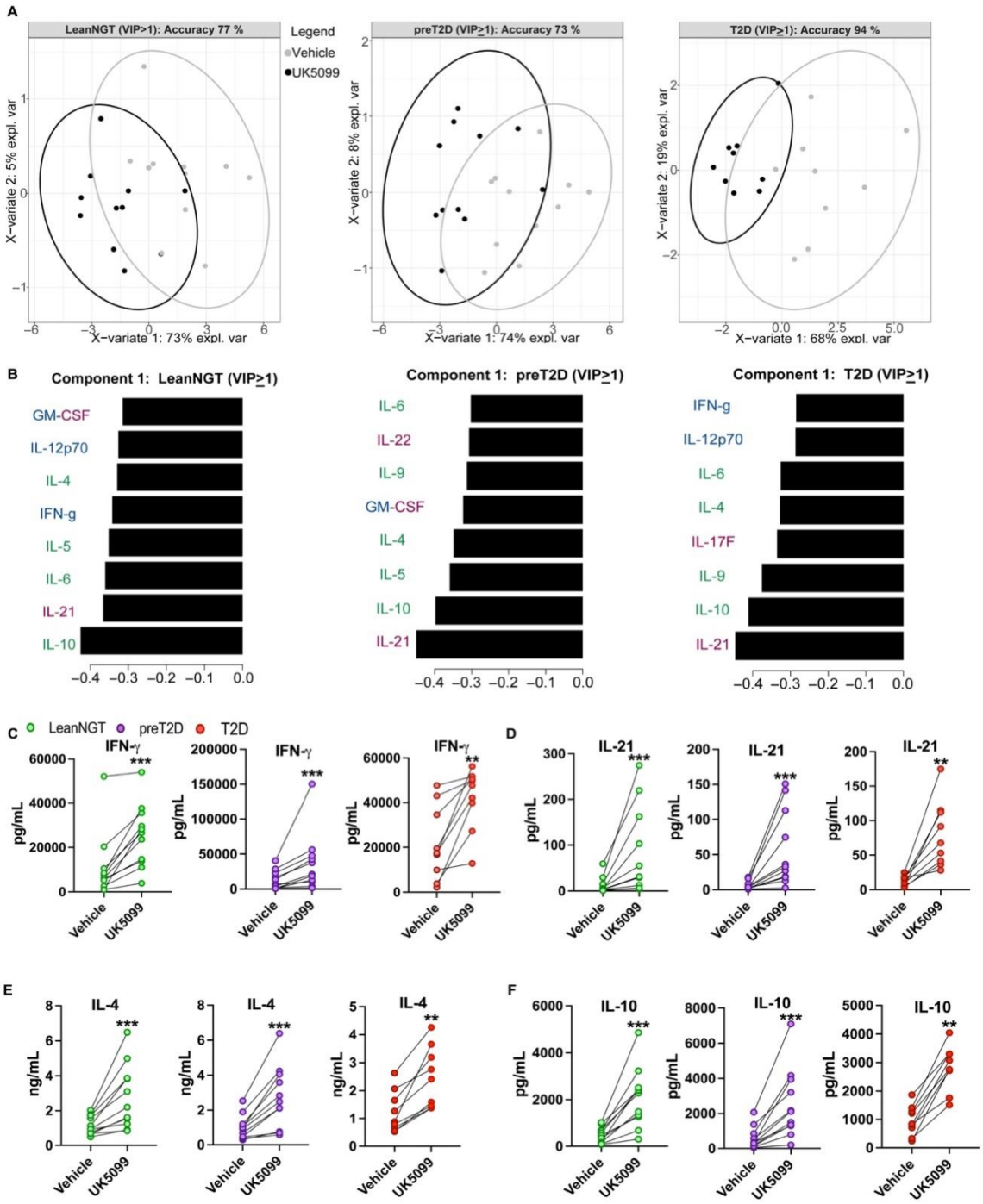

Figure 5.2 Mitochondrial pyruvate import uncouples T-cell metabolism from function

(**A-B**) PLSDA of inflammatory profiles generated by combining all cytokines measured after CD4⁺ Teff cell stimulation and treatment with vehicle (gray dots/bars) or UK5099 (black dots/bars) from leanNGT (left, *n* = 11), preT2D (middle, *n* = 11), and T2D (right- *n* = 9) donors showing (**A**) 2D projections of cytokine profiles in the first (most-distinguishing) component and **(B)** cytokines with a VIP score > 1 ranked from most (bottom) to least (top) important for defining treatment responses most *(continued on next page)*

Figure 5.2 (continued) characteristic of cells from the participant cohort indicated. Cytokines are color coded by T_{eff} subset as indicated- blue labels: Th1, green labels: Th2, and maroon labels: Th17. Representative cytokines for Th1 (**C**), Th17 (**D**), and Th2 (**E-F**) cells to show magnitude of treatment effect for each cohort. Differences assessed by paired two-tailed Wilcoxon test. **$p < 0.01$; ***$p < 0.001$. In panels A-B, data were analyzed and figures were generated by S. Saraswat and X.D. Zhang.

5.4.2 Blocking Cpt1a to limit FAO changes $CD4^+$ T-cell metabolism and T_{eff} cytokine production through disease-independent mechanisms

Thus far, we have demonstrated that high metabolism in total $CD4^+$ T cells associates with both preT2D and T2D, and is not reliant on pyruvate's contribution to the TCA cycle. Next, we used the FAO inhibitor etomoxir to test whether high OXPHOS in preT2D T cells, and now T2D T cells, is supported by FAO. Etomoxir is an irreversible inhibitor of the catalytic subunit of Cpt1a, which catalyzes the rate-limiting step of FAO. To avoid toxic effects of etomoxir such as loss of selectivity for Cpt1a and oxidative stress accumulation, thus creating impairments in OXPHOS, we used a low concentration of 3μM as previously demonstrated to optimally keep selectivity for Cpt1a.[323,324] Total $CD4^+$ T cells from lean NGT donors initially displayed elevated OCR and ECAR comparable to T2D T cells at baseline, and further augmented metabolic activity for T2D donors (Figure 5.3A,B); however, looking at the average of data points for each donor for both groups revealed that this higher OCR and ECAR appearance is driven by a higher trend in one or two data points as no net effect was detected (Figure5.3C-D). Higher non-mitochondrial oxygen consumption is an indicator of cellular stress.[325] Etomoxir treatment robustly increased non-mitochondrial oxygen consumption and modestly increased ATP-linked respiration in leanNGT donors' cells, suggesting that the effects of Cpt-1a inhibition on metabolism in the lean group are potentially driven by cellular stress. Lack of metabolic changes with etomoxir treatment for preT2D and T2D is consistent with our previous demonstrations in etomoxir-treated PBMCs from obese NGT and T2D donors.[46]

Although metabolism was unchanged in preT2D T cells with Cpt-1a inhibition, the T_{eff} cytokine profile adopts a more proinflammatory phenotype with enhanced production of Th1 cytokines (Figure 5.4B, blue labels; Figure 5.4C) and

Th17 cytokines (Figure 5.4B, maroon labels; Figure 5.4C) in the presence of etomoxir. This is similarly observed in the lean NGT and T2D T_{eff} profiles with etomoxir treatment, suggesting that Cpt1a

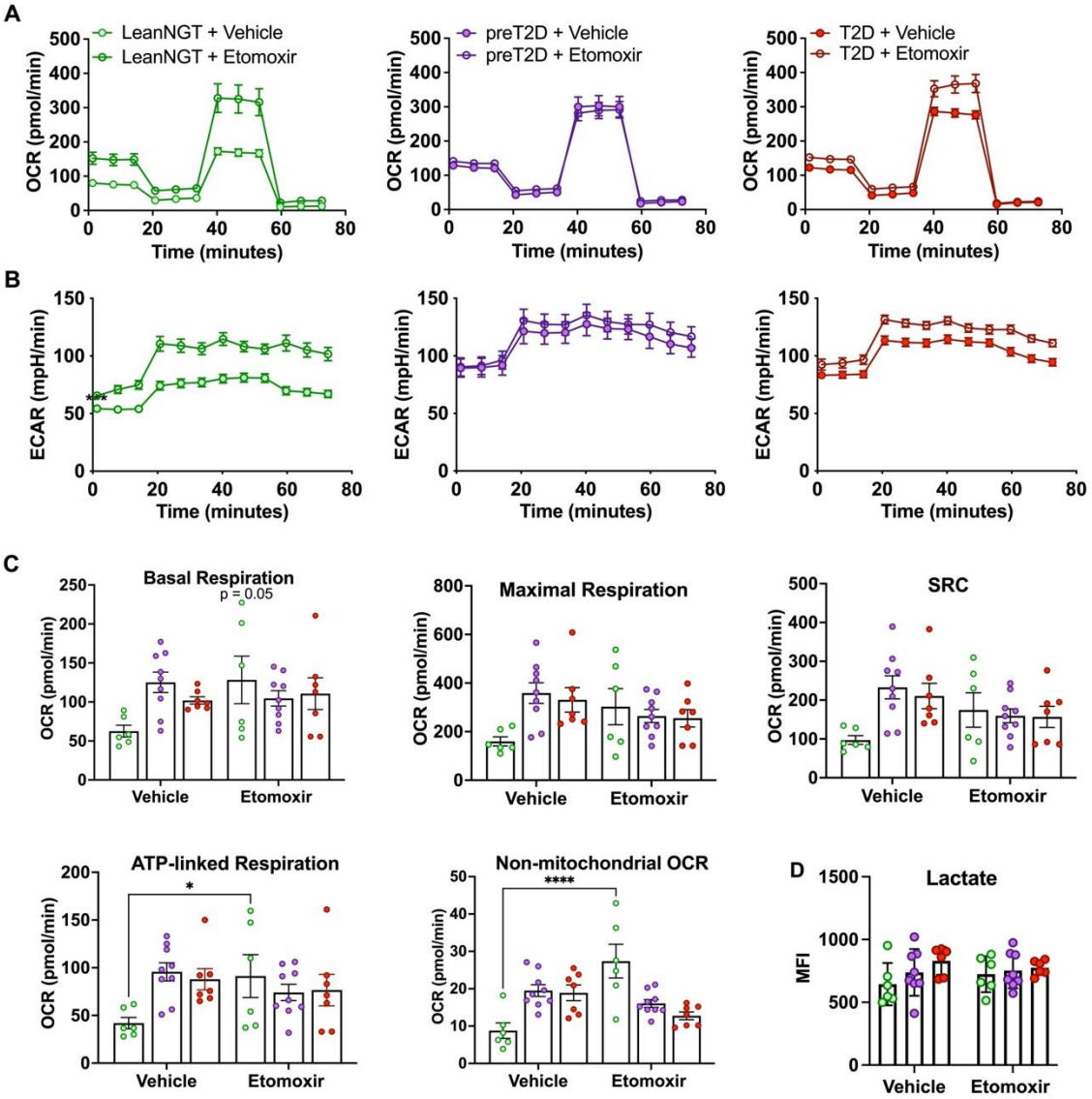

Figure 5.3 T cells from preT2D and T2D donors are insensitive to mild stress-induced changes to OXPHOS activity from Cpt1a inhibition
Mitochondrial stress test of CD3/CD28-stimulated total $CD4^+$ T cells treated with vehicle (DMSO- filled dots) or etomoxir (3μM- open dots) from LeanNGT (green dots- *n* = 6), preT2D (purple dots- *n* = 9), and T2D (red dots- *n* = 6) donors. OCR (**A**) and ECAR (**B**) plots as representations of OXPHOS and glycolysis, respectively. Dots at each time point represent the average OCR of samples as a group/treatment and plungers represent SEM. (**C**) OXPHOS parameters calculated as described in chapter 2. Bars represent average and SEM. Differences amongst cohorts by treatment and within cohorts by treatment were assessed by a two-way ANOVA with Bonferroni's multiple comparisons. *p < 0.05; **p < 0.01; ***p < 0.001.

inhibition does not have to significantly alter metabolism to change cytokine profiles, thereby uncoupling T-cell metabolism from function and echoing outcomes from MPC inhibition (Figures 5.1 & 5.2). An additional similarity in cytokine pattern observed in all cohorts was increased Th2 cytokines (Figure 5.4B green labels; Figure 5.4C), further emphasizing that aerobic glycolysis is the main driver of Th2 cytokine production and that T cells are likely, at least in part, relying on glycolysis with Cpt1a inhibition. Together, these data uncouple T-cell metabolism from function and we conclude that changes in metabolism, as determined by extracellular flux, are not necessarily required to elicit shifts in cytokine production.

5.4.3 Glutaminolysis supports high OXPHOS and proinflammatory effector responses in T2D pathogenesis

Upon activation, $CD4^+$ T cells shift their main carbon flux from glucose to glutaminolysis since glutaminolysis provides more reducing equivalents relative to pyruvate oxidation or FAO. Furthermore, glutaminolysis is one primary mechanism used to replenish key biosynthetic pathways, underscoring the critical role that glutamine plays in metabolic reprogramming. Like glucose, glutamine is an indispensable contributor to T-cell proliferation and survival, and differentiation into Th1 and Th17 subsets.[203,205,229,230] Thus far, we have demonstrated that total $CD4^+$ T cells from preT2D donors can overcome MPC or Cpt1a inhibition, as determined by extracellular flux analysis. Similar to MPC inhibition, changes in metabolism were not necessary to enhance cytokine production with etomoxir treatment, primarily shifting outcomes toward a pro-inflammatory phenotype marked by increases in Th1 and Th17 cytokines.

To determine if glutaminolysis differentially contributes to metabolism and inflammation in T2D T-cell pathogenesis, we utilized N,N'-[thiobis(2,1-ethanediyl-1,3,4-thiadiazole-5,2-diyl)]*bis*-benzeneacetamide (BPTES), an allosteric inhibitor against both isoforms of glutaminase-1 (GLS-1). GLS-1 is the enzyme that converts glutamine to glutamate in the mitochondria, which will then be converted to α-KG for TCA cycle anaplerosis and will ultimately yields 4 reducing equivalent

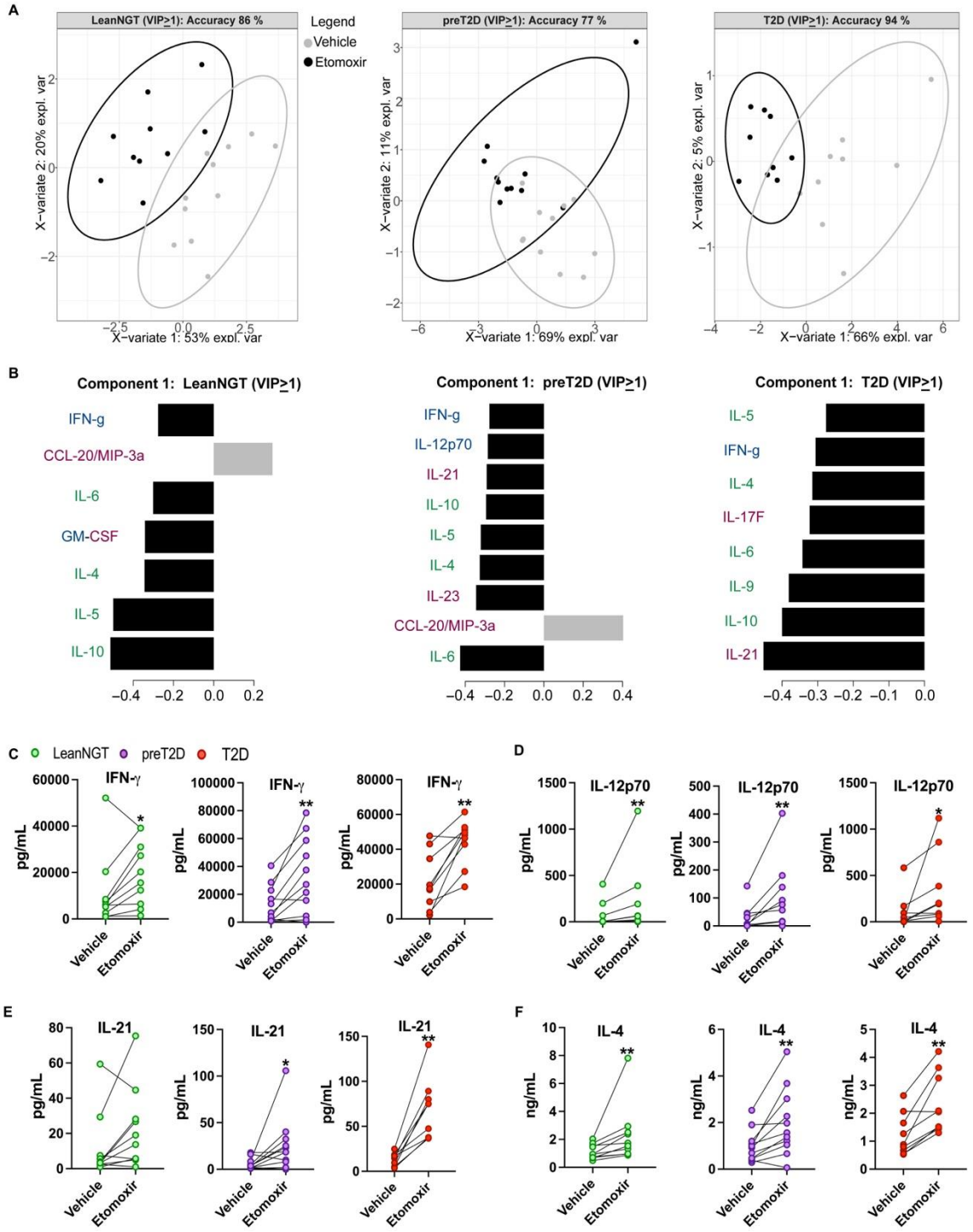

Figure 5.4 Cpt-1a inhibition uncouples T-cell metabolism from function
(**A-B**) PLSDA of inflammatory profiles generated by combining all cytokines measured after CD4⁺ Teff cell stimulation and treatment with vehicle (gray dots/bars) or etomoxir (black dots/bars) from leanNGT (left, *n* = 11), preT2D (middle, *n* = 11), and T2D (right- *n* = 9) donors showing (**A**) 2D projections of cytokine profiles in the first (most-distinguishing) component and (**B**) cytokines with a VIP score > 1 ranked from most (bottom) to least (top) important for defining treatment responses most *(continued on next page)*

Figure 5.4 (continued) characteristic of cells from the participant cohort indicated. Cytokines are color coded by T_{eff} subset as indicated- blue labels: Th1, green labels: Th2, and maroon labels: Th17. Representative cytokines for Th1 (**C**), Th17 (**D**), and Th2 (**E-F**) cells to show magnitude of treatment effect for each cohort. Differences assessed by paired two-tailed Wilcoxon test. $^{**}p < 0.01$; $^{***}p < 0.001$. In panels A-B, data were analyzed and figures were generated by S. Saraswat and X.D. Zhang.

molecules for the ETC. GLS-1 inhibition did not change basal and maximal respiration for cells from leanNGT donors (Figure 5.4A-B). In addition, other OCR parameters were unchanged by GLS-1 inhibition in the leanNGT cohort (Figure 5.4C), thus leanNGT donor cells appear to have fuel flexibility for glutamine. Considering results from MPC and Cpt1a inhibition, activated T cells in people with NGT may rely more on FAO to maintain optimal OXPHOS activity.

In contrast to leanNGT cells, BPTES significantly reduced all OXPHOS parameters in cells from preT2D and T2D donors (Figure 5.5 A-C). OCR was reduced for T2D donor cells, with BPTES treatment, comparable to that of leanNGT donor cells at baseline. Further assessment of OCR parameters revealed that basal respiration and ATP-linked respiration were most quantitatively affected by GLS-1 inhibition in the T2D group compared to preT2D, while spare respiratory capacity was decreased to a greater extent in preT2D T cells (Figure 5.5C). Furthermore, GLS-1 inhibition significantly increased non-mitochondrial oxygen consumption for leanNGT T cells comparable to preT2D and T2D (Figure 5.5C), suggesting that restricting glutaminolysis might induce stress in T cells from people with NGT but has no effect on T cells in preT2D and T2D. Higher non-mitochondrial oxygen consumption at baseline in T cells from preT2D and T2D donors that is unchanged with glutaminolysis restriction indicates that cytosolic oxidases may play a role in inflammatory pathogenesis that could be independent of glutamine's actions to limit oxidase activity. Altogether, these data suggest that glutaminolysis associates with higher T-cell OXPHOS in preT2D and T2D.

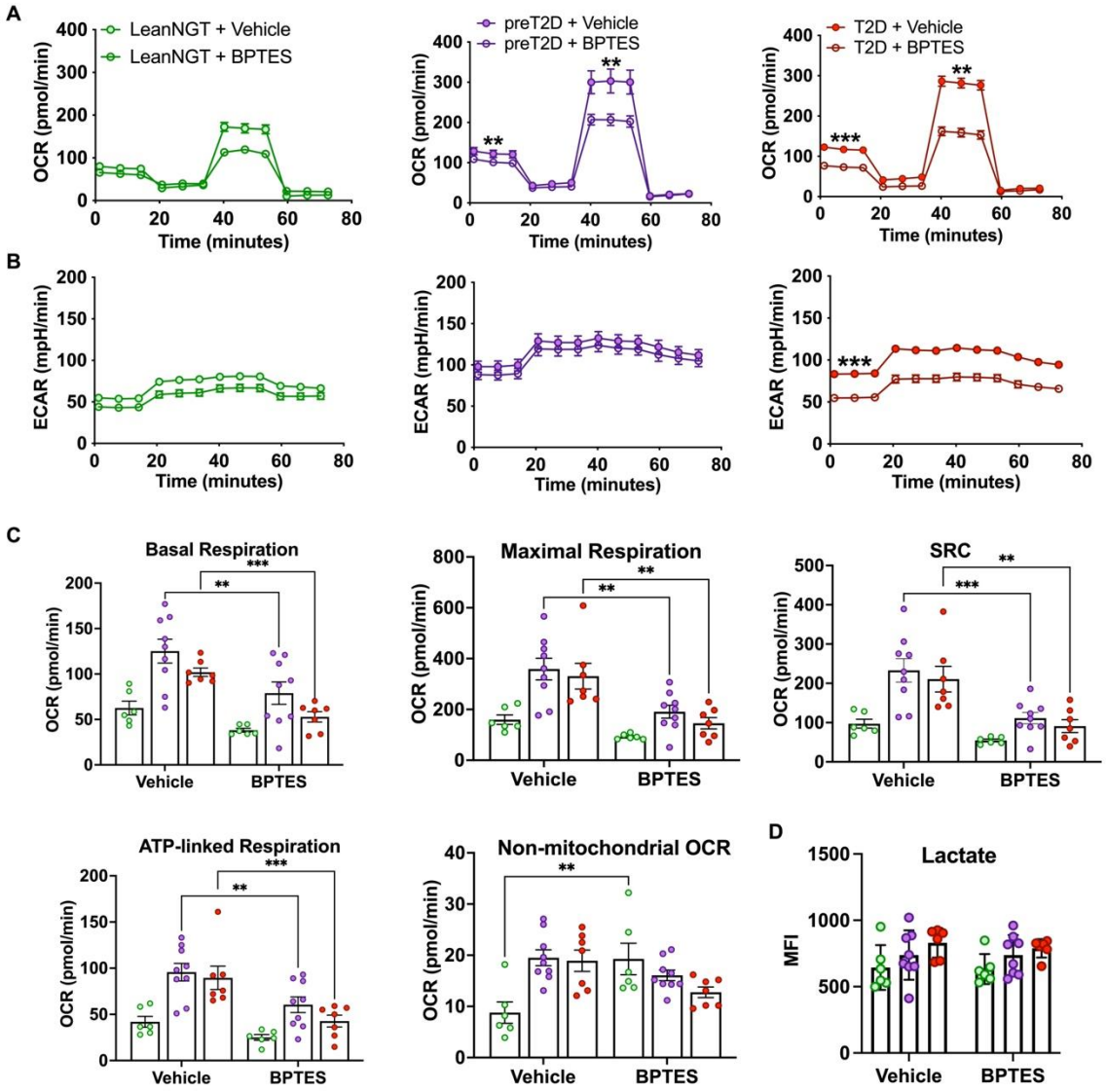

Figure 5.5 Glutaminolysis supports high T-cell OXPHOS in preT2D and T2D
Mitochondrial stress test of CD3/CD28-stimulated total $CD4^+$ T cells treated with vehicle (DMSO- filled dots) or BPTES (10μM) from LeanNGT (green dots- *n* = 6), preT2D (purple dots- *n* = 9), and T2D (red dots- *n* = 6) donors. OCR (**A**) and ECAR (**B**) plots as representations of OXPHOS and glycolysis, respectively. Plungers represent SEM. (**C**) OXPHOS parameters calculated as described in chapter 2. (**C**) OXPHOS parameters calculated as described in chapter 2. (**D**) Lactate production measured from supernatants represented as MFI from participant cohort as indicated. Bars represent average and SEM. Differences amongst cohorts by treatment and within cohorts by treatment were assessed by a two-way ANOVA with Bonferroni's multiple comparisons. *p < 0.05; **p < 0.01; ***p < 0.001.

GLS-1 inhibition in T_{eff} cells decreased most Th1 (Figure 5.6A-B, green labels; Figure 5.6C) and Th17 cytokines (Figure 5.6A-B, maroon labels; Figure 5.6C) for all cohorts. Furthermore, the Th2 cytokines IL-4 and IL-5 increased with BPTES treatment exclusively in T cells from T2D donors (Figure 5.6E,F). Given that glutaminolysis is required for high T-cell OXPHOS in preT2D and T2D, and for production of most Th1/Th17 cytokines (the T2D-associated cytokine profile), it's possible that glutamine reliance supports a pathogenic cytokine profile by also limiting Th2 function during T2D pathogenesis. Given these data, we conclude that glutaminolysis is instrumental to high T-cell OXPHOS in preT2D and T2D and to T2D-associated inflammation, specifically Th1 and Th17 cytokines.

Since glutaminolysis restriction reduced OXPHOS and classical pathogenic T-cell cytokines, we wanted to determine if replenishing α-KG, the downstream glutamine metabolite that enters the TCA cycle, by either acute injection or supplementing in the cell culture media with a physiological dose (10μM, reflective of plasma concentrations)[326-328] would reverse the effects of BPTES on metabolism and cytokine production, respectively. Glutaminolysis is a rapidly occurring process. Moreover, α-KG is taken out of the bloodstream within 5-min,[329] thus we posited that an acute injection of a cell-pemerable α-KG analog, dimethyl-2-ketoglutarate (DM2KG), in stimulated live T-cell culture should reveal if BPTES effects on metabolism are α-KG-dependent. Acute physiologic DM2KG injection demonstrated no change in metabolism with or without BPTES treatment (Figure 5.7 A-B), suggesting an α-KG independent mechanism by which BPTES treatment lowers metabolism in preT2D and T2D T cells; however, it is likely that a small dose, as is the physiological dose that was utilized here, may not be sufficient to rescue metabolism from GLS-1 inhibition.

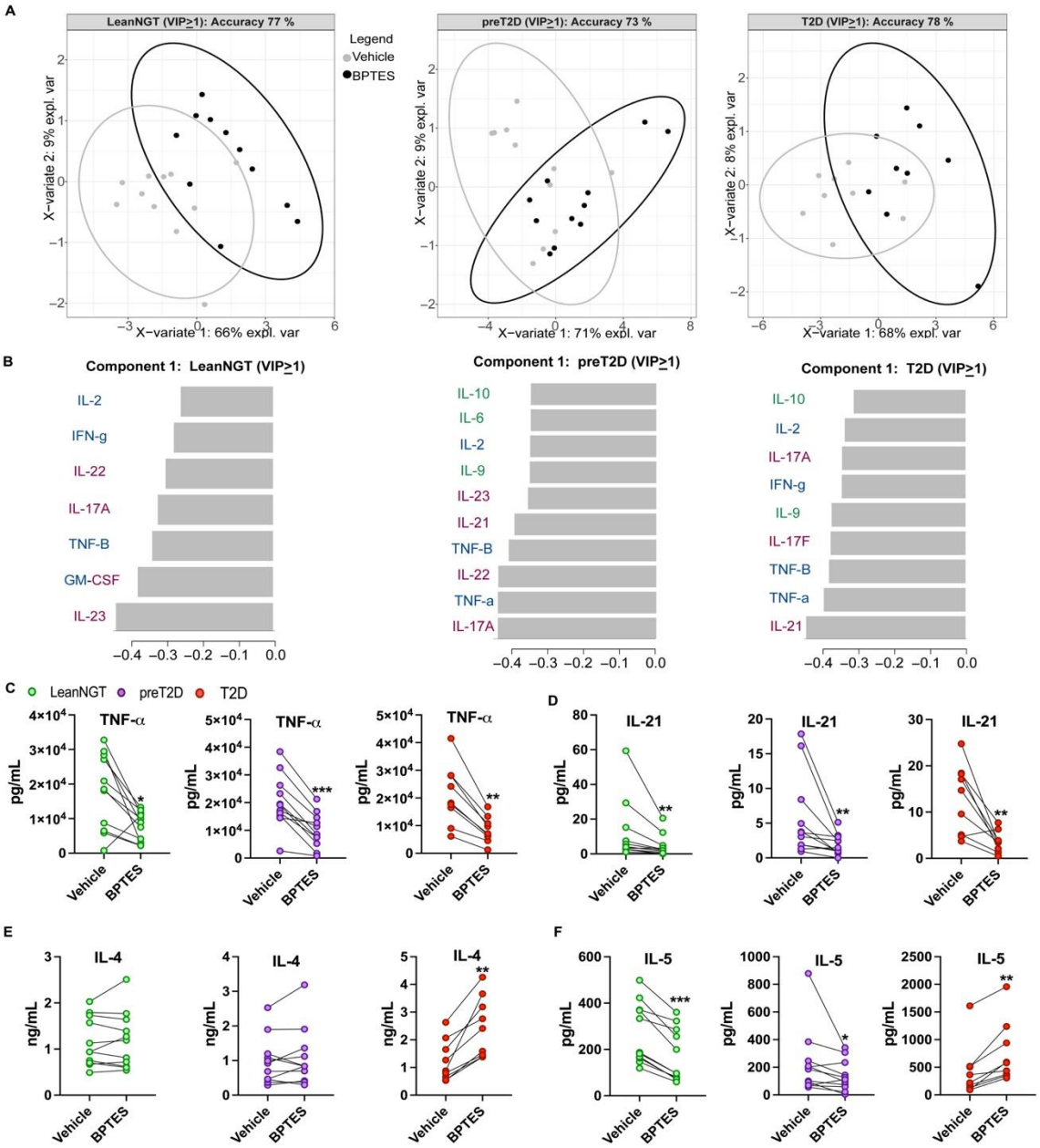

Figure 5.6 GLS-1 inhibition reduces Th1 and Th17 cytokines
(**A-B**) PLSDA of inflammatory profiles generated by combining all cytokines measured after CD4⁺ Teff cell stimulation and treatment with vehicle (gray dots/bars) or etomoxir (black dots/bars) from leanNGT (left, *n* = 11), preT2D (middle, *n* = 11), and T2D (right- *n* = 9) donors showing (**A**) 2D projections of cytokine profiles in the first (most-distinguishing) component and (**B**) cytokines with a VIP score > 1 ranked from most (bottom) to least (top) important for defining treatment responses most characteristic of cells from the participant cohort indicated. Cytokines are color coded by T_{eff} subset as indicated- blue labels: Th1, green labels: Th2, and maroon labels: Th17. Representative cytokines for Th1 (**C**), Th17 (**D**), and Th2 (**E-F**) cells to show magnitude of treatment effect for each cohort. Differences assessed by paired two-tailed Wilcoxon test. **p < 0.01; ***p < 0.001. In panels A-B, data were analyzed and figures were generated by S. Saraswat and X.D. Zhang.

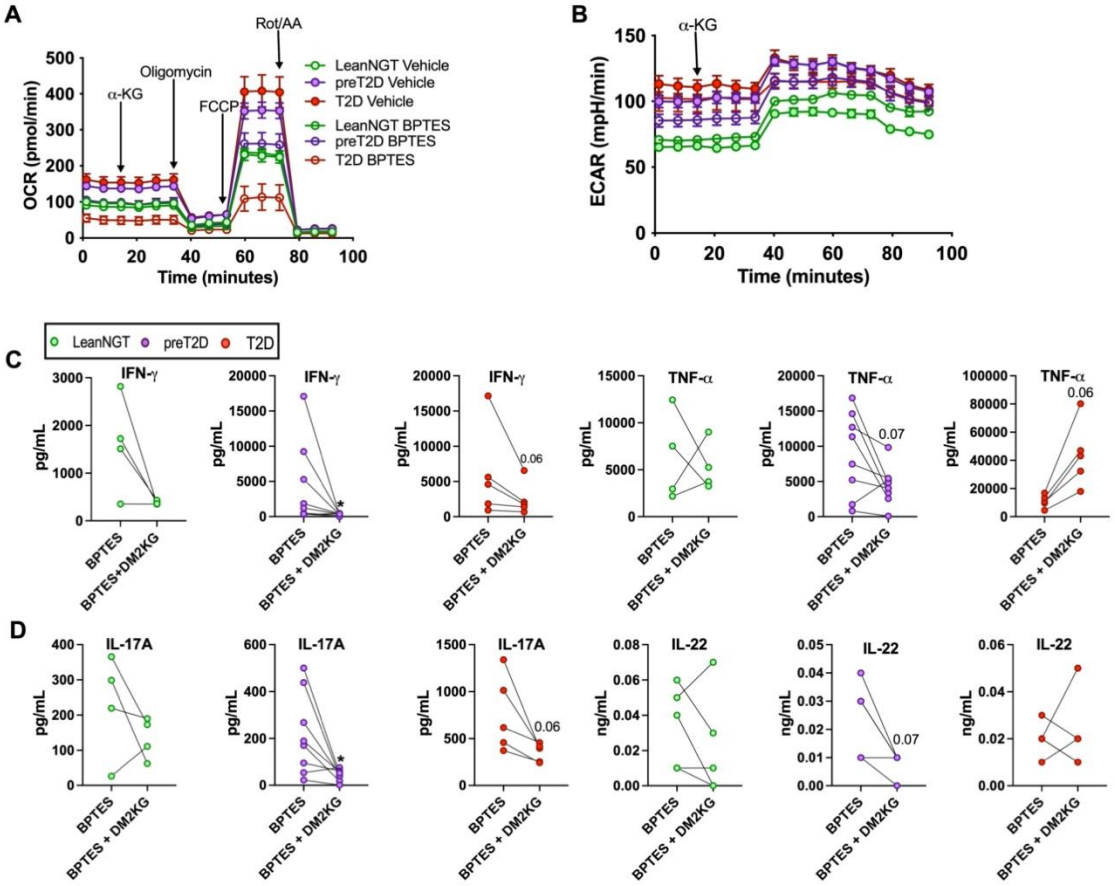

Figure 5.7 Alpha-ketoglutarate supplementation does not reverse the effects of GLS-1 inhibition on metabolism and inflammation

(**A-B**) OCR and ECAR plots of a mitochondrial stress test with an acute injection of a cell permeable α-KG analog (DM2KG, 10μM) in total $CD4^+$ T cell cultures with CD3/CD28 stimulation and treatment with vehicle or BPTES (preT2D, *n* = 5; T2D, *n* = 7; 2 leanNGT donors' cells run previously were used as an internal plate control). Representative cytokines of Th1 (**C**) and Th17 (**D**) cells from stimulated $CD4^+$ T_{eff} cells from leanNGT (green dots- n = 4), preT2D (n = 8), and T2D (n = 5) donors that were treated with BPTES or a combination of BPTES and DM2KG (added 20h and 32h post-stimulation). Differences were assessed by a paired two-tailed Wilcoxon rank test.

This was further demonstrated by an attenuated effect of BPTES on most Th1 and Th17 cytokines (Figure 5.7C-D) with the supplementation of cell culture medium with DM2KG at 24 and 32-hours post-stimulation in the presence of BPTES. Due to α-KG being a "promiscuous" metabolite, we recognize this experimental approach is flawed and stable isotope tracer studies labeling glutamine in the presence or absence of BPTES may better answer this question.

5.4.4 GLS-1 inhibition reduces mTORC1 activity in preT2D and T2D independent of inflammation

We have demonstrated that mitochondrial traits in peripheral $CD4^+$ T cells are not altered in preT2D or T2D and that higher T-cell OXPHOS associates with T2D pathogenesis. Since pyruvate oxidation and FAO was not an essential to high T-cell OXPHOS, T cells from preT2D and T2D donors may preferentially utilize glutaminolysis to sustain high OXPHOS as demonstrated by a reduction in OCR with glutaminolysis restriction. Moreover, Th2 cytokines were reduced with GLS-1 inhibition in leanNGT and preT2D donor cells but were increased in T2D donor cells. These data indicate that glutaminolysis supports T2D-associated inflammation by promoting Th1/Th17 cytokines over Th2 responses. T cells from preT2D donors may utilize FAO in combination with glycolysis to help maintain a more Th2-like profile as demonstrated by the relationship between Cpt1a activity and PPAR-γ to promote FAO in Th2/T_{reg} differentiation/function.[219]

Glutamine uptake and metabolism are part of a positive feedback loop with mTORC1 activity, which regulates both oxidative and glycolytic metabolism. In addition, mTORC1 promotes Th1 and Th17 responses by upregulating T-bet and ROR-γt expression, respectively.[227,228] Conversely, Th2 cells are thought to rely more on mTORC2 activity for cytokine production as mTORC2 upregulates GATA-3 expression and IL-4 production.[234,235] Given this knowledge, we tested the possibility that the effects of BPTES on inflammation worked through regulating mTORC1 activity. Expression of mTORC1 activity based on protein detection of pThr389-S6K in lysates from cultured T_{eff} cells revealed that mTORC1 activity is significantly reduced by BPTES in preT2D and T2D T_{eff} cells (Figure 5.8A).

Furthermore, treatment of T_{eff} cells with a physiologically relevant dose (0.01μM)[330] of the mTOR inhibitor everolimus produced similar reductions in Th1 and Th17 cytokines as BPTES (Figure 5.8B). Everolimus unsurprisingly reduced Th2 cytokines, consistent with demonstrations that it also inhibits NF-κB as a downstream consequence of PI3K-Akt-mTOR inhibition.[331] Together, these data suggest that effects of glutaminolysis restriction on inflammation may be dependent on reducing mTORC1 activity. Th1/Th17 cytokines could be supported in T2D inflammatory pathogenesis by coordination of glutamine metabolism and mTORC1 functions.

To determine if a reduction Th1/Th17 cytokines with glutaminolysis restriction is dependent on mTORC1 activity, we performed a rescue experiment by adding an mTORC1 agonist, NV-5138, at 24hr post-stimulation in the presence of BPTES. NV-5138 is a leucine analog that acts as an inhibitor of Sestrin-2, which is a negative regulator of mTORC1.[332] Agonism of mTORC1 activity with NV-5138 in total $CD4^+$ T cells was confirmed by protein expression of total S6K and pThr389-S6K (Figure 5.9A,B); however, only cells from the T2D cohort had enhanced mTORC1 activity with NV-5138 treatment (Figure 5.9B), potentially due to a higher sample size in the T2D cohort relative to lean NGT and preT2D cohorts. Despite an increase in mTORC1 activity in T2D donor cells, Th1 and Th17 cytokines were further augmented with NV-5138 in the presence of BPTES (Figure 5.9C-D), similar to what we observed in α-KG supplementation with BPTES (Figure 5.7). These data suggest that the effects of glutaminolysis restriction on Th1 and Th17 cytokines may not be solely dictated by mTORC1 activity. Alternatively, functions of GLS-1 might be downstream of mTORC1. Collectively, these data reveal that glutaminolysis supports high T-cell OXPHOS in peripheral $CD4^+$ T cells from preT2D and T2D donors and promotes Th1/Th17 cytokines independent of mTORC1.

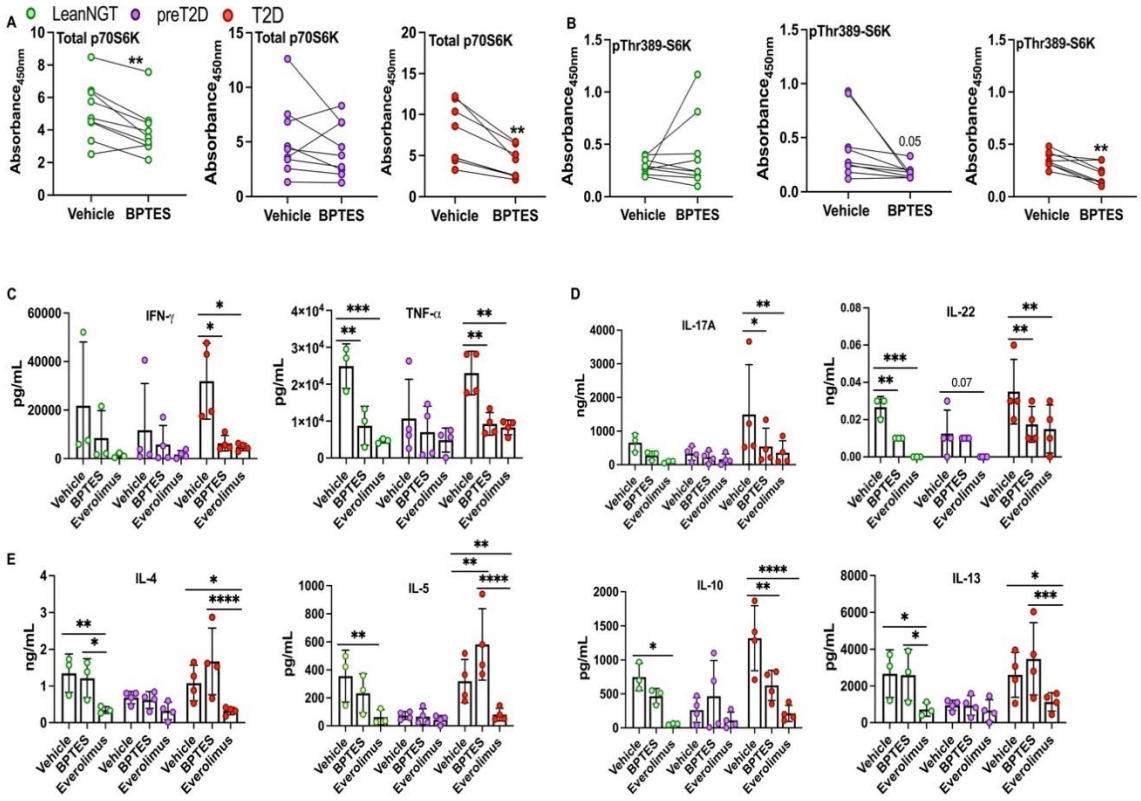

Figure 5.8 GLS-1 inhibition reduces mTORC1 activity in T2D T cells and mTOR inhibition mimics effects of GLS-1 on Th1 and Th17 cytokines

(**A-B**) Protein expression of mTORC1 activity measured in T_{eff} cells after stimulation with CD3/CD28 (40h) from leanNGT (green dots, n = 8), preT2D (purple dots n = 8), or T2D (red dots, n = 7) donors cultured with vehicle or BPTES and protein expression of mTORC1 activity was measured. Representative cytokines of Th1 (**C**), Th17 (**D**), and Th2 (**E**) cells measured from supernatants from cultures with vehicle, BPTES, or everolimus. Differences were assessed by a paired two-tailed Wilcoxon rank test (**A,B**) or by a two-way ANOVA (**C-E**).

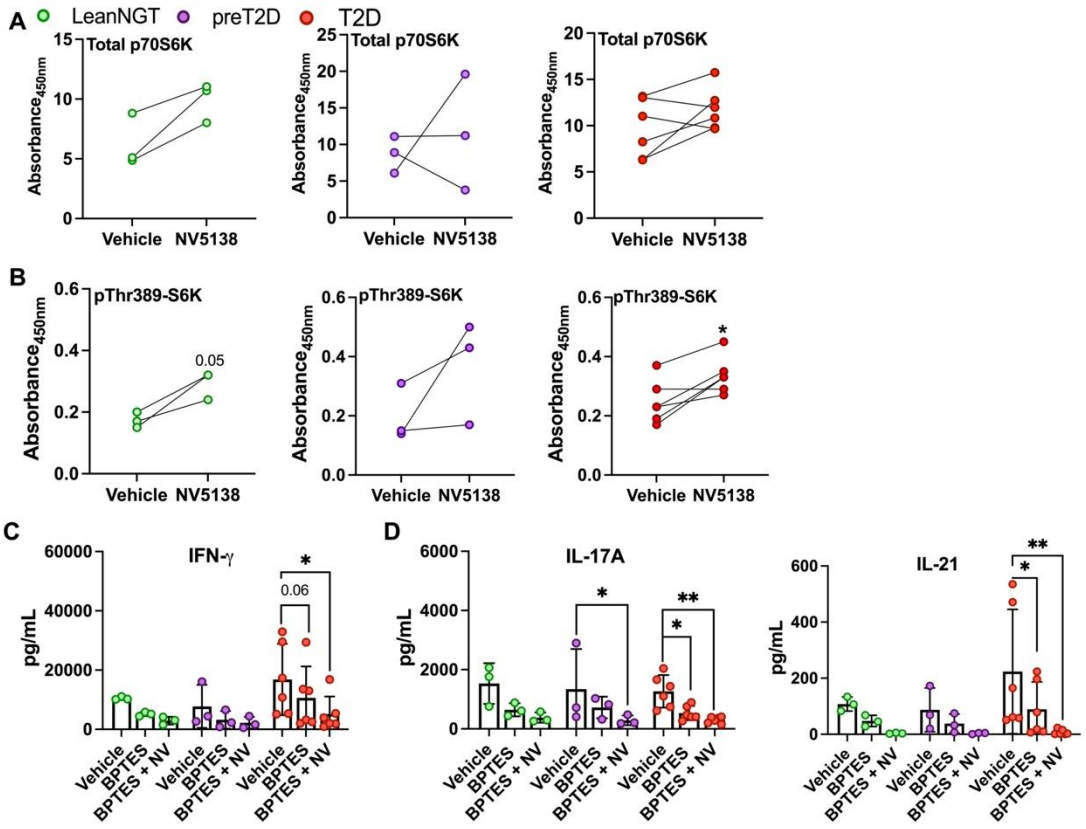

Figure 5.9 mTORC1 agonism does not reverse effects of GLS-1 inhibition on inflammation

Total CD4⁺ T cells stimulated with CD3/CD28 (40h) treated with (**A-B**) vehicle or NV5138 (10μM) and protein expression of mTORC1 activity was measured in whole cell extracts from lean NGT (green dots, *n* = 3), preT2D (purple dots, *n* = 3), and T2D (red dots, *n* = 5) donors. Representative cytokines for (**C**) Th1 and (**D**) Th17 cytokines from total CD4⁺ T cell cultures with CD3/CD28 and vehicle, BPTES, or a combination of BPTES and NV-5138. Differences were assessed by a paired Wilcoxon rank test (A,B) or a two-way ANOVA with Bonferroni's multiple comparisons. *p < 0.05; **p < 0.01.

5.5 Discussion

We have demonstrated that mitochondrial traits are not changed in preT2D T cells, thus leaving high T-cell OXPHOS unexplained. In this chapter, we revealed that total $CD4^+$ T cells from T2D donors also have high T-cell OXPHOS, linking outcomes in preT2D to T2D pathogenesis. Manipulation of the mitochondrial fuel sources pyruvate, fatty acids, and glutamine generated insightful outcomes on T cell metabolism and function. While pyruvate oxidation and FAO did not change OXPHOS or glycolysis in T cells from preT2D and T2D donors, as determined by extracellular flux and secreted lactate, respectively, cytokine production did change. Particularly, restricting FAO led to T cells from leanNGT and preT2D donors to adapt a more pro-inflammatory cytokine profile. Enhanced Th1 and Th17 cytokine production could be due to shifting to glycolysis and glutaminolysis to maintain reducing equivalent generation in the absence of FAO as glutaminolysis has been reported to support Th1 and Th17 differentiation/function.[182,205,230] Despite demonstrations that Cpt1a activity is not required for human T_{eff} responses,[324] metabolites generated through Cpt1a's ability to coordinate FA uptake and subsequent oxidation promotes anti-inflammatory profiles by limiting proinflammatory cytokines in metabolic disease.[219 333] Together, these results uncouple T-cell metabolism from function and emphasize that the numerous metabolites generated during T cell activation play a crucial role in T cell function rather than being solely dictated by individual pathways.

Restricting glutaminolysis mitigated high T-cell OXPHOS in preT2D and T2D donor cells and suggested that reductions in OCR were due to a dip in α-KG generated for the TCA cycle. However, acute injection of α-KG did not change OCR in cells treated with BPTES, implying that the effects of BPTES are not dependent on α-KG. Upon further scrutiny of the data, we realized the flaw in our approach to replenish α-KG in the TCA cycle. The multifunctional metabolite α-KG is not guaranteed to be utilized in its entirety by the TCA cycle, as α-KG is an essential cofactor for demethylases,[334] a precursor for citrate via reductive carboxylation to support *de novo* FAS,[335] and a ROS scavenger to mitigate oxidative stress;[336] therefore, the cell likely requires supraphysiological

concentrations of α-KG to ensure enough α-KG is shunted to the TCA cycle to bypass the effects of GLS-1 inhibition as supported by previous findings.[230,337]

Glutaminolysis restriction also reduced Th1 and Th17 cytokines from T_{eff} cells in all cohorts. Failure of α-KG to restore Th1 and Th17 cytokine production in the presence of BPTES was likely due to the multiple functions of α-KG discussed above. Since glutamine uptake and metabolism is involved in mTORC1 activation and Th1/Th17 differentiation, we postulated that the effects of BPTES on reducing Th1/Th17 cytokines was through reduced mTORC1 activity. This idea was supported by the reduction in mTORC1 activity in T_{eff} cells treated with BPTES. Furthermore, treating T_{eff} cells with the mTORC1 inhibitor everolimus reduced Th1 and Th17 cytokines similar to BPTES; however, mTORC1 agonism with NV-5138 did not rescue Th1/Th17 cytokine reduction by BPTES. These data indicate that Th1 and Th17 functions are not solely dictated by mTORC1 activity and points to other mechanisms involving glutamine metabolism as critical mediators for promoting T2D-associated inflammation, such as mitochondrial ROS scavenging and post-translational modifications facilitated by UDP-GlcNAc synthesis, or cell signaling functions mediated by GLS-1 (described further in chapter 6).

CHAPTER 6. SUMMARY AND FUTURE DIRECTIONS

Immunometabolism as a target of immunomodulatory therapies has become a popular area of interest for treating chronic inflammatory diseases such as autoimmunity (e.g., systemic lupus erythematous, rheumatoid arthritis, and inflammatory bowel disease), and cancer.[338-341] Current treatments for chronic inflammation include anti-TNFα, mTOR inhibitors, and NF-κB inhibitors.[342-344] While effective in reducing proinflammatory cytokine action/production, these treatments are accompanied by undesirable side effects as most generally suppress overall immune function by limiting cellular activation and proliferation. Furthermore, immunosuppression increases susceptibility to certain bacterial and/or viral infections and complicates infection clearance.[345-347] Although treatments for chronic inflammatory diseases have improved over the years, generating therapies that ameliorate inflammation with limited immunosuppressive effects could be achieved by targeting pathways that do not impair overall immune function. In this dissertation, I have shown that targeting individual mitochondrial fuel sources can change T-cell cytokine profiles without needing to change metabolism. These data are promising for future applications of immunometabolism research in designing new anti-inflammatory therapies since lowering cell metabolism to ameliorate inflammation poses similar limitations as immunosuppressive medications.

Anti-inflammatory therapies are not approved for T2D, as the primary goal of diabetes care/management is to lower blood glucose levels, which can be achieved by targeting non-immune components of disease pathogenesis. Unifying the mitigation of glycemic control and inflammatory sequelae could prove to be the missing piece for improving T2D prevention and disease management. Anti-TNFα and anti-IL1β therapies have been tested in clinical trials for the ability to improve glycemic control. While these therapies initially improved HbA1c and/or FBG, long-term improvement was not observed,[151,152,348] indicating that targeting individual cytokines in T2D is likely the wrong therapeutic approach. The premise for these studies was largely based on targeting pro-inflammatory monocytes and

macrophages, which were credited as being the dominant source of IR-supporting inflammation.[31,37,142,144,145,267] With addition of the work outlined in chapter 3, our lab has consistently demonstrated a critical and underappreciated role of T cells in T2D-associated meta-inflammation, thus indicating that underwhelming clinical trial outcomes could be a consequence, at least in part, of targeting an inappropriate cellular source of inflammation. Attitudes toward implementing immunosuppressives in T2D care are understandably apprehensive. People with T2D are already at risk of certain infections that can be particularly difficult to clear as hyperglycemia is thought to disrupt immune function.[349] Moreover, some glycemic control drugs such as metformin and sulfonylureas are reported to impair type 1 responses, potentially putting patients at an increased risk of fatal infections like *Mycobacterium tuberculosis*.[103-105] The work outlined in this dissertation supports published demonstrations of metabolic reprogramming directly manipulating immune cell function; thus, rewiring immune cells by manipulating certain fuel sources might also shift inflammatory outcomes to support peripheral insulin sensitization without eliciting immunosuppressive effects.

Higher oxidative metabolism in peripheral $CD4^+$ T cells is associated with elevated T2D risk and T2D pathogenesis as demonstrated by extracellular flux analysis in T cells from both preT2D and T2D donors. Peripheral T cells might lose fuel flexibility during obesity and T2D pathogenesis, and consequently rely on other fuel sources to preserve function. Glutaminolysis was the only anaplerotic pathway that significantly impacted overall oxidative metabolism in preT2D and T2D T cells. The glutamine switch likely occurs during preT2D since GLS-1 inhibition similarly reduced T-cell metabolism in both preT2D and T2D donors. GLS-1 inhibition reduced Th1 and Th17 cytokine production for all cohorts, with the most profound effect observed in T2D, highlighting the functional importance of Th17 cytokines in the T2D cytokine profile and supporting previous demonstrations that Th1 and Th17 cells require glutaminolysis for differentiation and effector functions.[205,215,229,230] As total $CD4^+$ T cells are a heterogenous mix, T-cell skewing studies may help identify if Th1 and/or Th17 subsets are responsible for the higher

OXPHOS profile in preT2D and T2D, given cell number limitations of naturally generated effector subsets .

Peripheral T cells in T2D may also be insensitive to glucose fluctuations (Figure A2.6) and could indicate glucose uptake impairments as demonstrated previously in peripheral T cells in T2D.[156] This could also explain, in part, why preT2D and T2D T cells did not secrete more lactate than leanNGT donor cells despite having higher ECAR measurements. Alternatively, ECAR is an unreliable and indirect surrogate measure of glycolysis, which is why measuring secreted lactate is important for data interpretation since lactate production is more indicative of glycolysis. Impaired migratory capacity of peripheral T cells in T2D is thought to be associated with impaired glucose uptake as aerobic glycolysis is essential to rapidly generate enough ATP to support migration.[156,239,350] Glutaminolysis reportedly enhances glucose uptake in T cells.[182,205,218] If glucose uptake is altered in T2D progression, enhanced glutaminolysis could also serve as a compensatory mechanism to help maintain aerobic glycolysis by boosting glucose uptake. Measuring glucose uptake in T2D T cells using flow cytometric analysis of intracellular accumulation of the glucose analog 2-(*N*-(7-Nitrobenz-2-oxa-1,3-diazol-4-yl)Amino)-2-Deoxyglucose (2-NDBG) could help us begin to understand why T cells shift to glutamine reliance in T2D pathogenesis. In addition, stable isotope tracer studies of glucose and glutamine after BPTES, etomoxir, and UK5099 treatment could inform how T cells from each cohort are compensating during TCA cycle anaplerosis. Additionally, analysis of glutamine transporter expression (Slc1a5) and/or GLS-1 could also help to identify easily testable targets for inhibiting glutaminolysis to determine if BPTES-mediated effects on metabolism and inflammation are glutaminolysis-dependent, as genetic knockdown of GLS-1 may not be feasible in primary human T cells due to a high rate of cell death and the requirement of GLS-1 function in T-cell survival.[203]

Interestingly, we observed enhanced Th2 responses exclusively in T2D donors with BPTES treatment, suggesting that GLS-1 activity somehow limits Th2 responses in T2D. This effect on enhanced Th2 cytokines is similar to our previous demonstrations in PBMCs from T2D donors under low glucose conditions.[46]

Moreover, T cells from leanNGT and preT2D donors adapted a pro-inflammatory cytokine profile when FAO was reduced by Cpt1a inhibition. This differs from our previously published work in PBMCs showing that some Th17 cytokines are reduced with a 3μM dose of etomoxir.[46] These differences could be due to different cell types (PBMCs vs purified T cells) and differences in the age of cohorts. We have previously shown that other cell types present in the PBMC fraction, such as monocytes and B cells, support Th17 cytokines in T2D donor cells;[42,44] therefore, these cells may have played a role in regulating Th17 cytokine production in the presence of etomoxir, which would not be captured in purified T cells alone.

PPAR-γ stimulates FAO by supporting CD36 and Cpt1a expression and function in T cells, and PPAR-γ agonism in naïve $CD4^+$ T cells induces T_{reg} differentiation and function by favoring FAO.[219] While Th2 cells have been shown to preferentially utilize aerobic glycolysis for differentiation and cytokine production, PPAR-γ activity is also critical for Th2 effector functions by coordinating ST2 and IL-5 gene transcription with GATA-3 signaling; however, ST2 expression is typically associated with pathogenic Th2 responses such as allergic airway inflammation, but this could be context-dependent.[232,351] More data is needed on the role of PPAR-γ activity in Th2 cells in metabolic disease to determine if this would be an effective target for shifting T2D-associated inflammation away from a Th17 signature. Additionally, it's possible that acetyl-CoA provided by pyruvate oxidation and/or FAO is critical for Th2 cytokines rather than strictly requiring glycolysis or FAO.

Our lab has previously shown that T cell-stimulated PBMCs from T2D donors display a low CACT:Cpt-1a ratio, indicating changes in FAO.[46] Knockdown of CACT in leanNGT donor cells coupled with LCFA supplementation recapitulated a T2D-like cytokine profile in which frequencies of $CD4^+IL\text{-}17^+$ cells significantly increased, suggesting that Th17 cytokine dominance in T2D is driven by changes in lipid flux and FAO.[242] If T cell FAO changes during T2D pathogenesis, T cells may turn to glutaminolysis to compensate for loss of a significant OXPHOS substrate source as glutaminolysis generates more reducing equivalents for the ETC,[220,352] further emphasizing the need for stable isotope tracer studies to solidify

our findings. Assessment of CACT expression in stimulated total $CD4^+$ T cells will be necessary to unify these results with PBMC findings.[46]

FAO changes may not occur in T cells from preT2D donors since Th2 cytokines dominate the preT2D cytokine profile and glutaminolysis restriction reduced Th2 cytokines in NGT and preT2D donors. Furthermore, Th2 cytokine production increased with Cpt1a or MPC inhibition independent of changes in metabolism, which may be due to compensatory increases in the acetyl-CoA pool to mitigate loss of either source. These results emphasize the oversimplification of our current understanding of metabolic reprogramming, which focuses on individual pathways dictating T cell lineage and function rather than the integration of the numerous metabolites generated during metabolic reprogramming of activated T cells. These data link T-cell metabolism in preT2D to T2D pathogenesis, with potential changes in FAO and upregulated glutaminolysis driving T2D-associated inflammation. Changes in FAO might decrease the acetyl-CoA pool and would deprive the hexosamine biosynthesis pathway of a key intermediate (N-acetylglucosamine) to produce UDP-GlcNAc used for O-GlcNAcylation and N-linked glycosylation modifications, of which directly modulate immune responses.[353,354] Additionally, enhanced aerobic glycolysis and glutaminolysis have been demonstrated to limit F-6P and glutamine availability in the hexosamine biosynthesis pathway by preferentially shunting these substrates to glycolysis and glutaminolysis to meet bioenergetic demands, resulting in decreased N-glycan branching of the TCR and CD25 in murine T-cell blasts.[218] Less N-glycan branching destabilizes CD25 expression, promoting intracellular retention, which supports a T_{eff} phenotype as T_{eff} cells express low levels of CD25 in contrast to T_{regs}, in which CD25 is constitutively expressed at high levels.[355] Moreover, increased β-1,6-GlcNAc-containing N-glycan branching of the TCR favors Th2 polarization over Th1,[356] demonstrating a key role of metabolite integration from glycolysis, glutaminolysis, and FAO in T cell lineage decisions, thus bridging T-cell metabolism with functional outcomes.

Lower N-glycan branching is associated with Th17 differentiation as a consequence of enhanced aerobic glycolysis and glutaminolysis.[218] Additionally,

Th17 cells have been shown to require GLS-1 activity by a mechanism that is not rescued by α-KG, consistent with our results, and was shown to be dependent on GLS1-mediated modulation of ROS.[230] GLS-1 activity was also required for initial Th1 differentiation and IFN-γ production; however, Th1 cells overcame these effects, but at the cost of developing an exhausted phenotype.[230] While we showed that T cells from T2D donors have lower mitochondrial superoxide production and speculated that this was due to metformin usage, measuring ROS production after BPTES treatment could have provided a preliminary indication on if GLS-1 inhibition reduces Th17 cytokines through ROS modulation. A schematic of proposed mechanisms is outlined in Figures 6.1 and 6.2.

PPAR-γ agonism has been shown to limit Th17 differentiation[357,358] and cytokine production by directly inhibiting GLS-1 activity, ultimately reducing α-KG levels and increasing ROS production.[358] The T cells that were used from T2D donors in the experiments discussed in chapters 4 and 5 were not taking TZDs (PPAR-γ agonists), which may be why these cells were sensitive to the effects of GLS-1 inhibition on Th1 and Th17 cytokine production. Repurposing PPAR-γ agonists to target GLS-1 activity and ameliorate T2D-associated inflammation may be an effective anti-inflammatory strategy for people with T2D. Using PPAR-γ agonists as an anti-inflammatory treatment might also be effective in delaying/preventing T2D onset in people with preT2D, since our data has consistently shown that T cells from preT2D donors do not yet display a Th17 cytokine profile, leading us to hypothesize that Th17 cytokine dominance may occur later in T2D pathogenesis as a consequence of shifting to glutaminolysis.

A consistent limitation to our studies was the disproportionate number of females in non-T2D cohorts, while T2D cohorts had a balanced ratio of males to females. Additionally, KY demographics further limit cohort diversity as most participants, regardless of participant cohort, were non-Hispanic white; therefore, we are not able to support conclusions on other populations that are disproportionately affected by obesity and T2D. Due to a limited sample size, we're not able to determine sex-specific or race-specific differences in inflammatory outcomes, which will be critical for aiding in T2D prevention/delay strategies.

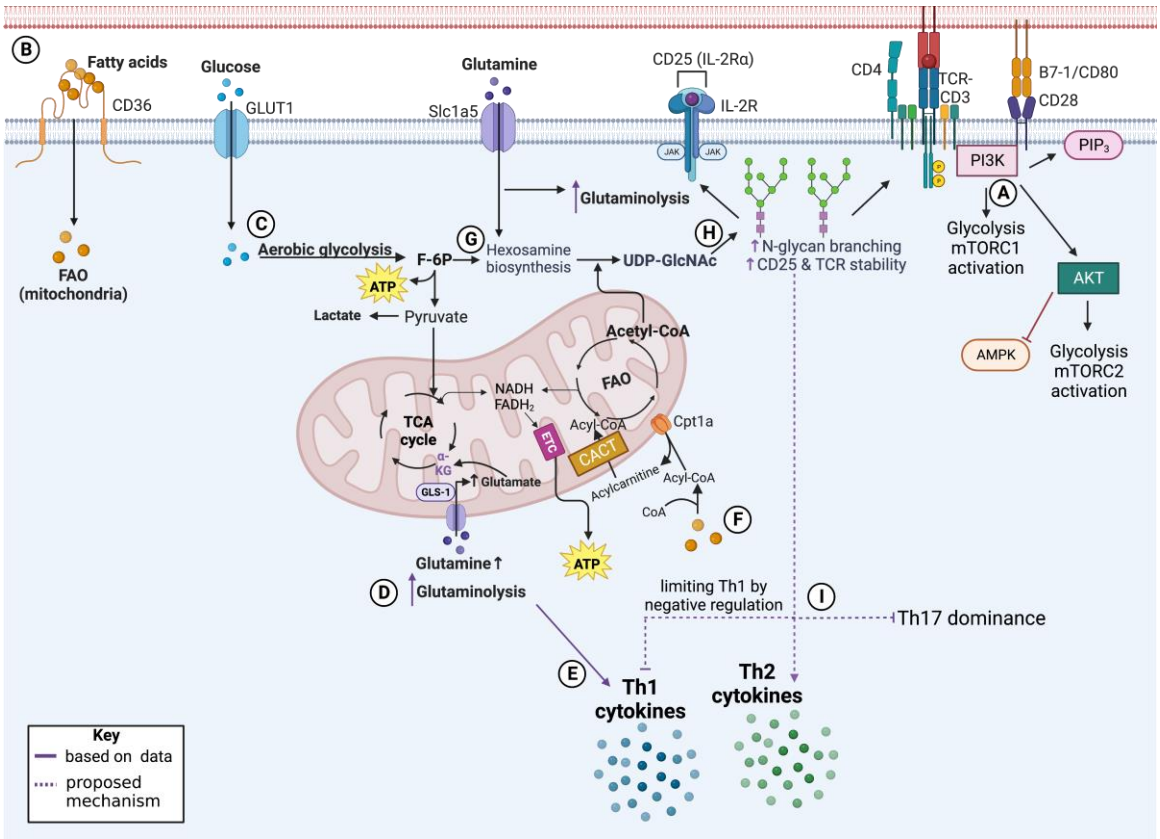

Figure 6.1 Schematic diagram of proposed mechanisms supporting CD4⁺ T-cell metabolism and T_{eff} cytokine production in preT2D

(**A**) T-cell activation by TCR engagement, CD3 activation, and co-stimulatory interactions activates the PI3K-Akt pathway to inhibit AMPK, subsequently activating mTORC1 and mTORC2 to support cell growth, proliferation, and survival and metabolism (e.g., glycolysis). (**B**) Activated T cells rapidly take in nutrients such as FAs, glucose, and glutamine for catabolism and anabolism. (**C**) Glucose is utilized for aerobic glycolysis, generating ATP, in addition to lactate (glycolysis) and acetyl-CoA (TCA cycle) from pyruvate, the latter supporting NADH and $FADH_2$ production for the ETC and OXPHOS. (**D**) Glutamine is transported into the mitochondria and is broken down into glutamate by the enzyme GLS-1, then to α-KG to replenish carbon loss via the TCA cycle, and (**E**) supports Th1 cytokine production from T_{eff} cells. (**F**) FAs are transported through Cpt1a on the outer mitochondrial membrane, converted into acylcarnitine, and further modified by CACT to generate acyl-CoA for FAO to generate NADH and $FADH_2$ for the ETC and OXPHOS and acetyl-CoA. (**G**) Products from glycolysis (F-6P), glutaminolysis (amino group), and FAO (acetyl-CoA) converge to generate UDP-GlcNAc in the hexosamine biosynthesis pathway. (**H**) UDP-GlcNAc generation enhances N-glycan branching of CD25 (IL-2Rα) and the TCR, of which support (**I**) Th2 differentiation/cytokine production over Th17 and limit Th1 function by negative regulation and might explain distinct CD4⁺ T cell cytokine profiles between preT2D and T2D.

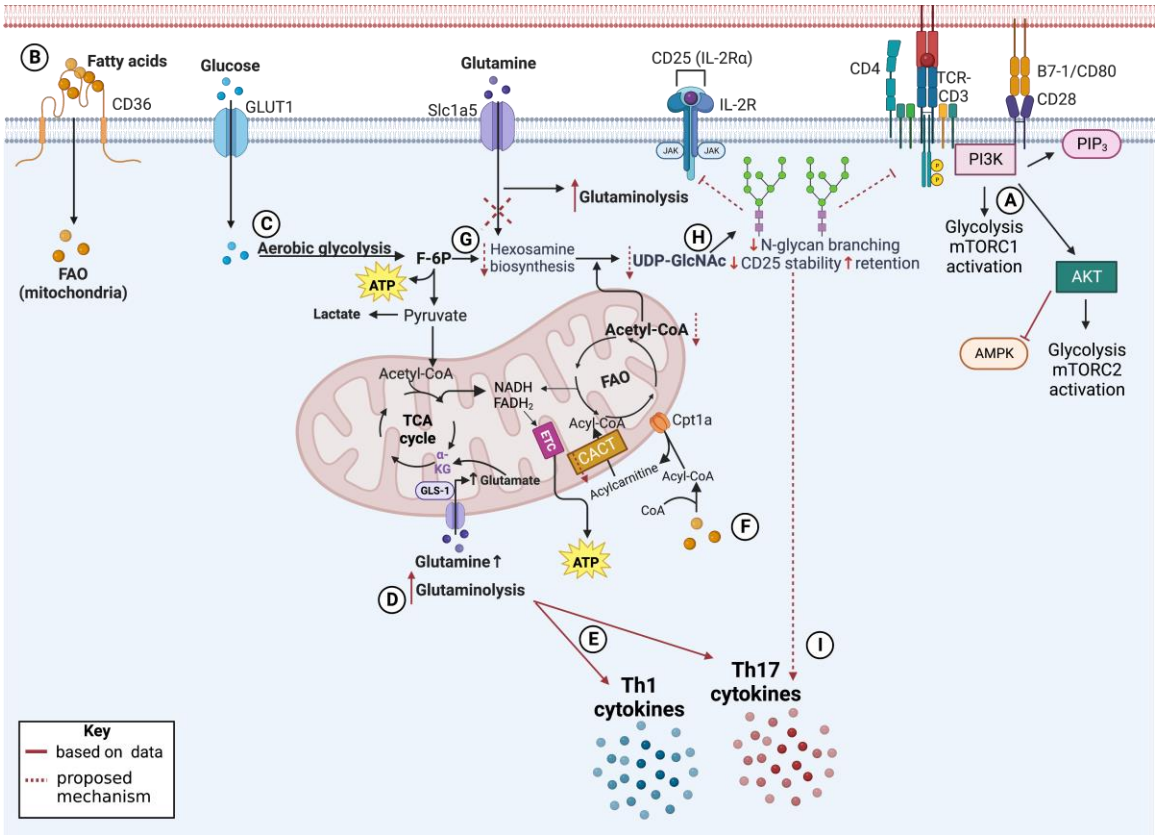

Figure 6.2 Schematic diagram of proposed mechanisms supporting CD4⁺ T-cell metabolism and T_{eff} cytokine production in T2D

(**A**) T-cell activation by TCR engagement, CD3 activation, and co-stimulatory interactions activates the PI3K-Akt pathway to inhibit AMPK, subsequently activating mTORC1 and mTORC2 to support cell growth, proliferation, and survival and metabolism (e.g., glycolysis). (**B**) Activated T cells rapidly take in nutrients such as FAs, glucose, and glutamine for catabolism and anabolism. (**C**) Glucose is utilized for aerobic glycolysis, generating ATP, in addition to lactate (glycolysis) and acetyl-CoA (TCA cycle) from pyruvate, the latter supporting NADH and $FADH_2$ production for the ETC and OXPHOS. (**D**) Glutamine is transported into the mitochondria and is broken down into glutamate by the enzyme GLS-1, then α-KG to replenish carbon loss via the TCA cycle, and (**E**) supports Th1 and Th17 cytokine production from T_{eff} cells. (**F**) FAs are transported and converted through Cpt1a on the outer mitochondrial membrane into acylcarnitine, then further modified by CACT to generate acyl-CoA, but changes in this mechanism as previously demonstrated (lower CACT expression)[46] might reduce the acetyl-CoA pool and could support a shift to glutamine reliance to bioenergetically compensate for changes in FAO (**G**) Products from glycolysis (F-6P), glutaminolysis (amino group), and FAO (acetyl-CoA) converge to generate UDP-GlcNAc in the hexosamine biosynthesis pathway, but potential reduction in available acetyl-CoA and a preferential utilization of glutamine to glutaminolysis might starve the hexosamine biosynthesis pathway. (**H**) Decreases in UDP-GlcNAc generation reduces N-glycan branching of CD25 (IL-2Rα) and the TCR, decreasing stability and leading to CD25 retention to support (**I**) Th17 differentiation/cytokine production over Th2 and might explain distinct CD4⁺ T cell cytokine profiles between preT2D and T2D.

APPENDICES

APPENDIX I. LIST OF ABBREVIATIONS

ACC	Acetyl-CoA carboxylase
AGE	Advanced glycated end-product
Akt	Protein kinase B
AMP	Adenosine monophosphate
AMPK	Adenosine monophosphate kinase
APC	Antigen-presenting cells
AT	Adipose tissue
ATM	Adipose tissue macrophage
ATP	Adenosine triphosphate
BPTES	N,N'-[thiobis(2,1-ethanediyl-1,3,4-thiadiazole-5,2-diyl)]*bis*-benzeneacetamide
CACT	Carnitine acylcarnitine transferase
CPT1a	Carnitine palmitoyltransferase 1a
DAMPs	Damage-associated molecular patterns
DIO	Diet-induced obesity
DPP4	Dipeptidyl peptidase 4
ER	Endoplasmic reticulum
ETC	Electron transport chain
F-6P	Fructose-6-phosphate

FA	Fatty acid
FACS	Fluorescence-activated cell sorting
FAO	Fatty acid oxidation
FBG	Fasting blood glucose
FFA	Free fatty acid
GI	Gastrointestinal
GIP	Glucose-dependent insulinotropic peptide
GLP-1	Glucagon-like peptide-1
GLS-1	Glutaminase-1
GPCR	G-protein coupled receptor
GSH	Glutathione
HbA1c	Hemoglobin A1c
IGT	Impaired glucose tolerance
IL	Interleukin
ILC2	Type 2 innate lymphoid cell
iNKT	Invariant natural killer T cell
InsR	Insulin receptor
IR	Insulin resistance
IRS	Insulin receptor substrate
JAK	Janus kinase

JNK	c-Jun N-terminal kinases
LAMP-1	Lysosomal associated membrane protein 1
LC3	1B-light chain 3
LCFA	Long-chain fatty acid
MAPK	Mitogen activated protein kinase
MPC	Mitochondrial pyruvate carrier
mtDNA	Mitochondrial DNA
mtROS	Mitochondrial ROS
ND	Non-diabetes
nDNA	Nuclear DNA
NF-κB	Nuclear factor kappa B
NFAT	Nuclear factor of activated T-cells
NGT	Normal glucose tolerance
OGTT	Oral glucose tolerance test
OXPHOS	Oxidative phosphorylation
PBMCs	Peripheral blood mononuclear cells
PFK1	Phosphofructokinase 1
PI3K	Phosphoinositide-3 kinase
PLC	Phospholipase C
PPAR-α	Peroxisome proliferator activated receptor-alpha

PPAR-γ	Peroxisome proliferator activated receptor-gamma
preT2D	Prediabetes
ROS	Reactive oxygen species
RTK	Receptor tyrosine kinase
S1P	Sphingosine-1 phosphate
SAT	Subcutaneous white adipose tissue
SFA	Saturated fatty acid
SGLT	Sodium-glucose cotransporter
T2D	Type 2 diabetes
T_{eff}	T-effector
T_{EM}	T-effector memory
Th1	T-helper 1
Th2	T-helper 2
Th17	T-helper 17
TG	Triglycerides
T_{reg}	T-regulatory
T_{RM}	Tissue-resident memory
TZDs	Thiazolidinediones
UPR	Unfolded protein response
SAT	Subcutaneous adipose tissue

STAT	Signal transducers of activation and transcription
VAT	Visceral adipose tissue
WAT	White adipose tissue

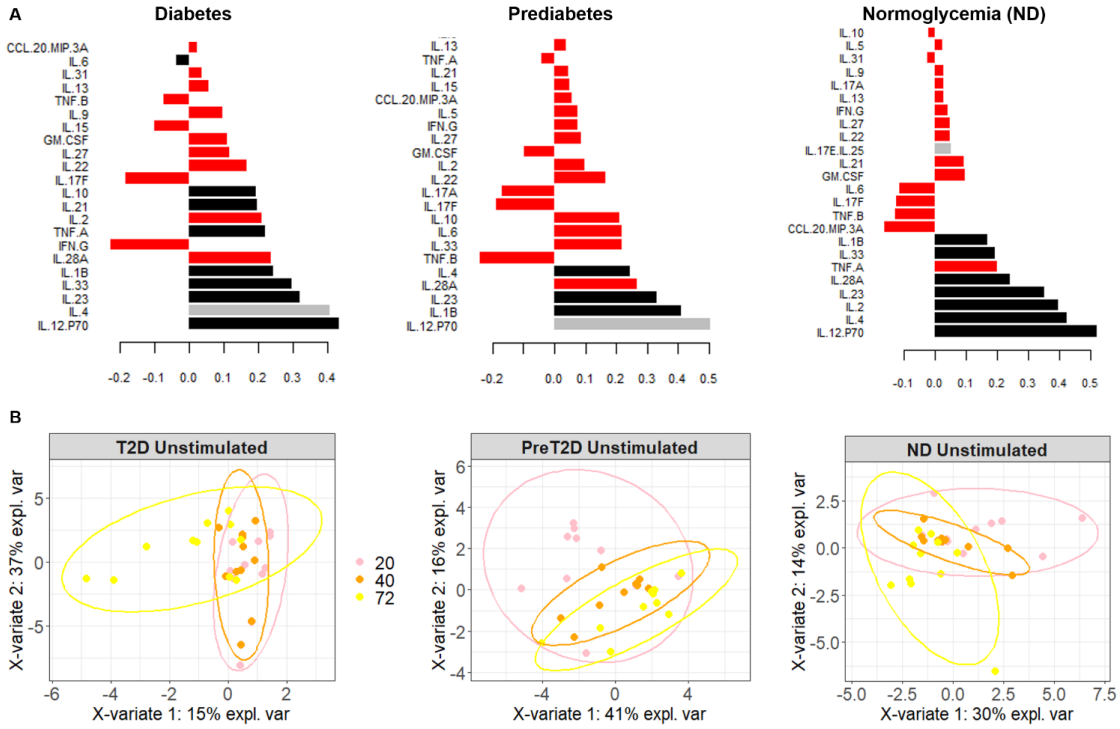

Figure A2.1: Cytokines produced by CD3/CD28- but not LPS- nor unstimulated PBMCs from cohorts indicated change over time as shown by PLSDA. (**A**) The second component that defines inflammation has more contribution from cytokines elicited by 40h CD3/CD28 stimulation (black bars), especially for samples from diabetes and non-diabetes (ND) subjects, than the first component (See Fig. 1). (**B**) Cytokine profiles produced by unstimulated PBMCs from the indicated cohort insignificantly change over time. Data were analyzed and figures were generated by X.D. Zhang

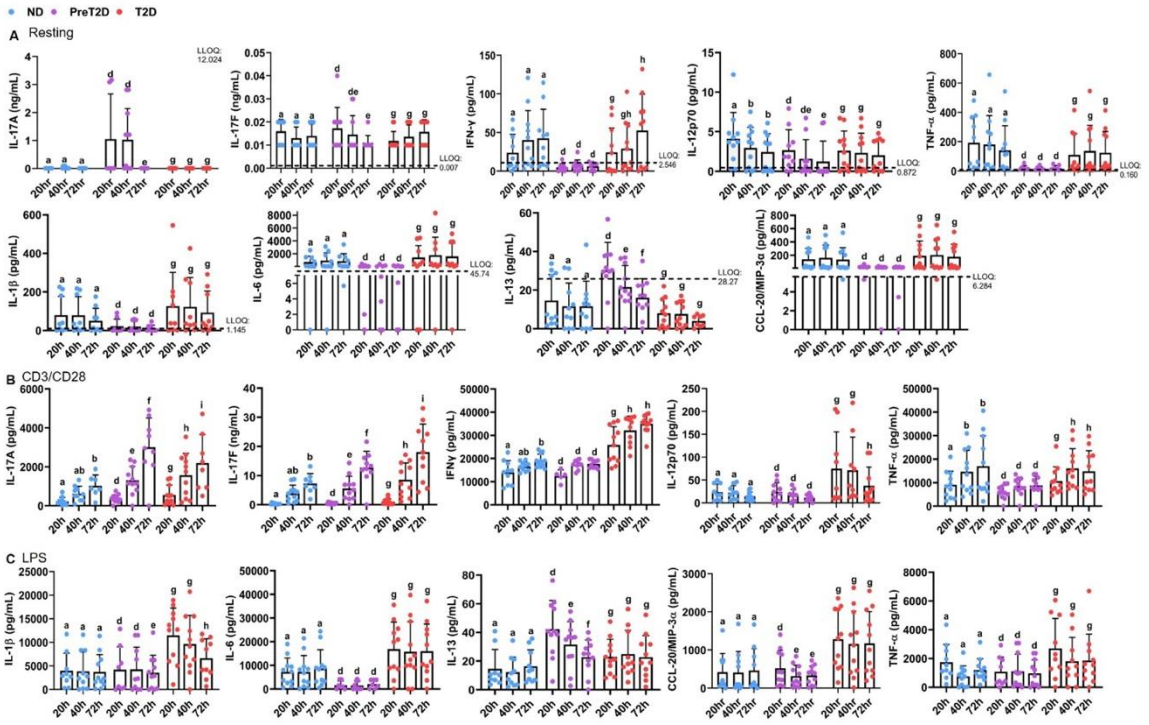

Figure A2.2: **Cytokines produced by CD3/CD28- but not LPS- nor unstimulated PBMCs from cohorts indicated change over time**

(**A**) Representative cytokines produced by PBMCs from each cohort without the presence of stimulation (resting). (**B**) Representative cytokines produced by PBMCs from each cohort stimulated with CD3/CD28 for 20-72h. (**C**) Representative cytokines produced by LPS stimulation (20-72hr) from each cohort. N's are shown in Table S1. Dashed lines represent the lower limit of quantification (LLOQ) to identify samples above or below this cut-off. Differences determined by a mixed-effects analysis and Tukey's multiple comparisons. Significance defined as $P < 0.05$ and represented as letters for each cohort (a-c for ND, d-f for preT2D, and g-i for T2D). Bars assigned the same letter indicate no statistical difference amongst time points within the same cohort.

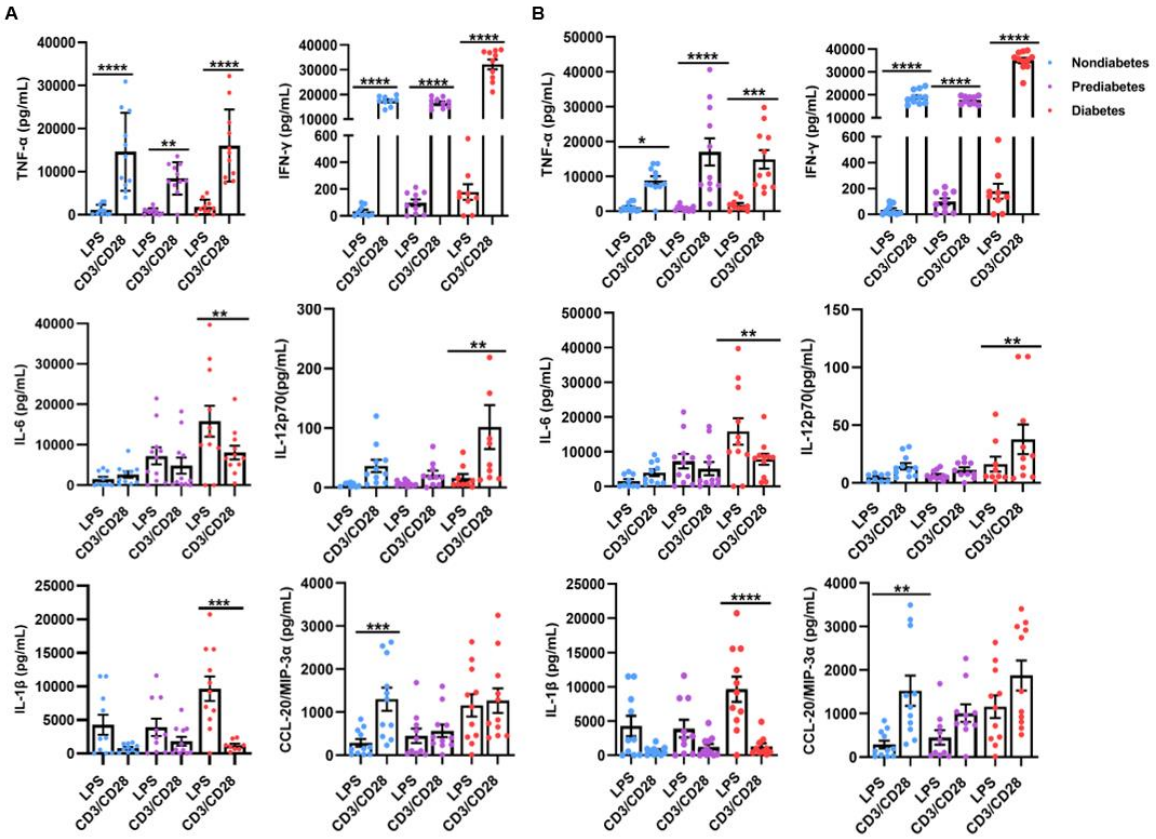

Figure A2.3. T cell and myeloid cell stimulation elicits approximately equivalent TNF-α production by PBMCs from all overweight/obese subjects

Direct comparison of cytokines elicited from PBMCs by (**A**) 20hr. LPS and 40 hr CD3/CD28 or (**B**) 72hrs CD/CD28 as measured in supernatants. PBMCs were from ND (blue), prediabetes (purple) or diabetes (red) subjects as indicated. Differences identified by two-way ANOVA are indicated. Bars show average and SD.

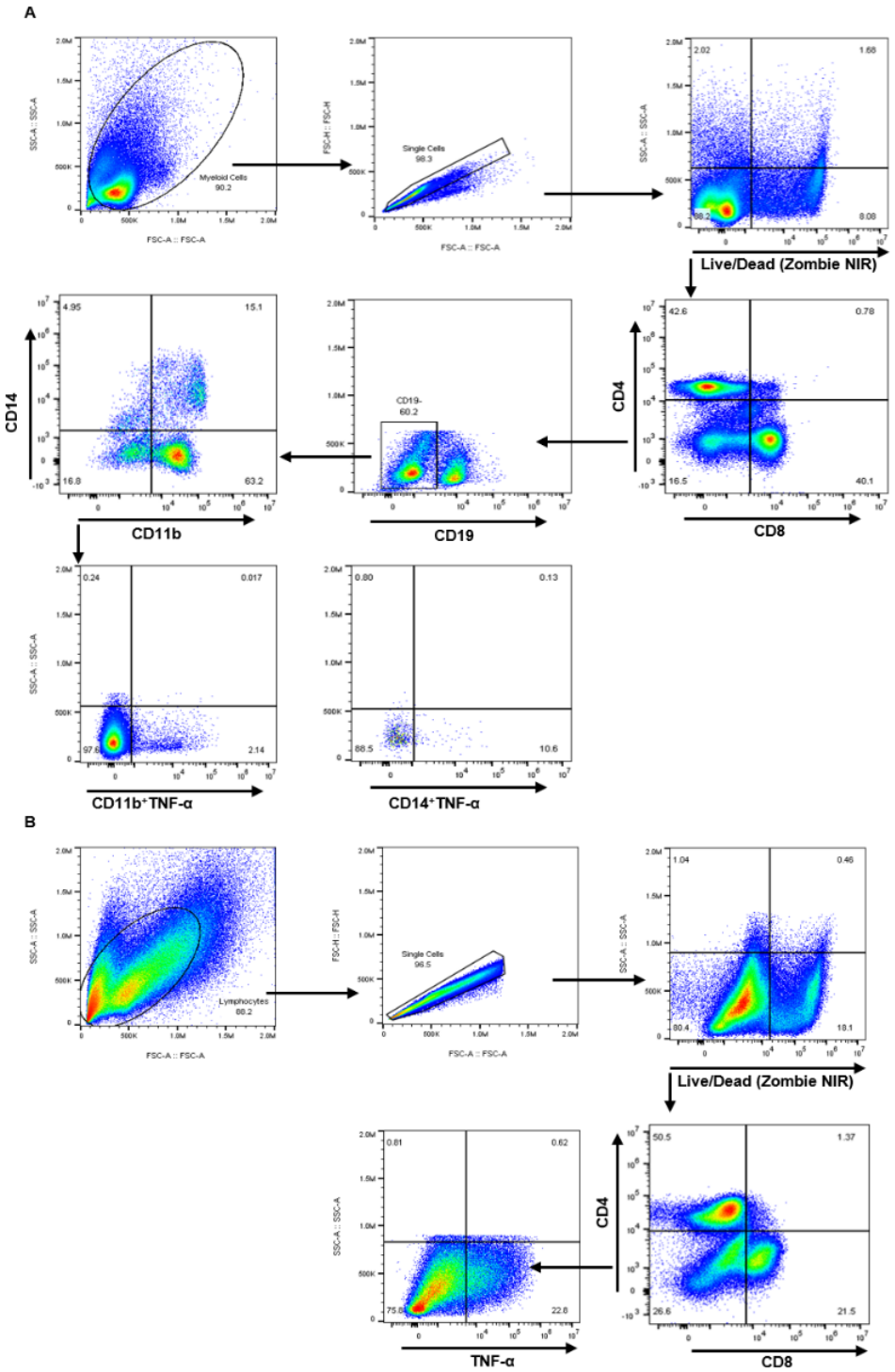

Figure A2.4. Gating Strategy for Intracellular TNF-α Staining of Myeloid Cell and CD4⁺ T cells (**A**) Gating for CD11b⁺ and CD14⁺ cells from LPS-stimulated PBMCS (20hrs) and intracellular TNF-α within these myeloid populations. (**B**) Gating for CD4⁺ T lymphocytes from CD3/CD28-stimulated PBMCs (40hrs) and intracellular TNF-α within the CD4⁺ population.

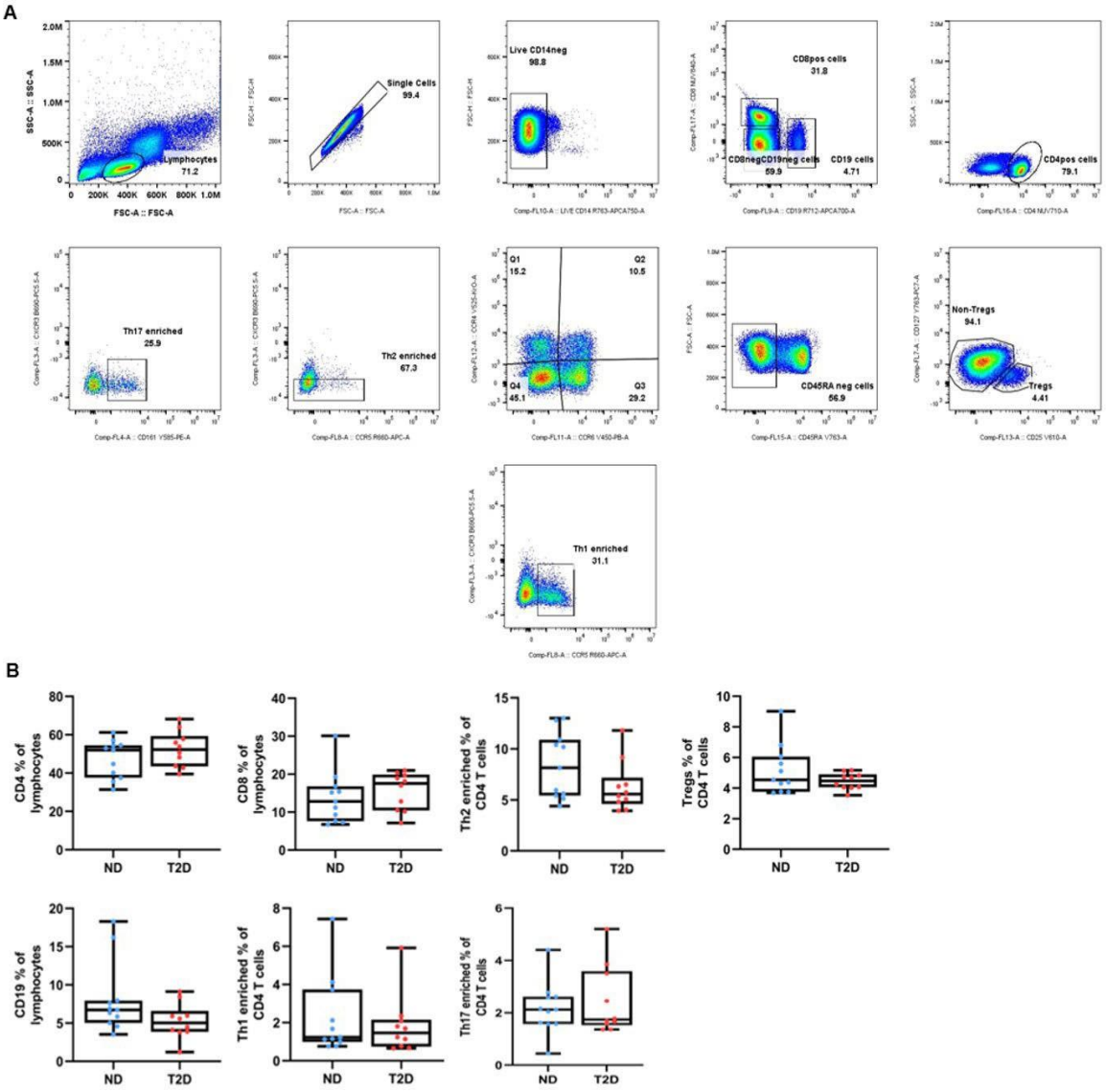

Figure A2.5. T cell and myeloid subset frequencies in PBMCs are similar between resting PBMCs from ND and diabetes subjects, and TNF-α production by myeloid cells is low in response to CD3/CD28 stimulation

(**A**) Flow cytometry gating strategy for quantification of immune cell subsets (**B**) Percentages of $CD4^+$, $CD8^+$, and $CD19^+$ cells in resting PBMCs determined per gating in panel A. Samples are from ND (blue), or T2D (red) subjects: ND (n=11), T2D (n=10). Statistical differences were determined by a Mann-Whitney U non-parametric t test. Figures and data analysis were generated by M.A. Agrawal.

Table A2.1 MRMR prediction of ND, preT2D, and T2D donors

Class	Precision	Recall	F1-score	AUC
ND	0.500	0.455	0.476	0.674
preT2D	0.500	0.545	0.522	0.682
T2D	0.909	0.909	0.909	0.893
Micro-average	0.636	0.636	0.636	0.757

Analysis generated by S. Fouladvand and J. Chen

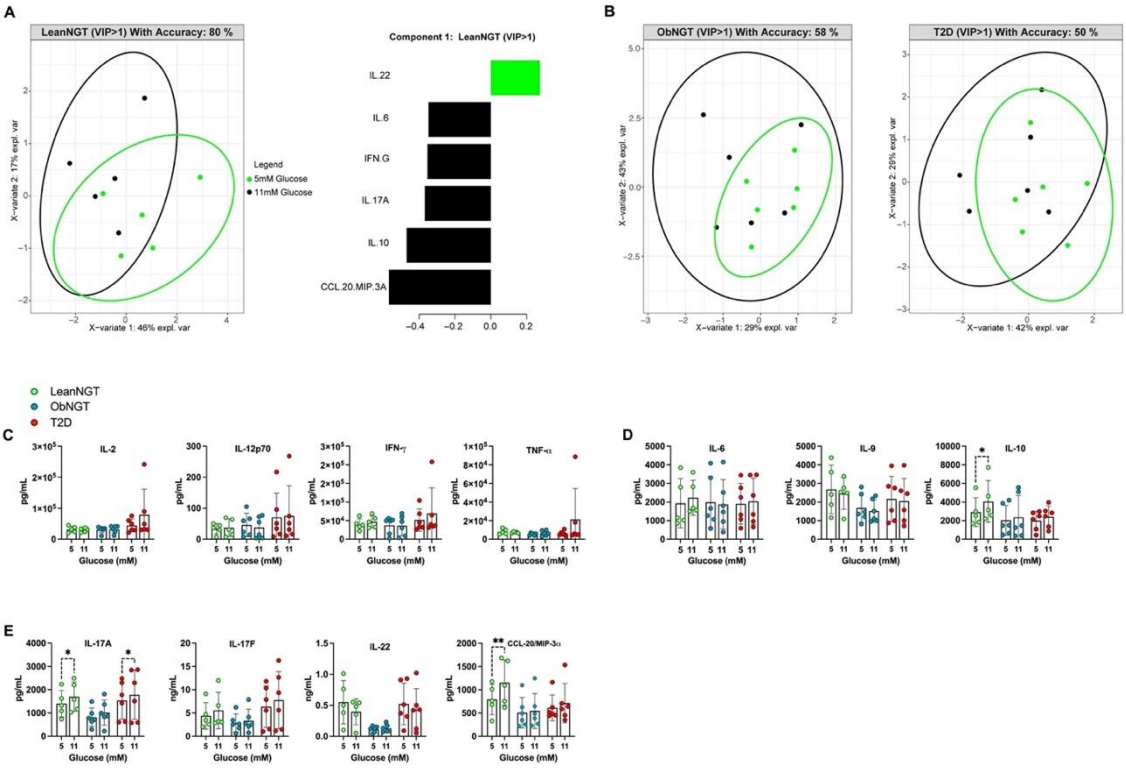

Figure A2.6 Insensitivity to glucose fluctuations associate with obesity and T2D
(**A-B**) PLSDA generated by combining all cytokines from PBMCs stimulated with CD3/CD28 (40h) from age-matched lean NGT (left), obese NGT (middle- right), and T2D (right) donors in euglycemic (5mM glucose- green dots/bars) or hyperglycemic (11mM glucose- black dots/bars) conditions. PLSDA are shown as 2D projections of cytokines in the first, most-distinguishing, component that ranks the optimal number of cytokine values (with a VIP score $\geq$ 1) that predict each cohort as indicated. The model was only able to generate reliable predictions (indicated by an accuracy $\geq$ 70 %), indicating no difference in cytokine production between glucose conditions in obesity/T2D. Cytokines that are higher under 5mM or 11mM glucose conditions are ranked for the lean NGT group (middle-left), showing higher production of Th1 (IFN-γ; IL-6), Th2 (IL-6; IL-10), Th17 (IL-17A; CCL-20), and Treg (IL-10). (**C-E**) Representative cytokines of Th1 (**C**), Th2/Treg (**D**), and Th17 cells (**E**). Analysis and figures in panels A and B were generated by S. Saraswat and X.D. Zhang.

REFERENCES

1. Hales, C.M., Fryar, C.D., Carroll, M.D., Freedman, D.S., and Ogden, C.L. (2018). Trends in Obesity and Severe Obesity Prevalence in US Youth and Adults by Sex and Age, 2007-2008 to 2015-2016. JAMA *319*, 1723-1725. 10.1001/jama.2018.3060.
2. Flegal, K.M., Kruszon-Moran, D., Carroll, M.D., Fryar, C.D., and Ogden, C.L. (2016). Trends in Obesity Among Adults in the United States, 2005 to 2014. JAMA *315*, 2284-2291. 10.1001/jama.2016.6458.
3. Ogden, C.L., Carroll, M.D., Lawman, H.G., Fryar, C.D., Kruszon-Moran, D., Kit, B.K., and Flegal, K.M. (2016). Trends in Obesity Prevalence Among Children and Adolescents in the United States, 1988-1994 Through 2013-2014. JAMA *315*, 2292-2299. 10.1001/jama.2016.6361.
4. Kannel, W.B., Cupples, L.A., Ramaswami, R., Stokes, J., 3rd, Kreger, B.E., and Higgins, M. (1991). Regional obesity and risk of cardiovascular disease; the Framingham Study. J Clin Epidemiol *44*, 183-190. 10.1016/0895-4356(91)90265-b.
5. Ruhl, C.E., and Everhart, J.E. (2003). Determinants of the association of overweight with elevated serum alanine aminotransferase activity in the United States. Gastroenterology *124*, 71-79. 10.1053/gast.2003.50004.
6. Okobi, O.E., Ajayi, O.O., Okobi, T.J., Anaya, I.C., Fasehun, O.O., Diala, C.S., Evbayekha, E.O., Ajibowo, A.O., Olateju, I.V., Ekabua, J.J., et al. (2021). The Burden of Obesity in the Rural Adult Population of America. Cureus *13*, e15770. 10.7759/cureus.15770.
7. Hill-Briggs, F., Adler, N.E., Berkowitz, S.A., Chin, M.H., Gary-Webb, T.L., Navas-Acien, A., Thornton, P.L., and Haire-Joshu, D. (2020). Social Determinants of Health and Diabetes: A Scientific Review. Diabetes Care *44*, 258-279. 10.2337/dci20-0053.
8. CDC Wonder, D.M. (2017).
9. Dall, T.M., Yang, W., Gillespie, K., Mocarski, M., Byrne, E., Cintina, I., Beronja, K., Semilla, A.P., Iacobucci, W., and Hogan, P.F. (2019). The Economic Burden of Elevated Blood Glucose Levels in 2017: Diagnosed and Undiagnosed Diabetes, Gestational Diabetes Mellitus, and Prediabetes. Diabetes Care *42*, 1661-1668. 10.2337/dc18-1226.
10. Zhang, Y., Pan, X.F., Chen, J., Xia, L., Cao, A., Zhang, Y., Wang, J., Li, H., Yang, K., Guo, K., et al. (2020). Combined lifestyle factors and risk of incident type 2 diabetes and prognosis among individuals with type 2 diabetes: a systematic review and meta-analysis of prospective cohort studies. Diabetologia *63*, 21-33. 10.1007/s00125-019-04985-9.
11. Lyssenko, V., Jonsson, A., Almgren, P., Pulizzi, N., Isomaa, B., Tuomi, T., Berglund, G., Altshuler, D., Nilsson, P., and Groop, L. (2008). Clinical risk factors, DNA variants, and the development of type 2 diabetes. N Engl J Med *359*, 2220-2232. 10.1056/NEJMoa0801869.
12. Cabrera, O., Berman, D.M., Kenyon, N.S., Ricordi, C., Berggren, P.O., and Caicedo, A. (2006). The unique cytoarchitecture of human pancreatic islets

has implications for islet cell function. Proc Natl Acad Sci U S A *103*, 2334-2339. 10.1073/pnas.0510790103.

13. DeFronzo, R.A., Jacot, E., Jequier, E., Maeder, E., Wahren, J., and Felber, J.P. (1981). The effect of insulin on the disposal of intravenous glucose. Results from indirect calorimetry and hepatic and femoral venous catheterization. Diabetes *30*, 1000-1007. 10.2337/diab.30.12.1000.
14. DeFronzo, R.A., Gunnarsson, R., Bjorkman, O., Olsson, M., and Wahren, J. (1985). Effects of insulin on peripheral and splanchnic glucose metabolism in noninsulin-dependent (type II) diabetes mellitus. J Clin Invest *76*, 149-155. 10.1172/JCI111938.
15. Edgerton, D.S., Lautz, M., Scott, M., Everett, C.A., Stettler, K.M., Neal, D.W., Chu, C.A., and Cherrington, A.D. (2006). Insulin's direct effects on the liver dominate the control of hepatic glucose production. J Clin Invest *116*, 521-527. 10.1172/JCI27073.
16. Michael, M.D., Kulkarni, R.N., Postic, C., Previs, S.F., Shulman, G.I., Magnuson, M.A., and Kahn, C.R. (2000). Loss of insulin signaling in hepatocytes leads to severe insulin resistance and progressive hepatic dysfunction. Mol Cell *6*, 87-97.
17. Harrison, L.C., and King-Roach, A.P. (1976). Insulin sensitivity of adipose tissue in vitro and the response to exogenous insulin in obese human subjects. Metabolism *25*, 1095-1101. 10.1016/0026-0495(76)90017-2.
18. Gastaldelli, A., Gaggini, M., and DeFronzo, R.A. (2017). Role of Adipose Tissue Insulin Resistance in the Natural History of Type 2 Diabetes: Results From the San Antonio Metabolism Study. Diabetes *66*, 815-822. 10.2337/db16-1167.
19. Yoneda, S., Uno, S., Iwahashi, H., Fujita, Y., Yoshikawa, A., Kozawa, J., Okita, K., Takiuchi, D., Eguchi, H., Nagano, H., et al. (2013). Predominance of beta-cell neogenesis rather than replication in humans with an impaired glucose tolerance and newly diagnosed diabetes. J Clin Endocrinol Metab *98*, 2053-2061. 10.1210/jc.2012-3832.
20. Hull, R.L., Kodama, K., Utzschneider, K.M., Carr, D.B., Prigeon, R.L., and Kahn, S.E. (2005). Dietary-fat-induced obesity in mice results in beta cell hyperplasia but not increased insulin release: evidence for specificity of impaired beta cell adaptation. Diabetologia *48*, 1350-1358. 10.1007/s00125-005-1772-9.
21. Gonzalez, A., Merino, B., Marroqui, L., Neco, P., Alonso-Magdalena, P., Caballero-Garrido, E., Vieira, E., Soriano, S., Gomis, R., Nadal, A., and Quesada, I. (2013). Insulin hypersecretion in islets from diet-induced hyperinsulinemic obese female mice is associated with several functional adaptations in individual beta-cells. Endocrinology *154*, 3515-3524. 10.1210/en.2013-1424.
22. Marchetti, P., Bugliani, M., Lupi, R., Marselli, L., Masini, M., Boggi, U., Filipponi, F., Weir, G.C., Eizirik, D.L., and Cnop, M. (2007). The endoplasmic reticulum in pancreatic beta cells of type 2 diabetes patients. Diabetologia *50*, 2486-2494. 10.1007/s00125-007-0816-8.

23. Rahier, J., Guiot, Y., Goebbels, R.M., Sempoux, C., and Henquin, J.C. (2008). Pancreatic beta-cell mass in European subjects with type 2 diabetes. Diabetes Obes Metab *10 Suppl 4*, 32-42. 10.1111/j.1463-1326.2008.00969.x.
24. Marchetti, P., and Masini, M. (2009). Autophagy and the pancreatic beta-cell in human type 2 diabetes. Autophagy *5*, 1055-1056. 10.4161/auto.5.7.9511.
25. Ling, W., Huang, Y., Huang, Y.M., Fan, R.R., Sui, Y., and Zhao, H.L. (2020). Global trend of diabetes mortality attributed to vascular complications, 2000-2016. Cardiovasc Diabetol *19*, 182. 10.1186/s12933-020-01159-5.
26. Schlesinger, S., Neuenschwander, M., Barbaresko, J., Lang, A., Maalmi, H., Rathmann, W., Roden, M., and Herder, C. (2022). Prediabetes and risk of mortality, diabetes-related complications and comorbidities: umbrella review of meta-analyses of prospective studies. Diabetologia *65*, 275-285. 10.1007/s00125-021-05592-3.
27. Cusick, M., Meleth, A.D., Agron, E., Fisher, M.R., Reed, G.F., Knatterud, G.L., Barton, F.B., Davis, M.D., Ferris, F.L., 3rd, Chew, E.Y., and Early Treatment Diabetc Retinopathy Study Research, G. (2005). Associations of mortality and diabetes complications in patients with type 1 and type 2 diabetes: early treatment diabetic retinopathy study report no. 27. Diabetes Care *28*, 617-625. 10.2337/diacare.28.3.617.
28. Ricardo-Gonzalez, R.R., Red Eagle, A., Odegaard, J.I., Jouihan, H., Morel, C.R., Heredia, J.E., Mukundan, L., Wu, D., Locksley, R.M., and Chawla, A. (2010). IL-4/STAT6 immune axis regulates peripheral nutrient metabolism and insulin sensitivity. Proc Natl Acad Sci U S A *107*, 22617-22622. 10.1073/pnas.1009152108.
29. Chang, Y.H., Ho, K.T., Lu, S.H., Huang, C.N., and Shiau, M.Y. (2012). Regulation of glucose/lipid metabolism and insulin sensitivity by interleukin-4. Int J Obes (Lond) *36*, 993-998. 10.1038/ijo.2011.168.
30. Chang, Y.H., Tsai, J.N., Chen, T.L., Ho, K.T., Cheng, H.Y., Hsiao, C.W., and Shiau, M.Y. (2019). Interleukin-4 Promotes Myogenesis and Boosts Myocyte Insulin Efficacy. Mediators Inflamm *2019*, 4182015. 10.1155/2019/4182015.
31. Dror, E., Dalmas, E., Meier, D.T., Wueest, S., Thevenet, J., Thienel, C., Timper, K., Nordmann, T.M., Traub, S., Schulze, F., et al. (2017). Postprandial macrophage-derived IL-1beta stimulates insulin, and both synergistically promote glucose disposal and inflammation. Nat Immunol *18*, 283-292. 10.1038/ni.3659.
32. Pradhan, A.D., Manson, J.E., Rifai, N., Buring, J.E., and Ridker, P.M. (2001). C-reactive protein, interleukin 6, and risk of developing type 2 diabetes mellitus. JAMA *286*, 327-334.
33. Qu, Y., Zhang, Q., Ma, S., Liu, S., Chen, Z., Mo, Z., and You, Z. (2016). Interleukin-17A Differentially Induces Inflammatory and Metabolic Gene Expression in the Adipose Tissues of Lean and Obese Mice. Int J Mol Sci *17*, 522. 10.3390/ijms17040522.

34. Stafeev, I.S., Michurina, S.S., Podkuychenko, N.V., Vorotnikov, A.V., Menshikov, M.Y., and Parfyonova, Y.V. (2018). Interleukin-4 Restores Insulin Sensitivity in Lipid-Induced Insulin-Resistant Adipocytes. Biochemistry (Mosc) *83*, 498-506. 10.1134/S0006297918050036.
35. Stanya, K.J., Jacobi, D., Liu, S., Bhargava, P., Dai, L., Gangl, M.R., Inouye, K., Barlow, J.L., Ji, Y., Mizgerd, J.P., et al. (2013). Direct control of hepatic glucose production by interleukin-13 in mice. J Clin Invest *123*, 261-271. 10.1172/JCI64941.
36. Tsao, C.H., Shiau, M.Y., Chuang, P.H., Chang, Y.H., and Hwang, J. (2014). Interleukin-4 regulates lipid metabolism by inhibiting adipogenesis and promoting lipolysis. J Lipid Res *55*, 385-397. 10.1194/jlr.M041392.
37. Lumeng, C.N., Deyoung, S.M., Bodzin, J.L., and Saltiel, A.R. (2007). Increased inflammatory properties of adipose tissue macrophages recruited during diet-induced obesity. Diabetes *56*, 16-23. 10.2337/db06-1076.
38. Lumeng, C.N., Bodzin, J.L., and Saltiel, A.R. (2007). Obesity induces a phenotypic switch in adipose tissue macrophage polarization. J Clin Invest *117*, 175-184. 10.1172/JCI29881.
39. Feuerer, M., Herrero, L., Cipolletta, D., Naaz, A., Wong, J., Nayer, A., Lee, J., Goldfine, A.B., Benoist, C., Shoelson, S., and Mathis, D. (2009). Lean, but not obese, fat is enriched for a unique population of regulatory T cells that affect metabolic parameters. Nat Med *15*, 930-939.
40. McLaughlin, T., Liu, L.F., Lamendola, C., Shen, L., Morton, J., Rivas, H., Winer, D., Tolentino, L., Choi, O., Zhang, H., et al. (2014). T-cell profile in adipose tissue is associated with insulin resistance and systemic inflammation in humans. Arterioscler Thromb Vasc Biol *34*, 2637-2643. 10.1161/ATVBAHA.114.304636.
41. Winer, D.A., Winer, S., Shen, L., Wadia, P.P., Yantha, J., Paltser, G., Tsui, H., Wu, P., Davidson, M.G., Alonso, M.N., et al. (2011). B cells promote insulin resistance through modulation of T cells and production of pathogenic IgG antibodies. Nat Med *17*, 610-617. 10.1038/nm.2353.
42. Defuria, J., Belkina, A.C., Jagannathan-Bogdan, M., Snyder-Cappione, J., Carr, J.D., Nersesova, Y.R., Markham, D., Strissel, K.J., Watkins, A.A., Zhu, M., et al. (2013). B cells promote inflammation in obesity and type 2 diabetes through regulation of T-cell function and an inflammatory cytokine profile. Proc Natl Acad Sci U S A *110*, 5133-5138. 10.1073/pnas.1215840110.
43. Ip, B., Cilfone, N.A., Belkina, A.C., DeFuria, J., Jagannathan-Bogdan, M., Zhu, M., Kuchibhatla, R., McDonnell, M.E., Xiao, Q., Kepler, T.B., et al. (2016). Th17 cytokines differentiate obesity from obesity-associated type 2 diabetes and promote TNFalpha production. Obesity (Silver Spring) *24*, 102-112. 10.1002/oby.21243.
44. Jagannathan-Bogdan, M., McDonnell, M.E., Shin, H., Rehman, Q., Hasturk, H., Apovian, C.M., and Nikolajczyk, B.S. (2011). Elevated proinflammatory cytokine production by a skewed T cell compartment requires monocytes and promotes inflammation in type 2 diabetes. J Immunol *186*, 1162-1172. 10.4049/jimmunol.1002615.

45. Liu, R., Pugh, G.H., Tevonian, E., Thompson, K., Lauffenburger, D.A., Kern, P.A., and Nikolajczyk, B.S. (2022). Regulatory T Cells Control Effector T Cell Inflammation in Human Prediabetes. Diabetes *71*, 264-274. 10.2337/db21-0659.
46. Nicholas, D.A., Proctor, E.A., Agrawal, M., Belkina, A.C., Van Nostrand, S.C., Panneerseelan-Bharath, L., Jones, A.R.t., Raval, F., Ip, B.C., Zhu, M., et al. (2019). Fatty Acid Metabolites Combine with Reduced beta Oxidation to Activate Th17 Inflammation in Human Type 2 Diabetes. Cell Metab *30*, 447-461 e445. 10.1016/j.cmet.2019.07.004.
47. Thorens, B., Sarkar, H.K., Kaback, H.R., and Lodish, H.F. (1988). Cloning and functional expression in bacteria of a novel glucose transporter present in liver, intestine, kidney, and beta-pancreatic islet cells. Cell *55*, 281-290. 10.1016/0092-8674(88)90051-7.
48. Permutt, M.A., Koranyi, L., Keller, K., Lacy, P.E., Scharp, D.W., and Mueckler, M. (1989). Cloning and functional expression of a human pancreatic islet glucose-transporter cDNA. Proc Natl Acad Sci U S A *86*, 8688-8692. 10.1073/pnas.86.22.8688.
49. Rumala, C.Z., Liu, J., Locasale, J.W., Corkey, B.E., Deeney, J.T., and Rameh, L.E. (2020). Exposure of Pancreatic beta-Cells to Excess Glucose Results in Bimodal Activation of mTORC1 and mTOR-Dependent Metabolic Acceleration. iScience *23*, 100858. 10.1016/j.isci.2020.100858.
50. Itoh, Y., Kawamata, Y., Harada, M., Kobayashi, M., Fujii, R., Fukusumi, S., Ogi, K., Hosoya, M., Tanaka, Y., Uejima, H., et al. (2003). Free fatty acids regulate insulin secretion from pancreatic beta cells through GPR40. Nature *422*, 173-176. 10.1038/nature01478.
51. Cen, J., Sargsyan, E., and Bergsten, P. (2016). Fatty acids stimulate insulin secretion from human pancreatic islets at fasting glucose concentrations via mitochondria-dependent and -independent mechanisms. Nutr Metab (Lond) *13*, 59. 10.1186/s12986-016-0119-5.
52. Oslowski, C.M., and Urano, F. (2010). The binary switch between life and death of endoplasmic reticulum-stressed beta cells. Curr Opin Endocrinol Diabetes Obes *17*, 107-112. 10.1097/MED.0b013e3283372843.
53. Brandhorst, H., Brandhorst, D., Brendel, M.D., Hering, B.J., and Bretzel, R.G. (1998). Assessment of intracellular insulin content during all steps of human islet isolation procedure. Cell Transplant *7*, 489-495. 10.1177/096368979800700508.
54. Lee, J.S., Wu, Y., Schnepp, P., Fang, J., Zhang, X., Karnovsky, A., Woods, J., Stemmer, P.M., Liu, M., Zhang, K., and Chen, X. (2015). Proteomics analysis of rough endoplasmic reticulum in pancreatic beta cells. Proteomics *15*, 1508-1511. 10.1002/pmic.201400345.
55. Weir, G.C., and Bonner-Weir, S. (2004). Five stages of evolving beta-cell dysfunction during progression to diabetes. Diabetes *53 Suppl 3*, S16-21. 10.2337/diabetes.53.suppl_3.s16.
56. Zhao, Y.F. (2022). Free fatty acid receptors in the endocrine regulation of glucose metabolism: Insight from gastrointestinal-pancreatic-adipose

interactions. Front Endocrinol (Lausanne) *13*, 956277. 10.3389/fendo.2022.956277.

57. Stefan, N., Stumvoll, M., Vozarova, B., Weyer, C., Funahashi, T., Matsuzawa, Y., Bogardus, C., and Tataranni, P.A. (2003). Plasma adiponectin and endogenous glucose production in humans. Diabetes Care *26*, 3315-3319. 10.2337/diacare.26.12.3315.
58. Miller, R.A., Chu, Q., Le Lay, J., Scherer, P.E., Ahima, R.S., Kaestner, K.H., Foretz, M., Viollet, B., and Birnbaum, M.J. (2011). Adiponectin suppresses gluconeogenic gene expression in mouse hepatocytes independent of LKB1-AMPK signaling. J Clin Invest *121*, 2518-2528. 10.1172/JCI45942.
59. Yamauchi, T., Kamon, J., Minokoshi, Y., Ito, Y., Waki, H., Uchida, S., Yamashita, S., Noda, M., Kita, S., Ueki, K., et al. (2002). Adiponectin stimulates glucose utilization and fatty-acid oxidation by activating AMP-activated protein kinase. Nat Med *8*, 1288-1295. 10.1038/nm788.
60. Seufert, J., Kieffer, T.J., Leech, C.A., Holz, G.G., Moritz, W., Ricordi, C., and Habener, J.F. (1999). Leptin suppression of insulin secretion and gene expression in human pancreatic islets: implications for the development of adipogenic diabetes mellitus. J Clin Endocrinol Metab *84*, 670-676. 10.1210/jcem.84.2.5460.
61. Rieusset, J., Andreelli, F., Auboeuf, D., Roques, M., Vallier, P., Riou, J.P., Auwerx, J., Laville, M., and Vidal, H. (1999). Insulin acutely regulates the expression of the peroxisome proliferator-activated receptor-gamma in human adipocytes. Diabetes *48*, 699-705. 10.2337/diabetes.48.4.699.
62. Sugii, S., Olson, P., Sears, D.D., Saberi, M., Atkins, A.R., Barish, G.D., Hong, S.H., Castro, G.L., Yin, Y.Q., Nelson, M.C., et al. (2009). PPARgamma activation in adipocytes is sufficient for systemic insulin sensitization. Proc Natl Acad Sci U S A *106*, 22504-22509. 10.1073/pnas.0912487106.
63. Chakrabarti, P., Kim, J.Y., Singh, M., Shin, Y.K., Kim, J., Kumbrink, J., Wu, Y., Lee, M.J., Kirsch, K.H., Fried, S.K., and Kandror, K.V. (2013). Insulin inhibits lipolysis in adipocytes via the evolutionarily conserved mTORC1-Egr1-ATGL-mediated pathway. Mol Cell Biol *33*, 3659-3666. 10.1128/MCB.01584-12.
64. Rosen, E.D., Sarraf, P., Troy, A.E., Bradwin, G., Moore, K., Milstone, D.S., Spiegelman, B.M., and Mortensen, R.M. (1999). PPAR gamma is required for the differentiation of adipose tissue in vivo and in vitro. Mol Cell *4*, 611-617. 10.1016/s1097-2765(00)80211-7.
65. Tontonoz, P., Hu, E., and Spiegelman, B.M. (1994). Stimulation of adipogenesis in fibroblasts by PPAR gamma 2, a lipid-activated transcription factor. Cell *79*, 1147-1156. 10.1016/0092-8674(94)90006-x.
66. Lasar, D., Rosenwald, M., Kiehlmann, E., Balaz, M., Tall, B., Opitz, L., Lidell, M.E., Zamboni, N., Krznar, P., Sun, W., et al. (2018). Peroxisome Proliferator Activated Receptor Gamma Controls Mature Brown Adipocyte Inducibility through Glycerol Kinase. Cell Rep *22*, 760-773. 10.1016/j.celrep.2017.12.067.

67. Ramos, L.S., Zippin, J.H., Kamenetsky, M., Buck, J., and Levin, L.R. (2008). Glucose and GLP-1 stimulate cAMP production via distinct adenylyl cyclases in INS-1E insulinoma cells. J Gen Physiol *132*, 329-338. 10.1085/jgp.200810044.
68. Carlessi, R., Chen, Y., Rowlands, J., Cruzat, V.F., Keane, K.N., Egan, L., Mamotte, C., Stokes, R., Gunton, J.E., Bittencourt, P.I.H., and Newsholme, P. (2017). GLP-1 receptor signalling promotes beta-cell glucose metabolism via mTOR-dependent HIF-1alpha activation. Sci Rep *7*, 2661. 10.1038/s41598-017-02838-2.
69. Seino, Y., Maekawa, R., Ogata, H., and Hayashi, Y. (2016). Carbohydrate-induced secretion of glucose-dependent insulinotropic polypeptide and glucagon-like peptide-1. J Diabetes Investig *7 Suppl 1*, 27-32. 10.1111/jdi.12449.
70. El, K., Gray, S.M., Capozzi, M.E., Knuth, E.R., Jin, E., Svendsen, B., Clifford, A., Brown, J.L., Encisco, S.E., Chazotte, B.M., et al. (2021). GIP mediates the incretin effect and glucose tolerance by dual actions on alpha cells and beta cells. Sci Adv *7*. 10.1126/sciadv.abf1948.
71. Naitoh, R., Miyawaki, K., Harada, N., Mizunoya, W., Toyoda, K., Fushiki, T., Yamada, Y., Seino, Y., and Inagaki, N. (2008). Inhibition of GIP signaling modulates adiponectin levels under high-fat diet in mice. Biochem Biophys Res Commun *376*, 21-25. 10.1016/j.bbrc.2008.08.052.
72. Kawasaki, T., Chen, W., Htwe, Y.M., Tatsumi, K., and Dudek, S.M. (2018). DPP4 inhibition by sitagliptin attenuates LPS-induced lung injury in mice. Am J Physiol Lung Cell Mol Physiol *315*, L834-L845. 10.1152/ajplung.00031.2018.
73. Casrouge, A., Sauer, A.V., Barreira da Silva, R., Tejera-Alhambra, M., Sanchez-Ramon, S., IcareB, Cancrini, C., Ingersoll, M.A., Aiuti, A., and Albert, M.L. (2018). Lymphocytes are a major source of circulating soluble dipeptidyl peptidase 4. Clin Exp Immunol *194*, 166-179. 10.1111/cei.13163.
74. Kaneto, H., Kimura, T., Shimoda, M., Obata, A., Sanada, J., Fushimi, Y., Nakanishi, S., Mune, T., and Kaku, K. (2021). Favorable Effects of GLP-1 Receptor Agonist against Pancreatic beta-Cell Glucose Toxicity and the Development of Arteriosclerosis: "The Earlier, the Better" in Therapy with Incretin-Based Medicine. Int J Mol Sci *22*. 10.3390/ijms22157917.
75. Kaneko, K., Fu, Y., Lin, H.Y., Cordonier, E.L., Mo, Q., Gao, Y., Yao, T., Naylor, J., Howard, V., Saito, K., et al. (2019). Gut-derived GIP activates central Rap1 to impair neural leptin sensitivity during overnutrition. J Clin Invest *129*, 3786-3791. 10.1172/JCI126107.
76. Sarkar, J., Nargis, T., Tantia, O., Ghosh, S., and Chakrabarti, P. (2019). Increased Plasma Dipeptidyl Peptidase-4 (DPP4) Activity Is an Obesity-Independent Parameter for Glycemic Deregulation in Type 2 Diabetes Patients. Front Endocrinol (Lausanne) *10*, 505. 10.3389/fendo.2019.00505.
77. Wilcock, C., and Bailey, C.J. (1994). Accumulation of metformin by tissues of the normal and diabetic mouse. Xenobiotica *24*, 49-57. 10.3109/00498259409043220.

78. Jensen, J.B., Sundelin, E.I., Jakobsen, S., Gormsen, L.C., Munk, O.L., Frokiaer, J., and Jessen, N. (2016). [11C]-Labeled Metformin Distribution in the Liver and Small Intestine Using Dynamic Positron Emission Tomography in Mice Demonstrates Tissue-Specific Transporter Dependency. Diabetes *65*, 1724-1730. 10.2337/db16-0032.
79. Gormsen, L.C., Sundelin, E.I., Jensen, J.B., Vendelbo, M.H., Jakobsen, S., Munk, O.L., Hougaard Christensen, M.M., Brosen, K., Frokiaer, J., and Jessen, N. (2016). In Vivo Imaging of Human 11C-Metformin in Peripheral Organs: Dosimetry, Biodistribution, and Kinetic Analyses. J Nucl Med *57*, 1920-1926. 10.2967/jnumed.116.177774.
80. He, L., and Wondisford, F.E. (2015). Metformin action: concentrations matter. Cell Metab *21*, 159-162. 10.1016/j.cmet.2015.01.003.
81. Kim, S.A., and Choi, H.C. (2012). Metformin inhibits inflammatory response via AMPK-PTEN pathway in vascular smooth muscle cells. Biochem Biophys Res Commun *425*, 866-872. 10.1016/j.bbrc.2012.07.165.
82. Takashima, M., Ogawa, W., Hayashi, K., Inoue, H., Kinoshita, S., Okamoto, Y., Sakaue, H., Wataoka, Y., Emi, A., Senga, Y., et al. (2010). Role of KLF15 in regulation of hepatic gluconeogenesis and metformin action. Diabetes *59*, 1608-1615. 10.2337/db09-1679.
83. Rittig, N., Aagaard, N.K., Sundelin, E., Villadsen, G.E., Sandahl, T.D., Holst, J.J., Hartmann, B., Brosen, K., Gronbaek, H., and Jessen, N. (2021). Metformin Stimulates Intestinal Glycolysis and Lactate Release: A single-Dose Study of Metformin in Patients With Intrahepatic Portosystemic Stent. Clin Pharmacol Ther *110*, 1329-1336. 10.1002/cpt.2382.
84. Tobar, N., Rocha, G.Z., Santos, A., Guadagnini, D., Assalin, H.B., Camargo, J.A., Goncalves, A., Pallis, F.R., Oliveira, A.G., Rocco, S.A., et al. (2023). Metformin acts in the gut and induces gut-liver crosstalk. Proc Natl Acad Sci U S A *120*, e2211933120. 10.1073/pnas.2211933120.
85. Bridges, H.R., Jones, A.J., Pollak, M.N., and Hirst, J. (2014). Effects of metformin and other biguanides on oxidative phosphorylation in mitochondria. Biochem J *462*, 475-487. 10.1042/BJ20140620.
86. Guigas, B., Detaille, D., Chauvin, C., Batandier, C., De Oliveira, F., Fontaine, E., and Leverve, X. (2004). Metformin inhibits mitochondrial permeability transition and cell death: a pharmacological in vitro study. Biochem J *382*, 877-884. 10.1042/BJ20040885.
87. Algire, C., Moiseeva, O., Deschenes-Simard, X., Amrein, L., Petruccelli, L., Birman, E., Viollet, B., Ferbeyre, G., and Pollak, M.N. (2012). Metformin reduces endogenous reactive oxygen species and associated DNA damage. Cancer Prev Res (Phila) *5*, 536-543. 10.1158/1940-6207.CAPR-11-0536.
88. Madiraju, A.K., Qiu, Y., Perry, R.J., Rahimi, Y., Zhang, X.M., Zhang, D., Camporez, J.G., Cline, G.W., Butrico, G.M., Kemp, B.E., et al. (2018). Metformin inhibits gluconeogenesis via a redox-dependent mechanism in vivo. Nat Med *24*, 1384-1394. 10.1038/s41591-018-0125-4.
89. Wang, Y., An, H., Liu, T., Qin, C., Sesaki, H., Guo, S., Radovick, S., Hussain, M., Maheshwari, A., Wondisford, F.E., et al. (2019). Metformin

Improves Mitochondrial Respiratory Activity through Activation of AMPK. Cell Rep *29*, 1511-1523 e1515. 10.1016/j.celrep.2019.09.070.

90. Caparrotta, T.M., Blackbourn, L.A.K., McGurnaghan, S.J., Chalmers, J., Lindsay, R., McCrimmon, R., McKnight, J., Wild, S., Petrie, J.R., Philip, S., et al. (2020). Prescribing Paradigm Shift? Applying the 2019 European Society of Cardiology-Led Guidelines on Diabetes, Prediabetes, and Cardiovascular Disease to Assess Eligibility for Sodium-Glucose Cotransporter 2 Inhibitors or Glucagon-Like Peptide 1 Receptor Agonists as First-Line Monotherapy (or Add-on to Metformin Monotherapy) in Type 2 Diabetes in Scotland. Diabetes Care *43*, 2034-2041. 10.2337/dc20-0120.
91. Davidson, M.B. (2020). Metformin Should Not Be Used to Treat Prediabetes. Diabetes Care *43*, 1983-1987. 10.2337/dc19-2221.
92. Kim, H., Haluzik, M., Gavrilova, O., Yakar, S., Portas, J., Sun, H., Pajvani, U.B., Scherer, P.E., and LeRoith, D. (2004). Thiazolidinediones improve insulin sensitivity in adipose tissue and reduce the hyperlipidaemia without affecting the hyperglycaemia in a transgenic model of type 2 diabetes. Diabetologia *47*, 2215-2225. 10.1007/s00125-004-1581-6.
93. Todd, M.K., Watt, M.J., Le, J., Hevener, A.L., and Turcotte, L.P. (2007). Thiazolidinediones enhance skeletal muscle triacylglycerol synthesis while protecting against fatty acid-induced inflammation and insulin resistance. Am J Physiol Endocrinol Metab *292*, E485-493. 10.1152/ajpendo.00080.2006.
94. Nesto, R.W., Bell, D., Bonow, R.O., Fonseca, V., Grundy, S.M., Horton, E.S., Le Winter, M., Porte, D., Semenkovich, C.F., Smith, S., et al. (2004). Thiazolidinedione use, fluid retention, and congestive heart failure: a consensus statement from the American Heart Association and American Diabetes Association. Diabetes Care *27*, 256-263. 10.2337/diacare.27.1.256.
95. Bashier, A., Khalifa, A.A., Rashid, F., Abdelgadir, E.I., Al Qaysi, A.A., Ali, R., Eltinay, A., Nafach, J., Alsayyah, F., and Alawadi, F. (2017). Efficacy and Safety of SGLT2 Inhibitors in Reducing Glycated Hemoglobin and Weight in Emirati Patients With Type 2 Diabetes. J Clin Med Res *9*, 499-507. 10.14740/jocmr2976w.
96. Huthmacher, J.A., Meier, J.J., and Nauck, M.A. (2020). Efficacy and Safety of Short- and Long-Acting Glucagon-Like Peptide 1 Receptor Agonists on a Background of Basal Insulin in Type 2 Diabetes: A Meta-analysis. Diabetes Care *43*, 2303-2312. 10.2337/dc20-0498.
97. Li, C., Luo, J., Jiang, M., and Wang, K. (2022). The Efficacy and Safety of the Combination Therapy With GLP-1 Receptor Agonists and SGLT-2 Inhibitors in Type 2 Diabetes Mellitus: A Systematic Review and Meta-analysis. Front Pharmacol *13*, 838277. 10.3389/fphar.2022.838277.
98. Martinez-Vizcaino, V., Diez-Fernandez, A., Alvarez-Bueno, C., Martinez-Alfonso, J., and Cavero-Redondo, I. (2021). Safety and Efficacy of SGLT2 Inhibitors: A Multiple-Treatment Meta-Analysis of Clinical Decision Indicators. J Clin Med *10*. 10.3390/jcm10122713.

99. Dube, M.P., Chan, E.S., Lake, J.E., Williams, B., Kinslow, J., Landay, A., Coombs, R.W., Floris-Moore, M., Ribaudo, H.J., and Yarasheski, K.E. (2019). A Randomized, Double-blinded, Placebo-controlled Trial of Sitagliptin for Reducing Inflammation and Immune Activation in Treated and Suppressed Human Immunodeficiency Virus Infection. Clin Infect Dis *69*, 1165-1172. 10.1093/cid/ciy1051.
100. Rizzo, M.R., Barbieri, M., Marfella, R., and Paolisso, G. (2012). Reduction of oxidative stress and inflammation by blunting daily acute glucose fluctuations in patients with type 2 diabetes: role of dipeptidyl peptidase-IV inhibition. Diabetes Care *35*, 2076-2082. 10.2337/dc12-0199.
101. Satoh-Asahara, N., Sasaki, Y., Wada, H., Tochiya, M., Iguchi, A., Nakagawachi, R., Odori, S., Kono, S., Hasegawa, K., and Shimatsu, A. (2013). A dipeptidyl peptidase-4 inhibitor, sitagliptin, exerts anti-inflammatory effects in type 2 diabetic patients. Metabolism *62*, 347-351. 10.1016/j.metabol.2012.09.004.
102. Koska, J., Osredkar, T., D'Souza, K., Sands, M., Sinha, S., Zhang, W., Meyer, C., and Reaven, P.D. (2019). Effects of saxagliptin on adipose tissue inflammation and vascular function in overweight and obese people: a placebo-controlled study. Diabet Med *36*, 1399-1407. 10.1111/dme.13889.
103. Kewcharoenwong, C., Prabowo, S.A., Bancroft, G.J., Fletcher, H.A., and Lertmemongkolchai, G. (2018). Glibenclamide Reduces Primary Human Monocyte Functions Against Tuberculosis Infection by Enhancing M2 Polarization. Front Immunol *9*, 2109. 10.3389/fimmu.2018.02109.
104. Stevenson, C.R., Forouhi, N.G., Roglic, G., Williams, B.G., Lauer, J.A., Dye, C., and Unwin, N. (2007). Diabetes and tuberculosis: the impact of the diabetes epidemic on tuberculosis incidence. BMC Public Health *7*, 234. 10.1186/1471-2458-7-234.
105. Yu, X., Li, L., Xia, L., Feng, X., Chen, F., Cao, S., and Wei, X. (2019). Impact of metformin on the risk and treatment outcomes of tuberculosis in diabetics: a systematic review. BMC Infect Dis *19*, 859. 10.1186/s12879-019-4548-4.
106. Collier, J.J., Batdorf, H.M., Martin, T.M., Rohli, K.E., Burk, D.H., Lu, D., Cooley, C.R., Karlstad, M.D., Jackson, J.W., Sparer, T.E., et al. (2021). Pancreatic, but not myeloid-cell, expression of interleukin-1alpha is required for maintenance of insulin secretion and whole body glucose homeostasis. Mol Metab *44*, 101140. 10.1016/j.molmet.2020.101140.
107. Ellingsgaard, H., Ehses, J.A., Hammar, E.B., Van Lommel, L., Quintens, R., Martens, G., Kerr-Conte, J., Pattou, F., Berney, T., Pipeleers, D., et al. (2008). Interleukin-6 regulates pancreatic alpha-cell mass expansion. Proc Natl Acad Sci U S A *105*, 13163-13168. 10.1073/pnas.0801059105.
108. Stephens, L.A., Thomas, H.E., Ming, L., Grell, M., Darwiche, R., Volodin, L., and Kay, T.W. (1999). Tumor necrosis factor-alpha-activated cell death pathways in NIT-1 insulinoma cells and primary pancreatic beta cells. Endocrinology *140*, 3219-3227. 10.1210/endo.140.7.6873.

109. Copps, K.D., and White, M.F. (2012). Regulation of insulin sensitivity by serine/threonine phosphorylation of insulin receptor substrate proteins IRS1 and IRS2. Diabetologia *55*, 2565-2582. 10.1007/s00125-012-2644-8.
110. Rui, L., Aguirre, V., Kim, J.K., Shulman, G.I., Lee, A., Corbould, A., Dunaif, A., and White, M.F. (2001). Insulin/IGF-1 and TNF-alpha stimulate phosphorylation of IRS-1 at inhibitory Ser307 via distinct pathways. J Clin Invest *107*, 181-189. 10.1172/JCI10934.
111. Lanuza-Masdeu, J., Arevalo, M.I., Vila, C., Barbera, A., Gomis, R., and Caelles, C. (2013). In vivo JNK activation in pancreatic beta-cells leads to glucose intolerance caused by insulin resistance in pancreas. Diabetes *62*, 2308-2317. 10.2337/db12-1097.
112. Solinas, G., Naugler, W., Galimi, F., Lee, M.S., and Karin, M. (2006). Saturated fatty acids inhibit induction of insulin gene transcription by JNK-mediated phosphorylation of insulin-receptor substrates. Proc Natl Acad Sci U S A *103*, 16454-16459. 10.1073/pnas.0607626103.
113. Jiang, L.Q., Franck, N., Egan, B., Sjogren, R.J., Katayama, M., Duque-Guimaraes, D., Arner, P., Zierath, J.R., and Krook, A. (2013). Autocrine role of interleukin-13 on skeletal muscle glucose metabolism in type 2 diabetic patients involves microRNA let-7. Am J Physiol Endocrinol Metab *305*, E1359-1366. 10.1152/ajpendo.00236.2013.
114. Kanety, H., Feinstein, R., Papa, M.Z., Hemi, R., and Karasik, A. (1995). Tumor necrosis factor alpha-induced phosphorylation of insulin receptor substrate-1 (IRS-1). Possible mechanism for suppression of insulin-stimulated tyrosine phosphorylation of IRS-1. J Biol Chem *270*, 23780-23784. 10.1074/jbc.270.40.23780.
115. Hotamisligil, G.S., Peraldi, P., Budavari, A., Ellis, R., White, M.F., and Spiegelman, B.M. (1996). IRS-1-mediated inhibition of insulin receptor tyrosine kinase activity in TNF-alpha- and obesity-induced insulin resistance. Science *271*, 665-668. 10.1126/science.271.5249.665.
116. Wong, N., Fam, B.C., Cempako, G.R., Steinberg, G.R., Walder, K., Kay, T.W., Proietto, J., and Andrikopoulos, S. (2011). Deficiency in interferon-gamma results in reduced body weight and better glucose tolerance in mice. Endocrinology *152*, 3690-3699. 10.1210/en.2011-0288.
117. Kolodin, D., van Panhuys, N., Li, C., Magnuson, A.M., Cipolletta, D., Miller, C.M., Wagers, A., Germain, R.N., Benoist, C., and Mathis, D. (2015). Antigen- and cytokine-driven accumulation of regulatory T cells in visceral adipose tissue of lean mice. Cell Metab *21*, 543-557. 10.1016/j.cmet.2015.03.005.
118. Ramos-Ramirez, P., Malmhall, C., Tliba, O., Radinger, M., and Bossios, A. (2021). Adiponectin/AdipoR1 Axis Promotes IL-10 Release by Human Regulatory T Cells. Front Immunol *12*, 677550. 10.3389/fimmu.2021.677550.
119. Surendar, J., Frohberger, S.J., Karunakaran, I., Schmitt, V., Stamminger, W., Neumann, A.L., Wilhelm, C., Hoerauf, A., and Hubner, M.P. (2019). Adiponectin Limits IFN-gamma and IL-17 Producing CD4 T Cells in Obesity

by Restraining Cell Intrinsic Glycolysis. Front Immunol *10*, 2555. 10.3389/fimmu.2019.02555.
120. Duffaut, C., Galitzky, J., Lafontan, M., and Bouloumie, A. (2009). Unexpected trafficking of immune cells within the adipose tissue during the onset of obesity. Biochem Biophys Res Commun *384*, 482-485. 10.1016/j.bbrc.2009.05.002.
121. Miya, A., Nakamura, A., Miyoshi, H., Takano, Y., Sunagoya, K., Hayasaka, K., Shimizu, C., Terauchi, Y., and Atsumi, T. (2018). Impact of Glucose Loading on Variations in CD4(+) and CD8(+) T Cells in Japanese Participants with or without Type 2 Diabetes. Front Endocrinol (Lausanne) *9*, 81. 10.3389/fendo.2018.00081.
122. Emerson, S.R., Kurti, S.P., Harms, C.A., Haub, M.D., Melgarejo, T., Logan, C., and Rosenkranz, S.K. (2017). Magnitude and Timing of the Postprandial Inflammatory Response to a High-Fat Meal in Healthy Adults: A Systematic Review. Adv Nutr *8*, 213-225. 10.3945/an.116.014431.
123. Hermier, D., Mathe, V., Lan, A., Santini, C., Quignard-Boulange, A., Huneau, J.F., and Mariotti, F. (2017). Postprandial low-grade inflammation does not specifically require TLR4 activation in the rat. Nutr Metab (Lond) *14*, 65. 10.1186/s12986-017-0220-4.
124. Hajmrle, C., Smith, N., Spigelman, A.F., Dai, X., Senior, L., Bautista, A., Ferdaoussi, M., and MacDonald, P.E. (2016). Interleukin-1 signaling contributes to acute islet compensation. JCI Insight *1*, e86055. 10.1172/jci.insight.86055.
125. Americo-Da-Silva, L., Aguilera, J., Quinteros-Waltemath, O., Sanchez-Aguilera, P., Russell, J., Cadagan, C., Meneses-Valdes, R., Sanchez, G., Estrada, M., Jorquera, G., et al. (2021). Activation of the NLRP3 Inflammasome Increases the IL-1beta Level and Decreases GLUT4 Translocation in Skeletal Muscle during Insulin Resistance. Int J Mol Sci *22*. 10.3390/ijms221910212.
126. Rajendran, S., Anquetil, F., Quesada-Masachs, E., Graef, M., Gonzalez, N., McArdle, S., Chu, T., Krogvold, L., Dahl-Jorgensen, K., and von Herrath, M. (2020). IL-6 is present in beta and alpha cells in human pancreatic islets: Expression is reduced in subjects with type 1 diabetes. Clin Immunol *211*, 108320. 10.1016/j.clim.2019.108320.
127. Karlsen, A.E., Ronn, S.G., Lindberg, K., Johannesen, J., Galsgaard, E.D., Pociot, F., Nielsen, J.H., Mandrup-Poulsen, T., Nerup, J., and Billestrup, N. (2001). Suppressor of cytokine signaling 3 (SOCS-3) protects beta -cells against interleukin-1beta - and interferon-gamma -mediated toxicity. Proc Natl Acad Sci U S A *98*, 12191-12196. 10.1073/pnas.211445998.
128. Kimura, A., Naka, T., Nagata, S., Kawase, I., and Kishimoto, T. (2004). SOCS-1 suppresses TNF-alpha-induced apoptosis through the regulation of Jak activation. Int Immunol *16*, 991-999. 10.1093/intimm/dxh102.
129. Lynch, L., Michelet, X., Zhang, S., Brennan, P.J., Moseman, A., Lester, C., Besra, G., Vomhof-Dekrey, E.E., Tighe, M., Koay, H.F., et al. (2015). Regulatory iNKT cells lack expression of the transcription factor PLZF and

control the homeostasis of T(reg) cells and macrophages in adipose tissue. Nat Immunol *16*, 85-95. 10.1038/ni.3047.
130. Horii, T., Kozawa, J., Fujita, Y., Kawata, S., Ozawa, H., Ishibashi, C., Yoneda, S., Nammo, T., Miyagawa, J.I., Eguchi, H., and Shimomura, I. (2022). Lipid droplet accumulation in beta cells in patients with type 2 diabetes is associated with insulin resistance, hyperglycemia and beta cell dysfunction involving decreased insulin granules. Front Endocrinol (Lausanne) *13*, 996716. 10.3389/fendo.2022.996716.
131. Uzilday, B., Ozgur, R., Sekmen, A.H., and Turkan, I. (2018). Endoplasmic reticulum stress regulates glutathione metabolism and activities of glutathione related enzymes in Arabidopsis. Funct Plant Biol *45*, 284-296. 10.1071/FP17151.
132. Chen, E., Tsai, T.H., Li, L., Saha, P., Chan, L., and Chang, B.H. (2017). PLIN2 is a Key Regulator of the Unfolded Protein Response and Endoplasmic Reticulum Stress Resolution in Pancreatic beta Cells. Sci Rep *7*, 40855. 10.1038/srep40855.
133. Talchai, C., Xuan, S., Lin, H.V., Sussel, L., and Accili, D. (2012). Pancreatic beta cell dedifferentiation as a mechanism of diabetic beta cell failure. Cell *150*, 1223-1234. 10.1016/j.cell.2012.07.029.
134. DeFronzo, R.A., Ferrannini, E., Groop, L., Henry, R.R., Herman, W.H., Holst, J.J., Hu, F.B., Kahn, C.R., Raz, I., Shulman, G.I., et al. (2015). Type 2 diabetes mellitus. Nat Rev Dis Primers *1*, 15019. 10.1038/nrdp.2015.19.
135. Guilherme, A., Virbasius, J.V., Puri, V., and Czech, M.P. (2008). Adipocyte dysfunctions linking obesity to insulin resistance and type 2 diabetes. Nat Rev Mol Cell Biol *9*, 367-377. 10.1038/nrm2391.
136. Ryden, M., and Arner, P. (2017). Subcutaneous Adipocyte Lipolysis Contributes to Circulating Lipid Levels. Arterioscler Thromb Vasc Biol *37*, 1782-1787. 10.1161/ATVBAHA.117.309759.
137. Garcia-Martinez, I., Shaker, M.E., and Mehal, W.Z. (2015). Therapeutic Opportunities in Damage-Associated Molecular Pattern-Driven Metabolic Diseases. Antioxid Redox Signal *23*, 1305-1315. 10.1089/ars.2015.6383.
138. Cinti, S., Mitchell, G., Barbatelli, G., Murano, I., Ceresi, E., Faloia, E., Wang, S., Fortier, M., Greenberg, A.S., and Obin, M.S. (2005). Adipocyte death defines macrophage localization and function in adipose tissue of obese mice and humans. J Lipid Res *46*, 2347-2355. 10.1194/jlr.M500294-JLR200.
139. Nishimura, S., Manabe, I., Nagasaki, M., Eto, K., Yamashita, H., Ohsugi, M., Otsu, M., Hara, K., Ueki, K., Sugiura, S., et al. (2009). CD8+ effector T cells contribute to macrophage recruitment and adipose tissue inflammation in obesity. Nat Med *15*, 914-920.
140. Pang, C., Gao, Z., Yin, J., Zhang, J., Jia, W., and Ye, J. (2008). Macrophage infiltration into adipose tissue may promote angiogenesis for adipose tissue remodeling in obesity. Am J Physiol Endocrinol Metab *295*, E313-322. 10.1152/ajpendo.90296.2008.
141. Kusminski, C.M., Ghaben, A.L., Morley, T.S., Samms, R.J., Adams, A.C., An, Y., Johnson, J.A., Joffin, N., Onodera, T., Crewe, C., et al. (2020). A

Novel Model of Diabetic Complications: Adipocyte Mitochondrial Dysfunction Triggers Massive beta-Cell Hyperplasia. Diabetes *69*, 313-330. 10.2337/db19-0327.

142. Apovian, C.M., Bigornia, S., Mott, M., Meyers, M.R., Ulloor, J., Gagua, M., McDonnell, M., Hess, D., Joseph, L., and Gokce, N. (2008). Adipose macrophage infiltration is associated with insulin resistance and vascular endothelial dysfunction in obese subjects. Arterioscler Thromb Vasc Biol *28*, 1654-1659. 10.1161/ATVBAHA.108.170316.
143. Coats, B.R., Schoenfelt, K.Q., Barbosa-Lorenzi, V.C., Peris, E., Cui, C., Hoffman, A., Zhou, G., Fernandez, S., Zhai, L., Hall, B.A., et al. (2017). Metabolically Activated Adipose Tissue Macrophages Perform Detrimental and Beneficial Functions during Diet-Induced Obesity. Cell Rep *20*, 3149-3161. 10.1016/j.celrep.2017.08.096.
144. Weisberg, S.P., McCann, D., Desai, M., Rosenbaum, M., Leibel, R.L., and Ferrante, A.W., Jr. (2003). Obesity is associated with macrophage accumulation in adipose tissue. J Clin Invest *112*, 1796-1808. 10.1172/JCI19246.
145. Wentworth, J.M., Naselli, G., Brown, W.A., Doyle, L., Phipson, B., Smyth, G.K., Wabitsch, M., O'Brien, P.E., and Harrison, L.C. (2010). Pro-inflammatory CD11c+CD206+ adipose tissue macrophages are associated with insulin resistance in human obesity. Diabetes *59*, 1648-1656. 10.2337/db09-0287.
146. Espinosa De Ycaza, A.E., Sondergaard, E., Morgan-Bathke, M., Lytle, K., Delivanis, D.A., Ramos, P., Carranza Leon, B.G., and Jensen, M.D. (2022). Adipose Tissue Inflammation Is Not Related to Adipose Insulin Resistance in Humans. Diabetes *71*, 381-393. 10.2337/db21-0609.
147. Caslin, H.L., Cottam, M.A., Pinon, J.M., Boney, L.Y., and Hasty, A.H. (2022). Weight cycling induces innate immune memory in adipose tissue macrophages. Front Immunol *13*, 984859. 10.3389/fimmu.2022.984859.
148. Spranger, J., Kroke, A., Mohlig, M., Hoffmann, K., Bergmann, M.M., Ristow, M., Boeing, H., and Pfeiffer, A.F. (2003). Inflammatory cytokines and the risk to develop type 2 diabetes: results of the prospective population-based European Prospective Investigation into Cancer and Nutrition (EPIC)-Potsdam Study. Diabetes *52*, 812-817. 10.2337/diabetes.52.3.812.
149. Aziz, N. (2015). Measurement of Circulating Cytokines and Immune-Activation Markers by Multiplex Technology in the Clinical Setting: What Are We Really Measuring? For Immunopathol Dis Therap *6*, 19-22. 10.1615/ForumImmunDisTher.2015014162.
150. Gupta, S., Maratha, A., Siednienko, J., Natarajan, A., Gajanayake, T., Hoashi, S., and Miggin, S. (2017). Analysis of inflammatory cytokine and TLR expression levels in Type 2 Diabetes with complications. Sci Rep *7*, 7633. 10.1038/s41598-017-07230-8.
151. Everett, B.M., Donath, M.Y., Pradhan, A.D., Thuren, T., Pais, P., Nicolau, J.C., Glynn, R.J., Libby, P., and Ridker, P.M. (2018). Anti-Inflammatory Therapy With Canakinumab for the Prevention and Management of Diabetes. J Am Coll Cardiol *71*, 2392-2401. 10.1016/j.jacc.2018.03.002.

152. Ridker, P.M., MacFadyen, J.G., Thuren, T., Everett, B.M., Libby, P., Glynn, R.J., and Group, C.T. (2017). Effect of interleukin-1beta inhibition with canakinumab on incident lung cancer in patients with atherosclerosis: exploratory results from a randomised, double-blind, placebo-controlled trial. Lancet *390*, 1833-1842. 10.1016/S0140-6736(17)32247-X.
153. Cavelti-Weder, C., Timper, K., Seelig, E., Keller, C., Osranek, M., Lassing, U., Spohn, G., Maurer, P., Muller, P., Jennings, G.T., et al. (2016). Development of an Interleukin-1beta Vaccine in Patients with Type 2 Diabetes. Mol Ther *24*, 1003-1012. 10.1038/mt.2015.227.
154. Kleiveland, C.R. (2015). Peripheral Blood Mononuclear Cells. In The Impact of Food Bioactives on Health: in vitro and ex vivo models, K. Verhoeckx, P. Cotter, I. Lopez-Exposito, C. Kleiveland, T. Lea, A. Mackie, T. Requena, D. Swiatecka, and H. Wichers, eds. pp. 161-167. 10.1007/978-3-319-16104-4_15.
155. Cossarizza, A., Ortolani, C., Paganelli, R., Barbieri, D., Monti, D., Sansoni, P., Fagiolo, U., Castellani, G., Bersani, F., Londei, M., and Franceschi, C. (1996). CD45 isoforms expression on CD4+ and CD8+ T cells throughout life, from newborns to centenarians: implications for T cell memory. Mech Ageing Dev *86*, 173-195. 10.1016/0047-6374(95)01691-0.
156. Lau, E.Y.M., Carroll, E.C., Callender, L.A., Hood, G.A., Berryman, V., Pattrick, M., Finer, S., Hitman, G.A., Ackland, G.L., and Henson, S.M. (2019). Type 2 diabetes is associated with the accumulation of senescent T cells. Clin Exp Immunol *197*, 205-213. 10.1111/cei.13344.
157. Yi, H.S., Kim, S.Y., Kim, J.T., Lee, Y.S., Moon, J.S., Kim, M., Kang, Y.E., Joung, K.H., Lee, J.H., Kim, H.J., et al. (2019). T-cell senescence contributes to abnormal glucose homeostasis in humans and mice. Cell Death Dis *10*, 249. 10.1038/s41419-019-1494-4.
158. Lamers, M.L., Almeida, M.E., Vicente-Manzanares, M., Horwitz, A.F., and Santos, M.F. (2011). High glucose-mediated oxidative stress impairs cell migration. PLoS One *6*, e22865. 10.1371/journal.pone.0022865.
159. Wang, G.S., Shen, Y.S., Chou, W.Y., Tang, C.H., Yeh, H.I., Wang, L.Y., Yen, J.Y., Huang, T.Y., Liu, S.C., Yang, C.Y., et al. (2018). Senescence Induces Dysfunctions in Endothelial Progenitor Cells and Osteoblasts by Interfering Translational Machinery and Bioenergetic Homeostasis. Int J Mol Sci *19*. 10.3390/ijms19071997.
160. Gessl, A., and Waldhausl, W. (1998). Increased CD69 and human leukocyte antigen-DR expression on T lymphocytes in insulin-dependent diabetes mellitus of long standing. J Clin Endocrinol Metab *83*, 2204-2209. 10.1210/jcem.83.6.4889.
161. Winer, S., Chan, Y., Paltser, G., Truong, D., Tsui, H., Bahrami, J., Dorfman, R., Wang, Y., Zielenski, J., Mastronardi, F., et al. (2009). Normalization of obesity-associated insulin resistance through immunotherapy. Nat Med *15*, 921-929.
162. Winer, S., Paltser, G., Chan, Y., Tsui, H., Engleman, E., Winer, D., and Dosch, H.M. (2009). Obesity predisposes to Th17 bias. Eur J Immunol *39*, 2629-2635. 10.1002/eji.200838893.

163. 2., A.D.A.P.P.C. (2022). Classification and diagnosis of diabetes: standards of medical care in diabetes - 2022. Diabetes Care *45* (*1*).
164. Force, U.P.S.T. (2021). Screening for prediabetes and type 2 diabetes US preventative services task force recommendation statement. JAMA *326*.
165. Radin, M.S. (2014). Pitfalls in hemoglobin A1c measurement: when results may be misleading. J Gen Intern Med *29*, 388-394. 10.1007/s11606-013-2595-x.
166. Flynn, M.C., Kraakman, M.J., Tikellis, C., Lee, M.K.S., Hanssen, N.M.J., Kammoun, H.L., Pickering, R.J., Dragoljevic, D., Al-Sharea, A., Barrett, T.J., et al. (2020). Transient Intermittent Hyperglycemia Accelerates Atherosclerosis by Promoting Myelopoiesis. Circ Res *127*, 877-892. 10.1161/CIRCRESAHA.120.316653.
167. Sagastume, D., Siero, I., Mertens, E., Cottam, J., Colizzi, C., and Penalvo, J.L. (2022). The effectiveness of lifestyle interventions on type 2 diabetes and gestational diabetes incidence and cardiometabolic outcomes: A systematic review and meta-analysis of evidence from low- and middle-income countries. EClinicalMedicine *53*, 101650. 10.1016/j.eclinm.2022.101650.
168. Buck, M.D., O'Sullivan, D., and Pearce, E.L. (2015). T cell metabolism drives immunity. J Exp Med *212*, 1345-1360. 10.1084/jem.20151159.
169. Gowans, G.J., Hawley, S.A., Ross, F.A., and Hardie, D.G. (2013). AMP is a true physiological regulator of AMP-activated protein kinase by both allosteric activation and enhancing net phosphorylation. Cell Metab *18*, 556-566. 10.1016/j.cmet.2013.08.019.
170. Shaw, R.J., Kosmatka, M., Bardeesy, N., Hurley, R.L., Witters, L.A., DePinho, R.A., and Cantley, L.C. (2004). The tumor suppressor LKB1 kinase directly activates AMP-activated kinase and regulates apoptosis in response to energy stress. Proc Natl Acad Sci U S A *101*, 3329-3335. 10.1073/pnas.0308061100.
171. Fullerton, M.D., Galic, S., Marcinko, K., Sikkema, S., Pulinilkunnil, T., Chen, Z.P., O'Neill, H.M., Ford, R.J., Palanivel, R., O'Brien, M., et al. (2013). Single phosphorylation sites in Acc1 and Acc2 regulate lipid homeostasis and the insulin-sensitizing effects of metformin. Nat Med *19*, 1649-1654. 10.1038/nm.3372.
172. Saggerson, D. (2008). Malonyl-CoA, a key signaling molecule in mammalian cells. Annu Rev Nutr *28*, 253-272. 10.1146/annurev.nutr.28.061807.155434.
173. Eguchi, S., Oshiro, N., Miyamoto, T., Yoshino, K., Okamoto, S., Ono, T., Kikkawa, U., and Yonezawa, K. (2009). AMP-activated protein kinase phosphorylates glutamine : fructose-6-phosphate amidotransferase 1 at Ser243 to modulate its enzymatic activity. Genes Cells *14*, 179-189. 10.1111/j.1365-2443.2008.01260.x.
174. Chang, Y.H., Weng, C.L., and Lin, K.I. (2020). O-GlcNAcylation and its role in the immune system. J Biomed Sci *27*, 57. 10.1186/s12929-020-00648-9.
175. Wellen, K.E., Lu, C., Mancuso, A., Lemons, J.M., Ryczko, M., Dennis, J.W., Rabinowitz, J.D., Coller, H.A., and Thompson, C.B. (2010). The

hexosamine biosynthetic pathway couples growth factor-induced glutamine uptake to glucose metabolism. Genes Dev *24*, 2784-2799. 10.1101/gad.1985910.
176. Zibrova, D., Vandermoere, F., Goransson, O., Peggie, M., Marino, K.V., Knierim, A., Spengler, K., Weigert, C., Viollet, B., Morrice, N.A., et al. (2017). GFAT1 phosphorylation by AMPK promotes VEGF-induced angiogenesis. Biochem J *474*, 983-1001. 10.1042/BCJ20160980.
177. Delgoffe, G.M., Kole, T.P., Zheng, Y., Zarek, P.E., Matthews, K.L., Xiao, B., Worley, P.F., Kozma, S.C., and Powell, J.D. (2009). The mTOR kinase differentially regulates effector and regulatory T cell lineage commitment. Immunity *30*, 832-844. 10.1016/j.immuni.2009.04.014.
178. Kato, H., and Perl, A. (2014). Mechanistic target of rapamycin complex 1 expands Th17 and IL-4+ CD4-CD8- double-negative T cells and contracts regulatory T cells in systemic lupus erythematosus. J Immunol *192*, 4134-4144. 10.4049/jimmunol.1301859.
179. Mossmann, D., Park, S., and Hall, M.N. (2018). mTOR signalling and cellular metabolism are mutual determinants in cancer. Nat Rev Cancer *18*, 744-757. 10.1038/s41568-018-0074-8.
180. Yang, K., Neale, G., Green, D.R., He, W., and Chi, H. (2011). The tumor suppressor Tsc1 enforces quiescence of naive T cells to promote immune homeostasis and function. Nat Immunol *12*, 888-897. 10.1038/ni.2068.
181. Jacobs, S.R., Herman, C.E., Maciver, N.J., Wofford, J.A., Wieman, H.L., Hammen, J.J., and Rathmell, J.C. (2008). Glucose uptake is limiting in T cell activation and requires CD28-mediated Akt-dependent and independent pathways. J Immunol *180*, 4476-4486. 10.4049/jimmunol.180.7.4476.
182. Macintyre, A.N., Gerriets, V.A., Nichols, A.G., Michalek, R.D., Rudolph, M.C., Deoliveira, D., Anderson, S.M., Abel, E.D., Chen, B.J., Hale, L.P., and Rathmell, J.C. (2014). The glucose transporter Glut1 is selectively essential for CD4 T cell activation and effector function. Cell Metab *20*, 61-72. 10.1016/j.cmet.2014.05.004.
183. Shaked, M., Ketzinel-Gilad, M., Cerasi, E., Kaiser, N., and Leibowitz, G. (2011). AMP-activated protein kinase (AMPK) mediates nutrient regulation of thioredoxin-interacting protein (TXNIP) in pancreatic beta-cells. PLoS One *6*, e28804. 10.1371/journal.pone.0028804.
184. Greiner, E.F., Guppy, M., and Brand, K. (1994). Glucose is essential for proliferation and the glycolytic enzyme induction that provokes a transition to glycolytic energy production. J Biol Chem *269*, 31484-31490.
185. Lepez, A., Pirnay, T., Denanglaire, S., Perez-Morga, D., Vermeersch, M., Leo, O., and Andris, F. (2020). Long-term T cell fitness and proliferation is driven by AMPK-dependent regulation of reactive oxygen species. Sci Rep *10*, 21673. 10.1038/s41598-020-78715-2.
186. Zubkova, I., Mostowski, H., and Zaitseva, M. (2005). Up-regulation of IL-7, stromal-derived factor-1 alpha, thymus-expressed chemokine, and secondary lymphoid tissue chemokine gene expression in the stromal cells

in response to thymocyte depletion: implication for thymus reconstitution. J Immunol *175*, 2321-2330. 10.4049/jimmunol.175.4.2321.
187. Tokoyoda, K., Egawa, T., Sugiyama, T., Choi, B.I., and Nagasawa, T. (2004). Cellular niches controlling B lymphocyte behavior within bone marrow during development. Immunity *20*, 707-718. 10.1016/j.immuni.2004.05.001.
188. Hara, T., Shitara, S., Imai, K., Miyachi, H., Kitano, S., Yao, H., Tani-ichi, S., and Ikuta, K. (2012). Identification of IL-7-producing cells in primary and secondary lymphoid organs using IL-7-GFP knock-in mice. J Immunol *189*, 1577-1584. 10.4049/jimmunol.1200586.
189. Link, A., Vogt, T.K., Favre, S., Britschgi, M.R., Acha-Orbea, H., Hinz, B., Cyster, J.G., and Luther, S.A. (2007). Fibroblastic reticular cells in lymph nodes regulate the homeostasis of naive T cells. Nat Immunol *8*, 1255-1265. 10.1038/ni1513.
190. Murray, A.M., Simm, B., and Beagley, K.W. (1998). Cytokine gene expression in murine fetal intestine: potential for extrathymic T cell development. Cytokine *10*, 337-345. 10.1006/cyto.1997.0302.
191. Heufler, C., Topar, G., Grasseger, A., Stanzl, U., Koch, F., Romani, N., Namen, A.E., and Schuler, G. (1993). Interleukin 7 is produced by murine and human keratinocytes. J Exp Med *178*, 1109-1114. 10.1084/jem.178.3.1109.
192. Sawa, Y., Arima, Y., Ogura, H., Kitabayashi, C., Jiang, J.J., Fukushima, T., Kamimura, D., Hirano, T., and Murakami, M. (2009). Hepatic interleukin-7 expression regulates T cell responses. Immunity *30*, 447-457. 10.1016/j.immuni.2009.01.007.
193. Rane, L., Rahman, S., Magalhaes, I., Ahmed, R., Spangberg, M., Kondova, I., Verreck, F., Andersson, J., Brighenti, S., and Maeurer, M.J. (2011). Increased (6 exon) interleukin-7 production after M. tuberculosis infection and soluble interleukin-7 receptor expression in lung tissue. Genes Immun *12*, 513-522. 10.1038/gene.2011.29.
194. Tan, J.T., Dudl, E., LeRoy, E., Murray, R., Sprent, J., Weinberg, K.I., and Surh, C.D. (2001). IL-7 is critical for homeostatic proliferation and survival of naive T cells. Proc Natl Acad Sci U S A *98*, 8732-8737. 10.1073/pnas.161126098.
195. Kim, G.Y., Ligons, D.L., Hong, C., Luckey, M.A., Keller, H.R., Tai, X., Lucas, P.J., Gress, R.E., and Park, J.H. (2012). An in vivo IL-7 requirement for peripheral Foxp3+ regulatory T cell homeostasis. J Immunol *188*, 5859-5866. 10.4049/jimmunol.1102328.
196. Osborne, L.C., Dhanji, S., Snow, J.W., Priatel, J.J., Ma, M.C., Miners, M.J., Teh, H.S., Goldsmith, M.A., and Abraham, N. (2007). Impaired CD8 T cell memory and CD4 T cell primary responses in IL-7R alpha mutant mice. J Exp Med *204*, 619-631. 10.1084/jem.20061871.
197. van Oers, N.S., Tao, W., Watts, J.D., Johnson, P., Aebersold, R., and Teh, H.S. (1993). Constitutive tyrosine phosphorylation of the T-cell receptor (TCR) zeta subunit: regulation of TCR-associated protein tyrosine kinase

activity by TCR zeta. Mol Cell Biol *13*, 5771-5780. 10.1128/mcb.13.9.5771-5780.1993.
198. Stefanova, I., Hemmer, B., Vergelli, M., Martin, R., Biddison, W.E., and Germain, R.N. (2003). TCR ligand discrimination is enforced by competing ERK positive and SHP-1 negative feedback pathways. Nat Immunol *4*, 248-254. 10.1038/ni895.
199. Camerer, E., Regard, J.B., Cornelissen, I., Srinivasan, Y., Duong, D.N., Palmer, D., Pham, T.H., Wong, J.S., Pappu, R., and Coughlin, S.R. (2009). Sphingosine-1-phosphate in the plasma compartment regulates basal and inflammation-induced vascular leak in mice. J Clin Invest *119*, 1871-1879. 10.1172/jci38575.
200. Fukuhara, S., Simmons, S., Kawamura, S., Inoue, A., Orba, Y., Tokudome, T., Sunden, Y., Arai, Y., Moriwaki, K., Ishida, J., et al. (2012). The sphingosine-1-phosphate transporter Spns2 expressed on endothelial cells regulates lymphocyte trafficking in mice. J Clin Invest *122*, 1416-1426. 10.1172/JCI60746.
201. Goetzl, E.J., Kong, Y., and Mei, B. (1999). Lysophosphatidic acid and sphingosine 1-phosphate protection of T cells from apoptosis in association with suppression of Bax. J Immunol *162*, 2049-2056.
202. Mendoza, A., Fang, V., Chen, C., Serasinghe, M., Verma, A., Muller, J., Chaluvadi, V.S., Dustin, M.L., Hla, T., Elemento, O., et al. (2017). Lymphatic endothelial S1P promotes mitochondrial function and survival in naive T cells. Nature *546*, 158-161. 10.1038/nature22352.
203. Sener, Z., Cederkvist, F.H., Volchenkov, R., Holen, H.L., and Skalhegg, B.S. (2016). T Helper Cell Activation and Expansion Is Sensitive to Glutaminase Inhibition under Both Hypoxic and Normoxic Conditions. PLoS One *11*, e0160291. 10.1371/journal.pone.0160291.
204. Angela, M., Endo, Y., Asou, H.K., Yamamoto, T., Tumes, D.J., Tokuyama, H., Yokote, K., and Nakayama, T. (2016). Fatty acid metabolic reprogramming via mTOR-mediated inductions of PPARgamma directs early activation of T cells. Nat Commun *7*, 13683. 10.1038/ncomms13683.
205. Nakaya, M., Xiao, Y., Zhou, X., Chang, J.H., Chang, M., Cheng, X., Blonska, M., Lin, X., and Sun, S.C. (2014). Inflammatory T cell responses rely on amino acid transporter ASCT2 facilitation of glutamine uptake and mTORC1 kinase activation. Immunity *40*, 692-705. 10.1016/j.immuni.2014.04.007.
206. Pugazhenthi, S., Nesterova, A., Sable, C., Heidenreich, K.A., Boxer, L.M., Heasley, L.E., and Reusch, J.E. (2000). Akt/protein kinase B up-regulates Bcl-2 expression through cAMP-response element-binding protein. J Biol Chem *275*, 10761-10766. 10.1074/jbc.275.15.10761.
207. Wieman, H.L., Wofford, J.A., and Rathmell, J.C. (2007). Cytokine stimulation promotes glucose uptake via phosphatidylinositol-3 kinase/Akt regulation of Glut1 activity and trafficking. Mol Biol Cell *18*, 1437-1446. 10.1091/mbc.e06-07-0593.
208. Cai, S.L., Tee, A.R., Short, J.D., Bergeron, J.M., Kim, J., Shen, J., Guo, R., Johnson, C.L., Kiguchi, K., and Walker, C.L. (2006). Activity of TSC2 is

inhibited by AKT-mediated phosphorylation and membrane partitioning. J Cell Biol *173*, 279-289. 10.1083/jcb.200507119.
209. Carroll, B., Maetzel, D., Maddocks, O.D., Otten, G., Ratcliff, M., Smith, G.R., Dunlop, E.A., Passos, J.F., Davies, O.R., Jaenisch, R., et al. (2016). Control of TSC2-Rheb signaling axis by arginine regulates mTORC1 activity. Elife *5*. 10.7554/eLife.11058.
210. Liu, D., and Uzonna, J.E. (2010). The p110 delta isoform of phosphatidylinositol 3-kinase controls the quality of secondary anti-Leishmania immunity by regulating expansion and effector function of memory T cell subsets. J Immunol *184*, 3098-3105. 10.4049/jimmunol.0903177.
211. Okkenhaug, K., Patton, D.T., Bilancio, A., Garcon, F., Rowan, W.C., and Vanhaesebroeck, B. (2006). The p110delta isoform of phosphoinositide 3-kinase controls clonal expansion and differentiation of Th cells. J Immunol *177*, 5122-5128. 10.4049/jimmunol.177.8.5122.
212. Patton, D.T., Garden, O.A., Pearce, W.P., Clough, L.E., Monk, C.R., Leung, E., Rowan, W.C., Sancho, S., Walker, L.S., Vanhaesebroeck, B., and Okkenhaug, K. (2006). Cutting edge: the phosphoinositide 3-kinase p110 delta is critical for the function of CD4+CD25+Foxp3+ regulatory T cells. J Immunol *177*, 6598-6602. 10.4049/jimmunol.177.10.6598.
213. Moloughney, J.G., Kim, P.K., Vega-Cotto, N.M., Wu, C.C., Zhang, S., Adlam, M., Lynch, T., Chou, P.C., Rabinowitz, J.D., Werlen, G., and Jacinto, E. (2016). mTORC2 Responds to Glutamine Catabolite Levels to Modulate the Hexosamine Biosynthesis Enzyme GFAT1. Mol Cell *63*, 811-826. 10.1016/j.molcel.2016.07.015.
214. Jewell, J.L., Kim, Y.C., Russell, R.C., Yu, F.X., Park, H.W., Plouffe, S.W., Tagliabracci, V.S., and Guan, K.L. (2015). Metabolism. Differential regulation of mTORC1 by leucine and glutamine. Science *347*, 194-198. 10.1126/science.1259472.
215. Yu, Q., Tu, H., Yin, X., Peng, C., Dou, C., Yang, W., Wu, W., Guan, X., Li, J., Yan, H., et al. (2022). Targeting Glutamine Metabolism Ameliorates Autoimmune Hepatitis via Inhibiting T Cell Activation and Differentiation. Front Immunol *13*, 880262. 10.3389/fimmu.2022.880262.
216. Nicklin, P., Bergman, P., Zhang, B., Triantafellow, E., Wang, H., Nyfeler, B., Yang, H., Hild, M., Kung, C., Wilson, C., et al. (2009). Bidirectional transport of amino acids regulates mTOR and autophagy. Cell *136*, 521-534. 10.1016/j.cell.2008.11.044.
217. Csibi, A., Fendt, S.M., Li, C., Poulogiannis, G., Choo, A.Y., Chapski, D.J., Jeong, S.M., Dempsey, J.M., Parkhitko, A., Morrison, T., et al. (2013). The mTORC1 pathway stimulates glutamine metabolism and cell proliferation by repressing SIRT4. Cell *153*, 840-854. 10.1016/j.cell.2013.04.023.
218. Araujo, L., Khim, P., Mkhikian, H., Mortales, C.L., and Demetriou, M. (2017). Glycolysis and glutaminolysis cooperatively control T cell function by limiting metabolite supply to N-glycosylation. Elife *6*. 10.7554/eLife.21330.
219. Miao, Y., Zhang, C., Yang, L., Zeng, X., Hu, Y., Xue, X., Dai, Y., and Wei, Z. (2022). The activation of PPARgamma enhances Treg responses

through up-regulating CD36/CPT1-mediated fatty acid oxidation and subsequent N-glycan branching of TbetaRII/IL-2Ralpha. Cell Commun Signal *20*, 48. 10.1186/s12964-022-00849-9.

220. Yang, C., Ko, B., Hensley, C.T., Jiang, L., Wasti, A.T., Kim, J., Sudderth, J., Calvaruso, M.A., Lumata, L., Mitsche, M., et al. (2014). Glutamine oxidation maintains the TCA cycle and cell survival during impaired mitochondrial pyruvate transport. Mol Cell *56*, 414-424. 10.1016/j.molcel.2014.09.025.
221. Angelini, G., Gardella, S., Ardy, M., Ciriolo, M.R., Filomeni, G., Di Trapani, G., Clarke, F., Sitia, R., and Rubartelli, A. (2002). Antigen-presenting dendritic cells provide the reducing extracellular microenvironment required for T lymphocyte activation. Proc Natl Acad Sci U S A *99*, 1491-1496. 10.1073/pnas.022630299.
222. Pacheco, R., Oliva, H., Martinez-Navio, J.M., Climent, N., Ciruela, F., Gatell, J.M., Gallart, T., Mallol, J., Lluis, C., and Franco, R. (2006). Glutamate released by dendritic cells as a novel modulator of T cell activation. J Immunol *177*, 6695-6704. 10.4049/jimmunol.177.10.6695.
223. Garg, S.K., Yan, Z., Vitvitsky, V., and Banerjee, R. (2011). Differential dependence on cysteine from transsulfuration versus transport during T cell activation. Antioxid Redox Signal *15*, 39-47. 10.1089/ars.2010.3496.
224. Grifka-Walk, H.M., Giles, D.A., and Segal, B.M. (2015). IL-12-polarized Th1 cells produce GM-CSF and induce EAE independent of IL-23. Eur J Immunol *45*, 2780-2786. 10.1002/eji.201545800.
225. Jayaraman, P., Sada-Ovalle, I., Nishimura, T., Anderson, A.C., Kuchroo, V.K., Remold, H.G., and Behar, S.M. (2013). IL-1beta promotes antimicrobial immunity in macrophages by regulating TNFR signaling and caspase-3 activation. J Immunol *190*, 4196-4204. 10.4049/jimmunol.1202688.
226. Yang, H., Youm, Y.H., Vandanmagsar, B., Ravussin, A., Gimble, J.M., Greenway, F., Stephens, J.M., Mynatt, R.L., and Dixit, V.D. (2010). Obesity increases the production of proinflammatory mediators from adipose tissue T cells and compromises TCR repertoire diversity: implications for systemic inflammation and insulin resistance. J Immunol *185*, 1836-1845. 10.4049/jimmunol.1000021.
227. Chornoguz, O., Hagan, R.S., Haile, A., Arwood, M.L., Gamper, C.J., Banerjee, A., and Powell, J.D. (2017). mTORC1 Promotes T-bet Phosphorylation To Regulate Th1 Differentiation. J Immunol *198*, 3939-3948. 10.4049/jimmunol.1601078.
228. Kurebayashi, Y., Nagai, S., Ikejiri, A., Ohtani, M., Ichiyama, K., Baba, Y., Yamada, T., Egami, S., Hoshii, T., Hirao, A., et al. (2012). PI3K-Akt-mTORC1-S6K1/2 axis controls Th17 differentiation by regulating Gfi1 expression and nuclear translocation of RORgamma. Cell Rep *1*, 360-373. 10.1016/j.celrep.2012.02.007.
229. Klysz, D., Tai, X., Robert, P.A., Craveiro, M., Cretenet, G., Oburoglu, L., Mongellaz, C., Floess, S., Fritz, V., Matias, M.I., et al. (2015). Glutamine-dependent alpha-ketoglutarate production regulates the balance between T

helper 1 cell and regulatory T cell generation. Sci Signal *8*, ra97. 10.1126/scisignal.aab2610.
230. Johnson, M.O., Wolf, M.M., Madden, M.Z., Andrejeva, G., Sugiura, A., Contreras, D.C., Maseda, D., Liberti, M.V., Paz, K., Kishton, R.J., et al. (2018). Distinct Regulation of Th17 and Th1 Cell Differentiation by Glutaminase-Dependent Metabolism. Cell *175*, 1780-1795 e1719. 10.1016/j.cell.2018.10.001.
231. Fiorentino, D.F., Bond, M.W., and Mosmann, T.R. (1989). Two types of mouse T helper cell. IV. Th2 clones secrete a factor that inhibits cytokine production by Th1 clones. J Exp Med *170*, 2081-2095. 10.1084/jem.170.6.2081.
232. Chen, T., Tibbitt, C.A., Feng, X., Stark, J.M., Rohrbeck, L., Rausch, L., Sedimbi, S.K., Karlsson, M.C.I., Lambrecht, B.N., Karlsson Hedestam, G.B., et al. (2017). PPAR-gamma promotes type 2 immune responses in allergy and nematode infection. Sci Immunol *2*. 10.1126/sciimmunol.aal5196.
233. Rincon, M., Anguita, J., Nakamura, T., Fikrig, E., and Flavell, R.A. (1997). Interleukin (IL)-6 directs the differentiation of IL-4-producing CD4+ T cells. J Exp Med *185*, 461-469. 10.1084/jem.185.3.461.
234. Cook, K.D., and Miller, J. (2010). TCR-dependent translational control of GATA-3 enhances Th2 differentiation. J Immunol *185*, 3209-3216. 10.4049/jimmunol.0902544.
235. Yang, J.Q., Kalim, K.W., Li, Y., Zhang, S., Hinge, A., Filippi, M.D., Zheng, Y., and Guo, F. (2016). RhoA orchestrates glycolysis for TH2 cell differentiation and allergic airway inflammation. J Allergy Clin Immunol *137*, 231-245 e234. 10.1016/j.jaci.2015.05.004.
236. Zeng, H., and Chi, H. (2017). mTOR signaling in the differentiation and function of regulatory and effector T cells. Curr Opin Immunol *46*, 103-111. 10.1016/j.coi.2017.04.005.
237. Langrish, C.L., Chen, Y., Blumenschein, W.M., Mattson, J., Basham, B., Sedgwick, J.D., McClanahan, T., Kastelein, R.A., and Cua, D.J. (2005). IL-23 drives a pathogenic T cell population that induces autoimmune inflammation. J Exp Med *201*, 233-240. 10.1084/jem.20041257.
238. Harrington, L.E., Hatton, R.D., Mangan, P.R., Turner, H., Murphy, T.L., Murphy, K.M., and Weaver, C.T. (2005). Interleukin 17-producing CD4+ effector T cells develop via a lineage distinct from the T helper type 1 and 2 lineages. Nat Immunol *6*, 1123-1132. 10.1038/ni1254.
239. Haas, R., Smith, J., Rocher-Ros, V., Nadkarni, S., Montero-Melendez, T., D'Acquisto, F., Bland, E.J., Bombardieri, M., Pitzalis, C., Perretti, M., et al. (2015). Lactate Regulates Metabolic and Pro-inflammatory Circuits in Control of T Cell Migration and Effector Functions. PLoS Biol *13*, e1002202. 10.1371/journal.pbio.1002202.
240. Hirota, K., Yoshitomi, H., Hashimoto, M., Maeda, S., Teradaira, S., Sugimoto, N., Yamaguchi, T., Nomura, T., Ito, H., Nakamura, T., et al. (2007). Preferential recruitment of CCR6-expressing Th17 cells to inflamed

joints via CCL20 in rheumatoid arthritis and its animal model. J Exp Med *204*, 2803-2812. 10.1084/jem.20071397.
241. Pugh, G.H., Fouladvand, S., SantaCruz-Calvo, S., Agrawal, M., Zhang, X.D., Chen, J., Kern, P.A., and Nikolajczyk, B.S. (2022). T cells dominate peripheral inflammation in a cross-sectional analysis of obesity-associated diabetes. Obesity (Silver Spring) *30*, 1983-1994. 10.1002/oby.23528.
242. Nicholas, D., Proctor, E.A., Raval, F.M., Ip, B.C., Habib, C., Ritou, E., Grammatopoulos, T.N., Steenkamp, D., Dooms, H., Apovian, C.M., et al. (2017). Advances in the quantification of mitochondrial function in primary human immune cells through extracellular flux analysis. PLoS One *12*, e0170975. 10.1371/journal.pone.0170975.
243. Maury, E., Ehala-Aleksejev, K., Guiot, Y., Detry, R., Vandenhooft, A., and Brichard, S.M. (2007). Adipokines oversecreted by omental adipose tissue in human obesity. Am J Physiol Endocrinol Metab *293*, E656-665. 10.1152/ajpendo.00127.2007.
244. Fruhbeck, G., Catalan, V., Rodriguez, A., Ramirez, B., Becerril, S., Salvador, J., Colina, I., and Gomez-Ambrosi, J. (2019). Adiponectin-leptin Ratio is a Functional Biomarker of Adipose Tissue Inflammation. Nutrients *11*. 10.3390/nu11020454.
245. Laparra, A., Tricot, S., Le Van, M., Damouche, A., Gorwood, J., Vaslin, B., Favier, B., Benoist, S., Ho Tsong Fang, R., Bosquet, N., et al. (2019). The Frequencies of Immunosuppressive Cells in Adipose Tissue Differ in Human, Non-human Primate, and Mouse Models. Front Immunol *10*, 117. 10.3389/fimmu.2019.00117.
246. Ip, B.C., Hogan, A.E., and Nikolajczyk, B.S. (2015). Lymphocyte roles in metabolic dysfunction: of men and mice. Trends Endocrinol Metab *26*, 91-100. 10.1016/j.tem.2014.12.001.
247. Goldfine, A.B., and Shoelson, S.E. (2017). Therapeutic approaches targeting inflammation for diabetes and associated cardiovascular risk. J Clin Invest *127*, 83-93. 10.1172/JCI88884.
248. Peng, H., Long, F., and Ding, C. (2005). Feature selection based on mutual information: criteria of max-dependency, max-relevance, and min-redundancy. IEEE Trans Pattern Anal Mach Intell *27*, 1226-1238. 10.1109/TPAMI.2005.159.
249. Chen, T., and Guestrin, C. (2016). XGBoost: A Scalable Tree Boosting System. Proceedings of the 22nd ACM SIGKDD International Conference on Knowledge Discovery and Data Mining.
250. F., P., Varoquaux, G., Gramfort, A., Michel, V., Thirion, B., Grisel, M., Prettenhofer, P., Weiss, R., Dubourg, V., Vanderplas, J., et al. (2011). Scikit-learn: Machine Learning in Python. Journal of Machine Learning Research *12*, 2825-2830.
251. Lars Ståhle, S.W. (1987). Partial least squares analysis with cross-validation for the two-class problem: A Monte Carlo study. Journal of Chemometrics *1*, 185-196. 10.1002/cem.1180010306.
252. Wynn, T.A. (2015). Type 2 cytokines: mechanisms and therapeutic strategies. Nat Rev Immunol *15*, 271-282. 10.1038/nri3831.

253. Coquet, J.M., Schuijs, M.J., Smyth, M.J., Deswarte, K., Beyaert, R., Braun, H., Boon, L., Karlsson Hedestam, G.B., Nutt, S.L., Hammad, H., and Lambrecht, B.N. (2015). Interleukin-21-Producing CD4(+) T Cells Promote Type 2 Immunity to House Dust Mites. Immunity *43*, 318-330. 10.1016/j.immuni.2015.07.015.
254. Gramaglia, I., Mauri, D.N., Miner, K.T., Ware, C.F., and Croft, M. (1999). Lymphotoxin alphabeta is expressed on recently activated naive and Th1-like CD4 cells but is down-regulated by IL-4 during Th2 differentiation. J Immunol *162*, 1333-1338.
255. Tejero, J.D., Armand, N.C., Finn, C.M., Dhume, K., Strutt, T.M., Chai, K.X., Chen, L.M., and McKinstry, K.K. (2018). Cigarette smoke extract acts directly on CD4 T cells to enhance Th1 polarization and reduce memory potential. Cell Immunol *331*, 121-129. 10.1016/j.cellimm.2018.06.005.
256. Hotamisligil, G.S., Shargill, N.S., and Spiegelman, B.M. (1993). Adipose expression of tumor necrosis factor-alpha: direct role in obesity-linked insulin resistance. Science *259*, 87-91.
257. Kern, P.A., Saghizadeh, M., Ong, J.M., Bosch, R.J., Deem, R., and Simsolo, R.B. (1995). The expression of tumor necrosis factor in human adipose tissue. Regulation by obesity, weight loss, and relationship to lipoprotein lipase. J Clin Invest *95*, 2111-2119. 10.1172/JCI117899.
258. Poitou, C., Dalmas, E., Renovato, M., Benhamo, V., Hajduch, F., Abdennour, M., Kahn, J.F., Veyrie, N., Rizkalla, S., Fridman, W.H., et al. (2011). CD14dimCD16+ and CD14+CD16+ monocytes in obesity and during weight loss: relationships with fat mass and subclinical atherosclerosis. Arterioscler Thromb Vasc Biol *31*, 2322-2330. 10.1161/ATVBAHA.111.230979.
259. Uysal, K.T., Wiesbrock, S.M., Marino, M.W., and Hotamisligil, G.S. (1997). Protection from obesity-induced insulin resistance in mice lacking TNF-alpha function. Nature *389*, 610-614.
260. Strissel, K.J., DeFuria, J., Shaul, M.E., Bennett, G., Greenberg, A.S., and Obin, M.S. (2010). T-cell recruitment and Th1 polarization in adipose tissue during diet-induced obesity in C57BL/6 mice. Obesity (Silver Spring) *18*, 1918-1925. 10.1038/oby.2010.1.
261. Zhu, M., and Nikolajczyk, B.S. (2014). Immune cells link obesity-associated type 2 diabetes and periodontitis. J Dent Res *93*, 346-352. 10.1177/0022034513518943.
262. Grossmann, V., Schmitt, V.H., Zeller, T., Panova-Noeva, M., Schulz, A., Laubert-Reh, D., Juenger, C., Schnabel, R.B., Abt, T.G., Laskowski, R., et al. (2015). Profile of the Immune and Inflammatory Response in Individuals With Prediabetes and Type 2 Diabetes. Diabetes Care *38*, 1356-1364. 10.2337/dc14-3008.
263. Brahimaj, A., Ligthart, S., Ghanbari, M., Ikram, M.A., Hofman, A., Franco, O.H., Kavousi, M., and Dehghan, A. (2017). Novel inflammatory markers for incident pre-diabetes and type 2 diabetes: the Rotterdam Study. Eur J Epidemiol *32*, 217-226. 10.1007/s10654-017-0236-0.

264. Wiggins, K.B., Smith, M.A., and Schultz-Cherry, S. (2021). The Nature of Immune Responses to Influenza Vaccination in High-Risk Populations. Viruses *13*. 10.3390/v13061109.
265. Yamamoto, S., Mizoue, T., Tanaka, A., Oshiro, Y., Inamura, N., Konishi, M., Ozeki, M., Miyo, K., Sugiura, W., Sugiyama, H., and Ohmagari, N. (2021). Sex-associated differences between body mass index and SARS-CoV-2 antibody titers following the BNT 162b2 vaccine among 2,435 healthcare workers in Japan. medRxiv.
266. Pacifico, L., Di Renzo, L., Anania, C., Osborn, J.F., Ippoliti, F., Schiavo, E., and Chiesa, C. (2006). Increased T-helper interferon-gamma-secreting cells in obese children. Eur J Endocrinol *154*, 691-697. 10.1530/eje.1.02138.
267. O'Rourke, R.W., White, A.E., Metcalf, M.D., Winters, B.R., Diggs, B.S., Zhu, X., and Marks, D.L. (2012). Systemic inflammation and insulin sensitivity in obese IFN-gamma knockout mice. Metabolism *61*, 1152-1161. 10.1016/j.metabol.2012.01.018.
268. Dwyer-Lindgren, L., Bertozzi-Villa, A., Stubbs, R.W. et al. (2017). Inequalities in life expectancy among US counties, 1980 to 2014: temporal trends and key drivers. JAMA Intern Med, 1003-1011.
269. Quevedo-Martinez, J.U., Garfias, Y., Jimenez, J., Garcia, O., Venegas, D., and Bautista de Lucio, V.M. (2021). Pro-inflammatory cytokine profile is present in the serum of Mexican patients with different stages of diabetic retinopathy secondary to type 2 diabetes. BMJ Open Ophthalmol *6*, e000717. 10.1136/bmjophth-2021-000717.
270. Rocha, V.Z., Folco, E.J., Sukhova, G., Shimizu, K., Gotsman, I., Vernon, A.H., and Libby, P. (2008). Interferon-gamma, a Th1 cytokine, regulates fat inflammation: a role for adaptive immunity in obesity. Circ Res *103*, 467-476.
271. Wang, Z., Shen, X.H., Feng, W.M., Ye, G.F., Qiu, W., and Li, B. (2016). Analysis of Inflammatory Mediators in Prediabetes and Newly Diagnosed Type 2 Diabetes Patients. J Diabetes Res *2016*, 7965317. 10.1155/2016/7965317.
272. Imoto, K., Kukidome, D., Nishikawa, T., Matsuhisa, T., Sonoda, K., Fujisawa, K., Yano, M., Motoshima, H., Taguchi, T., Tsuruzoe, K., et al. (2006). Impact of mitochondrial reactive oxygen species and apoptosis signal-regulating kinase 1 on insulin signaling. Diabetes *55*, 1197-1204. 10.2337/db05-1187.
273. Li, P.F., Dietz, R., and von Harsdorf, R. (1999). p53 regulates mitochondrial membrane potential through reactive oxygen species and induces cytochrome c-independent apoptosis blocked by Bcl-2. EMBO J *18*, 6027-6036. 10.1093/emboj/18.21.6027.
274. Deragon, M.A., McCaig, W.D., Patel, P.S., Haluska, R.J., Hodges, A.L., Sosunov, S.A., Murphy, M.P., Ten, V.S., and LaRocca, T.J. (2020). Mitochondrial ROS prime the hyperglycemic shift from apoptosis to necroptosis. Cell Death Discov *6*, 132. 10.1038/s41420-020-00370-3.

275. Loson, O.C., Song, Z., Chen, H., and Chan, D.C. (2013). Fis1, Mff, MiD49, and MiD51 mediate Drp1 recruitment in mitochondrial fission. Mol Biol Cell *24*, 659-667. 10.1091/mbc.E12-10-0721.
276. Redpath, C.J., Bou Khalil, M., Drozdzal, G., Radisic, M., and McBride, H.M. (2013). Mitochondrial hyperfusion during oxidative stress is coupled to a dysregulation in calcium handling within a C2C12 cell model. PLoS One *8*, e69165. 10.1371/journal.pone.0069165.
277. Abdullah, M.O., Zeng, R.X., Margerum, C.L., Papadopoli, D., Monnin, C., Punter, K.B., Chu, C., Al-Rofaidi, M., Al-Tannak, N.F., Berardi, D., et al. (2022). Mitochondrial hyperfusion via metabolic sensing of regulatory amino acids. Cell Rep *40*, 111198. 10.1016/j.celrep.2022.111198.
278. Rambold, A.S., Kostelecky, B., Elia, N., and Lippincott-Schwartz, J. (2011). Tubular network formation protects mitochondria from autophagosomal degradation during nutrient starvation. Proc Natl Acad Sci U S A *108*, 10190-10195. 10.1073/pnas.1107402108.
279. Sassano, M.L., van Vliet, A.R., Vervoort, E., Van Eygen, S., Van den Haute, C., Pavie, B., Roels, J., Swinnen, J.V., Spinazzi, M., Moens, L., et al. (2023). PERK recruits E-Syt1 at ER-mitochondria contacts for mitochondrial lipid transport and respiration. J Cell Biol *222*. 10.1083/jcb.202206008.
280. Chen, H., Detmer, S.A., Ewald, A.J., Griffin, E.E., Fraser, S.E., and Chan, D.C. (2003). Mitofusins Mfn1 and Mfn2 coordinately regulate mitochondrial fusion and are essential for embryonic development. J Cell Biol *160*, 189-200. 10.1083/jcb.200211046.
281. Ge, Y., Shi, X., Boopathy, S., McDonald, J., Smith, A.W., and Chao, L.H. (2020). Two forms of Opa1 cooperate to complete fusion of the mitochondrial inner-membrane. Elife *9*. 10.7554/eLife.50973.
282. Lee, H., Smith, S.B., and Yoon, Y. (2017). The short variant of the mitochondrial dynamin OPA1 maintains mitochondrial energetics and cristae structure. J Biol Chem *292*, 7115-7130. 10.1074/jbc.M116.762567.
283. Patten, D.A., Wong, J., Khacho, M., Soubannier, V., Mailloux, R.J., Pilon-Larose, K., MacLaurin, J.G., Park, D.S., McBride, H.M., Trinkle-Mulcahy, L., et al. (2014). OPA1-dependent cristae modulation is essential for cellular adaptation to metabolic demand. EMBO J *33*, 2676-2691. 10.15252/embj.201488349.
284. Zorova, L.D., Popkov, V.A., Plotnikov, E.Y., Silachev, D.N., Pevzner, I.B., Jankauskas, S.S., Babenko, V.A., Zorov, S.D., Balakireva, A.V., Juhaszova, M., et al. (2018). Mitochondrial membrane potential. Anal Biochem *552*, 50-59. 10.1016/j.ab.2017.07.009.
285. Duong, Q.V., Levitsky, Y., Dessinger, M.J., Strubbe-Rivera, J.O., and Bazil, J.N. (2021). Identifying Site-Specific Superoxide and Hydrogen Peroxide Production Rates From the Mitochondrial Electron Transport System Using a Computational Strategy. Function (Oxf) *2*, zqab050. 10.1093/function/zqab050.
286. Selivanov, V.A., Votyakova, T.V., Pivtoraiko, V.N., Zeak, J., Sukhomlin, T., Trucco, M., Roca, J., and Cascante, M. (2011). Reactive oxygen species production by forward and reverse electron fluxes in the mitochondrial

respiratory chain. PLoS Comput Biol *7*, e1001115. 10.1371/journal.pcbi.1001115.
287. Miller, I.P., Pavlovic, I., Poljsak, B., Suput, D., and Milisav, I. (2019). Beneficial Role of ROS in Cell Survival: Moderate Increases in H(2)O(2) Production Induced by Hepatocyte Isolation Mediate Stress Adaptation and Enhanced Survival. Antioxidants (Basel) *8*. 10.3390/antiox8100434.
288. Previte, D.M., O'Connor, E.C., Novak, E.A., Martins, C.P., Mollen, K.P., and Piganelli, J.D. (2017). Reactive oxygen species are required for driving efficient and sustained aerobic glycolysis during CD4+ T cell activation. PLoS One *12*, e0175549. 10.1371/journal.pone.0175549.
289. Sena, L.A., Li, S., Jairaman, A., Prakriya, M., Ezponda, T., Hildeman, D.A., Wang, C.R., Schumacker, P.T., Licht, J.D., Perlman, H., et al. (2013). Mitochondria are required for antigen-specific T cell activation through reactive oxygen species signaling. Immunity *38*, 225-236. 10.1016/j.immuni.2012.10.020.
290. Lian, G., Gnanaprakasam, J.R., Wang, T., Wu, R., Chen, X., Liu, L., Shen, Y., Yang, M., Yang, J., Chen, Y., et al. (2018). Glutathione de novo synthesis but not recycling process coordinates with glutamine catabolism to control redox homeostasis and directs murine T cell differentiation. Elife *7*. 10.7554/eLife.36158.
291. Zhao, Z., Wang, Y., Gao, Y., Ju, Y., Zhao, Y., Wu, Z., Gao, S., Zhang, B., Pang, X., Zhang, Y., and Wang, W. (2023). The PRAK-NRF2 axis promotes the differentiation of Th17 cells by mediating the redox homeostasis and glycolysis. Proc Natl Acad Sci U S A *120*, e2212613120. 10.1073/pnas.2212613120.
292. Cottet-Rousselle, C., Ronot, X., Leverve, X., and Mayol, J.F. (2011). Cytometric assessment of mitochondria using fluorescent probes. Cytometry A *79*, 405-425. 10.1002/cyto.a.21061.
293. Finlin, B.S., Memetimin, H., Confides, A.L., Kasza, I., Zhu, B., Vekaria, H.J., Harfmann, B., Jones, K.A., Johnson, Z.R., Westgate, P.M., et al. (2018). Human adipose beiging in response to cold and mirabegron. JCI Insight *3*. 10.1172/jci.insight.121510.
294. Roy, J.G., McElhaney, J.E., and Verschoor, C.P. (2020). Reliable reference genes for the quantification of mRNA in human T-cells and PBMCs stimulated with live influenza virus. BMC Immunol *21*, 4. 10.1186/s12865-020-0334-8.
295. Kirber, M.T., Chen, K., and Keaney, J.F., Jr. (2007). YFP photoconversion revisited: confirmation of the CFP-like species. Nat Methods *4*, 767-768. 10.1038/nmeth1007-767.
296. Balla, A., Vereb, G., Gulkan, H., Gehrmann, T., Gergely, P., Heilmeyer, L.M., Jr., and Antal, M. (2000). Immunohistochemical localisation of two phosphatidylinositol 4-kinase isoforms, PI4K230 and PI4K92, in the central nervous system of rats. Exp Brain Res *134*, 279-288. 10.1007/s002210000469.
297. Valente, A.J., Maddalena, L.A., Robb, E.L., Moradi, F., and Stuart, J.A. (2017). A simple ImageJ macro tool for analyzing mitochondrial network

morphology in mammalian cell culture. Acta Histochem *119*, 315-326. 10.1016/j.acthis.2017.03.001.
298. Conway, W., Kiewisz, R., Fabig, G., Kelleher, C.P., Wu, H.Y., Anjur-Dietrich, M., Muller-Reichert, T., and Needleman, D.J. (2022). Self-organization of kinetochore-fibers in human mitotic spindles. Elife *11*. 10.7554/eLife.75458.
299. Adler, J., and Parmryd, I. (2010). Quantifying colocalization by correlation: the Pearson correlation coefficient is superior to the Mander's overlap coefficient. Cytometry A *77*, 733-742. 10.1002/cyto.a.20896.
300. Wolf, D.M., Segawa, M., Kondadi, A.K., Anand, R., Bailey, S.T., Reichert, A.S., van der Bliek, A.M., Shackelford, D.B., Liesa, M., and Shirihai, O.S. (2019). Individual cristae within the same mitochondrion display different membrane potentials and are functionally independent. EMBO J *38*, e101056. 10.15252/embj.2018101056.
301. Hackenbrock, C.R. (1966). Ultrastructural bases for metabolically linked mechanical activity in mitochondria. I. Reversible ultrastructural changes with change in metabolic steady state in isolated liver mitochondria. J Cell Biol *30*, 269-297. 10.1083/jcb.30.2.269.
302. Hackenbrock, C.R., Schneider, H., Lemasters, J.J., and Hochli, M. (1980). Relationships between bilayer lipid, motional freedom of oxidoreductase components, and electron transfer in the mitochondrial inner membrane. Adv Exp Med Biol *132*, 245-263. 10.1007/978-1-4757-1419-7_26.
303. Mannella, C.A., Pfeiffer, D.R., Bradshaw, P.C., Moraru, II, Slepchenko, B., Loew, L.M., Hsieh, C.E., Buttle, K., and Marko, M. (2001). Topology of the mitochondrial inner membrane: dynamics and bioenergetic implications. IUBMB Life *52*, 93-100. 10.1080/15216540152845885.
304. Cogliati, S., Frezza, C., Soriano, M.E., Varanita, T., Quintana-Cabrera, R., Corrado, M., Cipolat, S., Costa, V., Casarin, A., Gomes, L.C., et al. (2013). Mitochondrial cristae shape determines respiratory chain supercomplexes assembly and respiratory efficiency. Cell *155*, 160-171. 10.1016/j.cell.2013.08.032.
305. Isoda, K., Young, J.L., Zirlik, A., MacFarlane, L.A., Tsuboi, N., Gerdes, N., Schonbeck, U., and Libby, P. (2006). Metformin inhibits proinflammatory responses and nuclear factor-kappaB in human vascular wall cells. Arterioscler Thromb Vasc Biol *26*, 611-617. 10.1161/01.ATV.0000201938.78044.75.
306. Kaufmann, U., Kahlfuss, S., Yang, J., Ivanova, E., Koralov, S.B., and Feske, S. (2019). Calcium Signaling Controls Pathogenic Th17 Cell-Mediated Inflammation by Regulating Mitochondrial Function. Cell Metab *29*, 1104-1118 e1106. 10.1016/j.cmet.2019.01.019.
307. Pugsley, H.R. (2017). Assessing Autophagic Flux by Measuring LC3, p62, and LAMP1 Co-localization Using Multispectral Imaging Flow Cytometry. J Vis Exp. 10.3791/55637.
308. Dominy, J.E., and Puigserver, P. (2013). Mitochondrial biogenesis through activation of nuclear signaling proteins. Cold Spring Harb Perspect Biol *5*. 10.1101/cshperspect.a015008.

309. Laporte, D., Gouleme, L., Jimenez, L., Khemiri, I., and Sagot, I. (2018). Mitochondria reorganization upon proliferation arrest predicts individual yeast cell fate. Elife *7*. 10.7554/eLife.35685.
310. Buck, M.D., O'Sullivan, D., Klein Geltink, R.I., Curtis, J.D., Chang, C.H., Sanin, D.E., Qiu, J., Kretz, O., Braas, D., van der Windt, G.J., et al. (2016). Mitochondrial Dynamics Controls T Cell Fate through Metabolic Programming. Cell *166*, 63-76. 10.1016/j.cell.2016.05.035.
311. Xiao, B., Deng, X., Zhou, W., and Tan, E.K. (2016). Flow Cytometry-Based Assessment of Mitophagy Using MitoTracker. Front Cell Neurosci *10*, 76. 10.3389/fncel.2016.00076.
312. Pendergrass, W., Wolf, N., and Poot, M. (2004). Efficacy of MitoTracker Green and CMXrosamine to measure changes in mitochondrial membrane potentials in living cells and tissues. Cytometry A *61*, 162-169. 10.1002/cyto.a.20033.
313. Li, A., Zhang, S., Li, J., Liu, K., Huang, F., and Liu, B. (2016). Metformin and resveratrol inhibit Drp1-mediated mitochondrial fission and prevent ER stress-associated NLRP3 inflammasome activation in the adipose tissue of diabetic mice. Mol Cell Endocrinol *434*, 36-47. 10.1016/j.mce.2016.06.008.
314. Schmitt, K., Grimm, A., Dallmann, R., Oettinghaus, B., Restelli, L.M., Witzig, M., Ishihara, N., Mihara, K., Ripperger, J.A., Albrecht, U., et al. (2018). Circadian Control of DRP1 Activity Regulates Mitochondrial Dynamics and Bioenergetics. Cell Metab *27*, 657-666 e655. 10.1016/j.cmet.2018.01.011.
315. Degtyarev, M., De Maziere, A., Orr, C., Lin, J., Lee, B.B., Tien, J.Y., Prior, W.W., van Dijk, S., Wu, H., Gray, D.C., et al. (2008). Akt inhibition promotes autophagy and sensitizes PTEN-null tumors to lysosomotropic agents. J Cell Biol *183*, 101-116. 10.1083/jcb.200801099.
316. Yazid, M.D., and Hung-Chih, C. (2021). Perturbation of PI3K/Akt signaling affected autophagy modulation in dystrophin-deficient myoblasts. Cell Commun Signal *19*, 105. 10.1186/s12964-021-00785-0.
317. Dodd, K.M., Yang, J., Shen, M.H., Sampson, J.R., and Tee, A.R. (2015). mTORC1 drives HIF-1alpha and VEGF-A signalling via multiple mechanisms involving 4E-BP1, S6K1 and STAT3. Oncogene *34*, 2239-2250. 10.1038/onc.2014.164.
318. Eid, W., Dauner, K., Courtney, K.C., Gagnon, A., Parks, R.J., Sorisky, A., and Zha, X. (2017). mTORC1 activates SREBP-2 by suppressing cholesterol trafficking to lysosomes in mammalian cells. Proc Natl Acad Sci U S A *114*, 7999-8004. 10.1073/pnas.1705304114.
319. Blanchard, P.G., Festuccia, W.T., Houde, V.P., St-Pierre, P., Brule, S., Turcotte, V., Cote, M., Bellmann, K., Marette, A., and Deshaies, Y. (2012). Major involvement of mTOR in the PPARgamma-induced stimulation of adipose tissue lipid uptake and fat accretion. J Lipid Res *53*, 1117-1125. 10.1194/jlr.M021485.
320. Nguyen, D.V., and Rocke, D.M. (2002). Tumor classification by partial least squares using microarray gene expression data. Bioinformatics *18*, 39-50. 10.1093/bioinformatics/18.1.39.

321. Hildyard, J.C., Ammala, C., Dukes, I.D., Thomson, S.A., and Halestrap, A.P. (2005). Identification and characterisation of a new class of highly specific and potent inhibitors of the mitochondrial pyruvate carrier. Biochim Biophys Acta *1707*, 221-230. 10.1016/j.bbabio.2004.12.005.
322. Zhong, Y., Li, X., Yu, D., Li, X., Li, Y., Long, Y., Yuan, Y., Ji, Z., Zhang, M., Wen, J.G., et al. (2015). Application of mitochondrial pyruvate carrier blocker UK5099 creates metabolic reprogram and greater stem-like properties in LnCap prostate cancer cells in vitro. Oncotarget *6*, 37758-37769. 10.18632/oncotarget.5386.
323. O'Connor, R.S., Guo, L., Ghassemi, S., Snyder, N.W., Worth, A.J., Weng, L., Kam, Y., Philipson, B., Trefely, S., Nunez-Cruz, S., et al. (2018). The CPT1a inhibitor, etomoxir induces severe oxidative stress at commonly used concentrations. Sci Rep *8*, 6289. 10.1038/s41598-018-24676-6.
324. Raud, B., Roy, D.G., Divakaruni, A.S., Tarasenko, T.N., Franke, R., Ma, E.H., Samborska, B., Hsieh, W.Y., Wong, A.H., Stuve, P., et al. (2018). Etomoxir Actions on Regulatory and Memory T Cells Are Independent of Cpt1a-Mediated Fatty Acid Oxidation. Cell Metab *28*, 504-515 e507. 10.1016/j.cmet.2018.06.002.
325. Chacko, B.K., Kramer, P.A., Ravi, S., Benavides, G.A., Mitchell, T., Dranka, B.P., Ferrick, D., Singal, A.K., Ballinger, S.W., Bailey, S.M., et al. (2014). The Bioenergetic Health Index: a new concept in mitochondrial translational research. Clin Sci (Lond) *127*, 367-373. 10.1042/CS20140101.
326. Rocchiccioli, F., Leroux, J.P., and Cartier, P.H. (1984). Microdetermination of 2-ketoglutaric acid in plasma and cerebrospinal fluid by capillary gas chromatography mass spectrometry; application to pediatrics. Biomed Mass Spectrom *11*, 24-28. 10.1002/bms.1200110105.
327. Wagner, B.M., Donnarumma, F., Wintersteiger, R., Windischhofer, W., and Leis, H.J. (2010). Simultaneous quantitative determination of alpha-ketoglutaric acid and 5-hydroxymethylfurfural in human plasma by gas chromatography-mass spectrometry. Anal Bioanal Chem *396*, 2629-2637. 10.1007/s00216-010-3479-0.
328. Halamkova, L., Mailloux, S., Halamek, J., Cooper, A.J., and Katz, E. (2012). Enzymatic analysis of alpha-ketoglutaramate--a biomarker for hyperammonemia. Talanta *100*, 7-11. 10.1016/j.talanta.2012.08.022.
329. Cynober, L., Coudray-Lucas, C., de Bandt, J.P., Guechot, J., Aussel, C., Salvucci, M., and Giboudeau, J. (1990). Action of ornithine alpha-ketoglutarate, ornithine hydrochloride, and calcium alpha-ketoglutarate on plasma amino acid and hormonal patterns in healthy subjects. J Am Coll Nutr *9*, 2-12. 10.1080/07315724.1990.10720343.
330. Kirchner, G.I., Meier-Wiedenbach, I., and Manns, M.P. (2004). Clinical pharmacokinetics of everolimus. Clin Pharmacokinet *43*, 83-95. 10.2165/00003088-200443020-00002.
331. Huang, X.Y., Hu, Q.P., Shi, H.Y., Zheng, Y.Y., Hu, R.R., and Guo, Q. (2021). Everolimus inhibits PI3K/Akt/mTOR and NF-kB/IL-6 signaling and protects seizure-induced brain injury in rats. J Chem Neuroanat *114*, 101960. 10.1016/j.jchemneu.2021.101960.

332. Sengupta, S., Giaime, E., Narayan, S., Hahm, S., Howell, J., O'Neill, D., Vlasuk, G.P., and Saiah, E. (2019). Discovery of NV-5138, the first selective Brain mTORC1 activator. Sci Rep *9*, 4107. 10.1038/s41598-019-40693-5.
333. Procaccini, C., Carbone, F., Di Silvestre, D., Brambilla, F., De Rosa, V., Galgani, M., Faicchia, D., Marone, G., Tramontano, D., Corona, M., et al. (2016). The Proteomic Landscape of Human Ex Vivo Regulatory and Conventional T Cells Reveals Specific Metabolic Requirements. Immunity *44*, 406-421. 10.1016/j.immuni.2016.01.028.
334. Chisolm, D.A., Savic, D., Moore, A.J., Ballesteros-Tato, A., Leon, B., Crossman, D.K., Murre, C., Myers, R.M., and Weinmann, A.S. (2017). CCCTC-Binding Factor Translates Interleukin 2- and alpha-Ketoglutarate-Sensitive Metabolic Changes in T Cells into Context-Dependent Gene Programs. Immunity *47*, 251-267 e257. 10.1016/j.immuni.2017.07.015.
335. Fendt, S.M., Bell, E.L., Keibler, M.A., Olenchock, B.A., Mayers, J.R., Wasylenko, T.M., Vokes, N.I., Guarente, L., Vander Heiden, M.G., and Stephanopoulos, G. (2013). Reductive glutamine metabolism is a function of the alpha-ketoglutarate to citrate ratio in cells. Nat Commun *4*, 2236. 10.1038/ncomms3236.
336. Whillier, S., Garcia, B., Chapman, B.E., Kuchel, P.W., and Raftos, J.E. (2011). Glutamine and alpha-ketoglutarate as glutamate sources for glutathione synthesis in human erythrocytes. FEBS J *278*, 3152-3163. 10.1111/j.1742-4658.2011.08241.x.
337. Matias, M.I., Yong, C.S., Foroushani, A., Goldsmith, C., Mongellaz, C., Sezgin, E., Levental, K.R., Talebi, A., Perrault, J., Riviere, A., et al. (2021). Regulatory T cell differentiation is controlled by alphaKG-induced alterations in mitochondrial metabolism and lipid homeostasis. Cell Rep *37*, 109911. 10.1016/j.celrep.2021.109911.
338. Guo, C., Chen, S., Liu, W., Ma, Y., Li, J., Fisher, P.B., Fang, X., and Wang, X.Y. (2019). Immunometabolism: A new target for improving cancer immunotherapy. Adv Cancer Res *143*, 195-253. 10.1016/bs.acr.2019.03.004.
339. Morel, L. (2017). Immunometabolism in systemic lupus erythematosus. Nat Rev Rheumatol *13*, 280-290. 10.1038/nrrheum.2017.43.
340. Weyand, C.M., and Goronzy, J.J. (2017). Immunometabolism in early and late stages of rheumatoid arthritis. Nat Rev Rheumatol *13*, 291-301. 10.1038/nrrheum.2017.49.
341. Zaiatz Bittencourt, V., Jones, F., Doherty, G., and Ryan, E.J. (2021). Targeting Immune Cell Metabolism in the Treatment of Inflammatory Bowel Disease. Inflamm Bowel Dis *27*, 1684-1693. 10.1093/ibd/izab024.
342. Mease, P.J. (2007). Adalimumab in the treatment of arthritis. Ther Clin Risk Manag *3*, 133-148. 10.2147/tcrm.2007.3.1.133.
343. Kawata, T., Tada, K., Kobayashi, M., Sakamoto, T., Takiuchi, Y., Iwai, F., Sakurada, M., Hishizawa, M., Shirakawa, K., Shindo, K., et al. (2018). Dual inhibition of the mTORC1 and mTORC2 signaling pathways is a promising therapeutic target for adult T-cell leukemia. Cancer Sci *109*, 103-111. 10.1111/cas.13431.

344. Noreen, S., Maqbool, I., and Madni, A. (2021). Dexamethasone: Therapeutic potential, risks, and future projection during COVID-19 pandemic. Eur J Pharmacol *894*, 173854. 10.1016/j.ejphar.2021.173854.
345. Kooistra, E.J., van Berkel, M., van Kempen, N.F., van Latum, C.R.M., Bruse, N., Frenzel, T., van den Berg, M.J.W., Schouten, J.A., Kox, M., and Pickkers, P. (2021). Dexamethasone and tocilizumab treatment considerably reduces the value of C-reactive protein and procalcitonin to detect secondary bacterial infections in COVID-19 patients. Crit Care *25*, 281. 10.1186/s13054-021-03717-z.
346. Schneeweiss, S., Setoguchi, S., Weinblatt, M.E., Katz, J.N., Avorn, J., Sax, P.E., Levin, R., and Solomon, D.H. (2007). Anti-tumor necrosis factor alpha therapy and the risk of serious bacterial infections in elderly patients with rheumatoid arthritis. Arthritis Rheum *56*, 1754-1764. 10.1002/art.22600.
347. Ibrahim, A., Ahmed, M., Conway, R., and Carey, J.J. (2018). Risk of Infection with Methotrexate Therapy in Inflammatory Diseases: A Systematic Review and Meta-Analysis. J Clin Med *8*. 10.3390/jcm8010015.
348. Malozowski, S., and Sahlroot, J.T. (2007). Interleukin-1-receptor antagonist in type 2 diabetes mellitus. N Engl J Med *357*, 302-303; author reply 303. 10.1056/NEJMc071324.
349. Martinez, N., Vallerskog, T., West, K., Nunes-Alves, C., Lee, J., Martens, G.W., Behar, S.M., and Kornfeld, H. (2014). Chromatin decondensation and T cell hyperresponsiveness in diabetes-associated hyperglycemia. J Immunol *193*, 4457-4468. 10.4049/jimmunol.1401125.
350. Kishore, M., Cheung, K.C.P., Fu, H., Bonacina, F., Wang, G., Coe, D., Ward, E.J., Colamatteo, A., Jangani, M., Baragetti, A., et al. (2017). Regulatory T Cell Migration Is Dependent on Glucokinase-Mediated Glycolysis. Immunity *47*, 875-889 e810. 10.1016/j.immuni.2017.10.017.
351. Nobs, S.P., Natali, S., Pohlmeier, L., Okreglicka, K., Schneider, C., Kurrer, M., Sallusto, F., and Kopf, M. (2017). PPARgamma in dendritic cells and T cells drives pathogenic type-2 effector responses in lung inflammation. J Exp Med *214*, 3015-3035. 10.1084/jem.20162069.
352. DeBerardinis, R.J., Mancuso, A., Daikhin, E., Nissim, I., Yudkoff, M., Wehrli, S., and Thompson, C.B. (2007). Beyond aerobic glycolysis: transformed cells can engage in glutamine metabolism that exceeds the requirement for protein and nucleotide synthesis. Proc Natl Acad Sci U S A *104*, 19345-19350. 10.1073/pnas.0709747104.
353. Yang, W.H., Park, S.Y., Nam, H.W., Kim, D.H., Kang, J.G., Kang, E.S., Kim, Y.S., Lee, H.C., Kim, K.S., and Cho, J.W. (2008). NFkappaB activation is associated with its O-GlcNAcylation state under hyperglycemic conditions. Proc Natl Acad Sci U S A *105*, 17345-17350. 10.1073/pnas.0806198105.
354. Kuball, J., Hauptrock, B., Malina, V., Antunes, E., Voss, R.H., Wolfl, M., Strong, R., Theobald, M., and Greenberg, P.D. (2009). Increasing functional avidity of TCR-redirected T cells by removing defined N-glycosylation sites in the TCR constant domain. J Exp Med *206*, 463-475. 10.1084/jem.20082487.

355. Chen, X., and Oppenheim, J.J. (2011). Resolving the identity myth: key markers of functional CD4+FoxP3+ regulatory T cells. Int Immunopharmacol *11*, 1489-1496. 10.1016/j.intimp.2011.05.018.
356. Morgan, R., Gao, G., Pawling, J., Dennis, J.W., Demetriou, M., and Li, B. (2004). N-acetylglucosaminyltransferase V (Mgat5)-mediated N-glycosylation negatively regulates Th1 cytokine production by T cells. J Immunol *173*, 7200-7208. 10.4049/jimmunol.173.12.7200.
357. Klotz, L., Burgdorf, S., Dani, I., Saijo, K., Flossdorf, J., Hucke, S., Alferink, J., Nowak, N., Beyer, M., Mayer, G., et al. (2009). The nuclear receptor PPAR gamma selectively inhibits Th17 differentiation in a T cell-intrinsic fashion and suppresses CNS autoimmunity. J Exp Med *206*, 2079-2089. 10.1084/jem.20082771.
358. Miao, Y., Zheng, Y., Geng, Y., Yang, L., Cao, N., Dai, Y., and Wei, Z. (2021). The role of GLS1-mediated glutaminolysis/2-HG/H3K4me3 and GSH/ROS signals in Th17 responses counteracted by PPARgamma agonists. Theranostics *11*, 4531-4548. 10.7150/thno.54803.

VITA

Gabriella H. Kalantar (née Pugh)

EDUCATION

2018 – 2023	University of Kentucky College of Medicine PhD in Microbiology and Immunology Thesis Advisor: Barbara S. Nikolajczyk *Expected August 2023*
2016 – 2018	Eastern Kentucky University M.S. in Biology Concentration: Microbiology Thesis Advisor: Oliver R. Oakley Graduated *Magna Cum Laude*
2012 – 2016	Eastern Kentucky University B.S. in Biology Concentration: Cellular, Molecular, & Microbial Biology

PROFESSIONAL POSITIONS

2019 – 2023	University of Kentucky, Department of Microbiology, Immunology, and Molecular Genetics Graduate Research Assistant Advisor: Barbara S. Nikolajczyk, PhD PhD dissertation research
2016 – 2018	Eastern Kentucky University, Department of Biological Sciences Graduate Research Assistant Advisor: Dr. Oliver R. Oakley, PhD M.S. thesis research
May – Aug 2016	University of Kentucky, Department of Physiology Temporary paraprofessional (summer internship) Advisor: Dr. Ming Gong, PhD

HONORS & AWARDS

Academic

2022	Vision Award, University of Kentucky College of Medicine
2022	Department of Microbiology, Immunology, and Molecular Genetics' Nominee for College of Medicine Graduate Student of the Year Award
2022	Department of Microbiology, Immunology, and Molecular Genetics' Nominee for College of Medicine Outstanding Graduate Student Thesis Award
2021 – 2023	University of Kentucky Center for Clinical and Translational Science, TL1 Predoctoral Training Program TL1TR001997
2019 – 2021	University of Kentucky Department of Pharmacology and Nutritional Sciences, T32 Training Program T32 DK007778
2016 – 2018	Eastern Kentucky University and University of Kentucky KY Bridge to a Doctorate Degree Scholar Program for Appalachian Students

Research

11/2022	Outstanding Research Poster Award, University of Kentucky, Barnstable-Brown Diabetes and Obesity Center Research Day

PUBLICATIONS

1. **Pugh, G.H.**, Fouladvand, S., SantaCruz-Calvo, S., Agrawal, M., Zhang, X.D., Chen, J., Kern, P.A., Nikolajczyk, B.S. T cells dominate peripheral inflammation in cross-sectional obesity-associated diabetes. *Obesity (Silver Spring)* 2022;1-11. doi:10.10002/oby.23528.
2. Conway, R., Donato Rockhold, J., SantaCruz-Calvo, S., Zukowski, E., **Pugh, G.H.**, Hasturk, H.; Kern, P.A., Nikolajczyk, B.S., Bharath, L.P. Obesity and fatty acids promote mitochondrial translocation of STAT3 through ROS-dependent mechanisms. *Front. Aging*. 2022;3:924003. doi:10.3389/fragi.2022.924003.
3. Liu, R., **Pugh, G.H.**, Tevonian, E., Thompson, K., Lauffenburger, D.A., Kern, P.A., Nikolajczyk, B.S. Regulatory T cells control effector T cell inflammation in human prediabetes. *Diabetes*. 2021;71(2):264-274.

doi:10.2337/db21-0659.
4. SantaCruz-Calvo, S.; Bharath, L.; **Pugh, G.**; SantaCruz-Calvo, L.; Lenin, R.R.; Lutshumba, L.; Liu, R.; Bachstetter, A.; Zhu, B.; Nikolajczyk, B.S. Adaptive immune cells shape obesity-associated type 2 diabetes mellitus and less prominent comorbidities. Nat. Rev. Endocrinol 2021;18:23-42. doi:10.1038/s41574-021-00575-1.